Spring 1-1-2012

Connections Between the Non-Migrating Semidiurnal Tide Over the South Pole and Stationary Planetary Waves in the Northern Hemisphere

Frederico Eduardo da Cunha Estante
University of Colorado at Boulder, estantef@gmail.com

Connections between the non-migrating semidiurnal tide over the South Pole and stationary planetary waves in the northern hemisphere

by

Frederico Eduardo da Cunha Estante

B.S., Embry-Riddle Aeronautical University, 2010

A thesis submitted to the

Faculty of the Graduate School of the

University of Colorado in partial fulfillment

of the requirements for the degree of

Master of Science

Department of Aerospace Engineering Sciences

2012

This thesis entitled:
Connections between the non-migrating semidiurnal tide over the South Pole and stationary planetary waves in the northern hemisphere
written by Frederico Eduardo da Cunha Estante
has been approved for the Department of Aerospace Engineering Sciences

_____
Professor Scott Palo

_____
Professor Jeffrey Forbes

_____
Professor Delores Knipp

Date _____

The final copy of this thesis has been examined by the signatories, and we find that both the content and the form meet acceptable presentation standards of scholarly work in the above mentioned discipline.

Estante, Frederico Eduardo da Cunha (M.S., Aerospace Engineering)

Connections between the non-migrating semidiurnal tide over the South Pole and stationary planetary waves in the northern hemisphere

Thesis directed by Professor Scott Palo

The westward propagating zonal wavenumber 1 non-migrating semidiurnal tide is a dominant dynamical feature present during the Austral summer over the South Pole. It has been hypothesized that this wave is generated by a non-linear interaction between the zonal wavenumber one stationary planetary wave in the northern hemisphere stratosphere and the zonal wavenumber two migrating diurnal tide. However, direct evidence of this interaction has yet to be observed.

Using observations from the South Pole meteor radar (SPMR) system we can unambiguously determine the structure of the non-migrating semidiurnal tide in the meridional wind field. These observations are correlated with the stationary planetary wave activity in the zonal and meridional wind fields in the northern hemisphere stratosphere. Data from the NASA Modern Era Retrospective-Analysis for Research and Applications (MERRA) global assimilative model are used to determine the structure of the zonal wavenumber 1,2, and 3 stationary planetary waves for this comparison.

In addition, temperature data from the NASA TIMED SABER mission was analyzed and compared to the MERRA temperature observations as validation of the MERRA model results. Correlation analysis has indicated periods of time with significant correlation between the zonal wave-number 1 stationary planetary wave and the SPMR data and other times with very strong anti-correlations. Similar features are observed with the zonal wave-number 3 stationary planetary wave.

Dedication

To my parents, Mayra Estante and Paulo Estante.

Acknowledgements

First and foremost, I would like to thank my advisor, Professor Scott Palo, for his support and patience to teach me even the simplest things about atmospheric dynamics and radars, without getting upset with my basic questions. He gave me the opportunity to work on this very exciting project and learn a lot about this subject, not only in theory, but also about the hardware used by sending me to conferences and workshops around the world. I really hope that the time you invested in me was worth and that this research I performed may lead to further understanding of the subject.

I would like to thank my professors at Embry-Riddle Aeronautical University for preparing me for this journey in graduate school, and in special Dr. Irfan Azeem, who gave me the opportunity to start working at the Space Physics Research Lab, where I first got in touch with this field.

I also would like to thank my professors at the University of Colorado at Boulder, which helped me tirelessly through my graduate career. Special thanks go to Dr. Cassano for teaching me about atmospheric dynamics and Dr. Knipp for showing me how complicated and relatively not well understood is Earth's aerospace environment. I also thank Dr. Forbes for the help and thoughtful comments about my work.

My lab-mate and fellow graduate student McArthur Jones Jr., thanks for the countless hours spent discussing atmospheric dynamics, IDL and MATLAB. I would also like to thank Boris Papazov, Simon Tardivel and Aaron Rosengren for the help in the most various topics we discussed. Also, Dr. Loren Chang who helped me transition to this research group and

had a lot of patience in the beginning to explain what it takes to be a graduate student at CU, and also for showing me what I needed in order to get started in this research project.

To my best friend Vanessa Dobuchak, thanks for all the support and the comfort words in the moments I needed them the most.

At last, but not least, for always standing by my side and cheering me up, believing in me, motivating me towards my goals and helping me with whatever was necessary, I thank my parents Paulo Estante and Mayra Estante, and my brother Paulo Roberto Estante. Without you I would have never accomplished anything, I will be forever grateful for all the unique opportunities you provided me.

Contents

Chapter

Tables

Table

Figures

Figure

Chapter 1

INTRODUCTION

This thesis is an investigation of the possible mechanisms that drive the non-migrating semidiurnal tide over the South Pole. It has been proposed that it is created due to non-linear interactions of other tides and waves in the northern hemisphere.

1.1 Earth's Aerospace Environment

Earth's aerospace environment is extremely active, dynamic and non-linear. It reacts to inputs from the ground (such as volcanoes, oceans, etc) and space (solar and space radiation, meteors, etc) [Roble et al, 1986]. Figure 1.1 depicts the layers of the atmosphere and this system. The disturbances caused by all the different forcing elements propagate through the atmosphere due to the global circulation, which affects the pressure, density, winds and temperature distributions across the atmosphere. Due to this circulation, the dynamics of our region of interest, the mesosphere and lower thermosphere (ranging from 50 - 120km in altitude, also simply referred to as the MLT) changes rapidly, making it highly variable. This short-term variability of the waves in this region is the focus of this project. We are interested in studying the MLT because it is the region that divides the electrically neutral fluid of the lower thermosphere and the strongly ionized upper thermosphere. The major driving mechanism of this variability in the MLT is wave activity. Planetary waves and atmospheric tides, which are global scale oscillations, transport energy and momentum (and therefore mass) through the atmosphere. Gravity waves also have a very important because

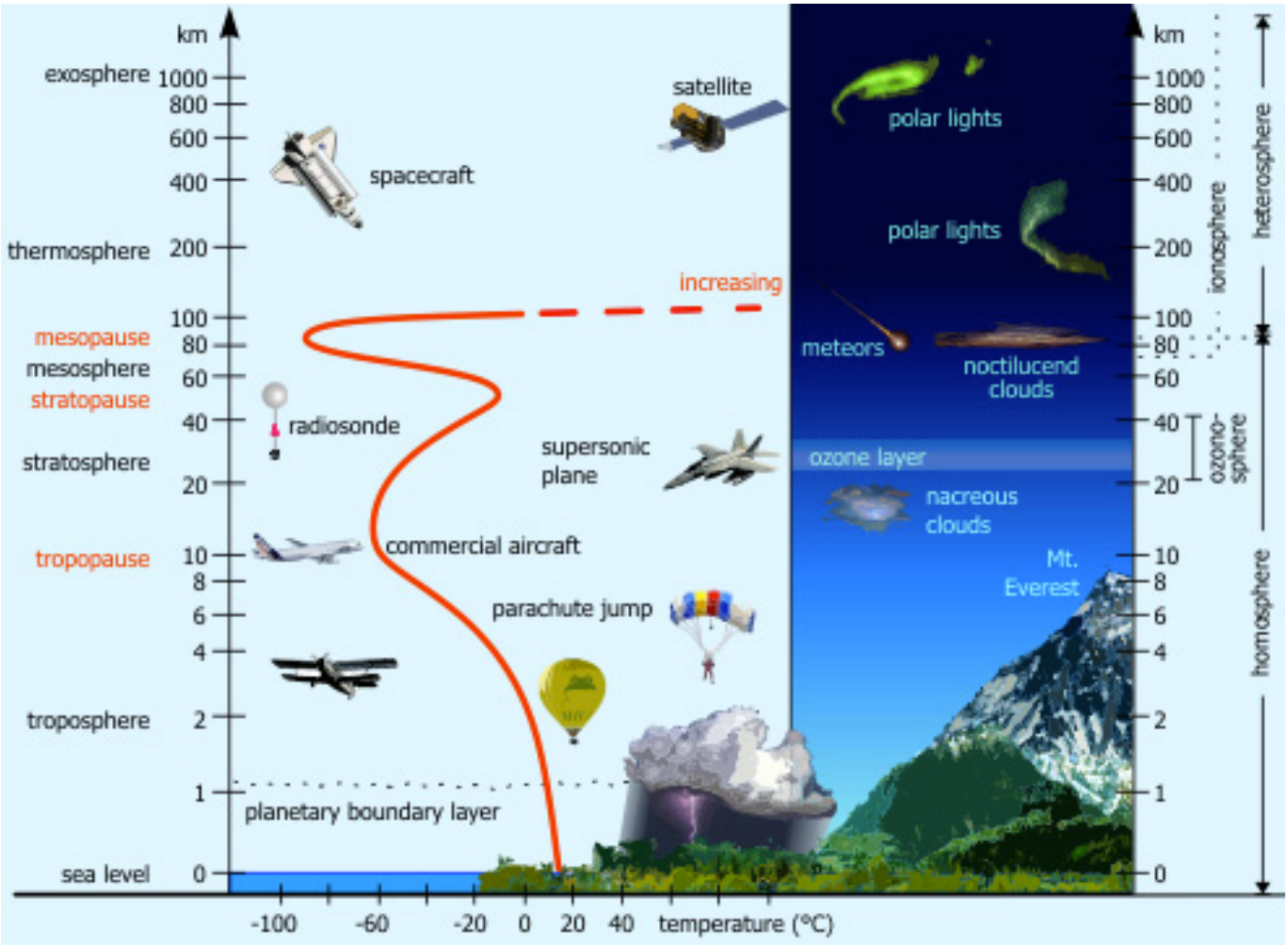

Figure 1.1: Structure of the layers of the atmosphere [The Ozone Hole, 2012]. The MLT, our region of interest, ranges from approximately 50km to 120km and includes the region around 90km where meteors usually break and leave an ionized trail, which allows us to obtain atmospheric tide information over the South Pole.

even though their dimensions are not as big as the other waves and tides, they are a major energy transport mechanism [Ebel, 1984].

This mass circulation can increase or decrease the density of the upper atmosphere. It can increase the mean molecular mass of the thermosphere, by depletion of atomic oxygen which causes a contraction of the thermosphere. This contraction then can cause a decrease in the neutral density that directly affects spacecraft drag in low Earth orbit (LEO) [Qian et al, 2009]. If this drag increases considerably, it will have various implications. First the spacecraft will loose altitude, which causes it to speed up and creates a problem for tracking; the spacecraft will not be where an orbit propagator would predict. This also accelerates the orbit decay process, because the spacecraft looses altitude with increased. Such variability of the ionosphere also has other implications. The waves that penetrate the ionosphere can modify the zonal structure of electron densities in the dynamo electric fields [Immel et al, 2006]. This can impact microwave communications and GPS accuracy.

1.2 Atmospheric Tides

Atmospheric tides are global scale oscillations in density, pressure, temperature and winds (zonal and meridional) with periods that are sub-harmonics of a solar day. The major forcing mechanism of the atmospheric tides is solar heating of the troposphere and stratosphere. The tides can either be vertically propagating or trapped (evanescent). The propagating disturbances originate in the lower layers of the atmosphere and propagate upwards towards lower densities [Forbes, 1995]. Due to conservation of energy, these tides grow in amplitude as atmospheric density decreases. This is the case until the waves reach an altitude around 90-100km, in the MLT. At this height, these tidal disturbances either break or dissipate due to increasing molecular diffusion.

The most significant tides are the terdiurnal (period of 8 hours), semidiurnal (period of 12 hours) and diurnal (period of 24 hours) components. The focus of this analysis is on the semidiurnal component. The tides can be classified not only by their periodicity, but also

Table 1.1: Comparison between migrating and non-migrating tides.

	Migrating Tides	Non-migrating Tides
Propagation	Sun-synchronous Westward	Non Sun-synchronous Westward, Eastward or Standing
Zonal wavenumber	1/Period (days)	Any (typically -6 to +6)
Forcing	Radiative	Latent heat Interaction with Planetary Waves

if they are migrating or non-migrating (Table 1.1). Migrating tides are so called since they follow the Sun's apparent motion in the sky, and are therefore propagate westward relative to an Earth-fixed observer. Non-migrating tides are not sun-synchronous and can propagate either eastward or westward or not propagate at all, being referred to as a standing.

In the MLT, the strongest component is the migrating diurnal tide with a zonal wavenumber of 1. In this study, the non-migrating semidiurnal tide with zonal wavenumber of 1 is considered. This component can be determined by the South Pole meteor radar (SPMR) which will be discussed on section 3.1.

1.3 Planetary (Rossby) Waves

Planetary waves have a global planetary structure but with greater periods (2, 4, 5, 10 days). Rossby waves are planetary waves that propagate westward. They can also be stationary (fixed to the Earth). Although these waves are referred to as stationary waves, it means they have a fix longitudinal structure, but can actually move in latitude and altitude. The modeling of these tides and waves is based on the classical tidal theory, which will be further discussed on chapter 2.

In this investigation a specific category of planetary waves will be analyzed, the stationary planetary waves. The stationary planetary waves are a very notable feature of the

winter stratosphere in the northern hemisphere because it is a stationary global scale disturbance that is superimposed on the circumpolar westerly wind [Matsuno, 1970]. These waves are coupled with events in the troposphere, which are ultimately linked to the dynamics occurring near the surface of the Earth. Due to this coupling, the stationary planetary waves are mainly forced by variations in the topography and geographical asymmetries in the land/water distribution, which directly affects the energy distribution [Chen, 2003].

1.4 NASA's Modern Era Retrospective Analysis for Research and Applications (MERRA)

The Modern Era Retrospective Analysis for Research and Applications (MERRA) is NASA's approach to a reanalysis model, which uses the newest version of the Goddard Earth Observing System Data Assimilation System Version 5 (GEOS-5) atmospheric general circulation model (AGCM) that is based on finite-volume dynamics [Rienecker, et al. 2008]. GEOS-5 uses a three-dimension variational data assimilation (3DVAR) analysis algorithm, which is based on the Gridpoint Statistical Interpolation Scheme [Rienecker, et al. 2011]. This model takes more than 10^6 data points as input for each iteration, which come from instruments aboard many NASA missions as well as data from ground based instruments, radiosondes, airborne instruments, etc.

It has a horizontal resolution of 1.25 degrees, temporal resolution of 3 hours and 42 vertical levels ranging from 1000hPa to 0.1hPa (approximately 64km). In the 10-0.1hPa interval there are 12 pressure levels.

1.5 South Pole meteor radar (SPMR)

The South Pole meteor radar (SPMR) was installed at the Amundsen-Scott South Pole station in 2001 and became fully operational in 2002. This is a VHF radar that has operated almost continuously since then and consists of four yagi antennas, which are switched on a pulse-to-pulse basis, every 3ms. This allows the unbiased determination of the zonal

wavenumber and direction of propagation of the observed perturbations [Portnyagin et al, 1998]. The system will be further discussed on section 3.1.

1.6 NASA's Sounding the Atmosphere by Broadband Emission Radiometry (SABER) Instrument

Thermosphere Ionosphere Mesosphere Energetics and Dynamics (TIMED) is a spacecraft operated by the National Aeronautics and Space Administration (NASA). This spacecraft carries the Sounding the Atmosphere by Broadband Emission Radiometry (SABER) instrument aboard [Remsberg et al, 2003], which is a limb viewing infrared radiometer that measures the thermal structure and composition from the upper troposphere (around 10km) until the thermosphere (around 120km). The instrument is positioned on the cold side of the TIMED spacecraft, which limits its field of view from 52° in one hemisphere to 83° in the opposite hemisphere. Every 60 days (approximately) the latitude ranges switch, as TIMED yaws in order to keep SABER on the cold side (not facing the Sun). The measurements are taken in the infrared spectral range, from 1.27μm to 17μm [Russell, et al. 1999].

1.7 Objectives

The goal of the research presented here is to understand the driving mechanism of the non-migrating semidiurnal tide wavenumber 1 over the South Pole due to a possible non-linear wave coupling with the stationary planetary waves in the northern winter hemisphere.

In order to achieve this, data from a meteor radar at the Amundsen-Scott South Pole Station is used, along with data from MERRA, which was validated by comparing it to measurements from the SABER instrument on NASA's TIMED spacecraft.

1.8 Thesis Outline

In Chapter 2, the classical tidal theory is discussed. The relevant equations are presented and explored in order to clarify the driving physics of this mechanism. In this chapter

the methodology of the analysis is also discussed.

In Chapter 3, the data sources are further discussed. The validation of the MERRA model is shown and the limitations of all the data sources are studied.

Chapter 4 brings the results of the analysis of the non-linear wave-wave interactions. Chapter 5 further discusses the results obtained, and Chapter 6 brings a conclusion of the study performed and goals for future work.

In the appendix one can find information on the nomenclature, list of acronyms and additional data.

Chapter 2

BACKGROUND

In this chapter, one can find the development and discussion of the physics behind the atmospheric tides, as well as the driving mechanisms of the response to tidal disturbances.

2.1 Tidal Theory

Laplace [1825] formulated current tidal theory where he described a set of linear partial differential equations to explain a two-dimensional barotropic flow (when pressure only depends on density and vice versa).

2.1.1 Primitive equations

Chapman and Lindzen derived a solution for the atmospheric tides using the primitive equations, by assuming the atmosphere is a layer of inviscid fluid on a rotating sphere [Chapman and Lindzen, 1970]. Based on this, the atmosphere can be treated as an invariant longitudinal zonal mean structure, which is modulated by temporal and spatial perturbations, as follows:

$$\{u, v, \Phi\} = \{\bar{u}, \bar{v}, \bar{\Phi}\} + \sum \{u', v', \Phi'\} \tag{2.1}$$

Equation 2.1 shows that the atmospheric fields can be split and treated as a mean, background field superimposed by perturbations.

The primitive equations consist of a system of 4 coupled, non-linear differential equations that describe an atmosphere which behaves like an ideal gas. The four equations are the two horizontal Navier-Stokes momentum equations, the continuity equation and the thermodynamic equation, as follows:

$$\frac{\vec{D}u}{Dt} = fv - \frac{1}{a\cos\phi}\frac{\partial\Phi}{\partial\lambda} - F_x \tag{2.2}$$

$$\frac{\vec{D}v}{Dt} = -fu - \frac{1}{a}\frac{\partial\Phi}{\partial\lambda} - F_y \tag{2.3}$$

$$\frac{1}{a\cos\phi}\frac{\partial u}{\partial\lambda} + \frac{1}{a\cos\phi}\frac{\partial}{\partial\phi}(v\cos\phi) + \frac{1}{\rho_0}\frac{\partial(\rho_0 w)}{\partial z} = 0 \tag{2.4}$$

$$\frac{\vec{D}\Phi_z}{Dt} + \frac{v}{a}\frac{\partial\Phi_z}{\partial\phi} + w\frac{\partial\Phi_z}{\partial z} + wN^2 = \frac{\kappa}{H}J - F_\Phi \tag{2.5}$$

A list of all the variables involved in these equations can be found on Appendix A. It is important to note that f is the Coriolis parameter, given by:

$$f = 2\Omega\sin\phi \tag{2.6}$$

Based on the assumption that equations 2.2 - 2.5 describe an atmosphere that behaves like an ideal gas, horizontally stratified and that the pressure is hydrostatic, it is known that:

$$\frac{\partial p_0}{\partial z} = -\rho_0 g \tag{2.7}$$

$$p_0 = \rho_0 R T_S \tag{2.8}$$

And the scale height H can be calculated by:

$$H = \frac{RT}{g} \tag{2.9}$$

Another important remark is the material derivative, which introduces the non-linearities in the system by advection of momentum and energy, is defined as:

$$\frac{\vec{D}}{Dt} = \frac{\partial}{\partial t} + (\bar{u} + u')\frac{\partial}{\partial x} + (\bar{v} + v')\frac{\partial}{\partial v} + (\bar{w} + w')\frac{\partial}{\partial z} \tag{2.10}$$

By substituting equations 2.1 and 2.10 into equations 2.2 - 2.5, a system of coupled non-linear equations arises. A few assumptions can be made: zonal and meridional mean winds are set to zero, the heating term (J) can be decomposed into a mean and perturbation, with the mean also set to zero. Another assumption is that perturbations are small enough so that terms containing quadratic perturbations can be neglected. External forces are also set to zero. These assumptions are valid assumptions, however they do affect the accuracy of the calculations. The system of linearized equations then becomes:

$$\frac{\partial u'}{\partial t} = fv' - \frac{1}{a\cos\phi}\frac{\partial \Phi'}{\partial \lambda} \tag{2.11}$$

$$\frac{\partial v'}{\partial t} = fu' - \frac{1}{a}\frac{\partial \Phi'}{\partial \phi} \tag{2.12}$$

$$\frac{1}{a\cos\phi}\frac{\partial u'}{\partial \lambda} + \frac{1}{a\cos\phi}\frac{\partial}{\partial \phi}(v'\cos\phi) + \frac{1}{\rho_0}\frac{\partial \rho_0 w'}{\partial z} = 0 \tag{2.13}$$

$$\frac{\partial \Phi_z{}'}{\partial t} + w'N^2 = \frac{\kappa J'}{H} \tag{2.14}$$

For a list of the variables with descriptions please refer to Appendix A.

2.1.2 Classical solution

Equations 2.11 - 2.14 represent the linearized equations. The horizontal and temporal dependences of these can also be decomposed from the vertical dependence through separation of variables. By doing so, the tidal perturbations can be defined as [Chang, 2010]:

$$u'(\lambda,\phi,z,t) = \sum_{\sigma}\sum_{s}\sum_{n} U_n^{\sigma,s}(\phi)G_n(z)e^{i(s\lambda-\sigma\Omega t)} \tag{2.15}$$

$$v'(\lambda,\phi,z,t) = \sum_{\sigma}\sum_{s}\sum_{n} V_n^{\sigma,s}(\phi)G_n(z)e^{i(s\lambda-\sigma\Omega t)} \tag{2.16}$$

$$\Phi'(\lambda,\phi,z,t) = \sum_{\sigma}\sum_{s}\sum_{n} \Theta_n^{\sigma,s}(\phi)G_n(z)e^{i(s\lambda-\sigma\Omega t)} \tag{2.17}$$

$$J'(\lambda,\phi,z,t) = \sum_{\sigma}\sum_{s}\sum_{n} \Theta_n^{\sigma,s}(\phi)J_n(z)e^{i(s\lambda-\sigma\Omega t)} \tag{2.18}$$

In these equations, s is the zonal wavenumber and n is the meridional index. If these equations are being solved for a specific tidal component, the perturbations are expressed as:

$$\hat{u}(\phi,z) = \sum_{n} U_n^{\sigma,s}(\phi)G_n(z) \tag{2.19}$$

$$\hat{v}(\phi,z) = \sum_{n} V_n^{\sigma,s}(\phi)G_n(z) \tag{2.20}$$

$$\hat{\Phi}(\phi,z) = \sum_{n} \Theta_n^{\sigma,s}(\phi)G_n(z) \tag{2.21}$$

By substituting equations 2.15 - 2.18 into the linearized primitive equations (equations 2.11 - 2.14), the solution (equations 2.19 - 2.20) arises in terms of the vertical structure equation, $G_n^{\sigma,s}(s)$. In these equations, U, V and Θ are known as Hough functions, which describe the structure of each Hough mode. These equations, when solved, turn out to be waves that either propagating (periodic) or trapped (evanescent) in the atmosphere. Propagating modes ($n > 0$) can propagate away from their region of excitation, whereas trapped modes ($n < 0$) are confined to the regions near where they were excited. As previously discussed, atmospheric tides have periods that are harmonics of a solar day.

When $\sigma = s$ the tidal disturbance is migrating, or Sun-synchronous. Therefore, the phase velocity of the migrating tides equals the rate of rotation of the Earth, Ω.

The latitudinal structure of tidal disturbances can be found by solving Laplace's tidal equation:

$$L\Theta_n^{\sigma,s} + \epsilon_n^{\sigma,s}\Theta_n^{\sigma,s} = 0 \tag{2.22}$$

The solution for this equation is given by the Hough functions $\Theta_n^{\sigma,s}$, which are the eigenvalues of Laplace's equation. Each Hough mode is a function of latitude and is expressed by an infinite sum of associated Legendre polynomials. The wind expansion functions are defined as [Hough, 1897, 1898]:

$$U_n^{\sigma,s}(\phi) = \frac{1}{2\Omega a(\sigma^2 - \sin^2\phi)}\left[\frac{\sigma s}{\cos\phi} + \sin\phi\frac{d}{d\phi}\right]\Theta_n^{\sigma,s}(\phi) \tag{2.23}$$

$$V_n^{\sigma,s}(\phi) = \frac{-i}{2\Omega a(\sigma^2 - \sin^2\phi)}\left[s\tan\phi + \sigma\frac{d}{d\phi}\right]\Theta_n^{\sigma,s}(\phi) \tag{2.24}$$

2.2 Non-linear Wave-Wave Interaction

As proposed by Teitelbaum and Vial [1991], planetary waves and atmospheric tides can interact through non-linear mechanisms and transfer energy to new tides and waves that are result from this interaction. In this process, the starting waves are called the "parent waves" and the waves that are created from their interaction are known as "child waves". This interaction arises from the non-linear advective terms of the primitive equations, due to the material derivative of the atmospheric fields.

If two waves of wavenumber/frequency pairs (s_1,ω_1) and (s_2,ω_2) are given by:

$$X = \cos(\omega_1 t + s_1\lambda) + \cos(\omega_2 t + s_2\lambda) \tag{2.25}$$

Their non-linear interaction yields:

$$X^2 = 1+\frac{1}{2}[\cos(2\omega_1 t+2s_1\lambda)+\cos(2\omega_2 t+2s_2\lambda)]+\cos[(\omega_1+\omega_2)t+(s_1+s_2)\lambda]-\cos[(\omega_1-\omega_2)t+(s_1-s_2)\lambda] \tag{2.26}$$

It can be seen that the child waves have a wavenumber/frequency dependence of the form $(2s_1,2\omega_1)$, $(2s_2,2\omega_2)$, $(s_1+s_2,\omega_1+\omega_2)$ and $(s_1-s_2,\omega_1-\omega_2)$. If the original waves were a stationary planetary wave with s=1 and a semidiurnal tide with s=2, their interaction would yield a semidiurnal s=1 tide, a semidiurnal s=3 tide, a quatradiurnal s=4 tide and a stationary planetary wave with s=2. These child waves, in turn, could interact with one another and other modal components present in the atmosphere to generate more oscillations, as it can be seen in Figure 2.1.

Angelats i Coll and Forbes [2002] performed a simulation using a three-dimensional nonlinear spectral model to study the non-linear wave-wave interaction and concluded that a non-migrating semidiurnal s=1 tide and a non-migrating semidiurnal s=3 tide result from the interaction between a stationary planetary wave s=1 and a migrating semidiurnal s=2 tide.

Another interesting analysis of non-linear interaction was performed by Smith et al [2007] by investigating the variability of the semidiurnal tides in the northern hemisphere induce by planetary wave activity in the southern hemisphere. They were not able to unambiguously determine the structure of the non-migrating semidiurnal s=1 tide due to the configuration of their radar, but they still concluded that the tide showed a strong correlation with the planetary wave s=1.

2.3 Structure and Dynamics of the Middle Atmosphere

The troposphere, which is the region from the surface of the Earth up to approximately 10km, contains more than 85% of the mass and virtually all water in the atmosphere. The troposphere is the layer of the atmosphere that contributes the most with the dynamics of

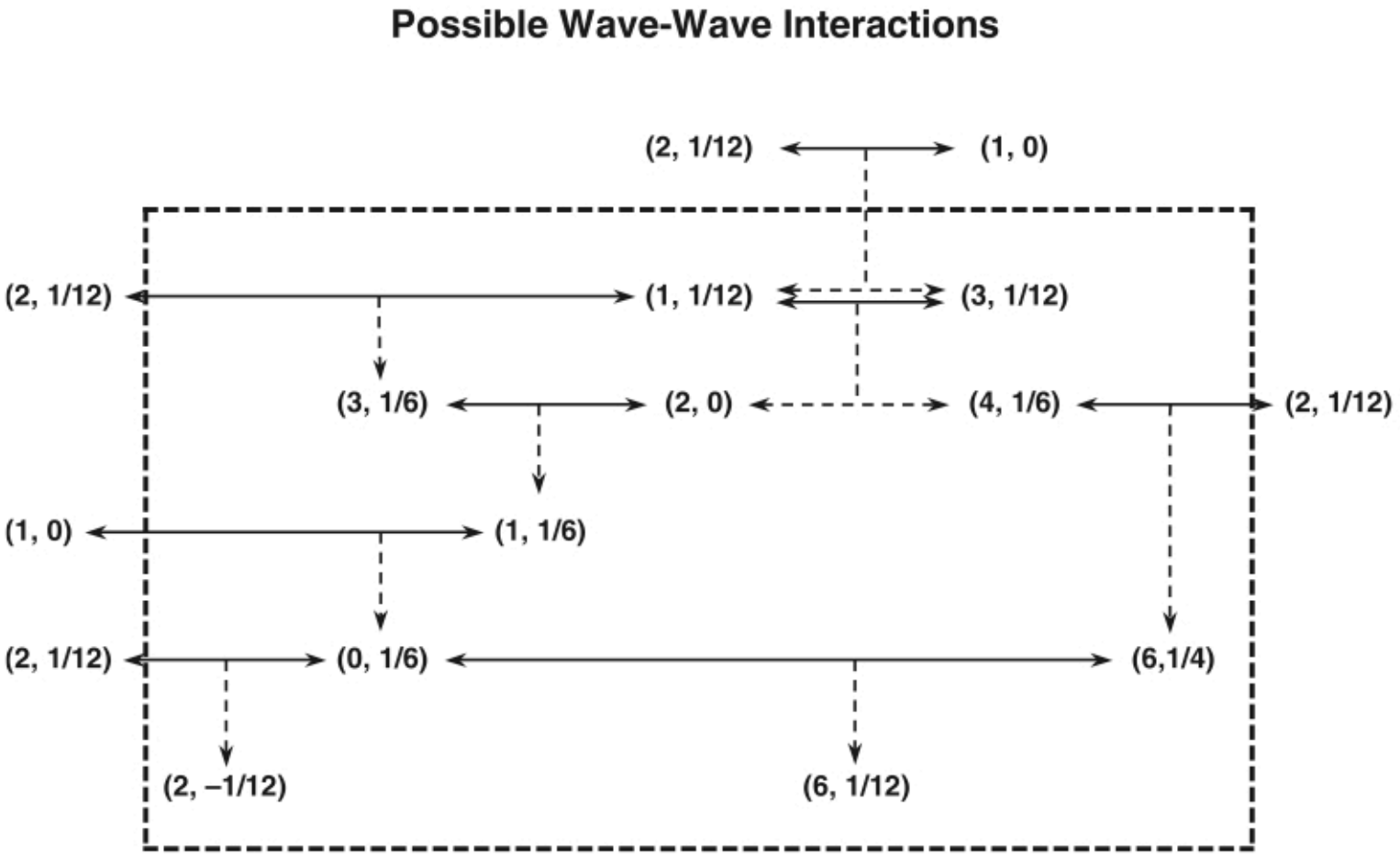

Figure 2.1: This graph shows possible non-linear wave-wave interactions. Each wave is shown by a zonal wavenumber/frequency pair. Solid lines show interactions between waves, while dashed lines denote their child waves [Angelats i Coll and Forbes, 2002].

climate variability and weather disturbances.

However, the troposphere and the middle atmosphere (from the tropopause to the mesopause, roughly the 10-90km region) are linked through radiative and dynamical processes, such as the upward propagation of waves which transport energy (and mass) away from the troposphere and the exchange of substances that are part of the photochemistry of the ozone layer (between 20 and 30km, inside the lower stratosphere). The ozone layer is responsible for absorbing 97-99% of the solar ultraviolet radiation.

The dynamics of the stratosphere are very complex. It loses energy through infrared radiative cooling, but also acquires energy by radiative heating due to the absorption of solar ultraviolet radiation by ozone. The temperature in this layer increases up to around 50km, in the stratopause. Above this level, the temperature starts to decrease due to reduced solar heating of ozone.

2.4 Variability

The atmosphere as a whole is extremely dynamical and non-linear. It is highly variable due to many factors, such as heterogenous surface terrain and large portions of water on the surface of the Earth which causes a differential heating on the surface. It also varies due to Earth's rotation and tilt angle with respect to the equatorial plane, with different parts of the planet receiving different amounts of solar radiation during the day. The dynamics of the oceans and atmosphere is also affected by lunar attraction, but to a lesser degree.

In the next sections two major phenomena that occur in the atmosphere will be discussed in more details: Sudden stratospheric warmings and the quasi-biennial oscillation.

2.4.1 Sudden Stratospheric Warming

In the stratosphere the mean flow is westerly during the winter and easterly during the summer. The winter stratosphere is characterized by a large vortex region that interacts with the winter mean flow. Sudden stratospheric warmings (SSW) occur when the polar

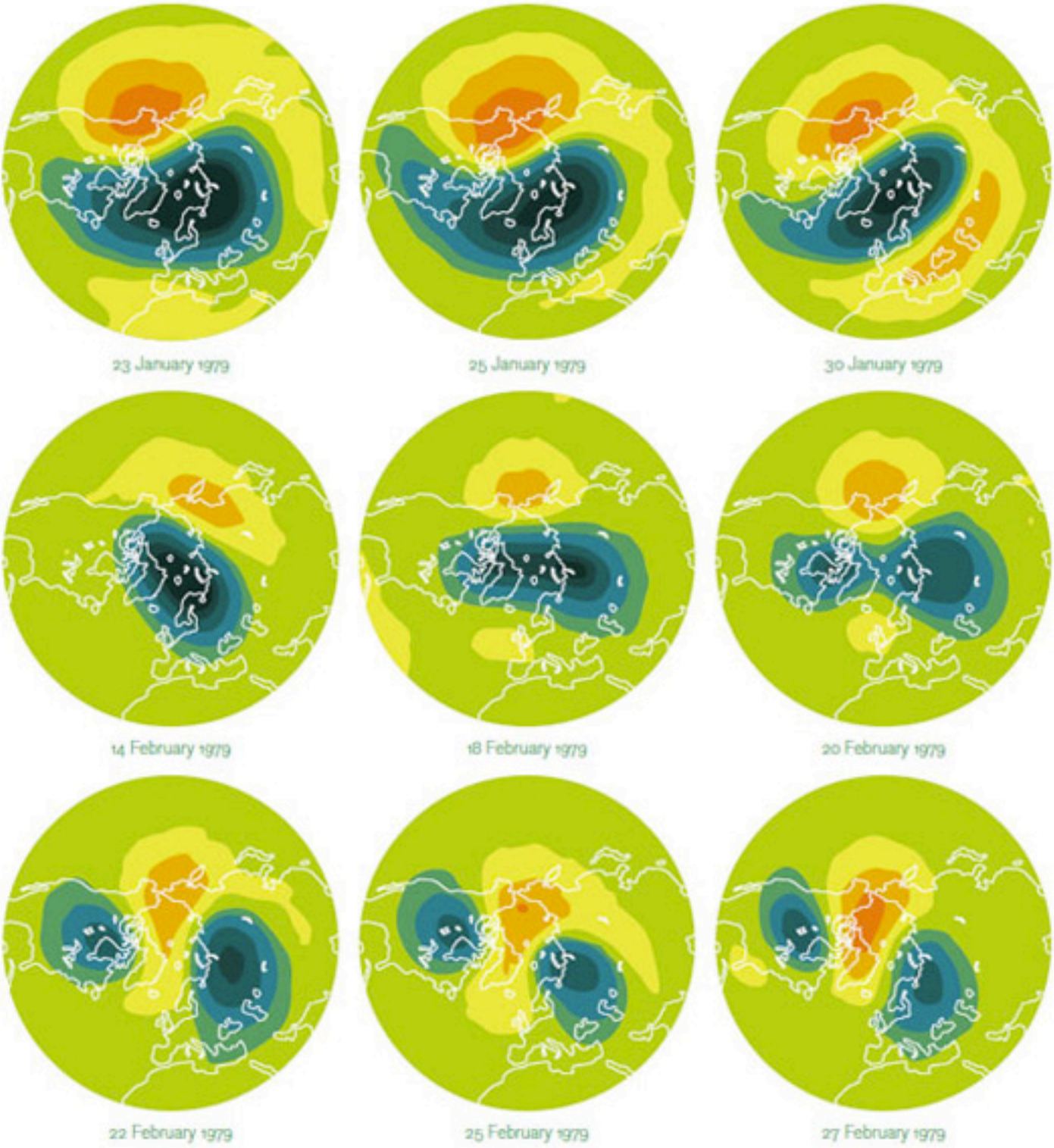

Figure 2.2: Polar vortex break-down during the 1979 Sudden Stratospheric Warming event. The low pressure (blue) area is distorted and ends up splitting due to the high pressure (red) region moving in [Charlton and Polvani, 2007].

vortex of westerly (or easterly) winds in the winter hemisphere quickly decelerates or even reverses direction, along with an increase of stratospheric temperature. SSW events can be subdivided into three main categories: Major, minor and final [Schoeberl, 1978]. A list of recent SSW events until 2009 can be seen on Table 2.1.

Figure 2.2 shows a coverage of the 1979 SSW event. This was the first SSW event observed by a satellite [Charlton and Polvani, 2007]. This figure clearly shows polar vortex displacing from the pole and subsequently splitting.

2.4.1.1 Major SSW

SSW events are considered major when the westerly winds at 10hPa and 60N reverse, becoming easterly. During these events, the polar vortex completely disrupts and is either split into two smaller vortices (also called daughter vortices), or displaced from its usual position over the pole. During a major SSW event the stratosphere can warm up by as much as 65K due to primarily increased eddy transport of heat from lower latitudes through vertical flow of energy carried by planetary waves [Schoeberl, 1978].

2.4.1.2 Minor SSW

Minor SSW events are classified similarly to major events, but less intense. In minor events the westerly winds only slow down, but do not actually reverse. Since there is not a change in the direction of the winds, the polar vortex does not break down. During a minor SSW event the stratosphere can warm up by as much as 25K [Schoeberl, 1978].

2.4.1.3 Final SSW

Final SSW events are named as such because they occur when the polar vortex winds reverse direction about the time the stratosphere enters the summer easterly phase, therefore the vortex does not revert back to a westerly phase until the next winter because there is not sufficient meridional gradient in solar heating to restore the polar night jet, allowing the the zonally averaged circulation to relax to an equinoctial instead of a solstitial circulation pattern [Schoeberl, 1978].

2.4.2 Quasi-Biennial Oscillation

The quasi-biennial oscillation (QBO) is a quasi-periodic oscillation (with a period of 28-29 months) between the westerly and easterly equatorial zonal winds in the tropical stratosphere. The QBO dominates the variability of the equatorial stratosphere. The alternating winds develop at the top of the lower stratosphere and propagate downwards towards the tropical tropopause at a rate of about 1km per month. At higher altitudes of the QBO the easterly winds dominate, whereas in the lower altitudes the westerly winds are more frequent. Also, the amplitude of westerly winds is about twice as strong as the amplitude of the easterly winds (refer to Figure 2.3).

Current studies suggested that the easterly momentum from the QBO comes from Rossby-gravity waves, and the westerly momentum originates from trapped equatorial Kelvin waves. At around 85km the QBO affects the variability of the mesosphere by filtering waves that propagate upwards through the equatorial stratosphere [Baldwin et al., 2001].

The QBO is a very important event in atmospheric dynamics because it impacts other phenomena in the atmosphere. Hurricanes form more often when westerly zonal wind anomalies occur, and less often when the QBO is on its easterly phase. It has also been observed that major SSW events occur mainly during the easterly phase of QBO [Baldwin et al., 2001].

Table 2.1: List of major Northern Hemisphere Sudden Stratospheric Warming events. Adapted from Charlton and Polvani [2006].

No.	Central date	Duration (days)	Emax (ms^{-1})	ΔT_{10} (K)	QBO phase
1	22 Feb 1979	8	-14.6	3.7	W
2	29 Feb 1980	12 (3 + 9)	-6.6	11.5	E
3	6 Feb 1981	1	-0.0	n\a	W
4	4 Dec 1981	2	-2.1	0.1	E
5	24 Feb 1984	40 (5 + 35)	-11.9	11.1	E
6	1 Jan 1985	6	-13.9	13.0	E
7	23 Jan 1987	31 (30 + 1)	-20.9	10.2	E
8	8 Dec 1987	9	-17.7	14.1	W
9	14 Mar 1988	11 (3 + 8)	-3.1	11.7	W
10	21 Feb 1989	30 (9 + 21)	-13.5	12.8	W
11	15 Dec 1998	6	-23.7	12.7	E
12	26 Feb 1999	21	-19.3	11.0	E
13	20 Mar 2000	3	-3.3	5.3	W
14	11 Feb 2001	13 (3 + 10)	-12.4	6.3	E
15	31 Dec 2001	3	-1.3	12.9	E
16	18 Jan 2003	1	-1.1	n\a	W
17	7 Jan 2004	9	-13.5	n\a	E
18	21 Jan 2006	26	-24.1	n\a	E
19	24 Feb 2007	4	-8.0	n\a	W
20	22 Feb 2008	7	-13.3	n\a	E
21	14 Mar 2008	7	-5.6	n\a	E
22	24 Jan 2009	30	-28.8	n\a	W

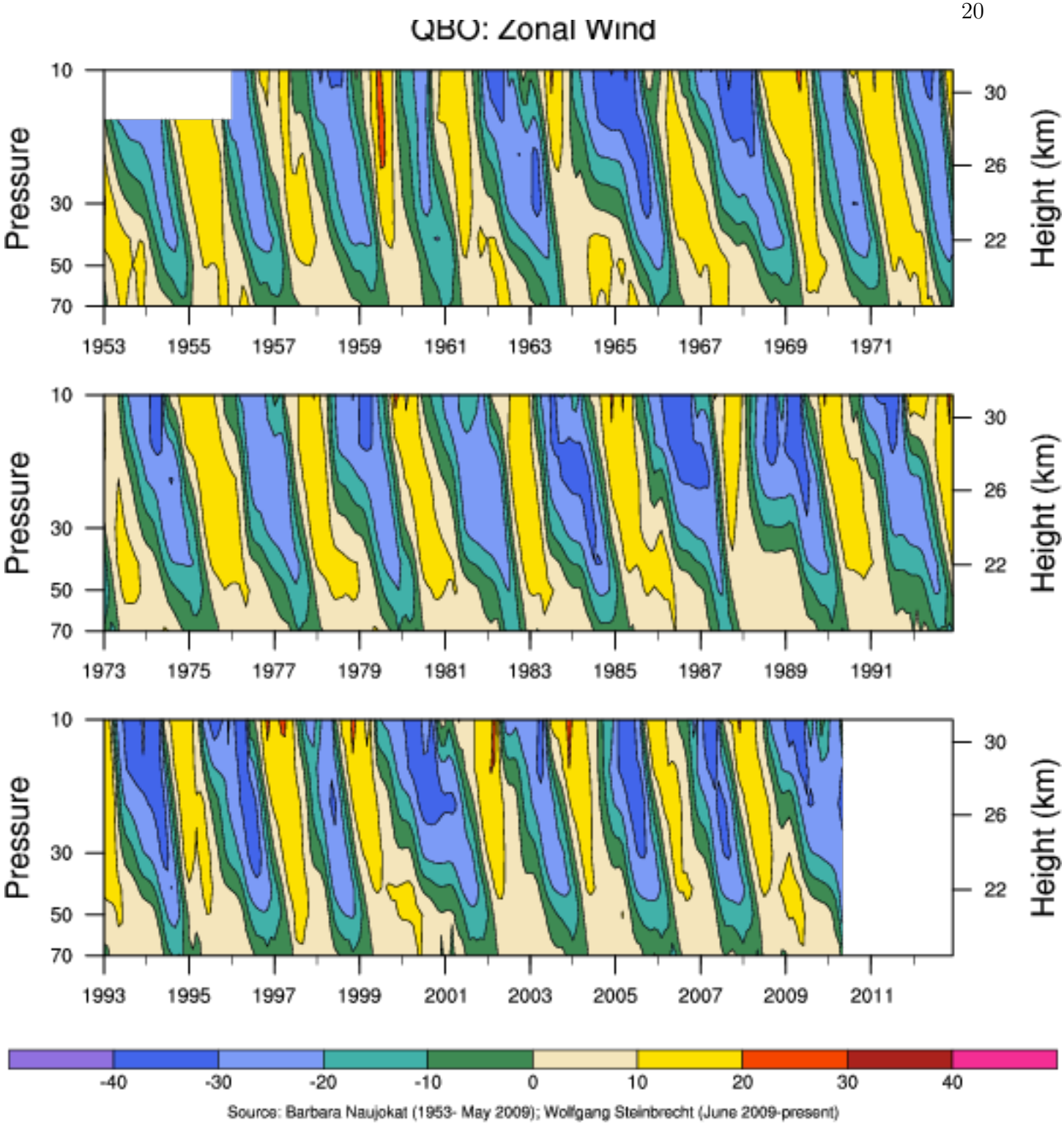

Figure 2.3: Structure of the QBO Zonal Wind from 1953 to 2010 [National Center for Atmospheric Research, 2012]. The westerly phase zonal wind amplitudes are denoted by the green to purple colors, and the easterly phase zonal wind amplitudes are showing by the beige to pink colors.

Chapter 3

DATA SOURCES

3.1 SPMR

The South Pole Meteor Radar (SPMR) is a quasi all-sky VHF meteor radar deployed about 1km from the geographic south pole [Lau, et al. 2006]. It is composed by four six-element yagi antennas mounted horizontally at $\frac{1}{2}$ wavelength above the ground reflector. The four yagi antennas point in the 0°, 90°E, 180° and 90°W directions. The system operates at 46.3 MHz, with a peak output power of 10kW which is modulated by a Gaussian pulse with a 36μs width and a pulse repetition frequency (PRF) of 305 Hz. Based on this configuration and its geographic position the system can unambiguously determine the structure of the non-migrating semidiurnal tides.

The combination of the yagi antennas with the radar controller and the data acquisition system is referred to as the Colorado Obninsk Radar (COBRA) system. The radar operates continuously in a search mode where the antennas are transmitting pulses constantly. The antennas are connected to the receiver through a transmit/receive (T/R) switch. The received data are transmitted to the computer that is processing the data in real-time looking for meteor echoes. When an event triggers an increase in the signal-to-noise ratio (SNR) above a predetermined threshold, the radar switches from search mode to acquisition mode where the system only transmits on the antenna where the signal was detected, and does so until the SNR drops below 3dB. This data are then stored for further processing. An additional data acquisition system is deployed with the radar to add interferometric capabil-

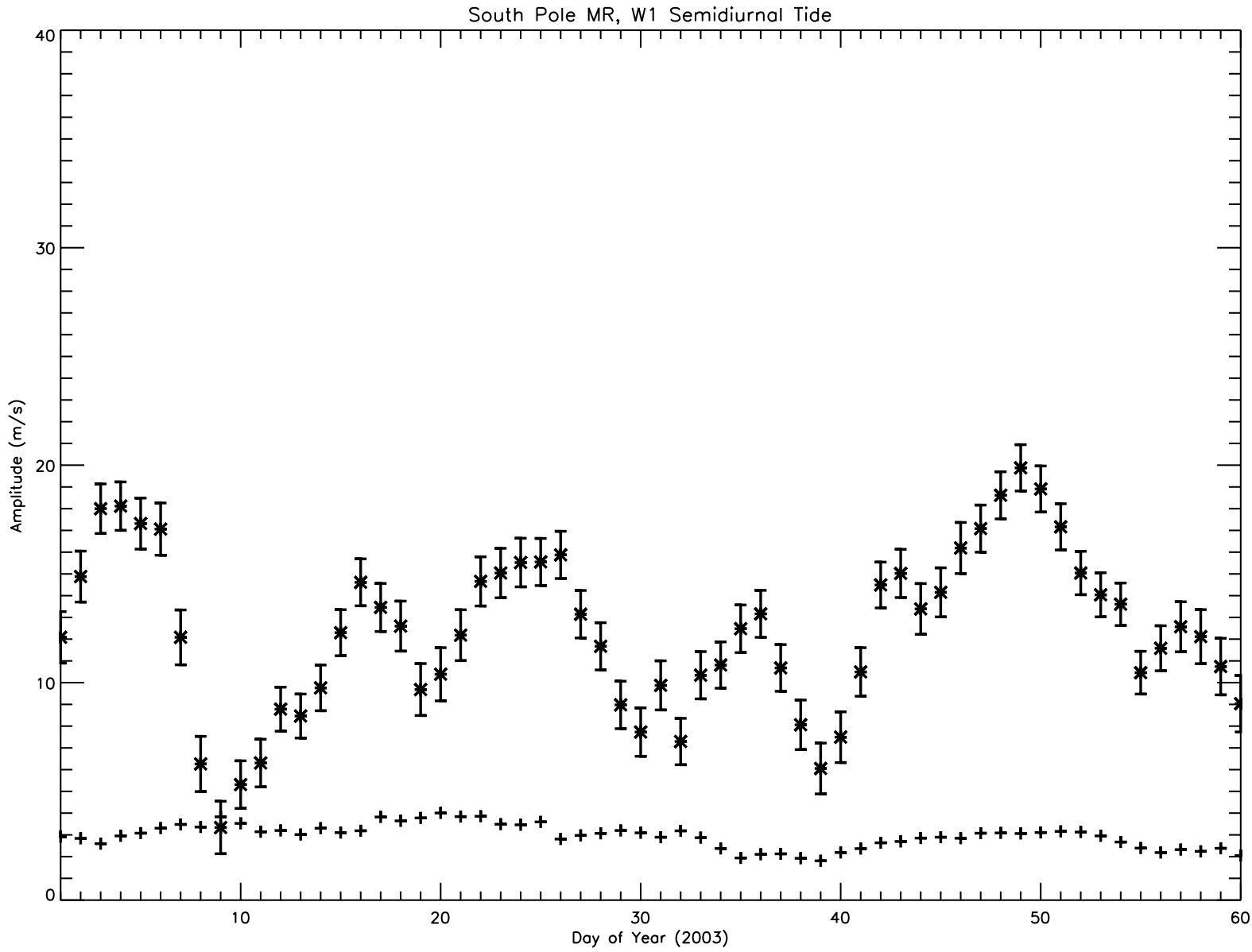

Figure 3.1: SPMR semidiurnal non-migrating s=1 tide data from 2003. The data are given by $*$, with the respective one sigma error bars. The DC component is shown by the $+$ symbols.

ities, this is the Meteor Echo Detection and Collection (MEDAC) system. A more complete description of the COBRA system is given by Janches et al [2004].

With multiple years of observations, the coherent seasonal structure of the large-scale oscillations has been studied. Large westward diurnal and semidiurnal components with zonal wavenumber 1 were observed, as well as non-migrating semidiurnal and migrating diurnal tides. Shorter period (<24 hours) westward propagating waves and longer period (>2 days) eastward propagating waves were also observed at the South Pole. Therefore, SPMR data will be used to extract these components so their variability can be studied. Figured 3.1 shows the structure of the non-migrating semidiurnal tide processed from the data collected by SPMR in 2003.

3.2 MERRA

As previously discussed, MERRA is a global reanalysis dataset that takes as input data collected from various NASA missions and ground based and airborne instruments [Rienecker, et al. 2008]. The objective is to resolve the structure of large-scale atmospheric oscillations in zonal and meridional winds. However, since continuous data of these fields is not available from either ground based instruments or instruments aboard spacecrafts, MERRA was chosen as the data source. In order to insure that the MERRA reanalysis dataset is appropriate for this investigation, it was validated by an analysis done by comparing its temperature fields to temperature data from the SABER instrument. This validation will be discussed on chapter 4. It is important to note that MERRA does not include SABER data in its reanalysis runs.

3.2.1 Reanalysis dataset

MERRA takes as input data from basically all NASA sponsored missions. Its access is open to the public through NASA's Global Modeling and Assimilation Office (GMAO) website [GMAO, 2010].

Although MERRA is a recent effort, the development team was able to process data starting in 1979 and production has already caught up to the present day. The access is very straight forward because the user can select on their website which atmospheric fields are desired (sea-level pressure, surface pressure, surface geopotential, geopotential height, ozone mixing ratio, specific humidity, relative humidity, zonal, meridional and vertical winds, temperature, etc.) and at which pressure levels (42 levels ranging from 1000hPa to 0.1hPa). The user can also select the data to be arranged at 3-hour measurements, or daily averages.

Figure 3.2 shows MERRA horizontal winds, temperature and geopotential height data during Austral summer on 2002-001. These fields are observed from MERRA at 550hPa and one can see the structure of the temperature and geopotential height distributions are fairly similar, with the maximum around the equator and a slightly higher gradient towards the summer hemisphere in the southern latitudes. The latitudinal structure of the zonal winds can also be easily seen from the upper right plot.

3.2.2 Vertical coordinate in pressure levels

As previously noted, MERRA uses pressure levels as its vertical coordinate system. This can be easily converted to a geometric height if a hydrostatic atmosphere is assumed. Also, below 100km of altitude, the atmospheric scale height H, which is the altitude required for the pressure to drop by a factor of e, can be approximated to 7km. MERRA's upper boundary is at 0.1hPa, this translates to approximately 64km in altitude. In this region, the assumption that H is constant is valid and the geometric height can be calculated through:

$$z^* = H \ln\left(\frac{p_0}{p}\right) \tag{3.1}$$

3.3 SABER

Data from the SABER instrument aboard the TIMED spacecraft was used in this research with the sole objective of validating the MERRA dataset. Figure 3.3 shows temper-

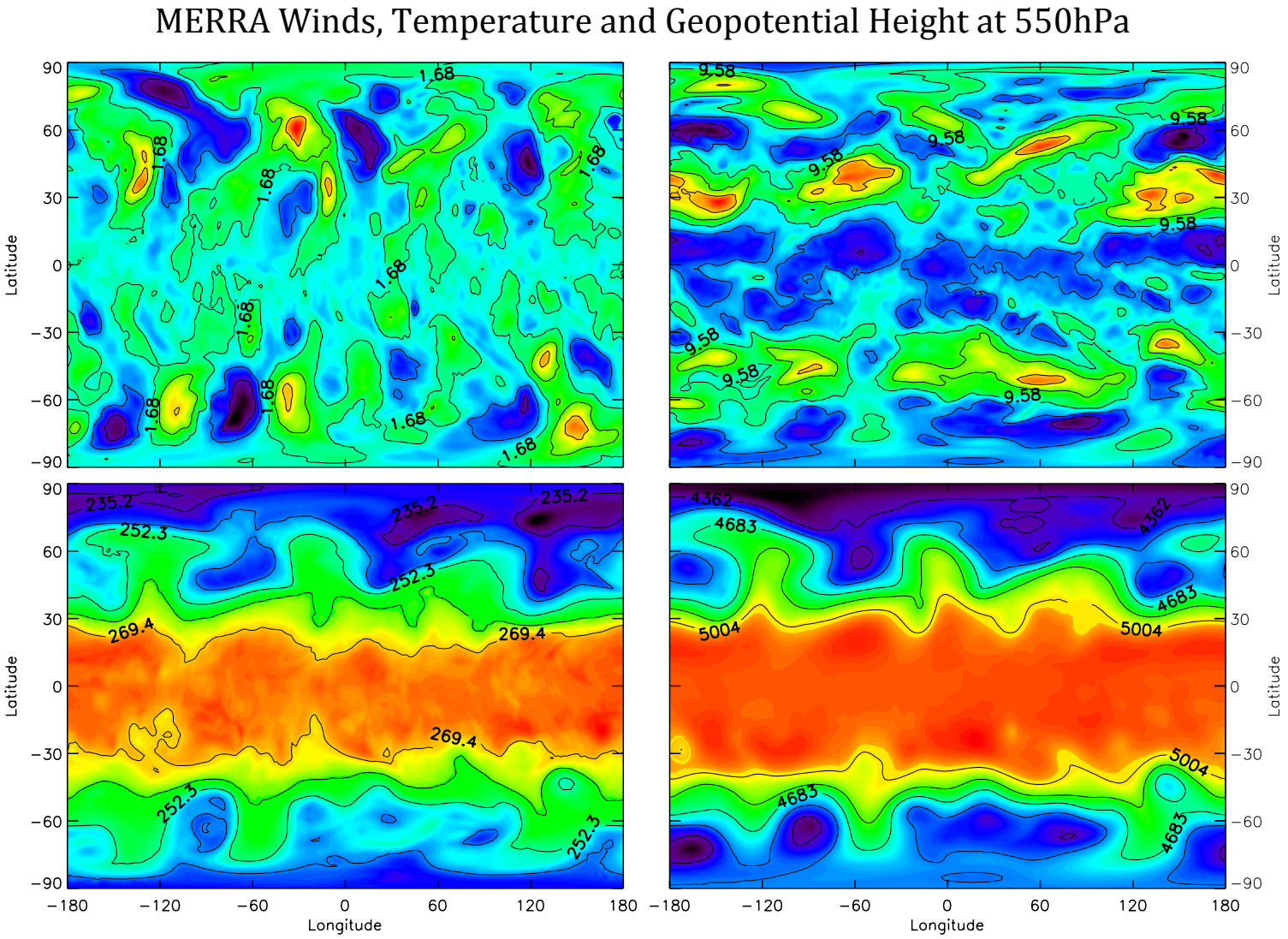

Figure 3.2: MERRA meridional and zonal winds (top left and top right respectively, in m/s), temperature (bottom left, in K) and geopotential height (bottom right, in m) fields at 550hPa on day 2002-001.

ature perturbation data resulting from 30-day least square fits associated with the stationary planetary waves (SPW) 1, 2, 3 and 4.

3.4 Data Analysis Methodology

This section will discuss the mathematical tools used to process the data sets and extract the necessary tidal and wave components from the atmospheric fields.

3.4.1 Least squares fitting

Least squares fitting is used in this study in order to extract components of the atmospheric tides and planetary waves from the database of observed winds, temperature and geopotential. This technique projects the data onto a basis function with a sinusoidal temporal and longitudinal form, with an associated frequency ω, a wavenumber s, wavelength λ and phase ψ as follows:

$$y(t, z, \phi) = A(z, \phi)\cos(s\lambda - \omega t + \psi(z, \phi)) \tag{3.2}$$

$$y(t, z, \phi) = A\cos(\psi)\cos(s\lambda - \omega t) - A\sin(\psi)\sin(s\lambda - \omega t) \tag{3.3}$$

In order to calculate the fit, the perturbations must be expressed as a linear combination in the form of y = Hx. The next step is to apply the least squares fit:

$$\hat{x} = (H^T H)^{-1} H^T \hat{y} \tag{3.4}$$

The data at each point in latitude and altitude is fitted to the sinusoidal basis function with a specific wavenumber and frequency. For a data vector of size n, y becomes a column vector of length nx1 containing the data collected along a latitude circle and H becomes a matrix of size nx2 with each row represented by:

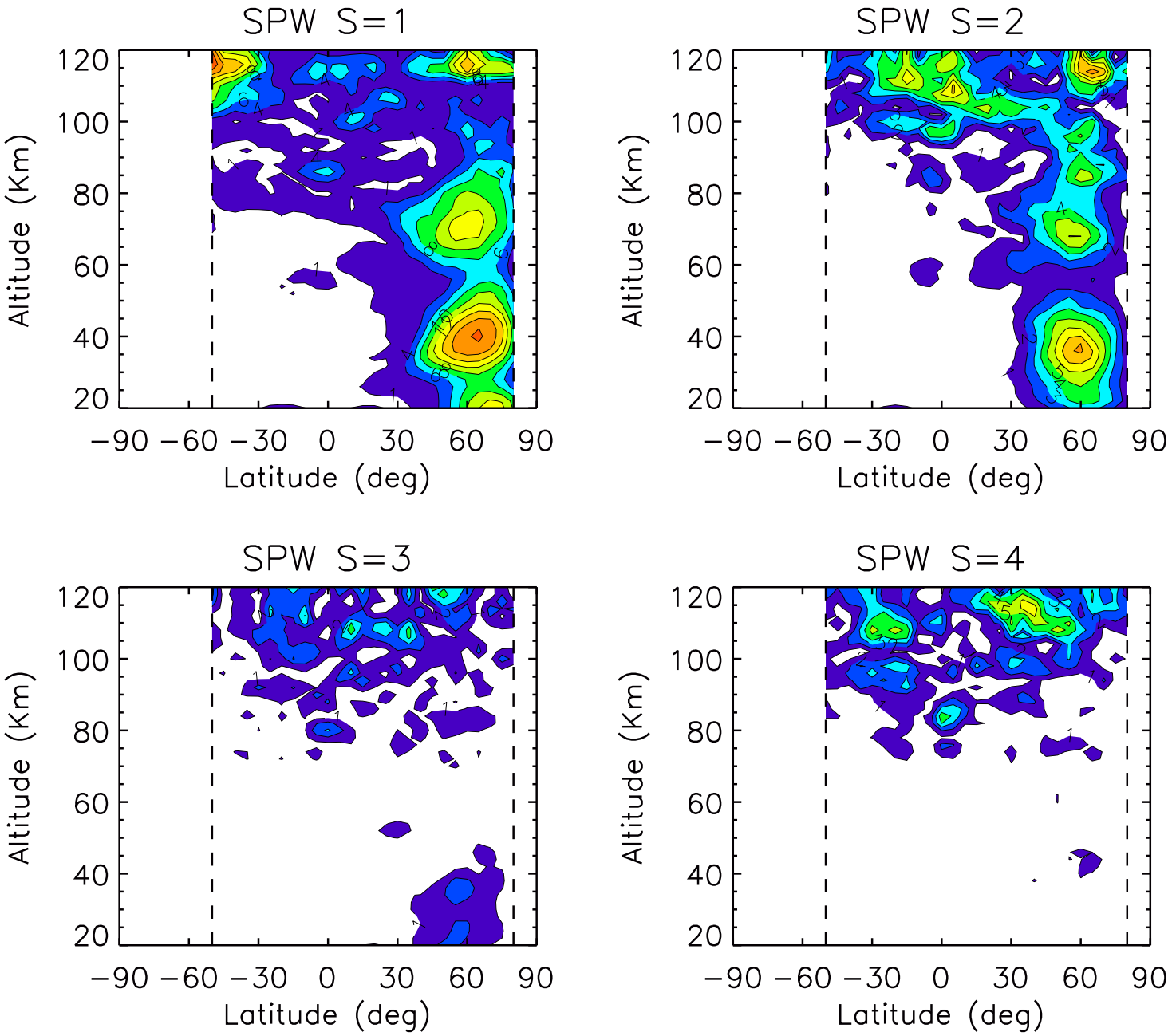

Figure 3.3: SABER temperature perturbation data associated with stationary planetary waves with zonal wavenumber 1,2,3 and 4 on day 050 of year 2002. Data courtesy from Dr. Xiaoli Zhang.

$$H_k = \begin{bmatrix} \cos(s\lambda_k - \omega t_k) & -\sin(s\lambda_k - \omega t_k) \end{bmatrix} \tag{3.5}$$

Where k represents the index of a data value along the latitude circle. Solving this equation yields $\hat{x}$ to be:

$$\hat{x} = \begin{bmatrix} A\cos(\psi) \\ A\sin(\psi) \end{bmatrix} \tag{3.6}$$

From this form, the amplitude and phase dependences can be separated, yielding the following expressions:

$$\hat{A} = \sqrt{(A\cos(\psi))^2 + (A\sin(\psi))^2} \tag{3.7}$$

$$\hat{\psi} = \tan^{-1}\left(\frac{A\sin(\psi)}{A\cos(\psi)}\right) \tag{3.8}$$

This is a very powerful technique because when compared to a Fourier Transform, it has multiple advantages. This method does not require evenly spaced data, and also provides an error estimate and covariance.

3.4.2 Linear correlation

In order to measure the association between two different time series (in the case of this study, the non-migrating semidiurnal tide obtained from SPMR and the planetary wave and tide components extracted from MERRA), the method of linear correlation is used. However, it is also of interest to identify which time series is leading the other, which is done by calculating the linear correlation as function of a lag L. This analysis is also known as a cross correlation, which for a data set of length N is represented by a scalar value r and calculated as follows:

$$r_{xy}(L) = \begin{cases} \dfrac{\sum_{k=0}^{N-|L|-1} (x_{k+|L|} - \bar{x})(y_k - \bar{y})}{\sqrt{\left[\sum_{k=0}^{N-1}(x_k - \bar{x})^2\right]\left[\sum_{k=0}^{N-1}(y_k - \bar{y})^2\right]}} & L < 0 \\ \dfrac{\sum_{k=0}^{N-L-1} (x_k - \bar{x})(y_{k+L} - \bar{y})}{\sqrt{\left[\sum_{k=0}^{N-1}(x_k - \bar{x})^2\right]\left[\sum_{k=0}^{N-1}(y_k - \bar{y})^2\right]}} & L \geq 0 \end{cases} \tag{3.9}$$

A correlation r always lies in the domain -1≤r≤1. It takes the value of 1 when the data points from both time series lie on a perfectly straight line with a positive slope and increase together, which is called a complete positive correlation [Numerical Recipes in C, 1988]. When r takes a value near zero, the series x and y are said to be uncorrelated. The last scenario is for r equal -1, which happens only when both time series lie on a perfect straight line with negative slope, meaning y is decreasing as x increases, which is called a complete negative correlation.

3.4.3 Statistical significance

A correlation value of r is a standard way to summarize the strength of the relationship between two data sets. However, it does not provide a strong argument whether the observed correlation is statistically significant or not. This happens because r is unaware of the individual distributions of the two data sets, implying that there is no concrete way to compute its distribution in the case of a null hypothesis. For example, two data sets can yield a complete positive correlation, but if the time series are extremely short when compared to the complete event under consideration, it can be meaningless and maybe just happened by a coincidence. Therefore, in order to make a stcientifically justified argument about the validity of the computed correlation, one must also provide a statistical significance.

For an event, if the null hypothesis is that the data sets are uncorrelated, large (usually N>20) and have enough convergent moments, it can be inferred that r is distributed normally, with a standard deviation of $\frac{1}{\sqrt{N}}$ and a mean of zero. Therefore, the probability that $|r|$ is larger than the observed value of the null hypothesis is the statistical significance s(r) and can be calculated through:

$$s(r) = erfc\left(\frac{|r|\sqrt{N}}{\sqrt{2}}\right) \tag{3.10}$$

Where N is the number of values used in computing r and erfc is the complementary error function, given by:

$$erfc(x) = 1 - erf(x) = \frac{2}{\sqrt{\pi}}\int_0^x e^{-t^2}dt \tag{3.11}$$

$$erfc(x) = \frac{2}{\sqrt{\pi}}\int_x^\infty e^{-t^2}dt \tag{3.12}$$

A small value of s means that the two distributions are significantly correlated [Numerical Recipes in C, 1988].

Chapter 4

RESULTS

4.1 MERRA Validation

As previously discussed, for this project the MERRA reanalysis dataset was chosen to provide global information of horizontal winds. This is the first time that MERRA has been used for such a study. To gain confidence in the use of MERRA data for this study, MERRA temperature fields were compared to the temperature measurements made by SABER. This data was obtained from a 30-day fit centered on day 2003-030, when SABER had a coverage of high latitudes in the winter hemisphere. The dashed line on the MERRA plots represent the latitudinal extent of SABER measurements on this day.

Figure 4.1 shows a comparison between the SABER and MERRA datasets. This figure shows that both the structure and amplitude of the SPW (stationary planetary waves) from MERRA and SABER match surprisingly well, specially given the fact that MERRA does not ingest SABER data when processing its reanalysis.

4.2 Stationary planetary wave correlation with SPMR

This section will present the results from an analysis that was performed by correlating the non-migrating semidiurnal tide s=1 obtained from SPMR on the summer hemisphere and the stationary planetary wave from MERRA on the winter hemisphere.

This analysis is done by first analyzing the time series of the MERRA fields at different latitudes and the SPMR non-migrating semidiurnal s=1 tide. These time series were then

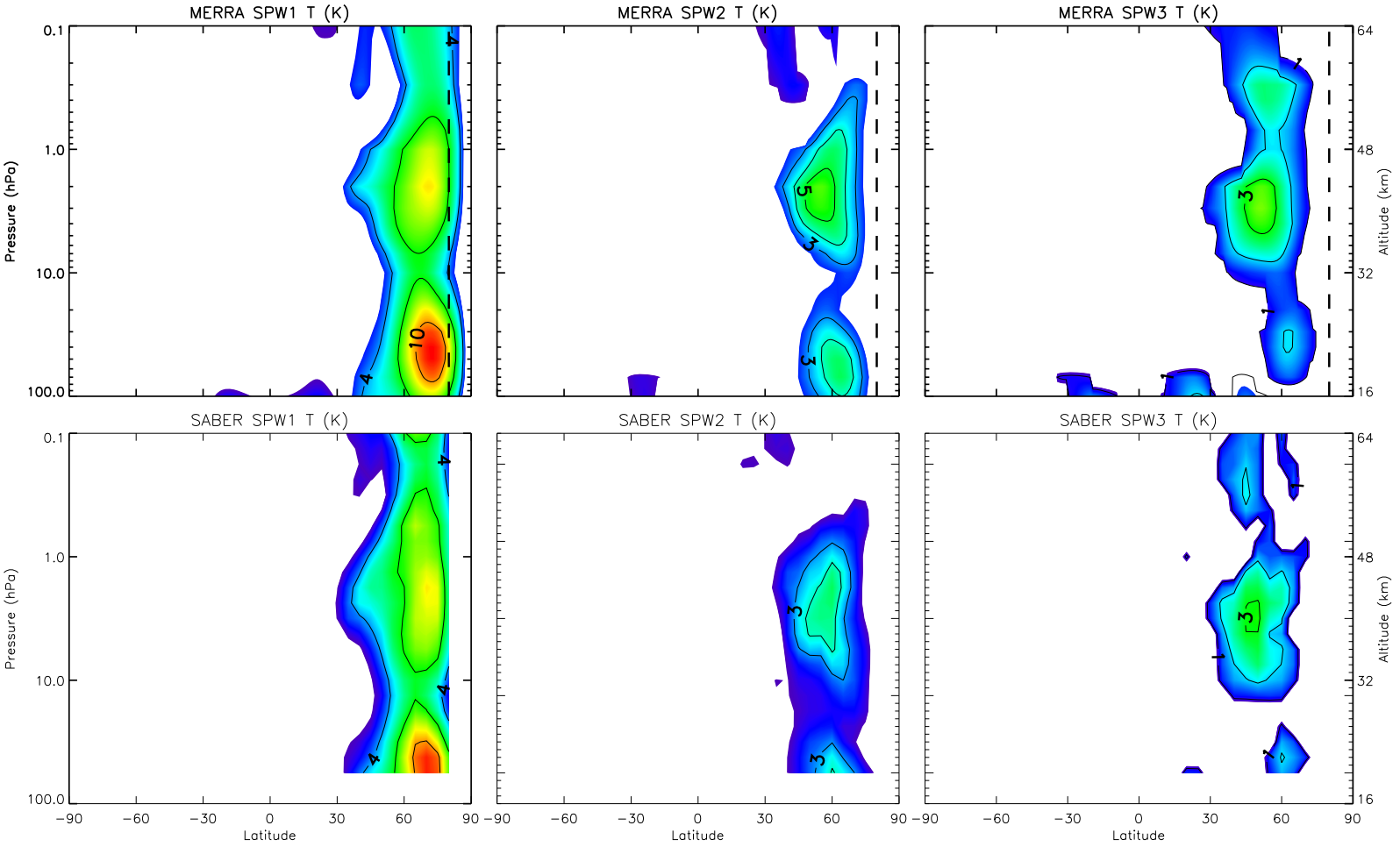

Figure 4.1: Top panes show stationary planetary wave s=1, 2 and 3 temperature structure from MERRA, while bottom panes show the same fields obtained from SABER. Data comes from a 30-day fit centered on 2003-030.

correlated using the procedure discussed on Chapter 3. In the correlation plots, symbols that are filled represent correlation points where the statistical significance is at least 95%. The correlation is calculated as a function of the lag between the two time series. Lag is a feature that arises in the cross correlation and basically means the quantity of steps (in this case the number of days, since each point is a daily average) one dataset is leading or trailing the other. The way this analysis was set up is that a negative lag (e.g. lag=-1) means that SPW leads 12hW1 by one day. A lag of zero means that the events are simultaneous, occurring in the same day.

4.2.1 2002 events

4.2.1.1 2002 - 325-342

One of the events studied in this research occurred near the end of 2002, on days 325-342. Figure 4.2 shows SPW1 and SPW3 temperature and horizontal wind fields from a 5-day fit centered on day 2002-340, which is within the period of interest for this event. It can be seen that both SPW1 and SPW3 have amplitudes above nominal, which might be due to some pre-conditioning for the SSW event that happened around one month later, on mid-January 2003. Figure 4.3 shows data from a 30-day fit of MERRA and SABER SPW1, SPW2 and SPW3 temperature fields also centered on 2002-340. From this figure it can be seen that the structure of the temperature field in both datasets is very similar. Even though during this time period SABER does not have a field of view covering the higher latitudes of the Northern Hemisphere, the equatorward edge of SPW1 and SPW2 can be observed, while most of SPW3 can be seen because it typically maximizes at lower latitudes.. The MERRA plots, shown on the top row, have dashed lines, which denote the field of view of SABER. By inspection it can be seen that the three components are well matched between the MERRA and SABER datasets, which gives us confidence that MERRA is reproducing the behavior of the atmosphere during this event.

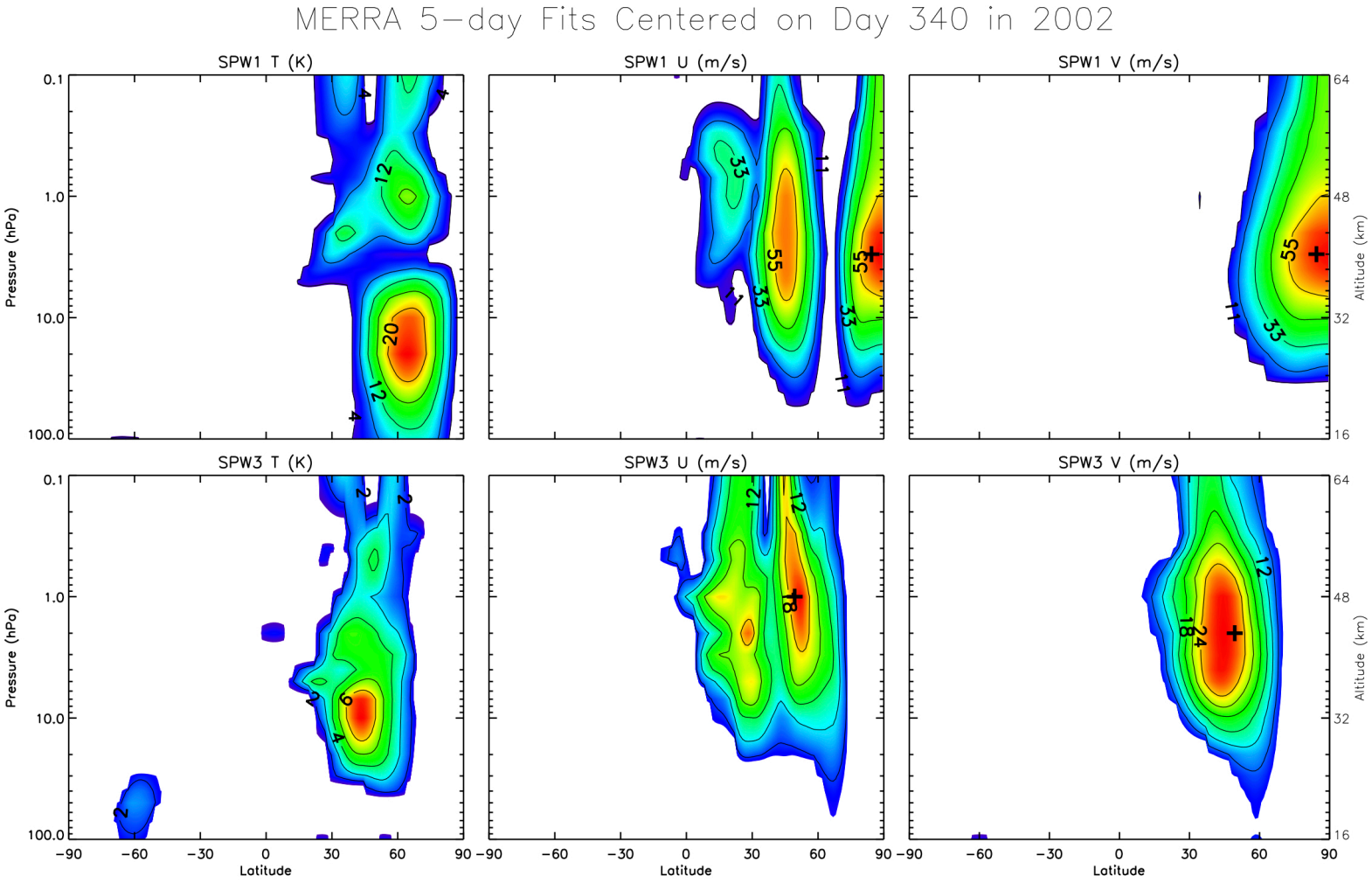

Figure 4.2: Top panes show SPW1 temperature, zonal and meridional fields from MERRA, while bottom panes show the same fields obtained from MERRA but SPW3. Data comes from a 5-day fit centered on 2002-340. The '+' sign represents the point with the maximum aplitude.

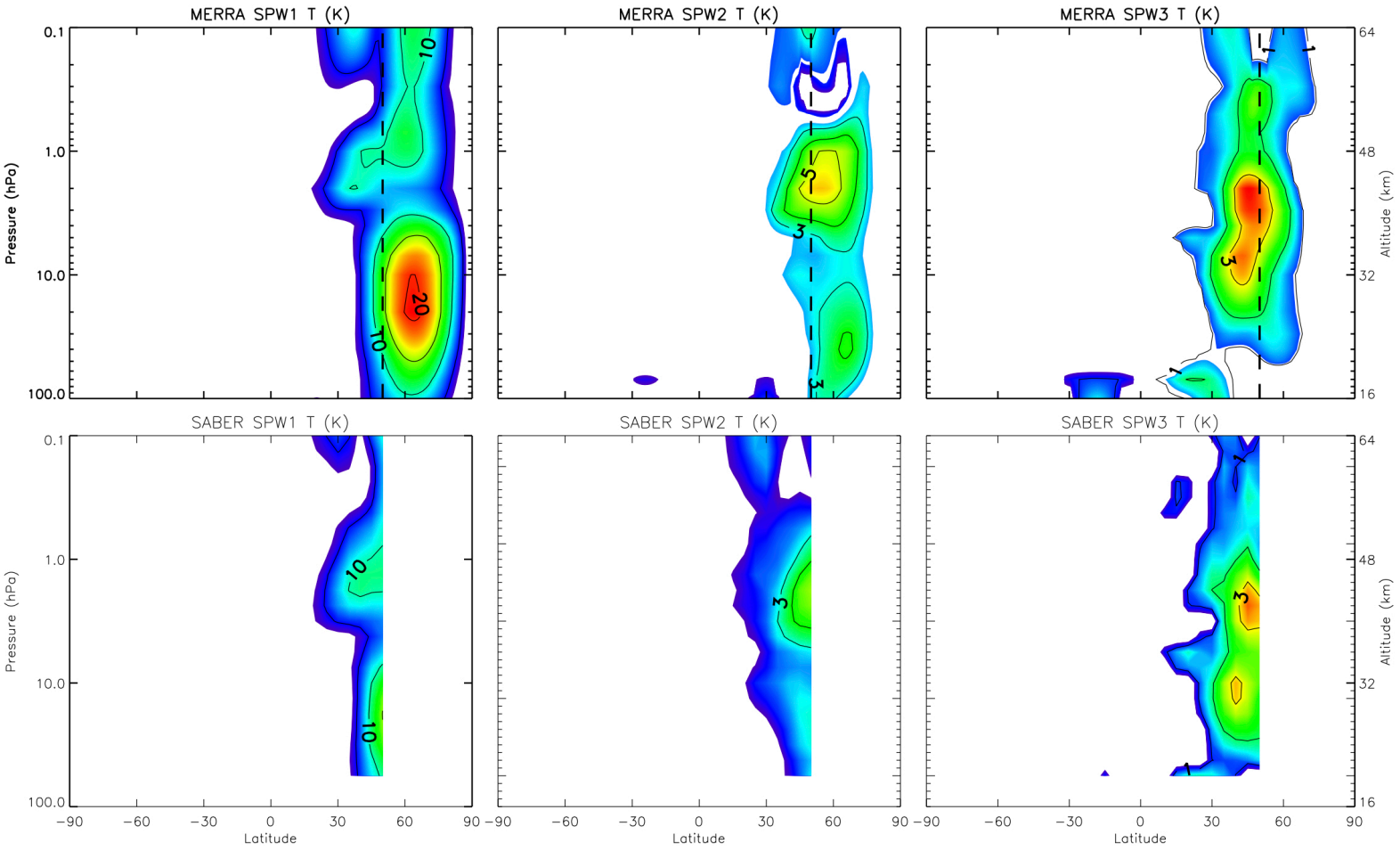

Figure 4.3: Top panes show SPW s=1,2,3 temperature fields from MERRA, while bottom panes show the same fields obtained from SABER. Data comes from a 30-day fit centered on 2002-340.

Figure 4.4 shows three panes with normalized zonal winds from MERRA over-plotted with the semidiurnal tide (12hW1) SPMR data represented by '+' over the austral summer period in 2002-2003. Top panel shows SPW1 data, middle panel shows SPW2 and bottom panel shows SPW3. The different time series in each plot correspond to daily averages at different latitudes (fixed latitude but variable height, where the maximum occurs on each day). The event being studied in this subsection lies between days 325 and 342. From this plot it can be seen that as 12hW1 decreases with a sharp gradient, SPW1 (which always has its strongest amplitudes between 80°N and 85°N) is also decreasing in this region. However, at lower altitudes (70°N and below) it is actually increasing. This means that during this time period SPW1 is moving south. SPW2 is always very variable and somewhat difficult to characterize. During this period SPW2 is mostly decreasing as well. SPW3 shows a clear increase at almost the same rate as 12hW1 decreases.

Figure 4.5 shows the correlation analysis done between zonal and meridional winds from SPW1, SPW2 and SPW3 and 12hW1 at different latitude slices as a function of lag. The filled symbols mean that the correlation point is statistically significant with a confidence of at least 95%. It can be seen that for almost every plot in this figure, the significant correlation points happen close or at a lag of zero (considering only the negative portion of the lag spectrum since it's mathematically inconsistent to consider positive lags for this scenario).

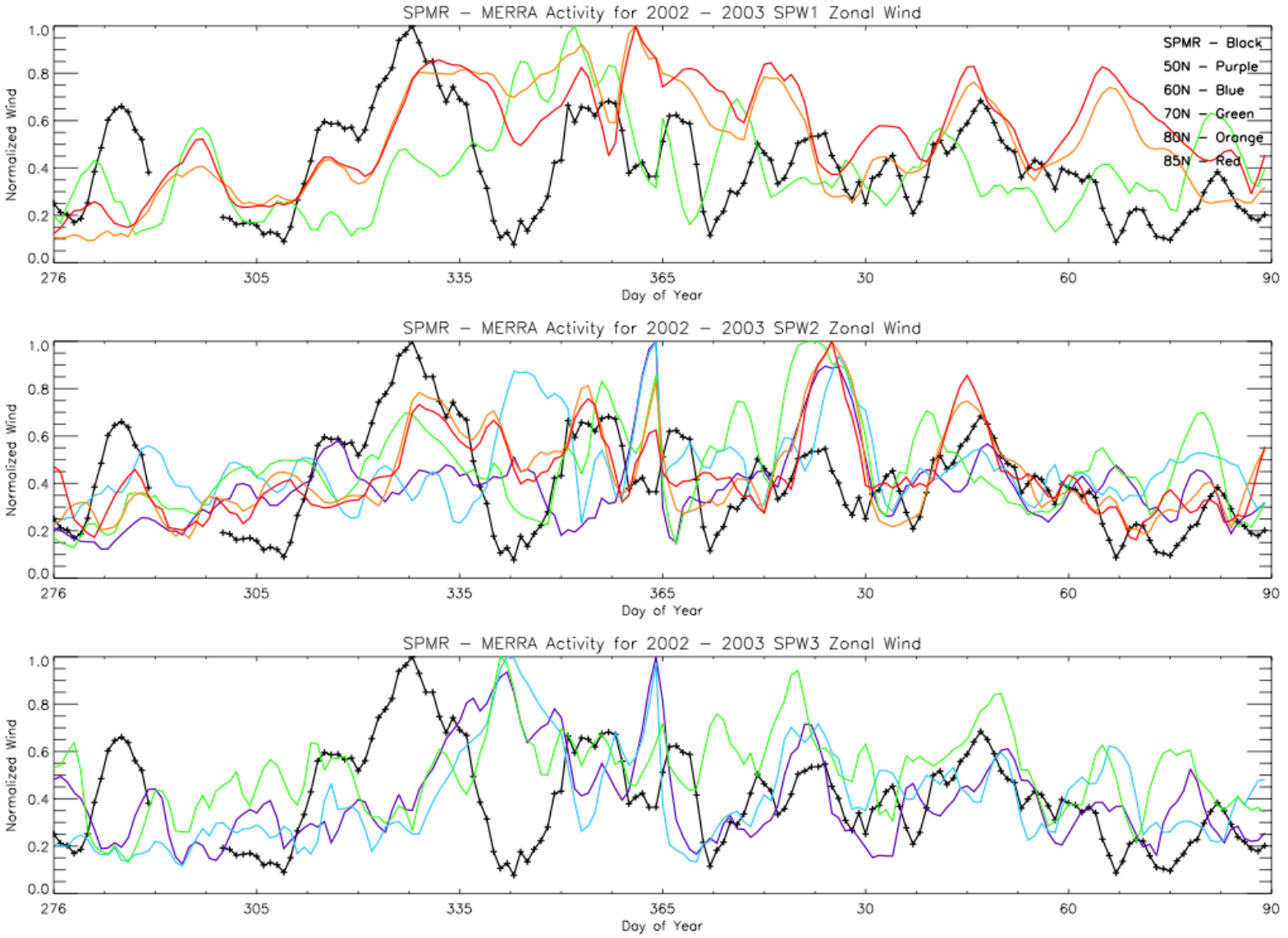

Figure 4.4: Top panel shows normalized SPW1 zonal wind and SPMR data. Middle panel shows SPW2 and SPMR, and bottom panel shows SPW3 and SPMR data. SPMR data shown by the black line, MERRA at 50N is purple, 60°N is blue, 70°N is green, 80°N is oransge and 85°N is red. Data is from 2002-2003.

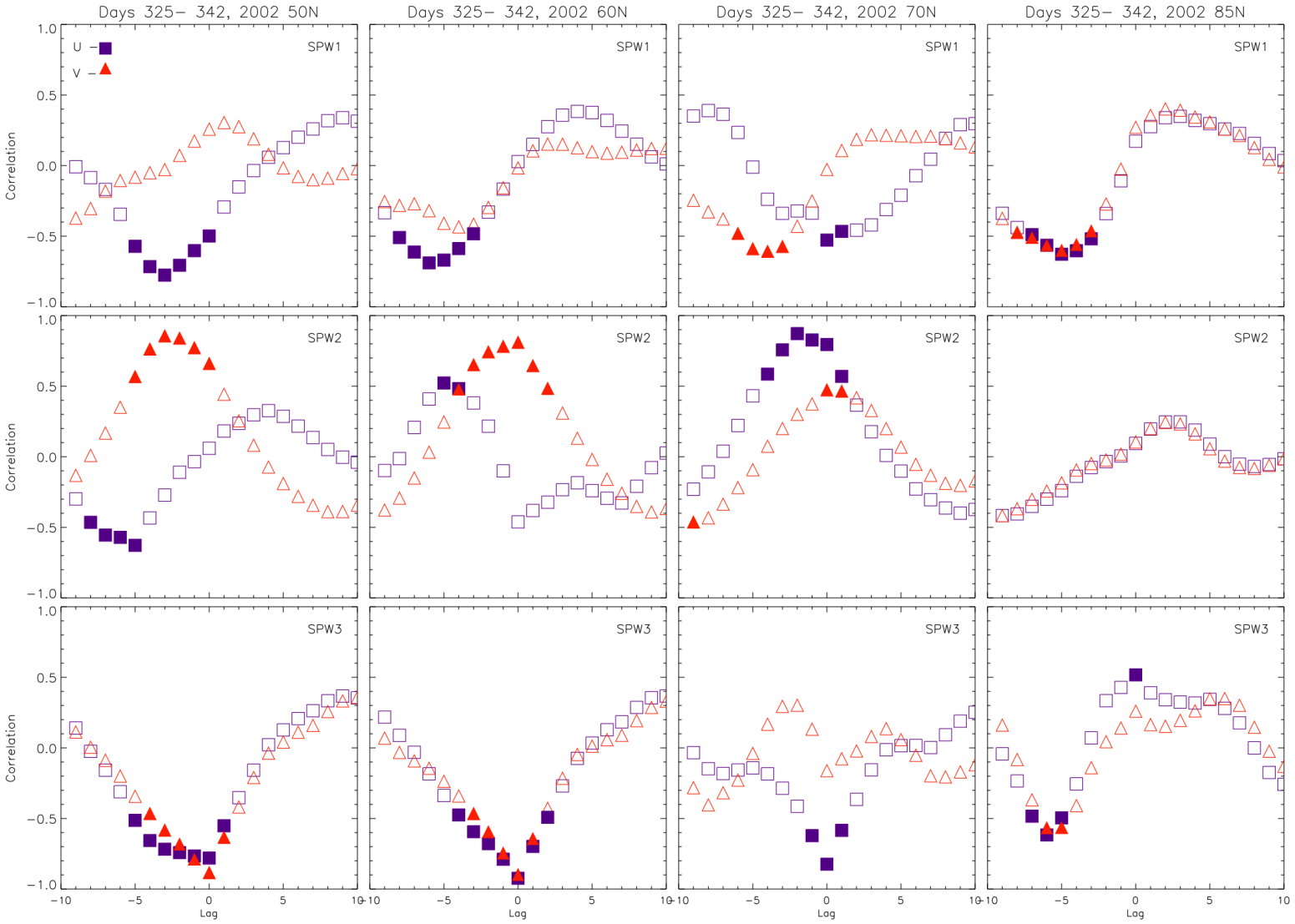

Figure 4.5: This figure shows the correlation between MERRA zonal and meridional winds and SPMR data in 2002, days 325-342 as a function of lag. Left column shows correlations using data from MERRA at 50°N, second column at 60°N, third column at 70°N and last column at 85°N. First row correlates the MERRA SPW1 components with 12hW1 from SPMR, middle row correlates MERRA SPW2 and bottom row correlates MERRA SPW3. Correlation of zonal winds is shown by blue squares and meridional winds by red triangles. In the correlation figures, filled symbols mean that the statistical significance of a correlation point is equal or greater than 95%.

The figures in the next few pages show correlation maps. These maps were composed by correlating the 12hW1 data from the period of interest to each SPW (U and V) grid point (in latitude and altitude). In these plots the shaded areas means the statistical significance is less than 95%, which are not reliable. Therefore attention must be focused on the white areas. Solid contour lines denote a positive correlation, while dashed lines represent negative correlations.

Figure 4.6 correlates SPW1 U with 12hW1. It can be seen that at higher latitudes and levels (where the SPW1 has its peak), the correlation gets higher than 0.7. At lower latitudes and heights, an anti-correlation of up to -0.7 is present. Since during this period the 12hW1 is decreasing this means that SPW1 is moving southward and down. Figure 4.7 correlates SPW1 V and shows a very similar structure to the correlation just analyzed with the zonal wind, with the only difference is that the correlation gets as high as 0.9 and covers a larger part of the winter hemisphere.

Figure 4.8 correlates SPW2 U, which is usually very variable structure-wise and has discontinuities between its peaks, which causes a sudden change from a correlation of around 0.8 to an anti-correlation of -0.9 and then back to a positive correlation of 0.7 northward. Figure 4.9, which correlates the meridional wind, shows a similar structure. The correlation of SPW3 U and V can be seen on figures 4.10 and 4.11, respectively. Both figures show a clear and strong anti-correlation covering most part of the winter hemisphere.

Appendix C brings similar correlation plots for different lags. Figures C.1, C.3 and C.5 show the correlation of the SPW U components for lag=0,-1,-2 respectively. SPW1 decreases the intensity of the positive correlation around its peak region as the lag moves from 0 to -2. SPW2 has a relatively constant correlation around this lag window. SPW3 decreases its anti-correlation as we move further away from a lag=0, but is still significant at lag=-2.

Similarly, figures C.2, C.4 and C.6 show the correlation of the SPW V components for lag=0,-1,-2. SPW1 has the largest positive correlation region at lag=0, but it maintains the basic structure up to lag=-2. SPW2 and SPW3 stay almost constant in this period.

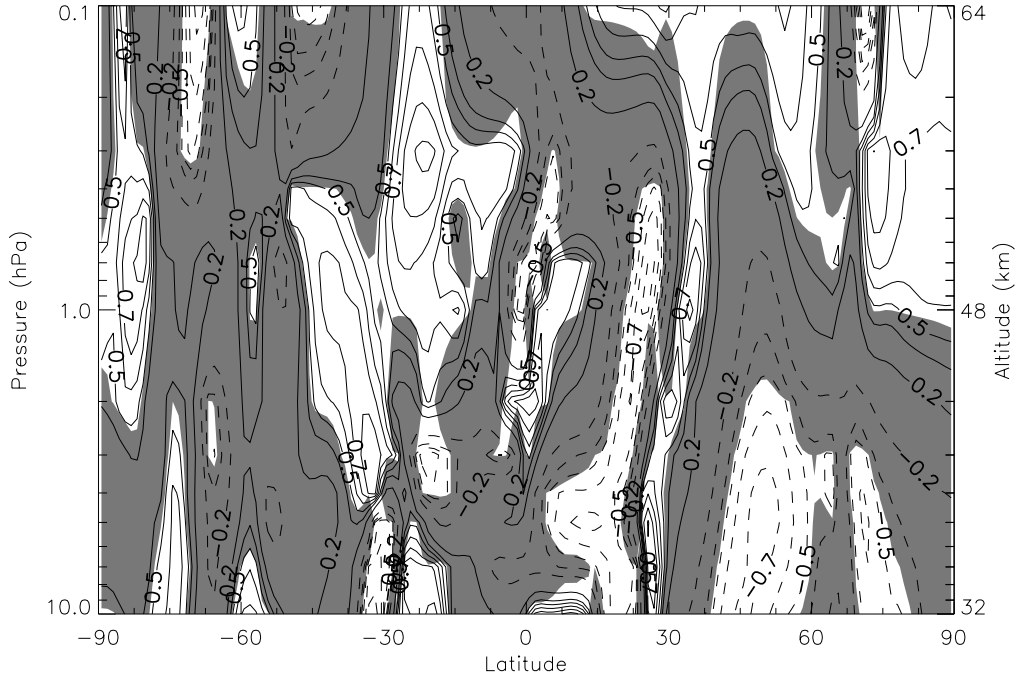

Figure 4.6: Correlation map of SPW1 U on 2002 - 325-342 with a lag of 0. Solid contour lines represent a positive correlation and dashed lines mean negative correlation. Shaded areas mean that the statistical significance of a correlation point is less than 95%.

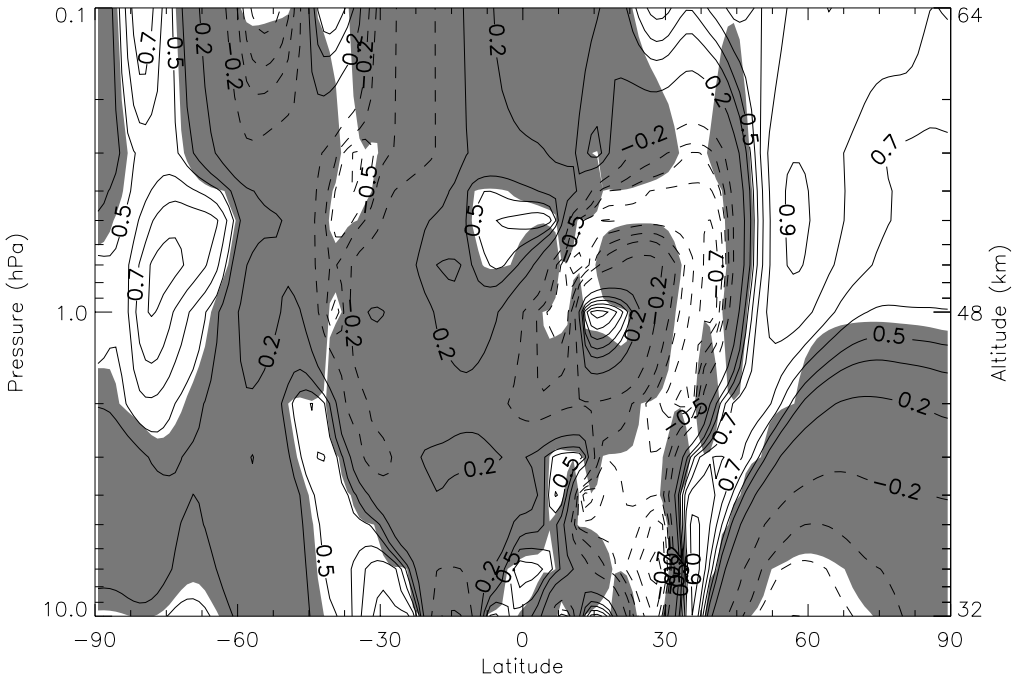

Figure 4.7: Correlation map of SPW1 V on 2002 - 325-342 with a lag of 0. Solid contour lines represent a positive correlation and dashed lines mean negative correlation. Shaded areas mean that the statistical significance of a correlation point is less than 95%.

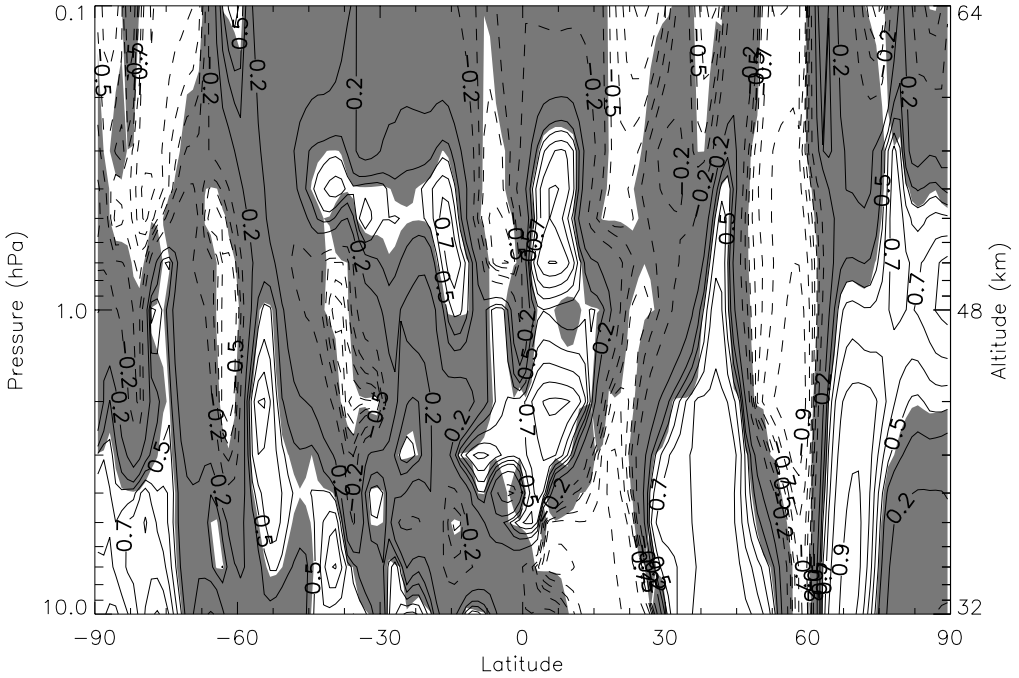

Figure 4.8: Correlation map of SPW2 U on 2002 - 325-342 with a lag of 0. Solid contour lines represent a positive correlation and dashed lines mean negative correlation. Shaded areas mean that the statistical significance of a correlation point is less than 95%.

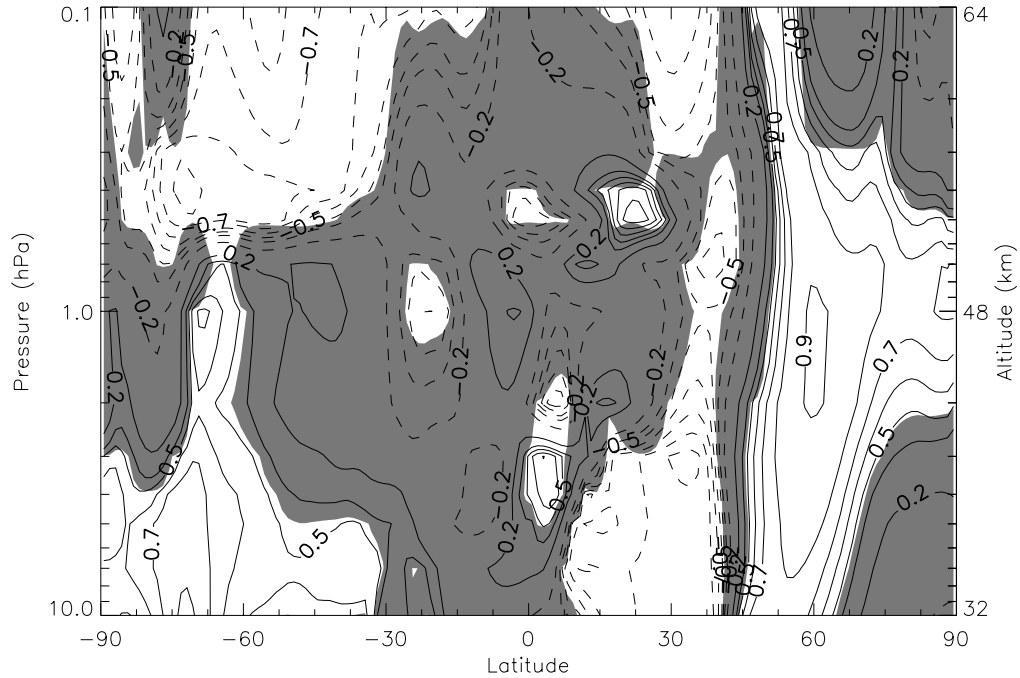

Figure 4.9: Correlation map of SPW2 V on 2002 - 325-342 with a lag of 0. Solid contour lines represent a positive correlation and dashed lines mean negative correlation. Shaded areas mean that the statistical significance of a correlation point is less than 95%.

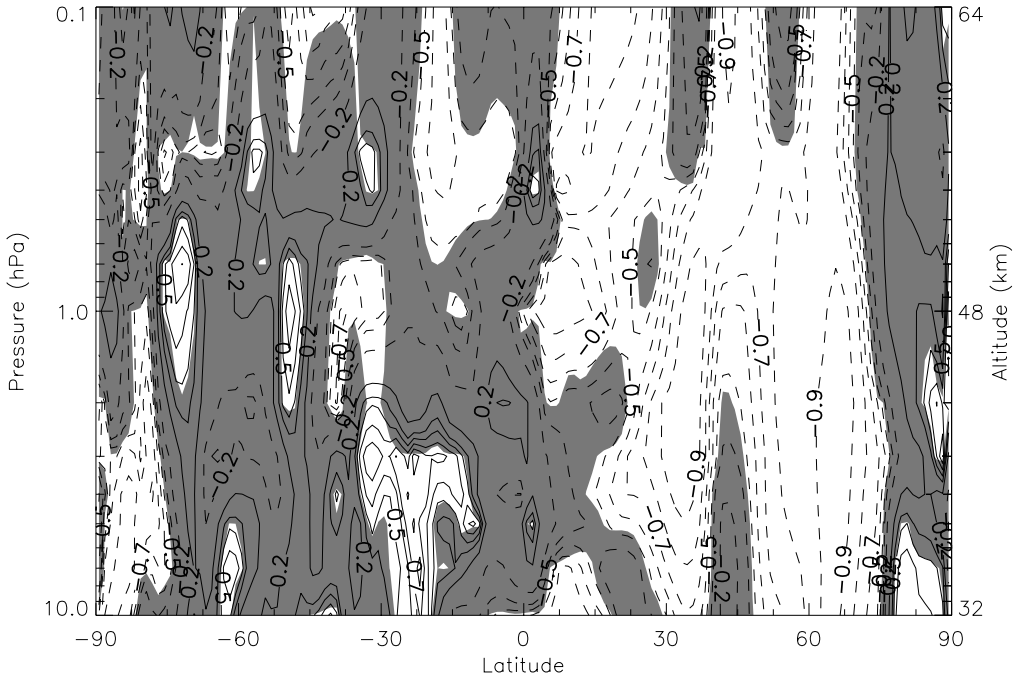

Figure 4.10: Correlation map of SPW3 U on 2002 - 325-342 with a lag of 0. Solid contour lines represent a positive correlation and dashed lines mean negative correlation. Shaded areas mean that the statistical significance of a correlation point is less than 95%.

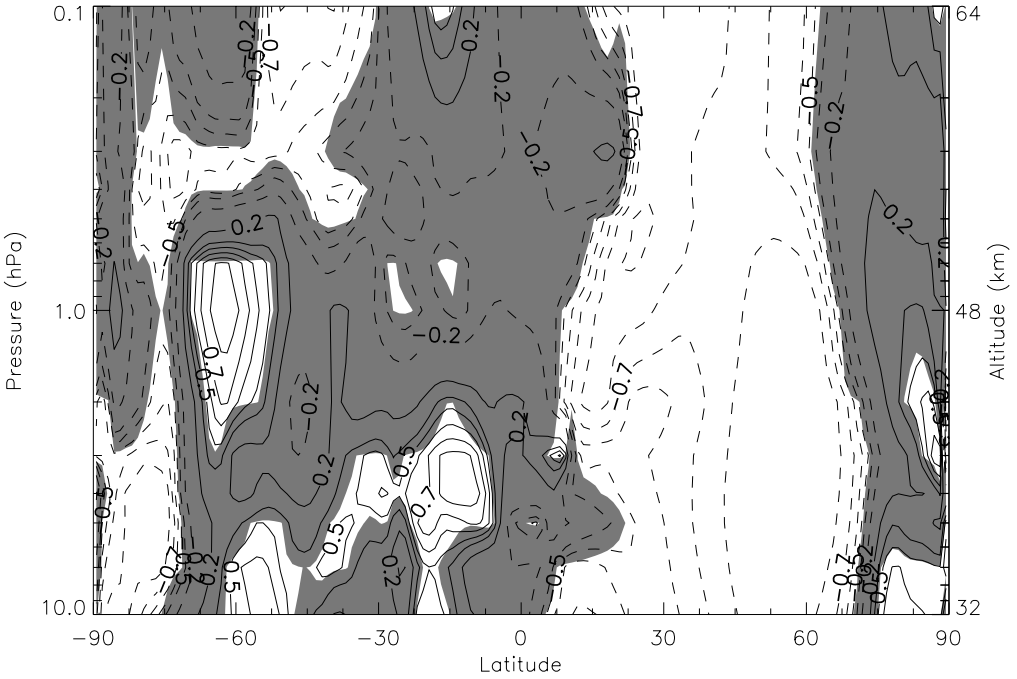

Figure 4.11: Correlation map of SPW3 V on 2002 - 325-342 with a lag of 0. Solid contour lines represent a positive correlation and dashed lines mean negative correlation. Shaded areas mean that the statistical significance of a correlation point is less than 95%.

4.2.1.2 2002 - 345-365

Another event of interest in 2002 happened right after the previous event, during days 345 and 365. From figures 4.12 and 4.13 show that during this event, SPW1 U and V correlate well with the structure of the nonmigrating semidiurnal tide over the South Pole, with positive correlations as strong as 0.8. Both components of SPW1 have a large positive correlation region starting around 80-85°N, and covering a large vertical structure.

Figure 4.14 shows a strong positive correlation between SPW2 U and 12hW1 at higher latitudes and a strong anti-correlation at mid-latitudes, which corresponds to the motion of SPW2 in the northern hemisphere during this period. Figure 4.15 shows a similar structure but with a much larger region of positive correlation in the higher latitudes and covering most of the vertical structure.

Figures 4.16 and 4.17 show the correlation of 12hW1 and SPW3 U and V, respectively. Both SPW components show a strong anti-correlation covering much of the winter hemisphere across the latitudes and altitudes where SPW3 peaks.

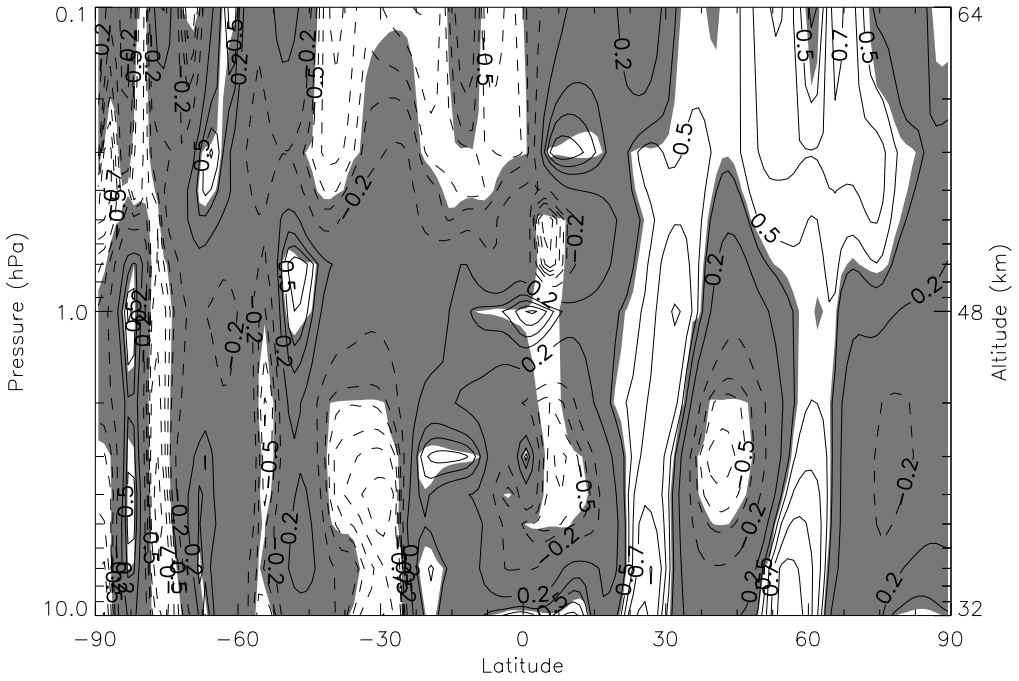

Figure 4.12: Correlation map of SPW1 U on 2002 - 345-365 with a lag of 0. Solid contour lines represent a positive correlation and dashed lines mean negative correlation. Shaded areas mean that the statistical significance of a correlation point is less than 95%.

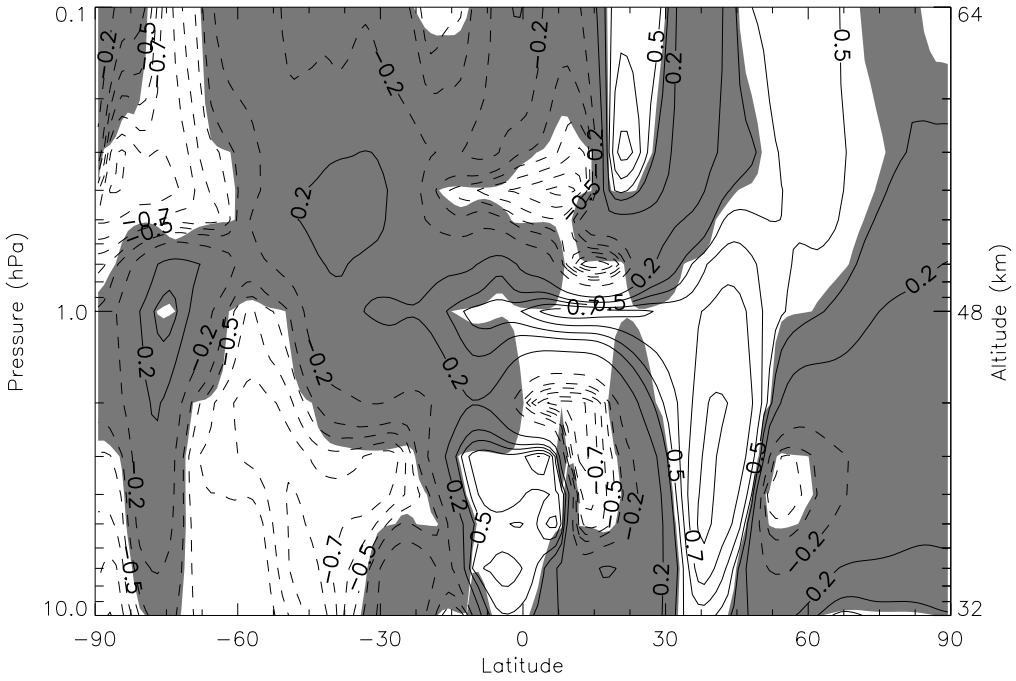

Figure 4.13: Correlation map of SPW1 V on 2002 - 345-365 with a lag of 0. Solid contour lines represent a positive correlation and dashed lines mean negative correlation. Shaded areas mean that the statistical significance of a correlation point is less than 95%.

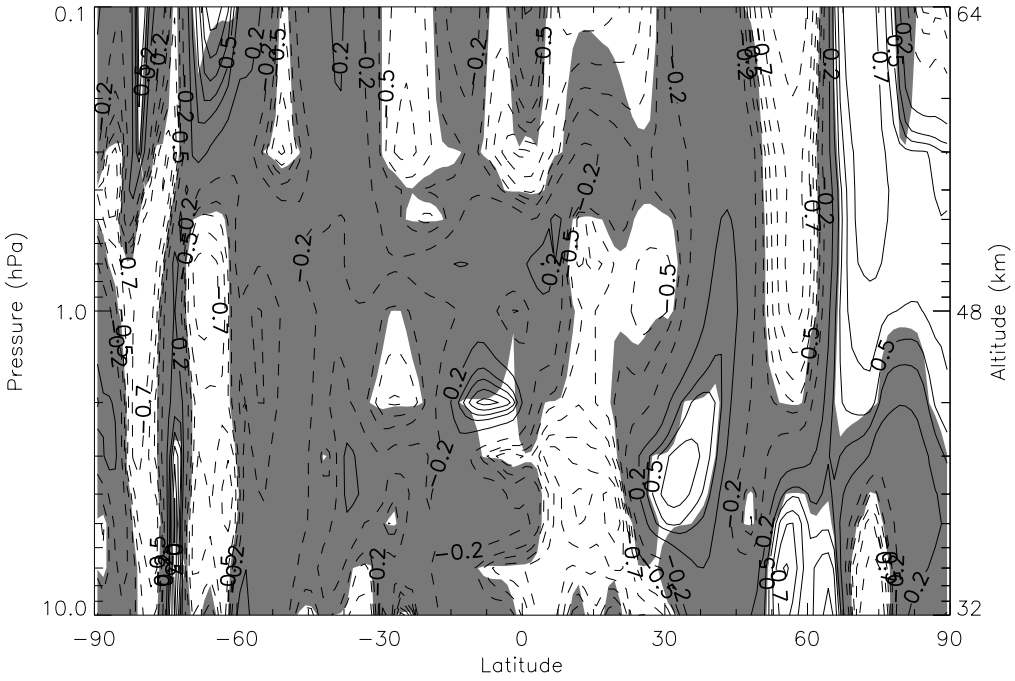

Figure 4.14: Correlation map of SPW2 U on 2002 - 345-365 with a lag of 0. Solid contour lines represent a positive correlation and dashed lines mean negative correlation. Shaded areas mean that the statistical significance of a correlation point is less than 95%.

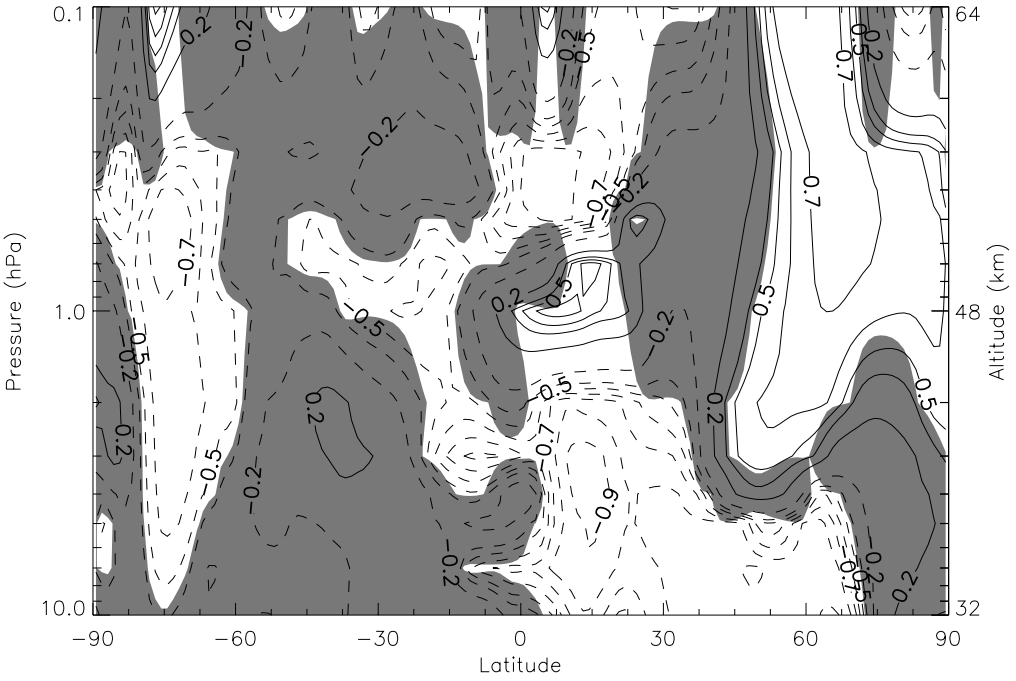

Figure 4.15: Correlation map of SPW2 V on 2002 - 345-365 with a lag of 0. Solid contour lines represent a positive correlation and dashed lines mean negative correlation. Shaded areas mean that the statistical significance of a correlation point is less than 95%.

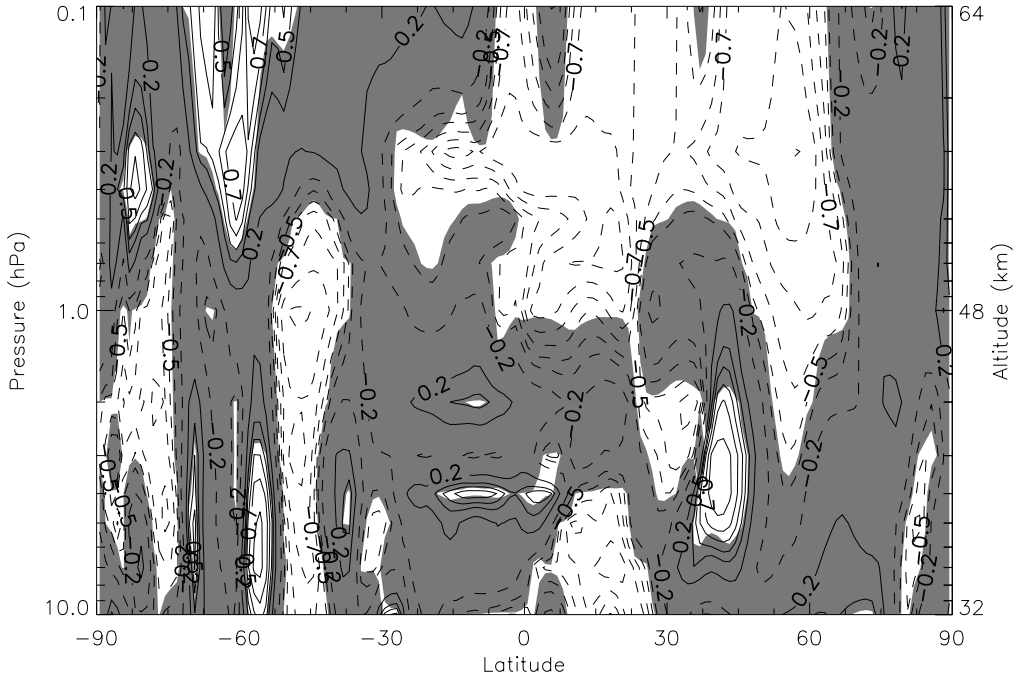

Figure 4.16: Correlation map of SPW3 U on 2002 - 345-365 with a lag of 0. Solid contour lines represent a positive correlation and dashed lines mean negative correlation. Shaded areas mean that the statistical significance of a correlation point is less than 95%.

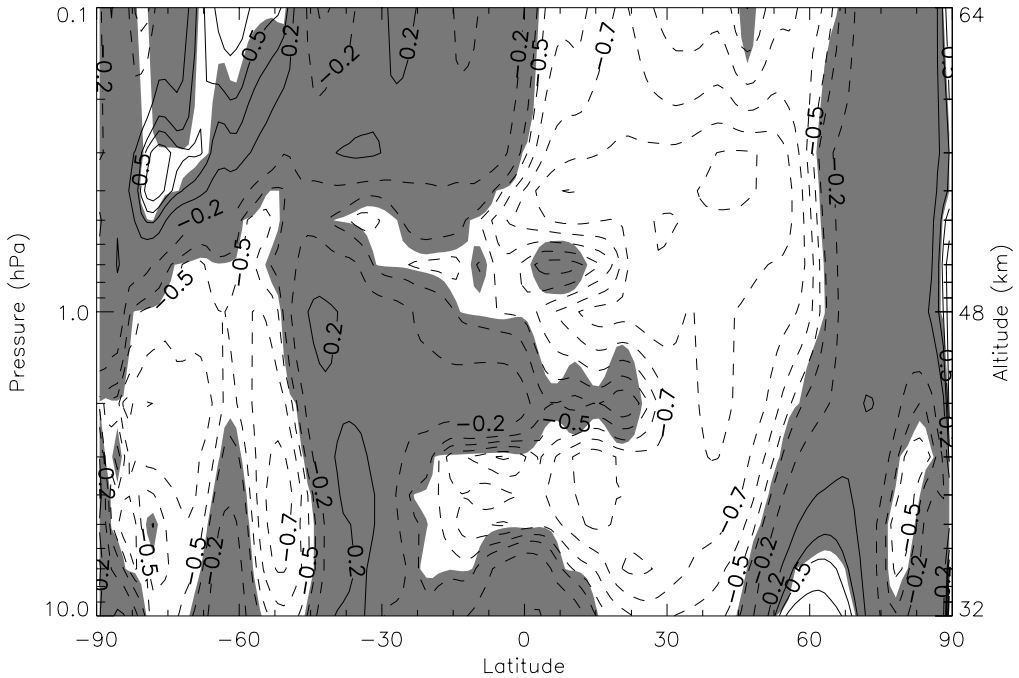

Figure 4.17: Correlation map of SPW3 V on 2002 - 345-365 with a lag of 0. Solid contour lines represent a positive correlation and dashed lines mean negative correlation. Shaded areas mean that the statistical significance of a correlation point is less than 95%.

4.2.2 2003 events

4.2.2.1 2003 - 1-13

This event in the early days of 2003 immediately follows the event just discussed in the end of 2002. Even though this event only happens between days 1-13, it shows a very interesting feature that will be discussed next.

Figure 4.18 shows the correlation between 12hW1 and SPW1 U wind. An extremely strong anti-correlation can be seen at high latitudes and altitudes, where SPW1 peaks. It can also be seen a strong positive correlation at lower altitudes, which correlations with the vertical movement of SPW1 during this period. Figure 4.19 shows the correlation of SPW1 V wind and 12hW1, with a structure that resembles the one seen for SPW1 U.

Figures 4.20 and 4.21 show the correlation between 12hW1 and SPW2 U and V, respectively. Both plots show a clear, strong anti-correlation covering most of the winter hemisphere.

Figures 4.22 and 4.23 show the correlation between 12hW1 and SPW3 U and V, respectively. There is an anti-correlation, however it only happens on a relatively small region and does not seem to be extremely significant.

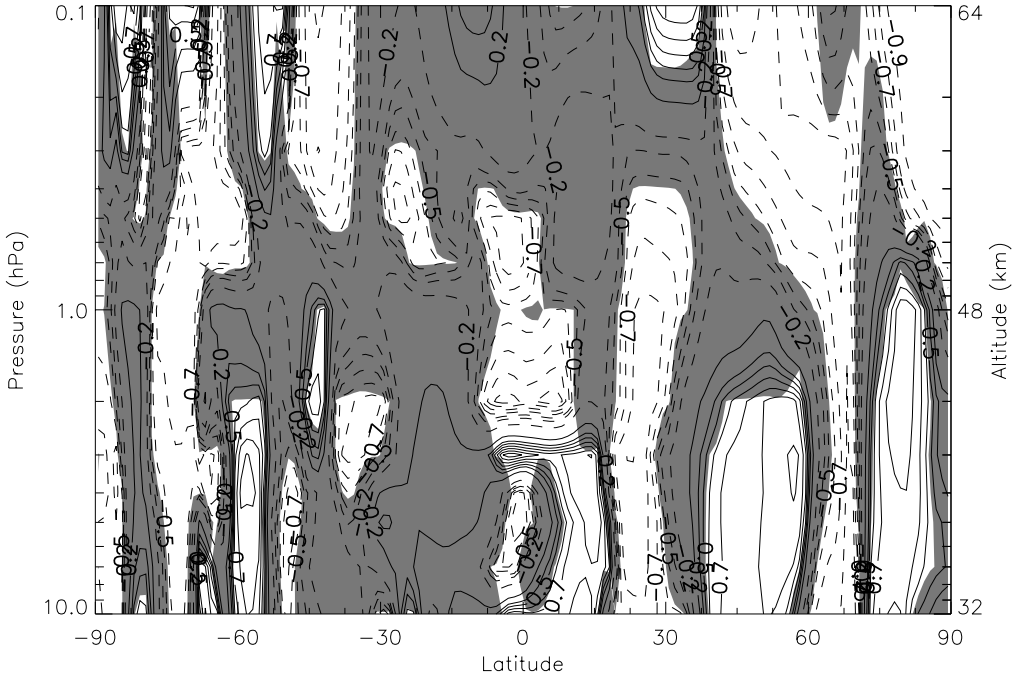

Figure 4.18: Correlation map of SPW1 U on 2003 - 1-13 with a lag of 0. Solid contour lines represent a positive correlation and dashed lines mean negative correlation. Shaded areas mean that the statistical significance of a correlation point is less than 95%.

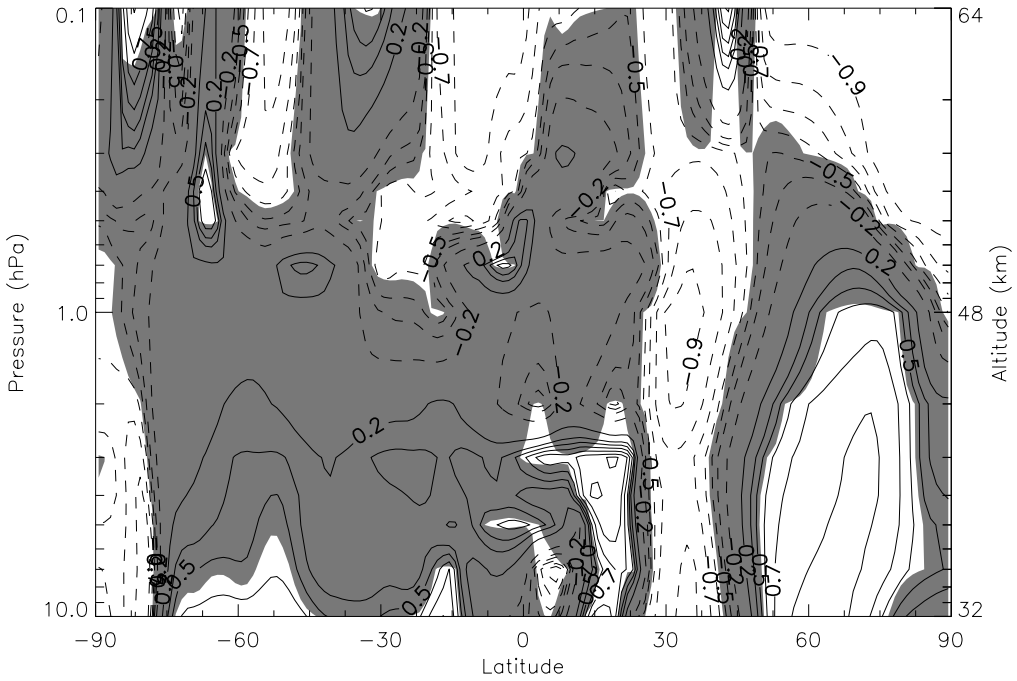

Figure 4.19: Correlation map of SPW1 V on 2003 - 1-13 with a lag of 0. Solid contour lines represent a positive correlation and dashed lines mean negative correlation. Shaded areas mean that the statistical significance of a correlation point is less than 95%.

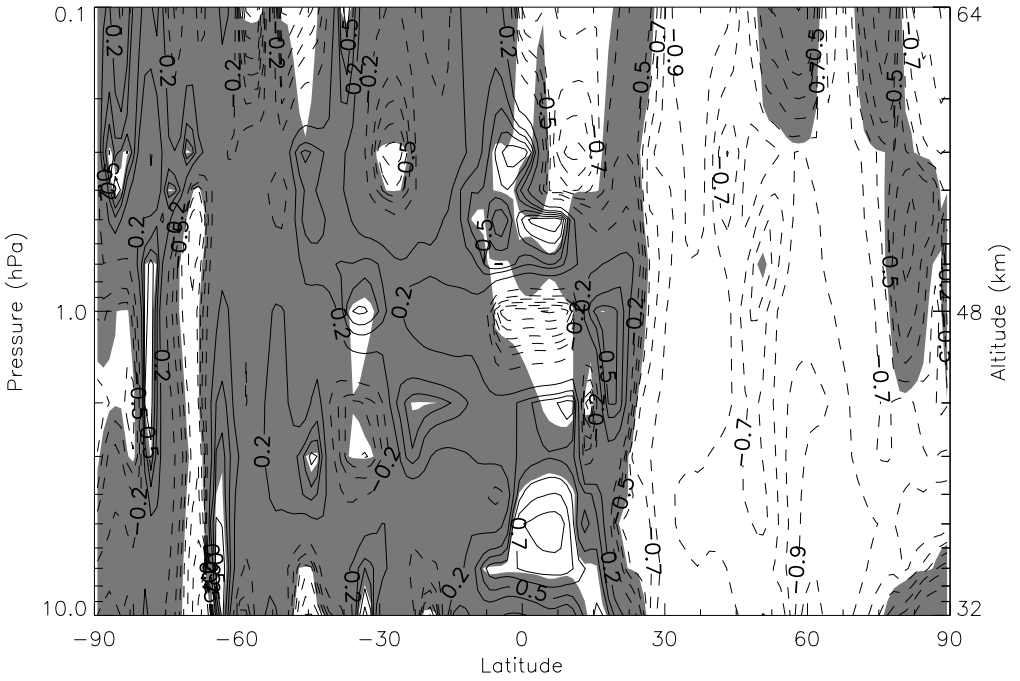

Figure 4.20: Correlation map of SPW2 U on 2003 - 1-13 with a lag of 0. Solid contour lines represent a positive correlation and dashed lines mean negative correlation. Shaded areas mean that the statistical significance of a correlation point is less than 95%.

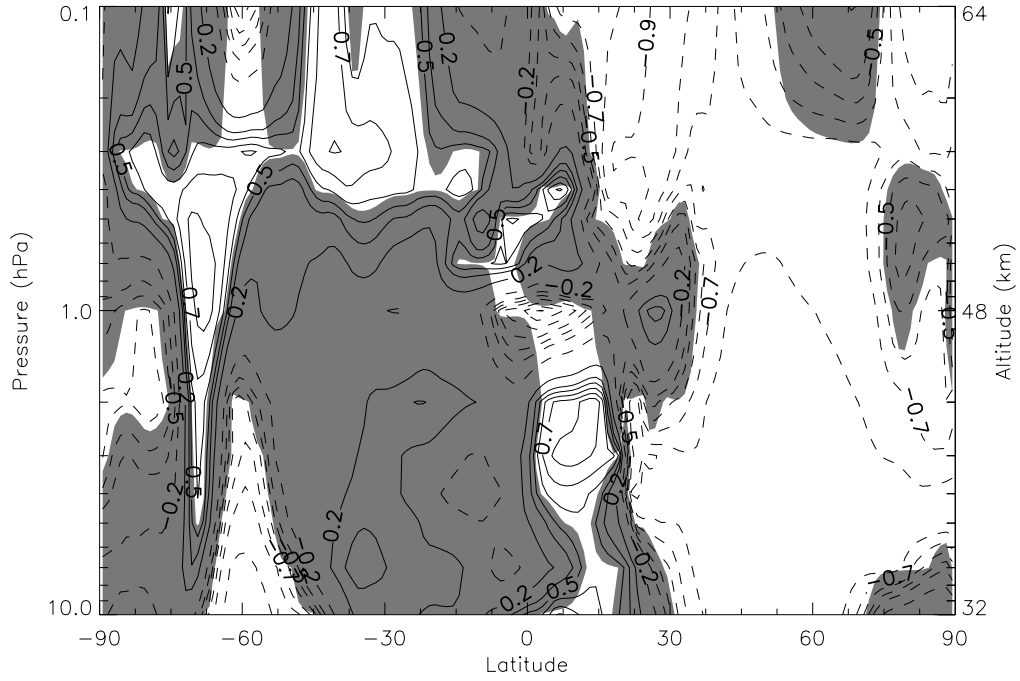

Figure 4.21: Correlation map of SPW2 V on 2003 - 1-13 with a lag of 0. Solid contour lines represent a positive correlation and dashed lines mean negative correlation. Shaded areas mean that the statistical significance of a correlation point is less than 95%.

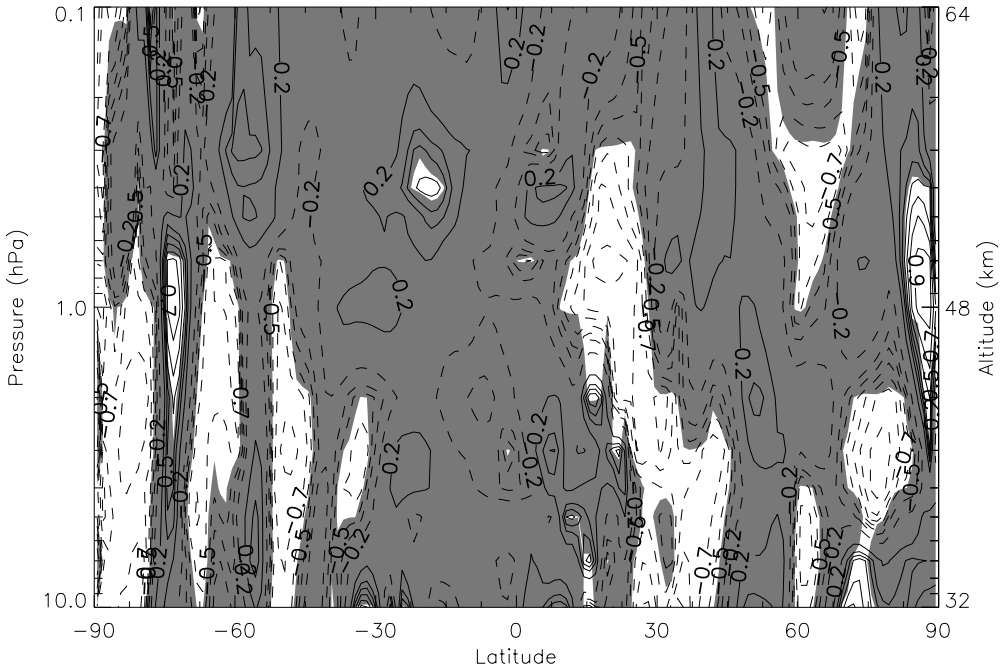

Figure 4.22: Correlation map of SPW3 U on 2003 - 1-13 for lag=0

Correlation map of SPW3 U on 2003 - 1-13 with a lag of 0. Solid contour lines represent a positive correlation and dashed lines mean negative correlation. Shaded areas mean that the statistical significance of a correlation point is less than 95%.

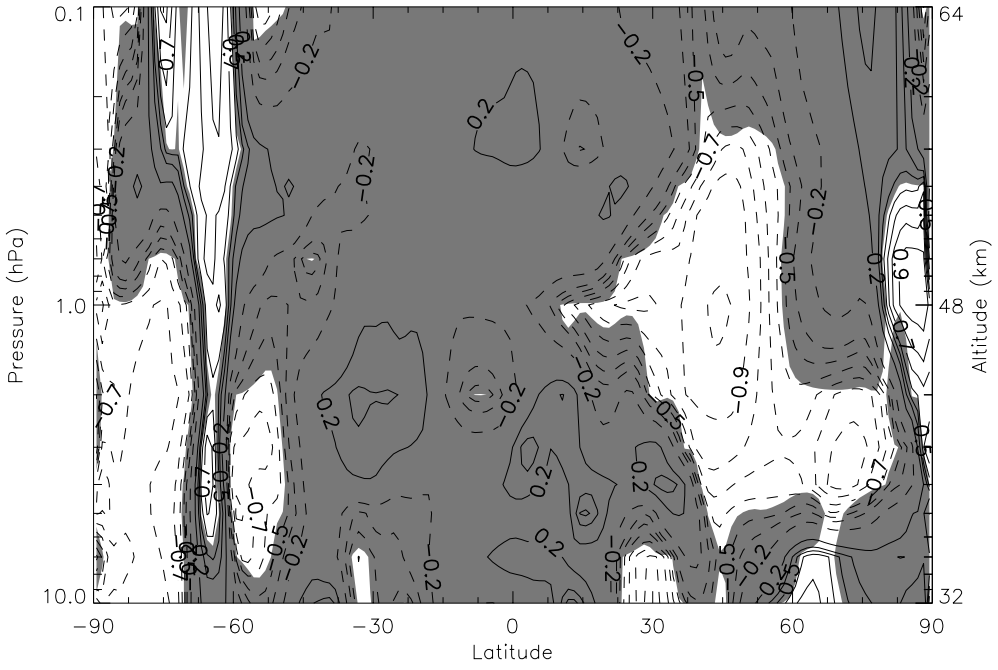

Figure 4.23: Correlation map of SPW3 V on 2003 - 1-13 with a lag of 0. Solid contour lines represent a positive correlation and dashed lines mean negative correlation. Shaded areas mean that the statistical significance of a correlation point is less than 95%.

4.2.2.2 2003 - 10-30

Going back to Figure 4.4, there is another period of interest on days 10-30 in 2003 because there was a major SSW event centered on day 2003-18, as it can be seen on Table 2.1. Figure 4.24 shows that SPW1 has an anti-correlation around lag zero, while SPW2 and SPW3 have a positive correlation.

Figures 4.25 and 4.26 show the correlation from SPW1 U and V. Both plots depict an anti-correlation that gets larger than -0.7. However, these regions of stronger anti-correlation happen at latitudes much lower than where SPW1 peaks, therefore the amplitudes in this region is much smaller.

The correlation from SPW2 U and V, shown by Figures 4.27 and 4.28 respectively, depict a positive correlation at mid-to-high latitudes, which is where SPW2 peaks.

Figures 4.29 and 4.30 correlate SPW3 U and V, with a moderate correlation of around 0.5 and 0.6 in the mid latitudes, where SPW3 peaks.

The extra figures on Appendix C show the correlation of this event up to lag=-2. Figures C.7, C.9 and C.11 show the correlation of the SPW U fields for lag=0, lag=-1 and lag=-2 respectively. In all the cases SPW1 shows a strong anti-correlation but around 60°N, which is south of its peak. SPW2 shows a strong positive correlation for lag=0, and SPW3 shows a strong correlation up to lag=-2 around its peak region. Similarly, figures C.8, C.10 and C.12 show the correlation of the SPW V fields for lag=0, lag=-1 and lag=-2, which happen to have the same behavior as the U correlations.

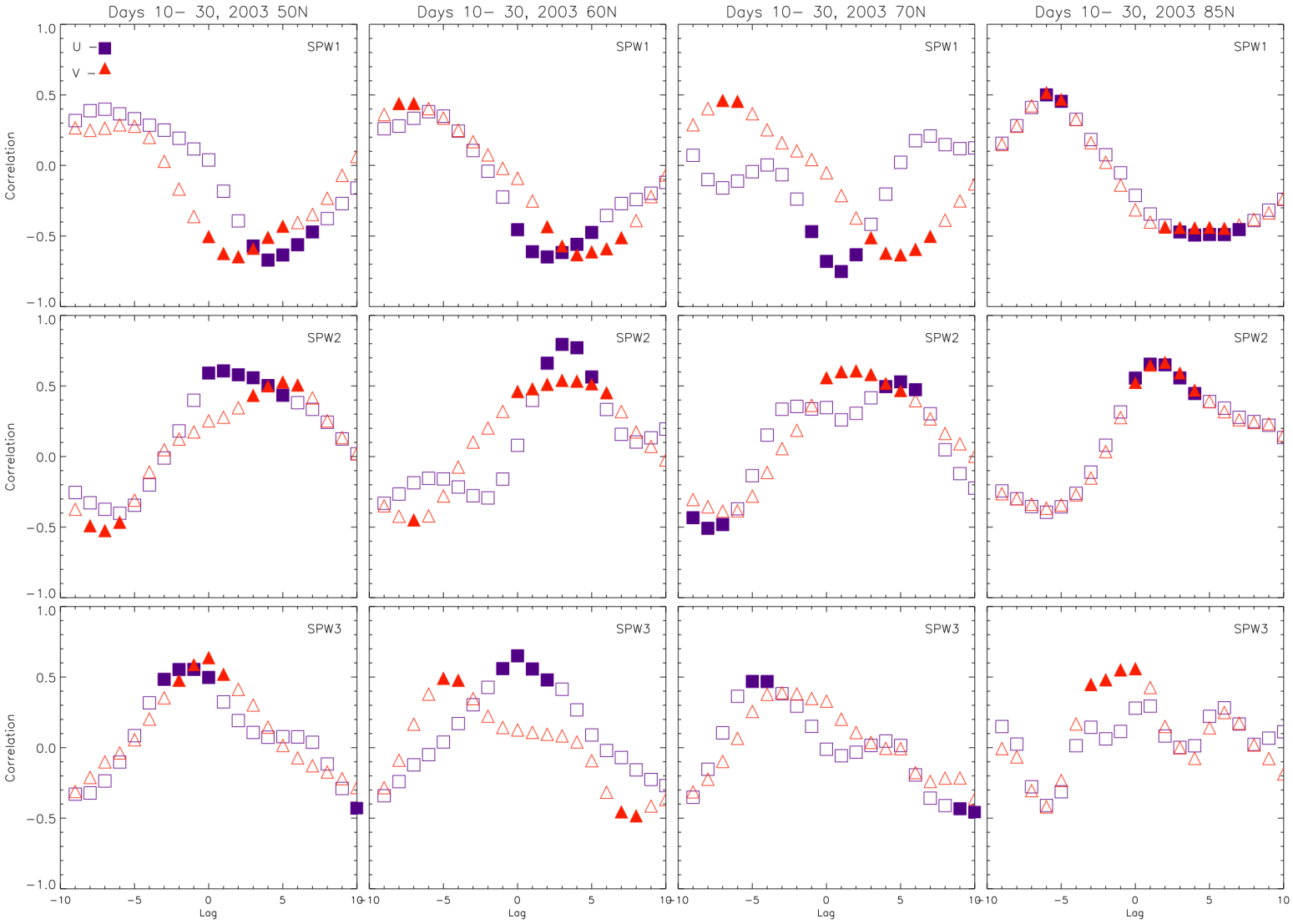

Figure 4.24: This figure shows the correlation between MERRA zonal and meridional winds and SPMR data in 2003, days 10-30 as a function of lag. Left column shows correlations using data from MERRA at 50°N, second column at 60°N, third column at 70°N and last column at 85°N. First row correlates the MERRA SPW1 components with 12hW1 from SPMR, middle row correlates MERRA SPW2 and bottom row correlates MERRA SPW3. Correlation of zonal winds is shown by blue squares and meridional winds by red triangles. Filled symbols mean that the statistical significance of a correlation point is equal or greater than 95%.

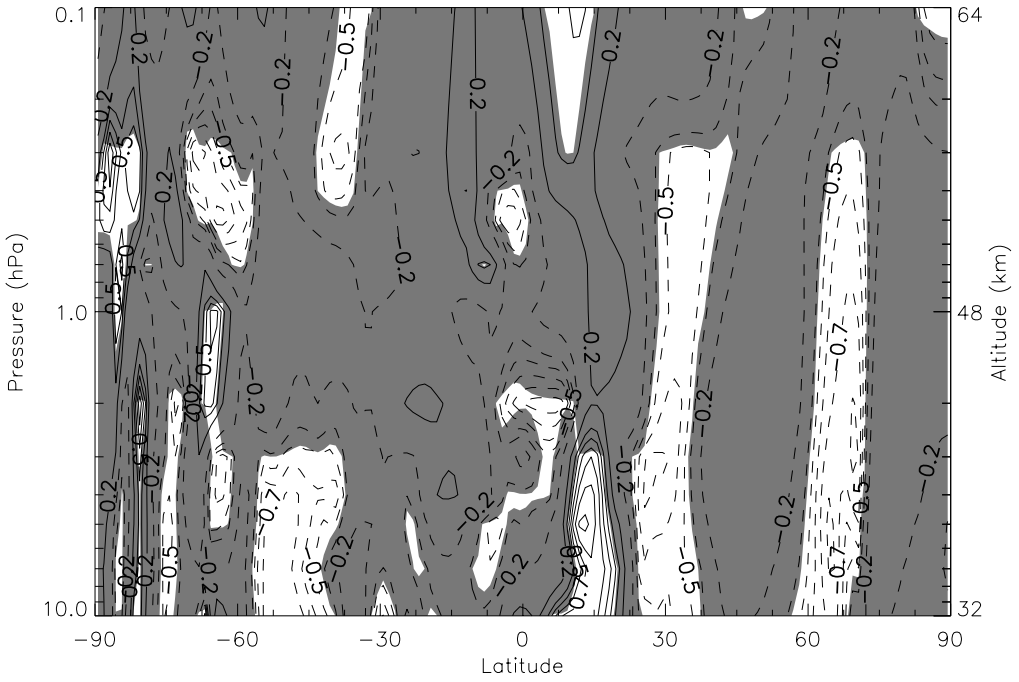

Figure 4.25: Correlation map of SPW1 U on 2003 - 10-30 with a lag of 0. Solid contour lines represent a positive correlation and dashed lines mean negative correlation. Shaded areas mean that the statistical significance of a correlation point is less than 95%.

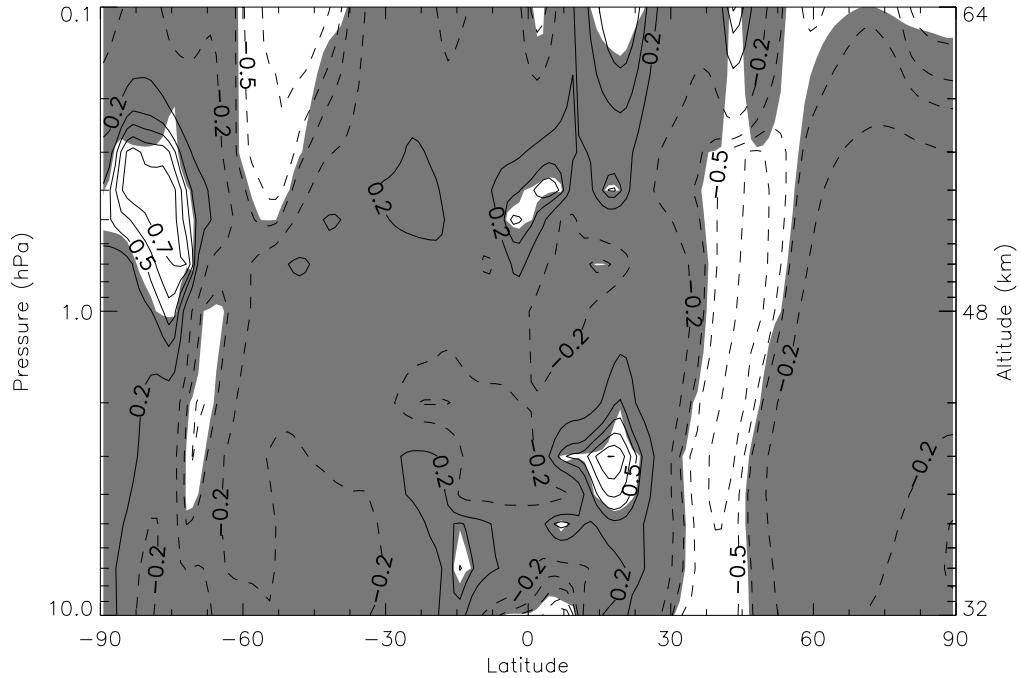

Figure 4.26: Correlation map of SPW1 V on 2003 - 10-30 with a lag of 0. Solid contour lines represent a positive correlation and dashed lines mean negative correlation. Shaded areas mean that the statistical significance of a correlation point is less than 95%.

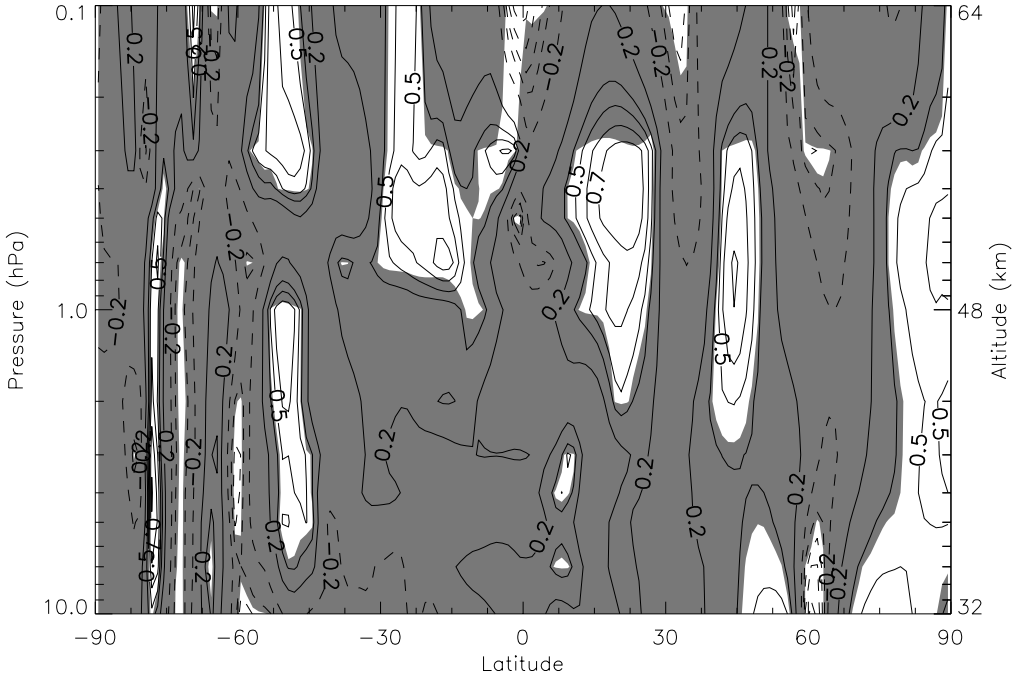

Figure 4.27: Correlation map of SPW2 U on 2003 - 10-30 with a lag of 0. Solid contour lines represent a positive correlation and dashed lines mean negative correlation. Shaded areas mean that the statistical significance of a correlation point is less than 95%.

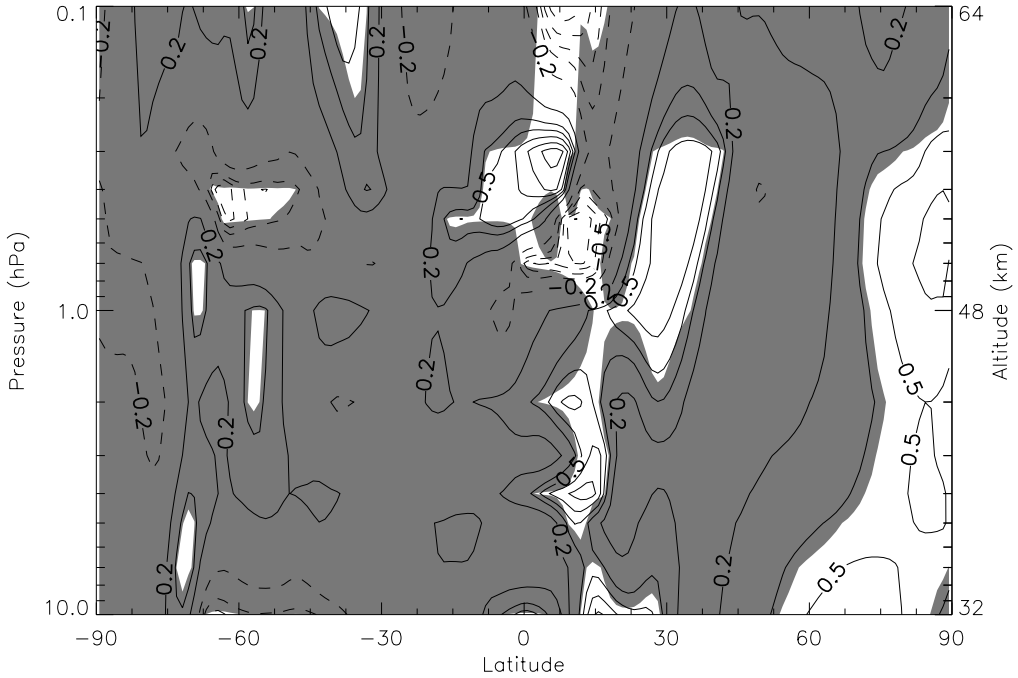

Figure 4.28: Correlation map of SPW2 V on 2003 - 10-30 with a lag of 0. Solid contour lines represent a positive correlation and dashed lines mean negative correlation. Shaded areas mean that the statistical significance of a correlation point is less than 95%.

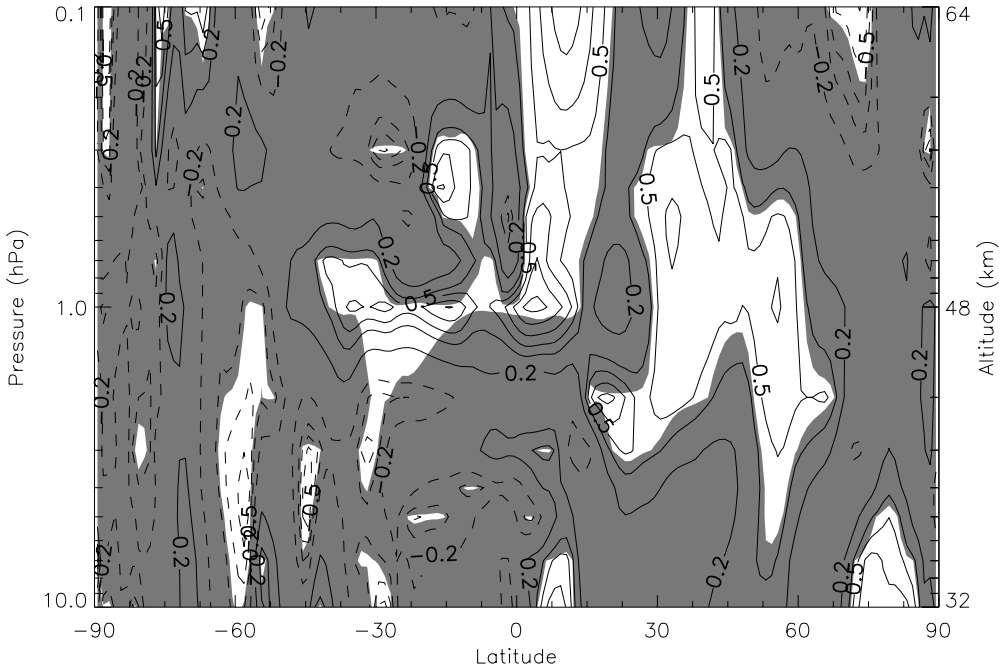

Figure 4.29: Correlation map of SPW3 U on 2003 - 10-30 for lag=0

Correlation map of SPW3 U on 2003 - 10-30 with a lag of 0. Solid contour lines represent a positive correlation and dashed lines mean negative correlation. Shaded areas mean that the statistical significance of a correlation point is less than 95%.

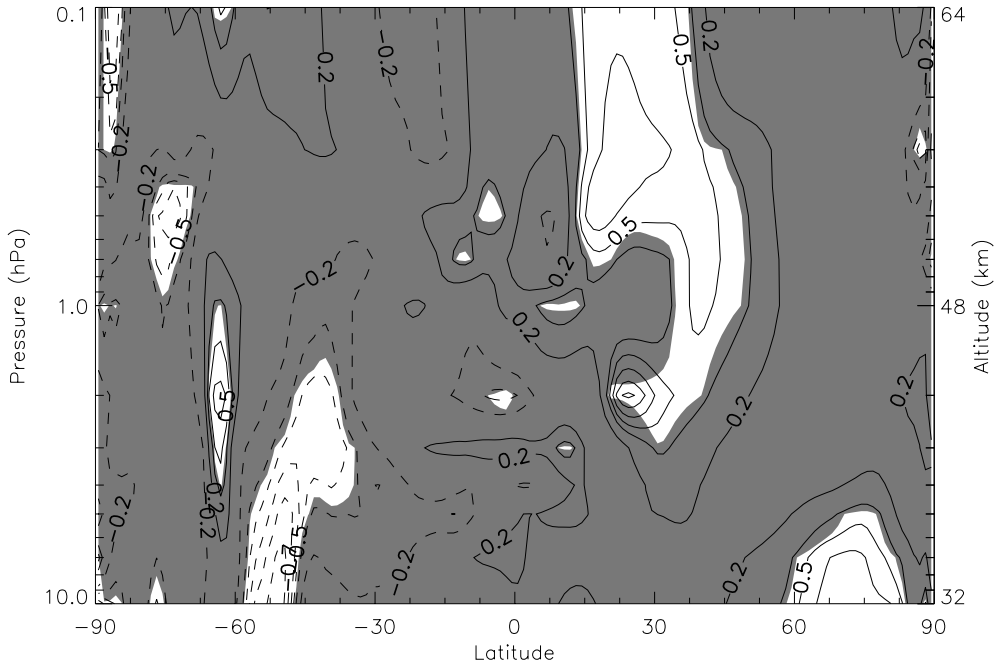

Figure 4.30: Correlation map of SPW3 V on 2003 - 10-30 with a lag of 0. Solid contour lines represent a positive correlation and dashed lines mean negative correlation. Shaded areas mean that the statistical significance of a correlation point is less than 95%.

4.2.2.3 2003 - 45-70

This event happens towards the end of the 2002-2003 austral summer season and covers a large period between days 45 and 70.

It can be clearly seen from figures 4.31 and 4.32 that the correlation between 12hW1 and SPW1 U and V is strong in the higher latitudes and altitudes during this period.

Figure 4.33 shows that the correlation between 12hW1 and SPW2 U has regions of positive and negative anti-correlation in the winter hemisphere, but none stands out as being significant. Figure 4.34 which shows the correlation with SPW2 V has larger regions of positive and negative correlation, but it is still complicated to decide which one is dominant since during this event SPW2 is highly variable in its structure.

Figure 4.35 shows that the correlation between 12hW1 and SPW3 U is very strong and covers most of the winter hemisphere, with its strongest correlation occurring where SPW3 peaks. Figure 4.36 shows an even wider and better correlation with SPW3 V.

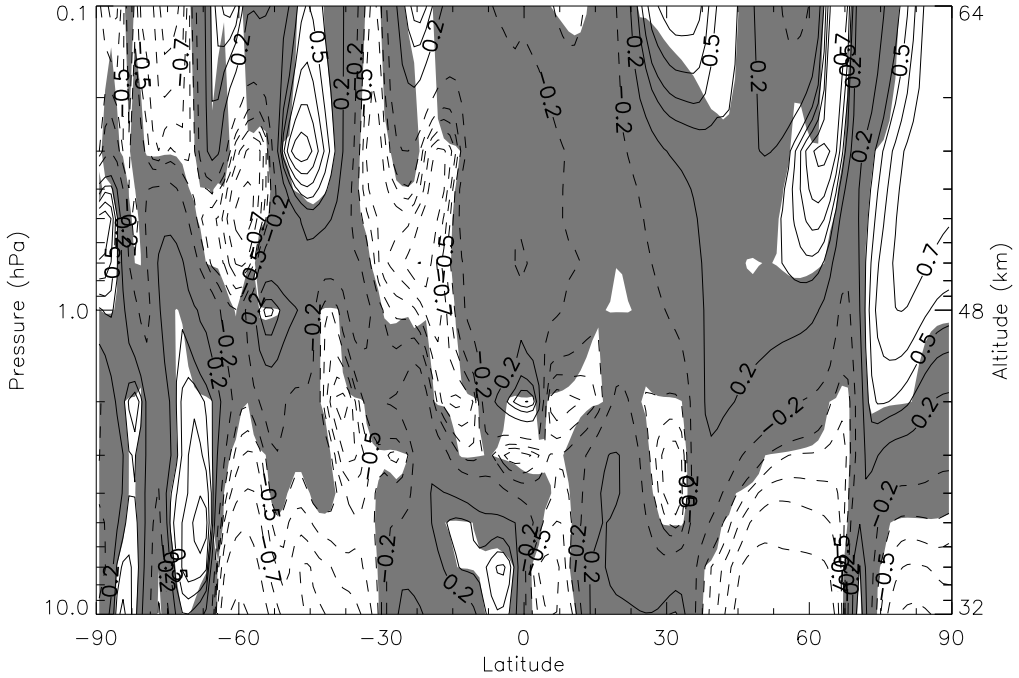

Figure 4.31: Correlation map of SPW1 U on 2003 - 45-70 with a lag of 0. Solid contour lines represent a positive correlation and dashed lines mean negative correlation. Shaded areas mean that the statistical significance of a correlation point is less than 95%.

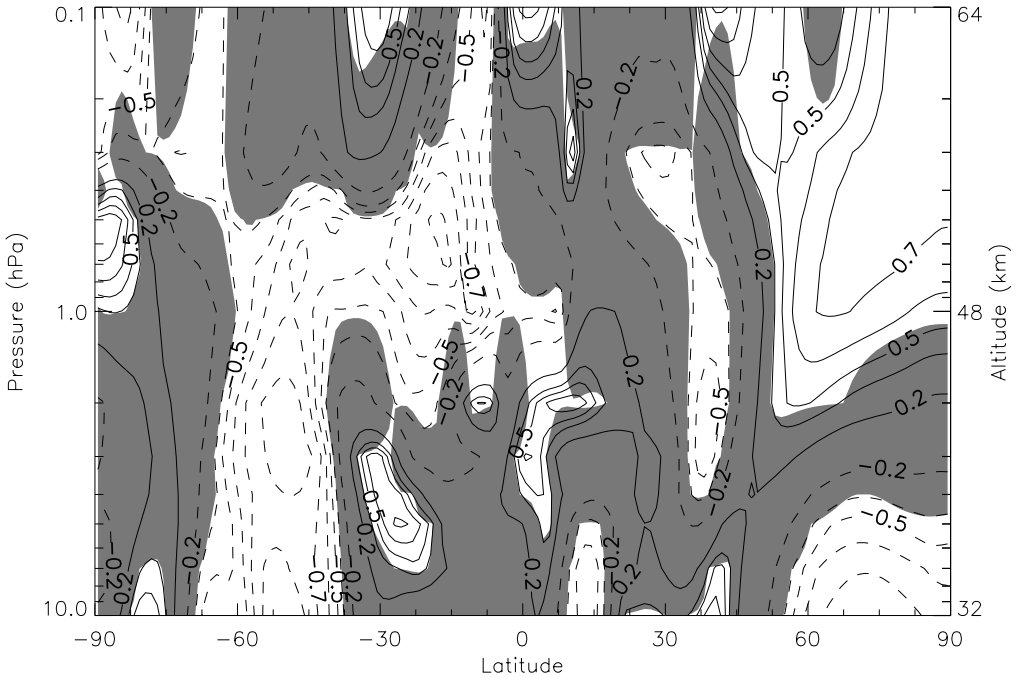

Figure 4.32: Correlation map of SPW1 V on 2003 - 45-70 with a lag of 0. Solid contour lines represent a positive correlation and dashed lines mean negative correlation. Shaded areas mean that the statistical significance of a correlation point is less than 95%.

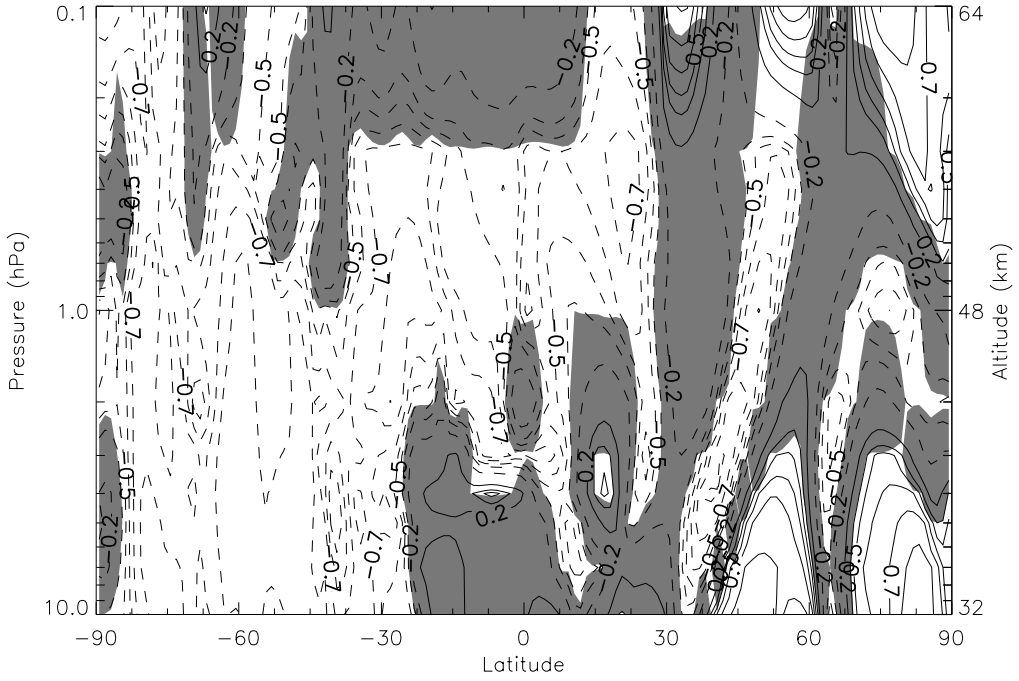

Figure 4.33: Correlation map of SPW2 U on 2003 - 45-70 with a lag of 0. Solid contour lines represent a positive correlation and dashed lines mean negative correlation. Shaded areas mean that the statistical significance of a correlation point is less than 95%.

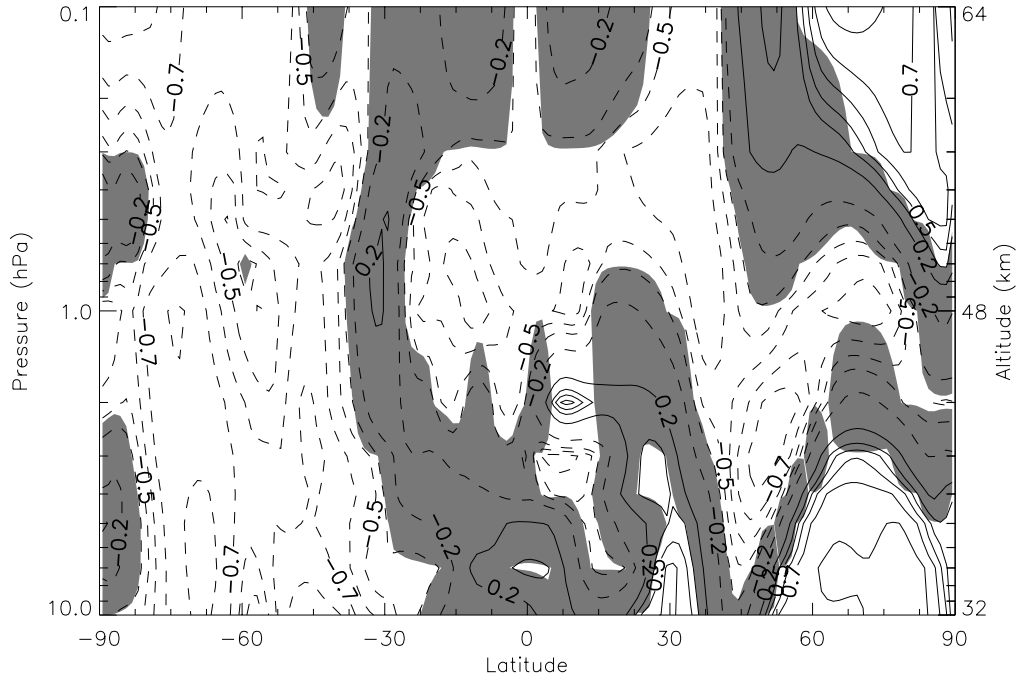

Figure 4.34: Correlation map of SPW2 V on 2003 - 45-70 with a lag of 0. Solid contour lines represent a positive correlation and dashed lines mean negative correlation. Shaded areas mean that the statistical significance of a correlation point is less than 95%.

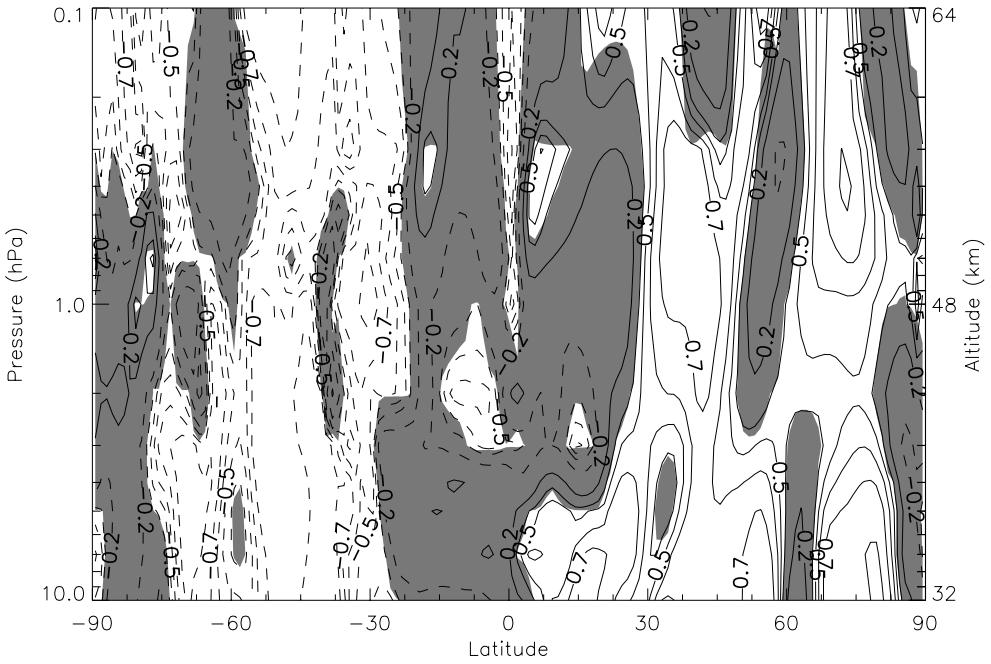

Figure 4.35: Correlation map of SPW3 U on 2003 - 45-70 for lag=0

Correlation map of SPW3 U on 2003 - 45-70 with a lag of 0. Solid contour lines represent a positive correlation and dashed lines mean negative correlation. Shaded areas mean that the statistical significance of a correlation point is less than 95%.

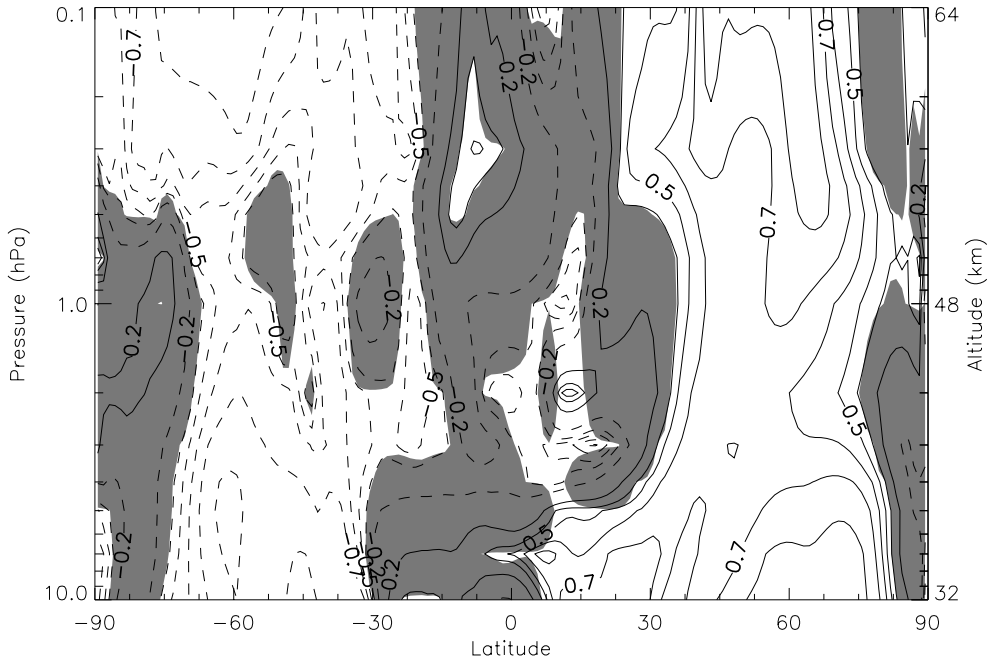

Figure 4.36: Correlation map of SPW3 V on 2003 - 45-70 with a lag of 0. Solid contour lines represent a positive correlation and dashed lines mean negative correlation. Shaded areas mean that the statistical significance of a correlation point is less than 95%.

4.2.3 2004 events

4.2.3.1 2004 - 10-50

The next event analyzed in more details is actually a long period between days 10-50 in 2004. As it can be seen on Figure 4.37, in this period SPMR 12hW1 data has a sharp increase and then starts decreasing again but with a much smaller gradient. Figure 4.38 shows correlation between the SPW fields at different latitude slices and different lags. Keeping in mind that filled symbols mean that the correlation is statistically significant with a confidence of least 95%, it can easily be seen that this event is of interest. Specially by noting that, according to Table 2.1, there was a SSW event on January 7th, 2004, right before this event started being analyzed.

By inspecting figures 4.39 and 4.40, which correlate SPW1 U and V respectively, it can be seen an extremely strong (at points almost perfect) correlation dominating most of the winter hemisphere at mid to high latitudes and all levels.

SPW2 U correlation, shown by Figure 4.41 depicts a narrow region of strong anti-correlation around the region where SPW2 peaks, and then a very strong positive correlation northward. Figure 4.42 shows the SPW2 V correlation and most of the significant correlation is region is actually given by a strong positive correlation in the mid to high latitudes.

Figure 4.43 and Figure 4.44 show the correlation of SPW3 U and V respectively. Both components show a strong anti-correlation in the lower levels, up to 3hPa, and then strong correlation above that in most of the winter hemisphere.

The structure of the correlation of the SPW U fields for lag=0,-1,-2 shown by figures C.13, C.15 and C.17 is basically static for the different lags. This is the same case for figures C.14, C.16 and C.18 which show the SPW V correlations. This indicates that this event is indeed very solid, with strong correlation that last for a long period of time.

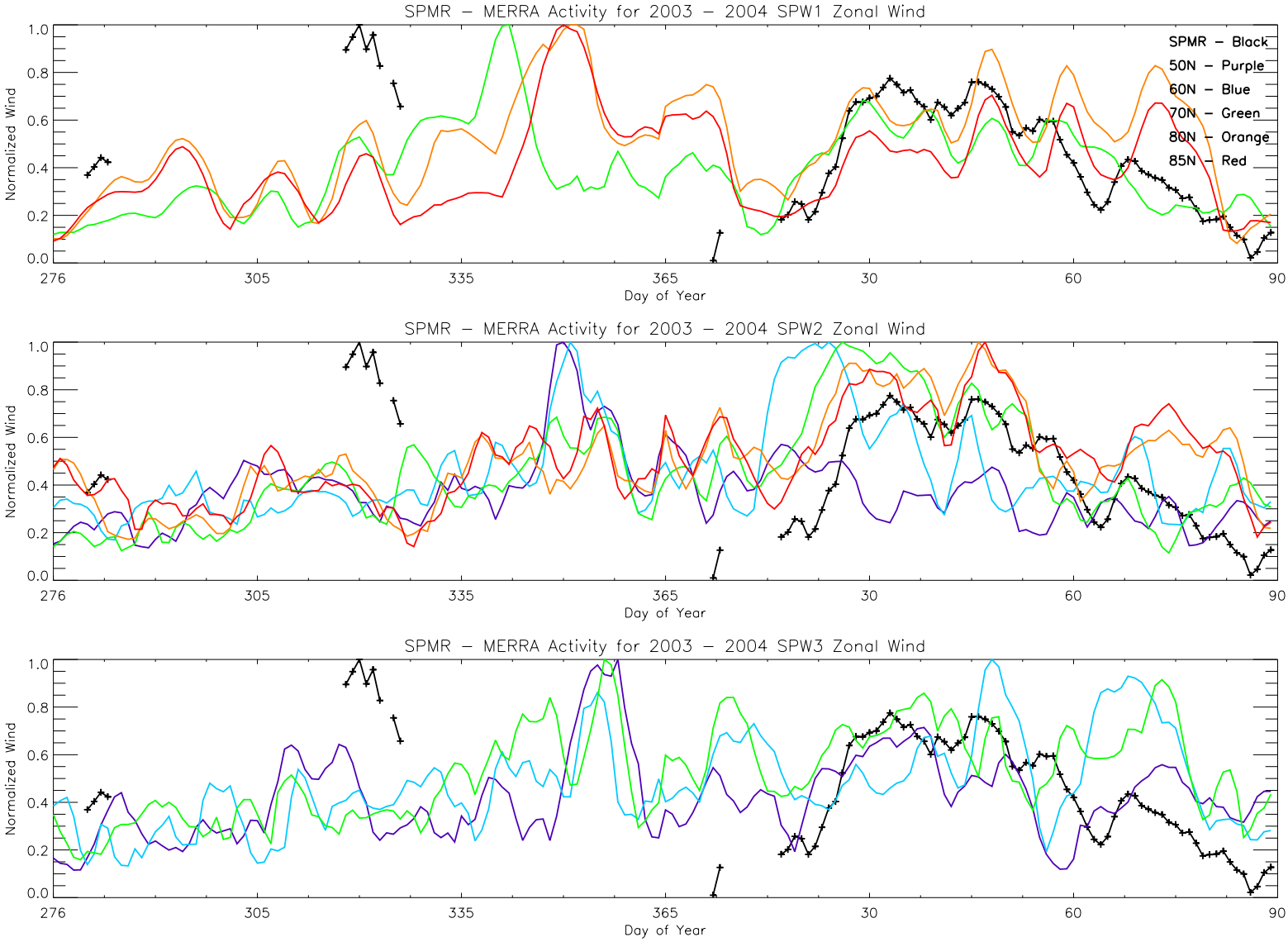

Figure 4.37: Top panel shows normalized SPW1 zonal wind and SPMR data. Middle panel shows SPW2 and SPMR, and bottom panel shows SPW3 and SPMR data. SPMR data shown by the black line, MERRA at 50°N is purple, 60°N is blue, 70°N is green, 80°N is orange and 85°N is red. Data is from 2003-2004.

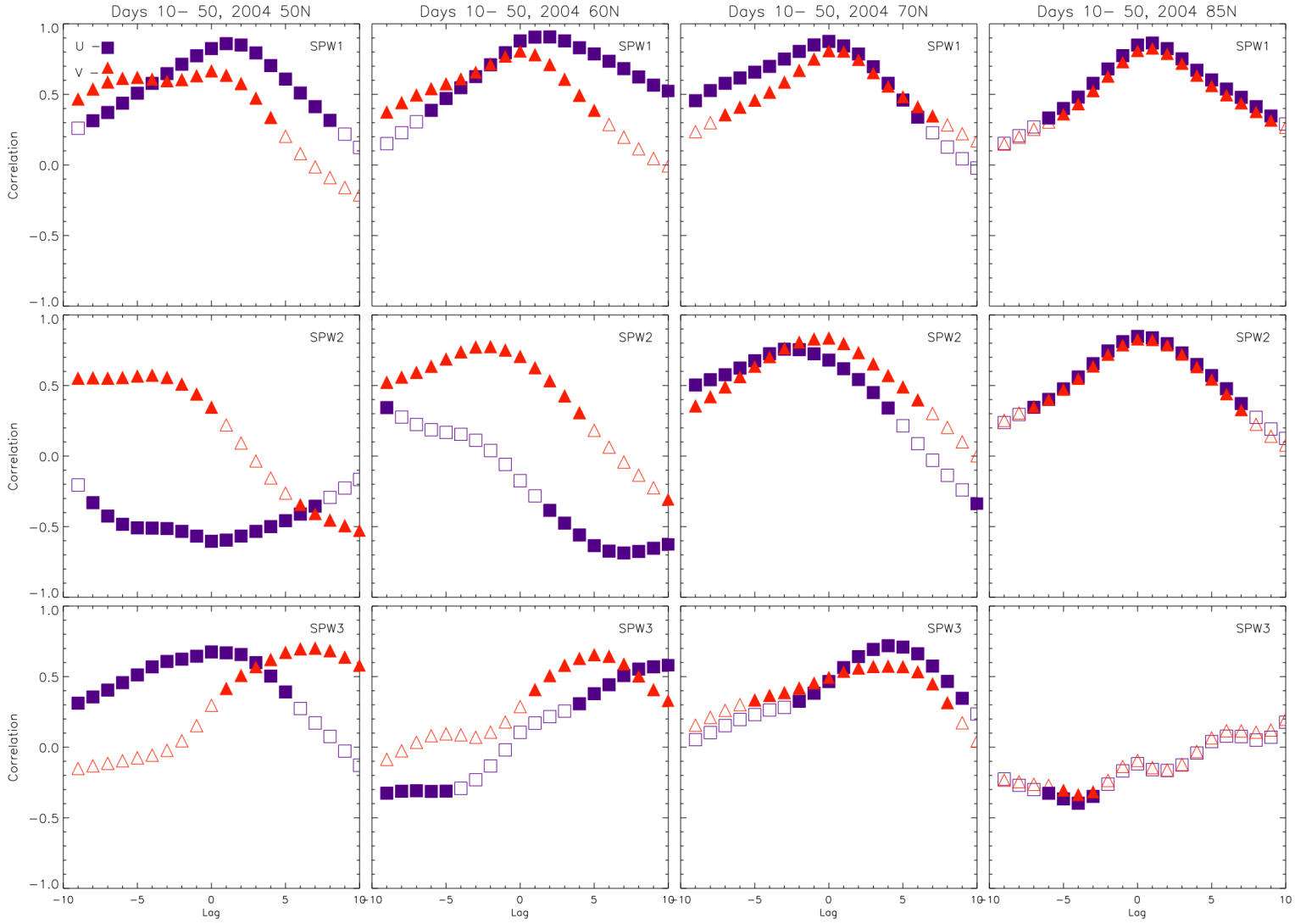

Figure 4.38: This figure shows the correlation between MERRA zonal and meridional winds and SPMR data in 2004, days 10-50 as a function of lag. Left column shows correlations using data from MERRA at 50°N, second column at 60°N, third column at 70°N and last column at 85°N. First row correlates the MERRA SPW1 components with 12hW1 from SPMR, middle row correlates MERRA SPW2 and bottom row correlates MERRA SPW3. Correlation of zonal winds is shown by blue squares and meridional winds by red triangles. Filled symbols mean that the statistical significance of a correlation point is equal or greater than 95%.

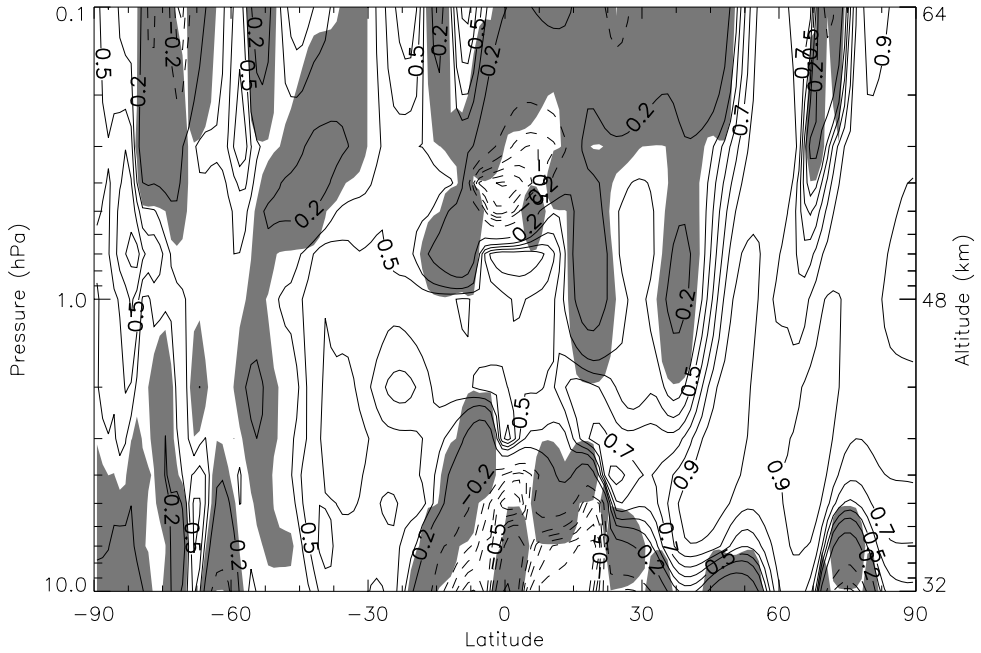

Figure 4.39: Correlation map of SPW1 U on 2004 - 10-50 with a lag of 0. Solid contour lines represent a positive correlation and dashed lines mean negative correlation. Shaded areas mean that the statistical significance of a correlation point is less than 95%.

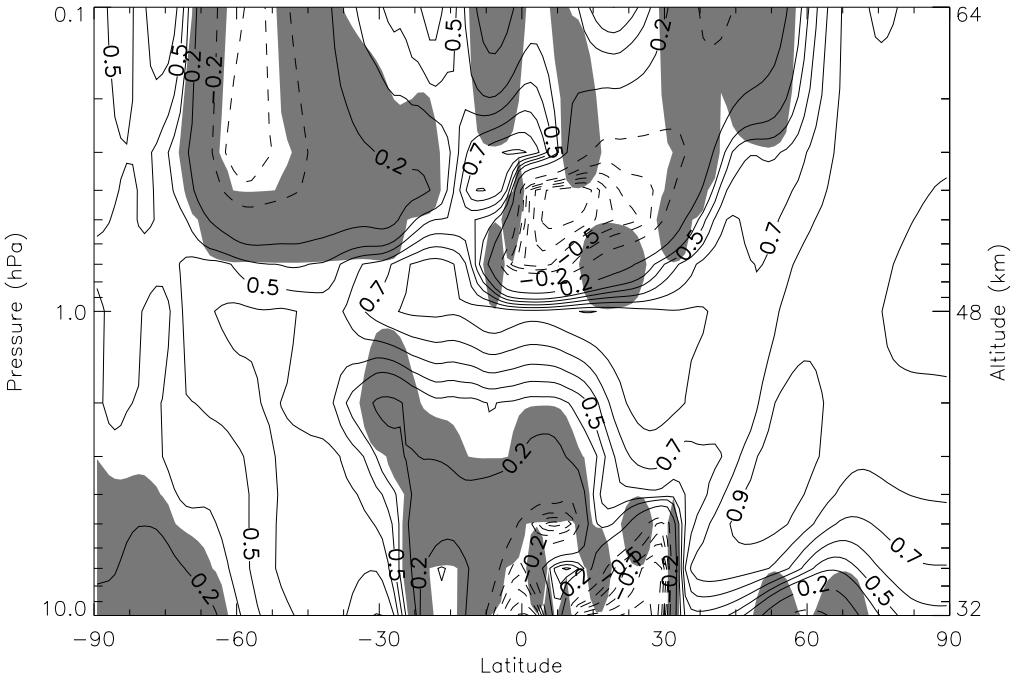

Figure 4.40: Correlation map of SPW1 V on 2004 - 10-50 with a lag of 0. Solid contour lines represent a positive correlation and dashed lines mean negative correlation. Shaded areas mean that the statistical significance of a correlation point is less than 95%.

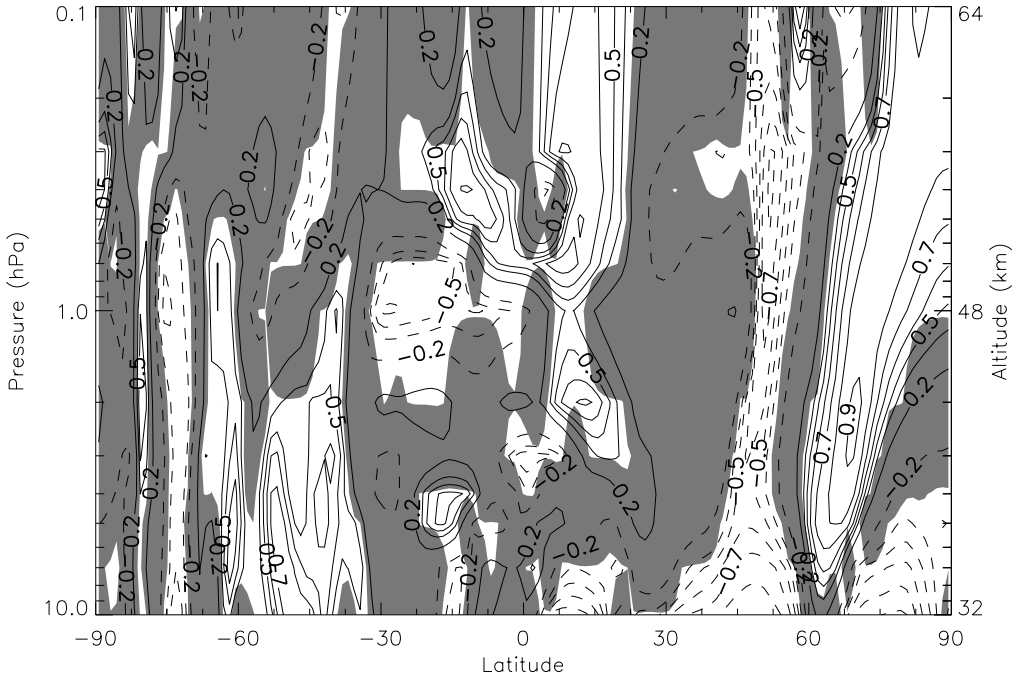

Figure 4.41: Correlation map of SPW2 U on 2004 - 10-50 with a lag of 0. Solid contour lines represent a positive correlation and dashed lines mean negative correlation. Shaded areas mean that the statistical significance of a correlation point is less than 95%.

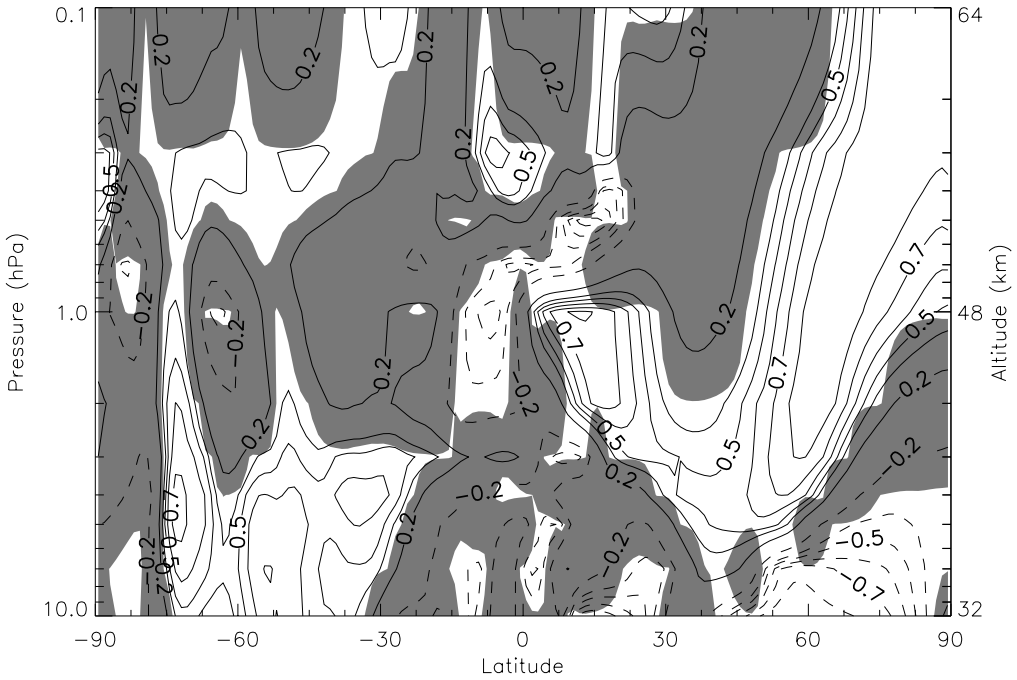

Figure 4.42: Correlation map of SPW2 V on 2004 - 10-50 with a lag of 0. Solid contour lines represent a positive correlation and dashed lines mean negative correlation. Shaded areas mean that the statistical significance of a correlation point is less than 95%.

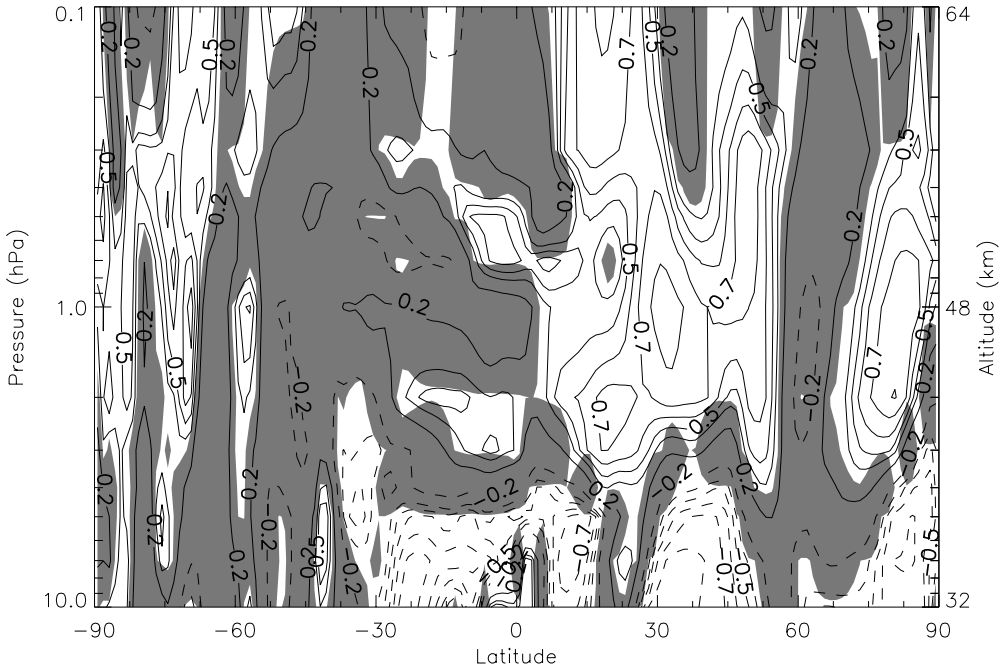

Figure 4.43: Correlation map of SPW3 U on 2004 - 10-50 for lag=0

Correlation map of SPW3 U on 2004 - 10-50 with a lag of 0. Solid contour lines represent a positive correlation and dashed lines mean negative correlation. Shaded areas mean that the statistical significance of a correlation point is less than 95%.

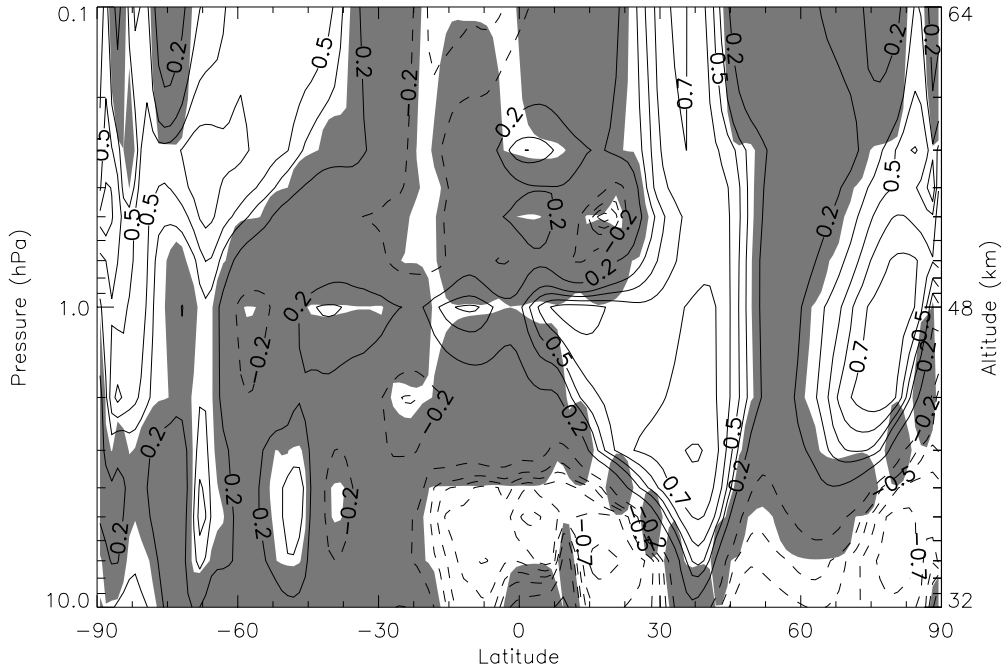

Figure 4.44: Correlation map of SPW3 V on 2004 - 10-50 with a lag of 0. Solid contour lines represent a positive correlation and dashed lines mean negative correlation. Shaded areas mean that the statistical significance of a correlation point is less than 95%.

4.2.3.2 2004 - 55-85

The next event to be studied in the 2003-2004 austral summer season spans a long period between days 55 and 85.

Figures 4.45 and 4.46, which represent the correlations with SPW1 U and V, respectively, show a strong positive correlation that covers most of the winter hemisphere.

Figures 4.47 and 4.48 correlate 12hW1 with SPW2 U and V, respectively, show a very similar structure for both components. A positive correlation can be observed at mid-latitudes and mid-altitudes, and also at high latitudes and high altitudes (close to 64km), while a negative correlation can be seen in the high latitudes and low altitudes. This is related to the motion of SPW2 both vertically and horizontally during this period.

Figures 4.49 and 4.50 show the correlation with SPW3 U and V. On this event, there is no significant correlation with this component of the SPW.

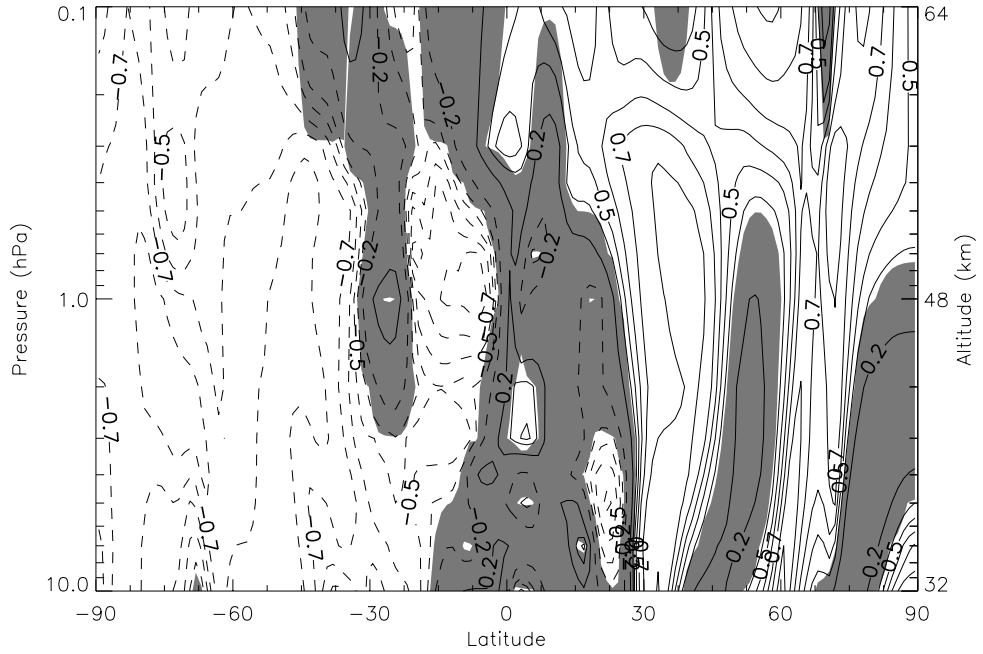

Figure 4.45: Correlation map of SPW1 U on 2004 - 55-85 with a lag of 0. Solid contour lines represent a positive correlation and dashed lines mean negative correlation. Shaded areas mean that the statistical significance of a correlation point is less than 95%.

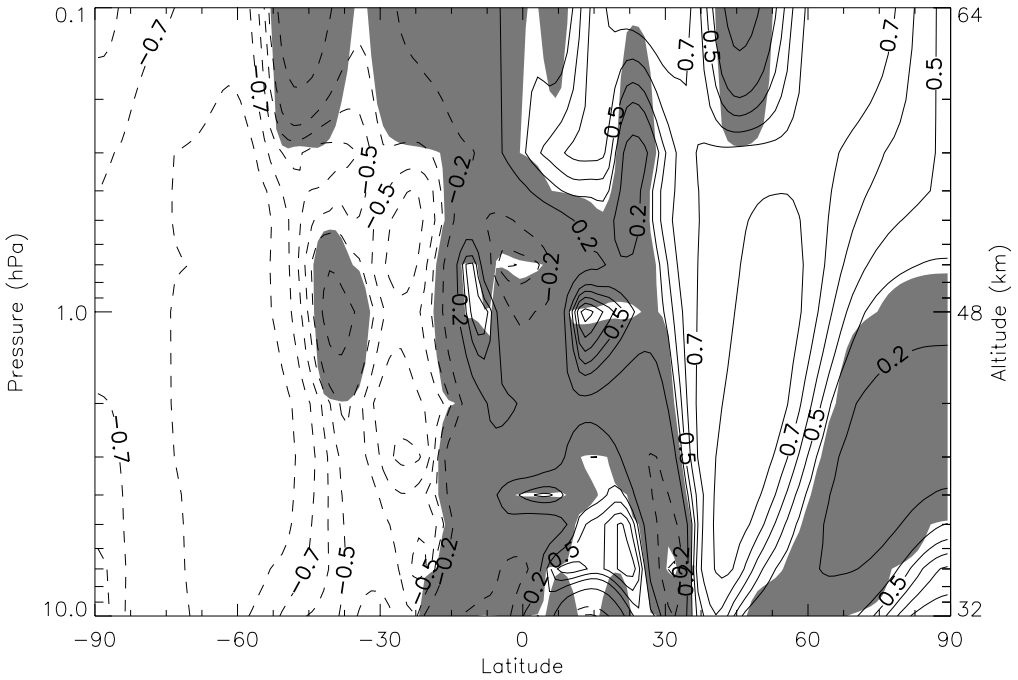

Figure 4.46: Correlation map of SPW1 V on 2004 - 55-85 with a lag of 0. Solid contour lines represent a positive correlation and dashed lines mean negative correlation. Shaded areas mean that the statistical significance of a correlation point is less than 95%.

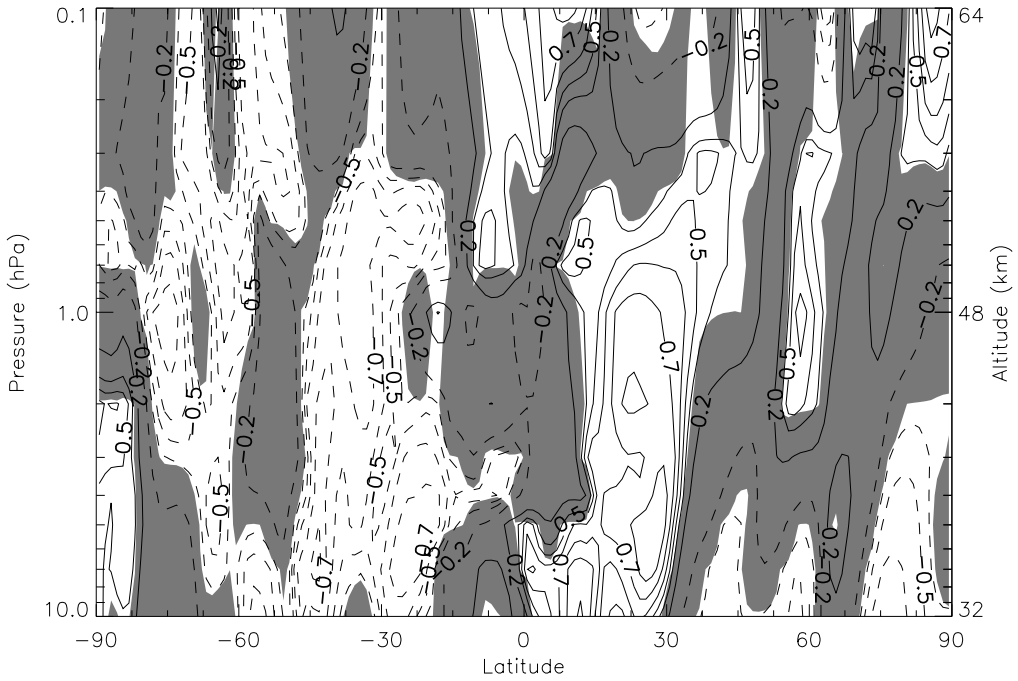

Figure 4.47: Correlation map of SPW2 U on 2004 - 55-85 with a lag of 0. Solid contour lines represent a positive correlation and dashed lines mean negative correlation. Shaded areas mean that the statistical significance of a correlation point is less than 95%.

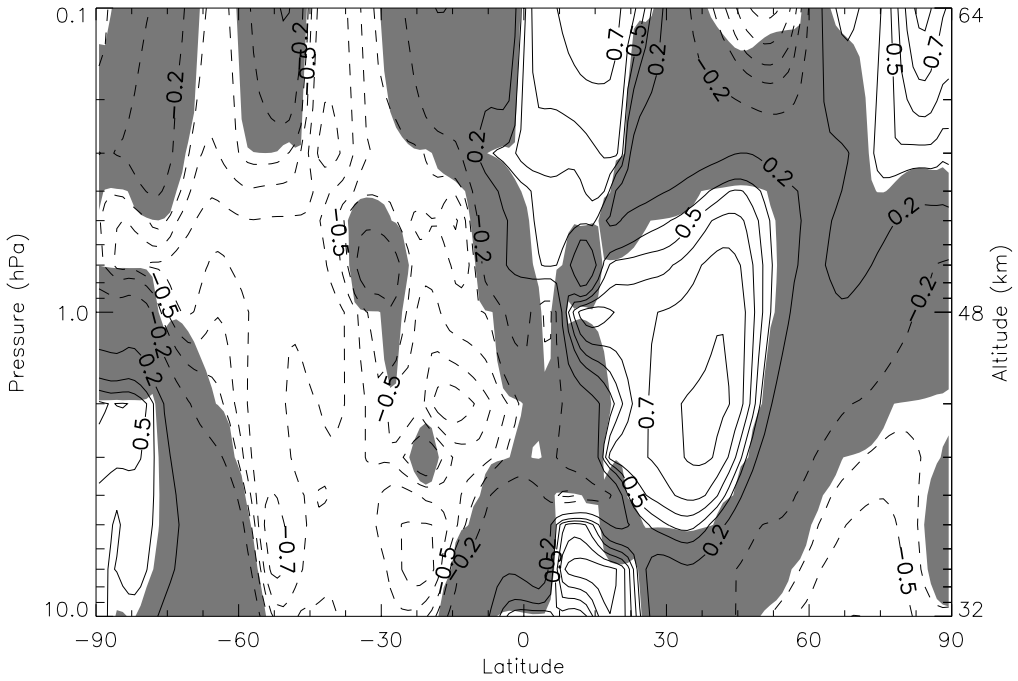

Figure 4.48: Correlation map of SPW2 V on 2004 - 55-85 with a lag of 0. Solid contour lines represent a positive correlation and dashed lines mean negative correlation. Shaded areas mean that the statistical significance of a correlation point is less than 95%.

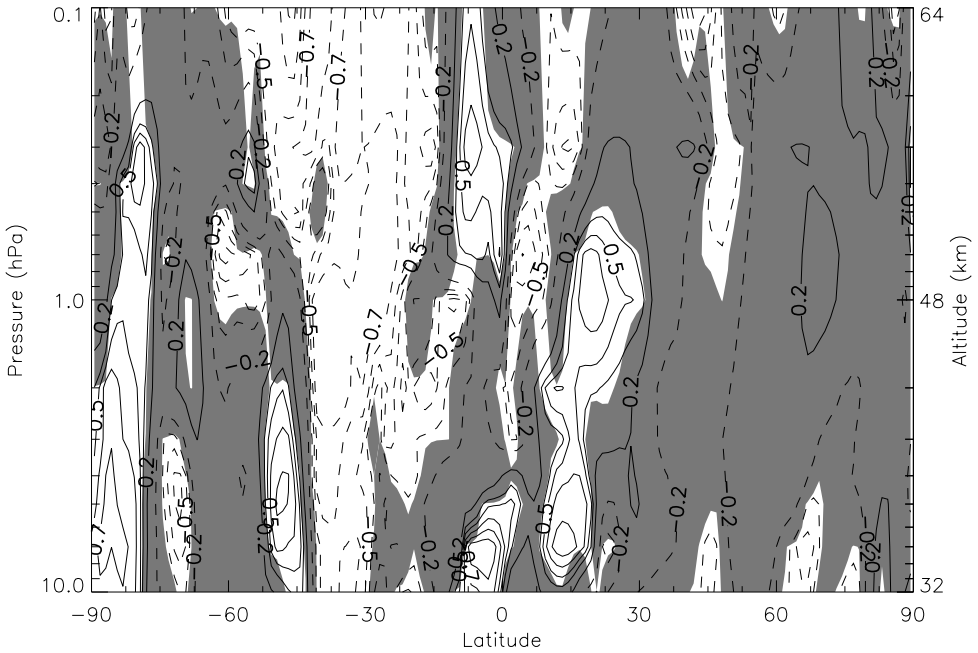

Figure 4.49: Correlation map of SPW3 U on 2004 - 55-85 for lag=0

Correlation map of SPW3 U on 2004 - 55-85 with a lag of 0. Solid contour lines represent a positive correlation and dashed lines mean negative correlation. Shaded areas mean that the statistical significance of a correlation point is less than 95%.

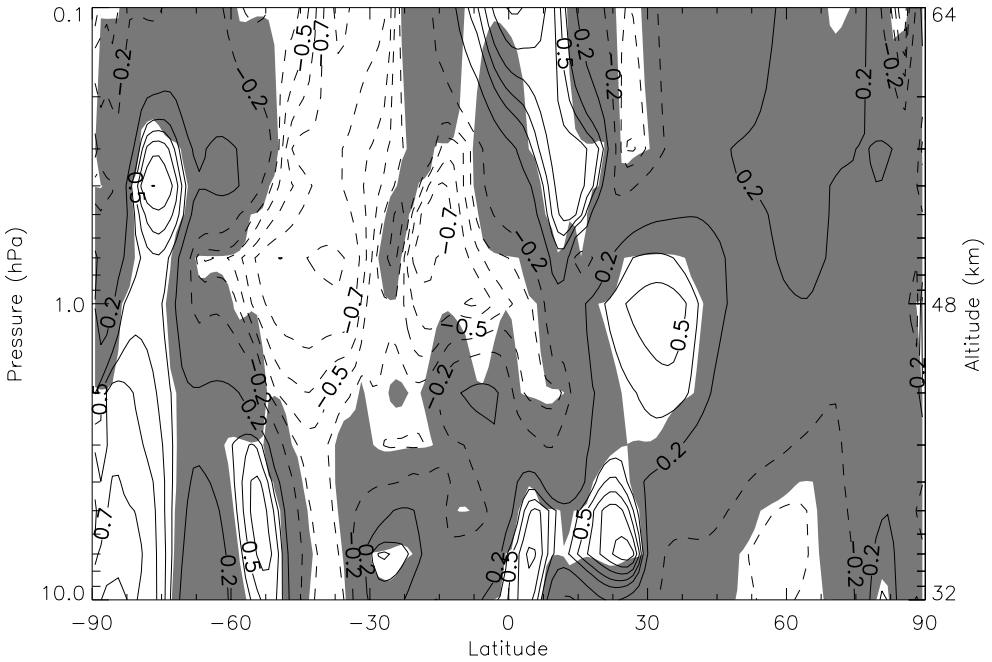

Figure 4.50: Correlation map of SPW3 V on 2004 - 55-85 with a lag of 0. Solid contour lines represent a positive correlation and dashed lines mean negative correlation. Shaded areas mean that the statistical significance of a correlation point is less than 95%.

4.2.4 2005 events

4.2.4.1 2005 - 50-75

The next event to be analyzed happened between days 50 and 75 at the end of the austral summer in 2005. Figure 4.51 shows the normalized amplitudes of 12hW1 and SPW1, SPW2 and SPW3.

Figure 4.52 shows that the correlation between 12hW1 and SPW1 U for this event is positive but happens at lower altitudes than where SPW1 usually peaks. Figure 4.53 shows a similar structure but with a larger positive correlation region in lower altitudes.

Figures 4.54 and 4.55 show the correlation with SPW2 U and V. Both components show a strong anti-correlation at lower altitudes and mid-to-high latitudes.

Figures 4.56 and 4.57 represent the correlation between 12hW1 and SPW3 U and V, respectively. This is the most interesting feature of this event because both components show a strong positive correlation covering a large region of the winter hemisphere, specifically where SPW3 peaks.

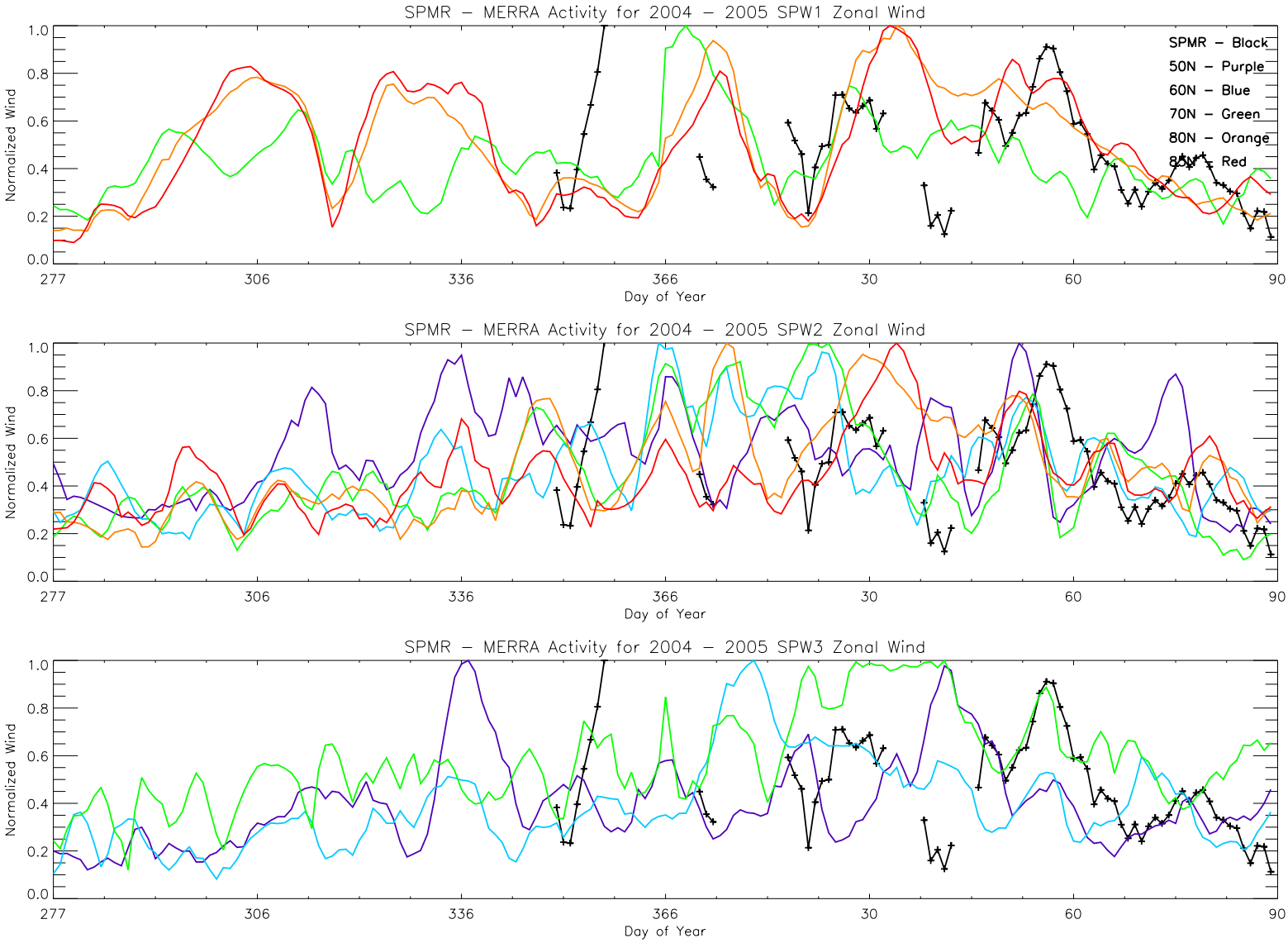

Figure 4.51: Top panel shows normalized SPW1 zonal wind and SPMR data. Middle panel shows SPW2 and SPMR, and bottom panel shows SPW3 and SPMR data. SPMR data shown by the black line, MERRA at 50°N is purple, 60°N is blue, 70°N is green, 80°N is orange and 85°N is red. Data is from 2004-2005.

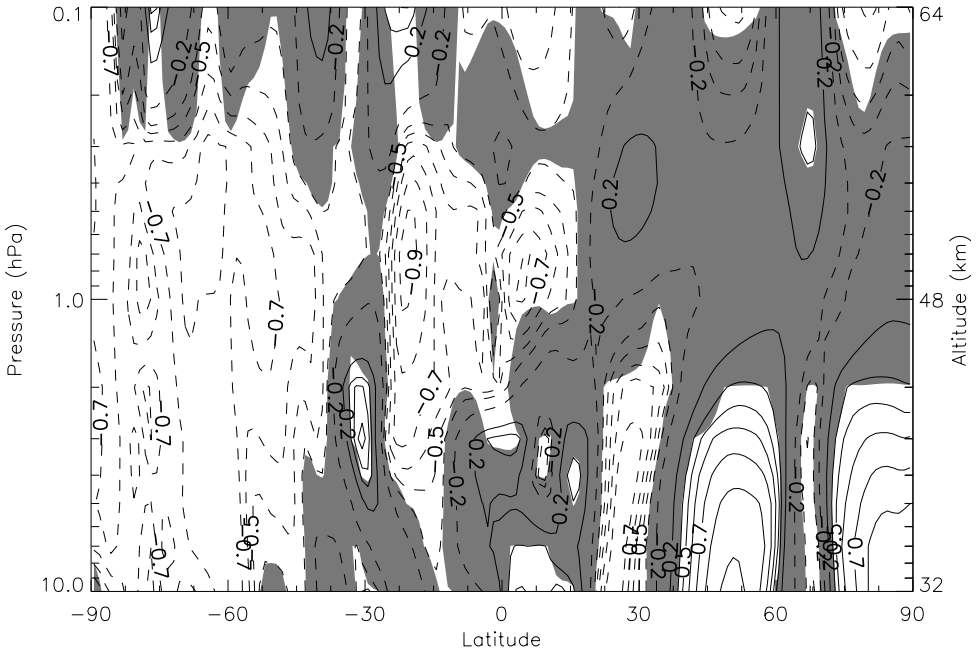

Figure 4.52: Correlation map of SPW1 U on 2005 - 50-75 with a lag of 0. Solid contour lines represent a positive correlation and dashed lines mean negative correlation. Shaded areas mean that the statistical significance of a correlation point is less than 95%.

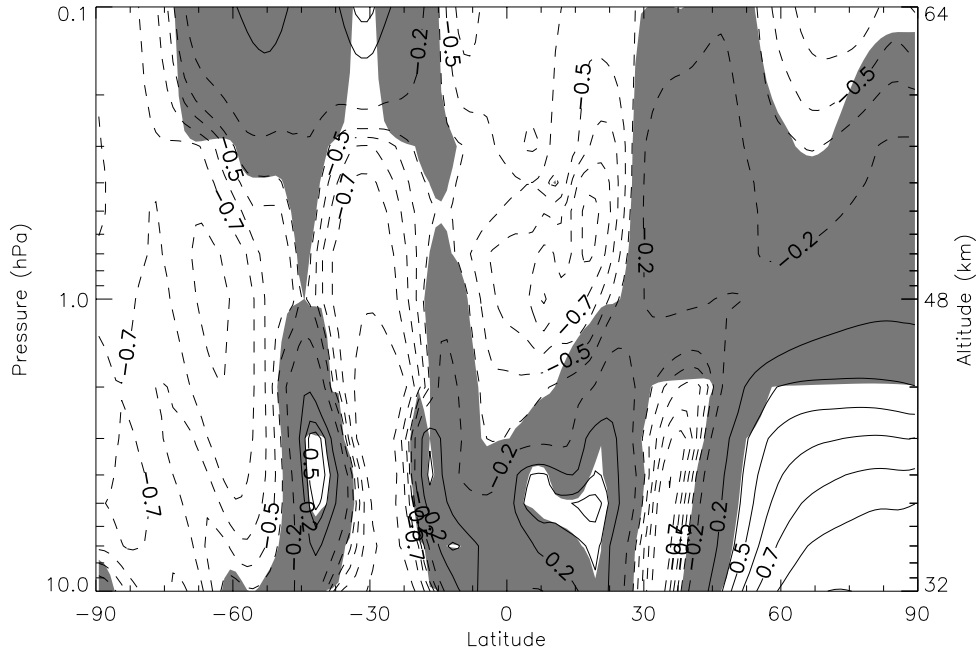

Figure 4.53: Correlation map of SPW1 V on 2005 - 50-75 with a lag of 0. Solid contour lines represent a positive correlation and dashed lines mean negative correlation. Shaded areas mean that the statistical significance of a correlation point is less than 95%.

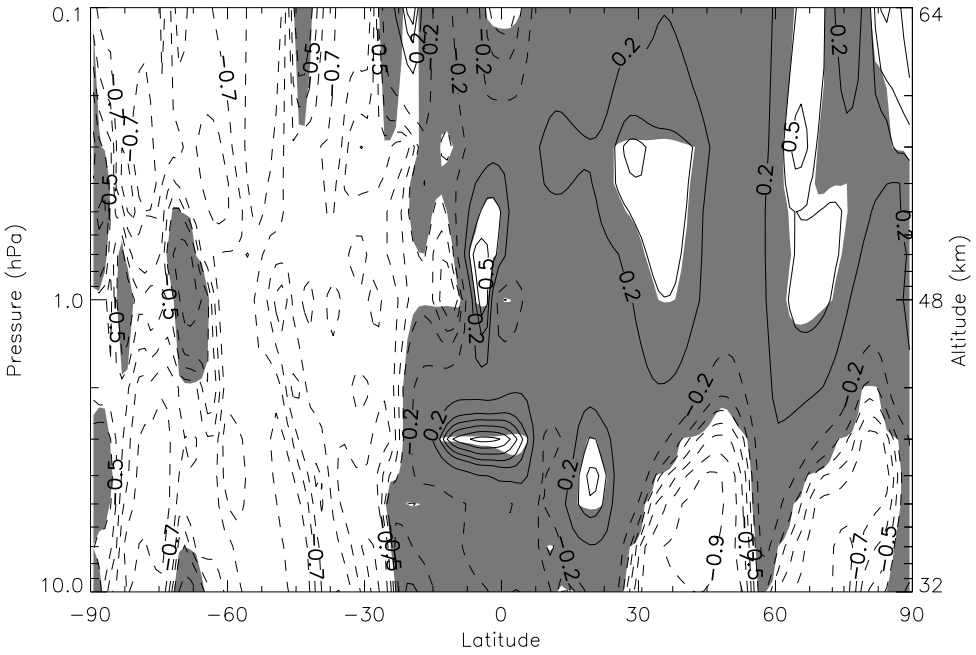

Figure 4.54: Correlation map of SPW2 U on 2005 - 50-75 with a lag of 0. Solid contour lines represent a positive correlation and dashed lines mean negative correlation. Shaded areas mean that the statistical significance of a correlation point is less than 95%.

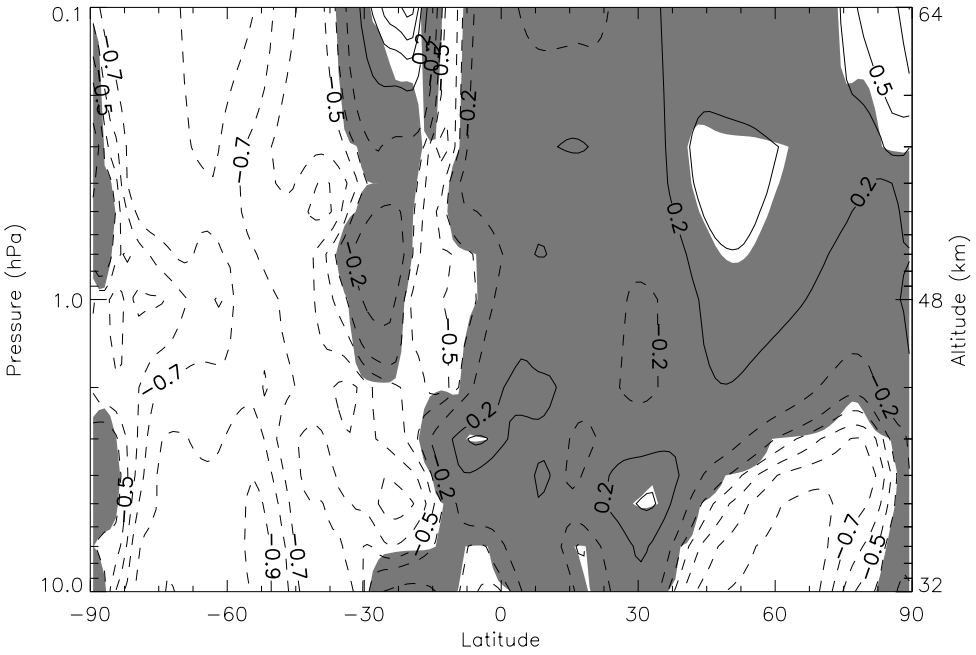

Figure 4.55: Correlation map of SPW2 V on 2005 - 50-75 with a lag of 0. Solid contour lines represent a positive correlation and dashed lines mean negative correlation. Shaded areas mean that the statistical significance of a correlation point is less than 95%.

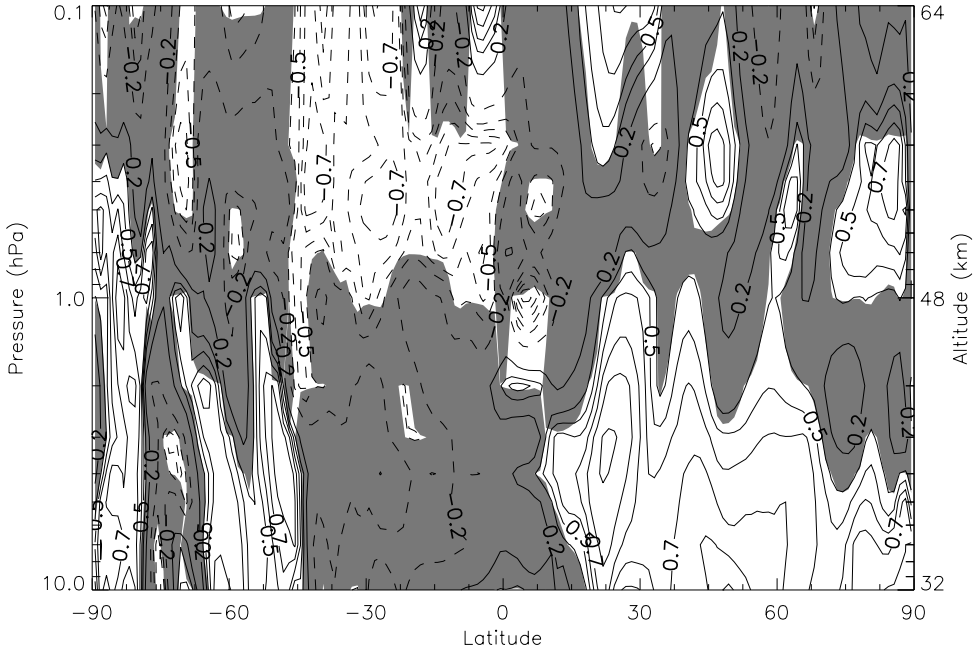

Figure 4.56: Correlation map of SPW3 U on 2005 - 50-75 for lag=0

Correlation map of SPW3 U on 2005 - 50-75 with a lag of 0. Solid contour lines represent a positive correlation and dashed lines mean negative correlation. Shaded areas mean that the statistical significance of a correlation point is less than 95%.

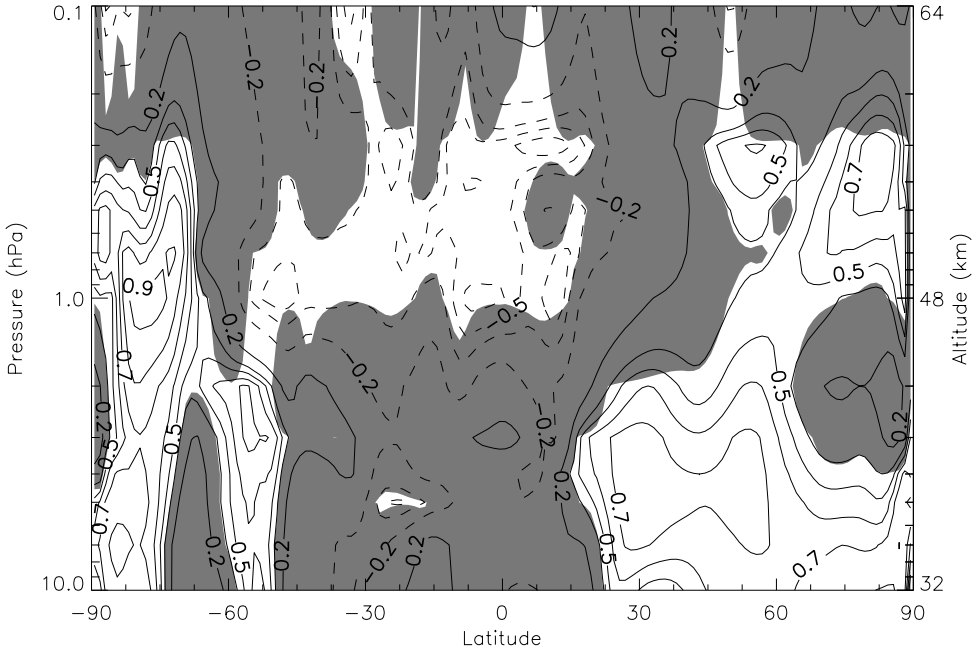

Figure 4.57: Correlation map of SPW3 V on 2005 - 50-75 with a lag of 0. Solid contour lines represent a positive correlation and dashed lines mean negative correlation. Shaded areas mean that the statistical significance of a correlation point is less than 95%.

4.2.4.2 2005 - 277-291

The next event to be considered happened in the beginning of the 2005-2006 austral summer season, during days 277 through 291 of 2005. Figure 4.58 shows the normalized behavior of 12hW1 and SPW components during this season.

Figures 4.59 and 4.60 show that the correlation between 12hW1 and SPW1 U and V is extremely strong (with correlations as high as 0.9) and covers most of the winter hemisphere.

Figures 4.61 and 4.62 shows that SPW2 U and V have regions with positive and negative correlation in the winter hemisphere, however these regions are relatively small and do not seem to effectively impact the variability observed on 12hW1.

Figures 4.63 and 4.64 depict the correlation between 12hW1 and SPW3 U and V components. Both plots show a region of strong positive correlation in the mid-latitudes, where SPW3 peaks.

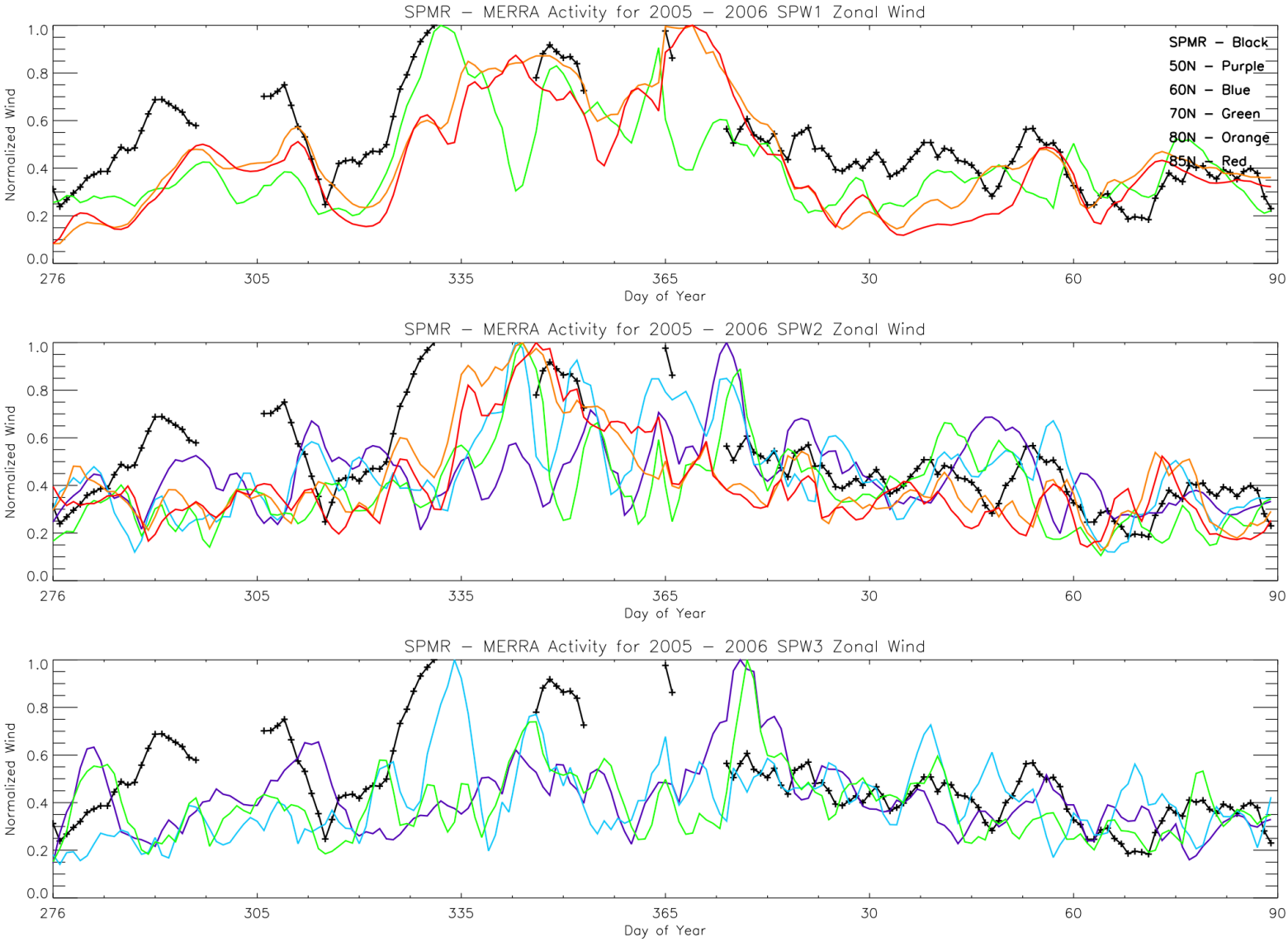

Figure 4.58: Top panel shows normalized SPW1 zonal wind and SPMR data. Middle panel shows SPW2 and SPMR, and bottom panel shows SPW3 and SPMR data. SPMR data shown by the black line, MERRA at 50°N is purple, 60°N is blue, 70°N is green, 80°N is orange and 85°N is red. Data is from 2005-2006.

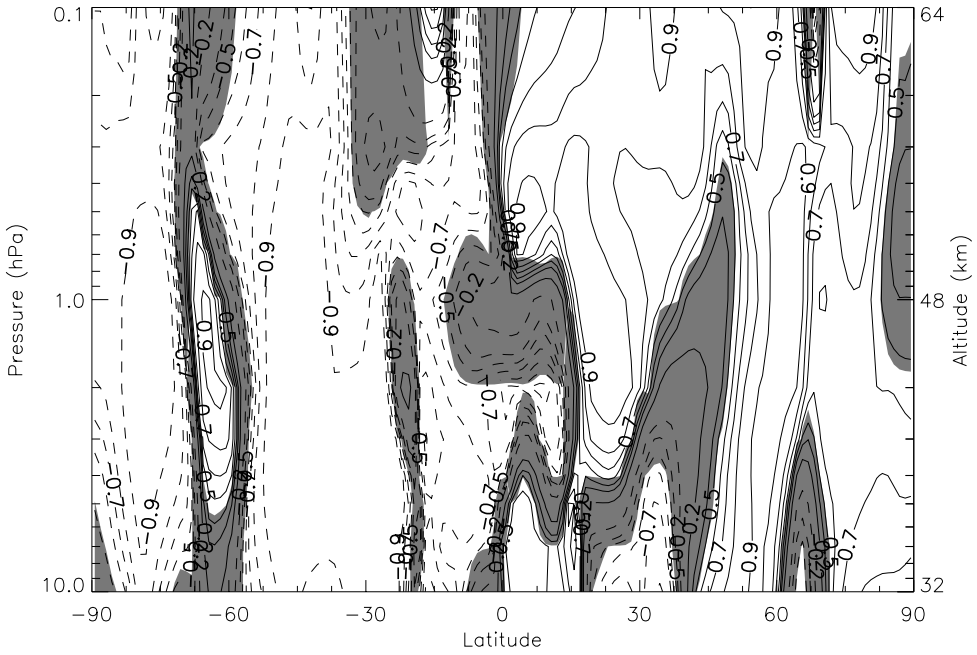

Figure 4.59: Correlation map of SPW1 U on 2005 - 277-291 with a lag of 0. Solid contour lines represent a positive correlation and dashed lines mean negative correlation. Shaded areas mean that the statistical significance of a correlation point is less than 95%.

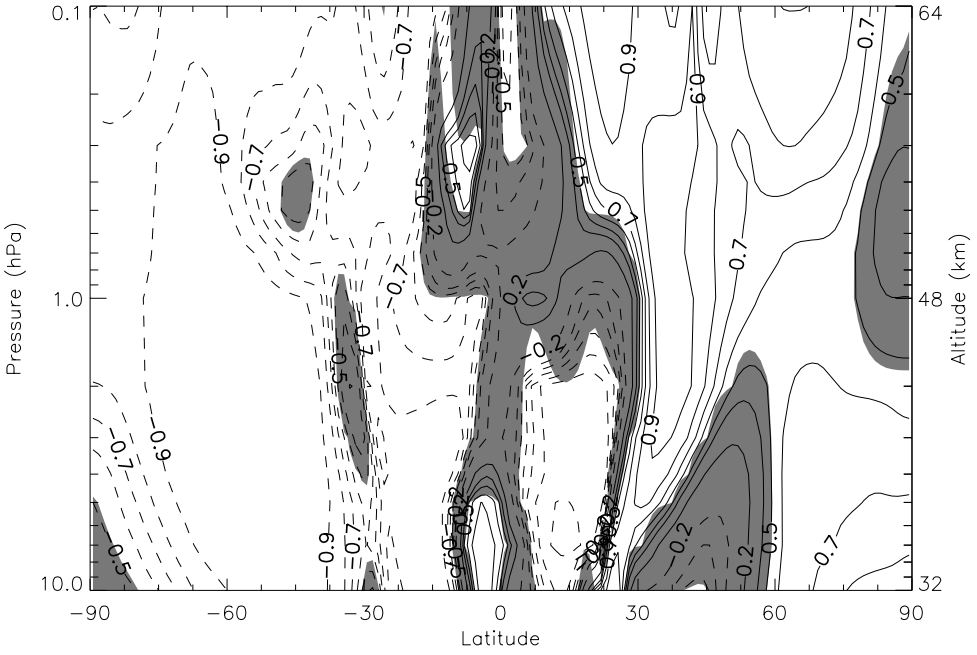

Figure 4.60: Correlation map of SPW1 V on 2005 - 277-291 with a lag of 0. Solid contour lines represent a positive correlation and dashed lines mean negative correlation. Shaded areas mean that the statistical significance of a correlation point is less than 95%.

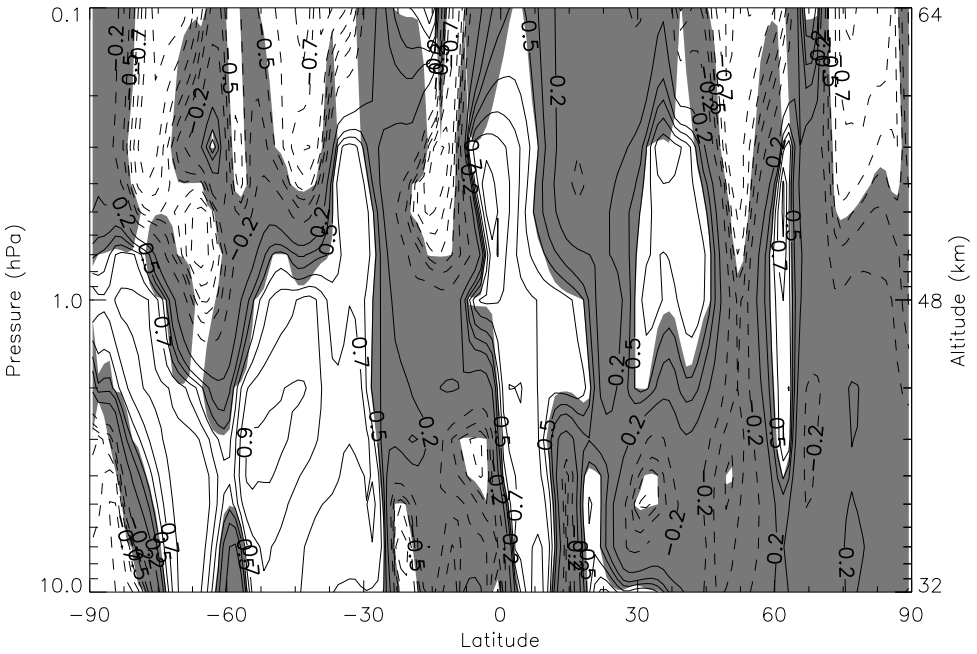

Figure 4.61: Correlation map of SPW2 U on 2005 - 277-291 with a lag of 0. Solid contour lines represent a positive correlation and dashed lines mean negative correlation. Shaded areas mean that the statistical significance of a correlation point is less than 95%.

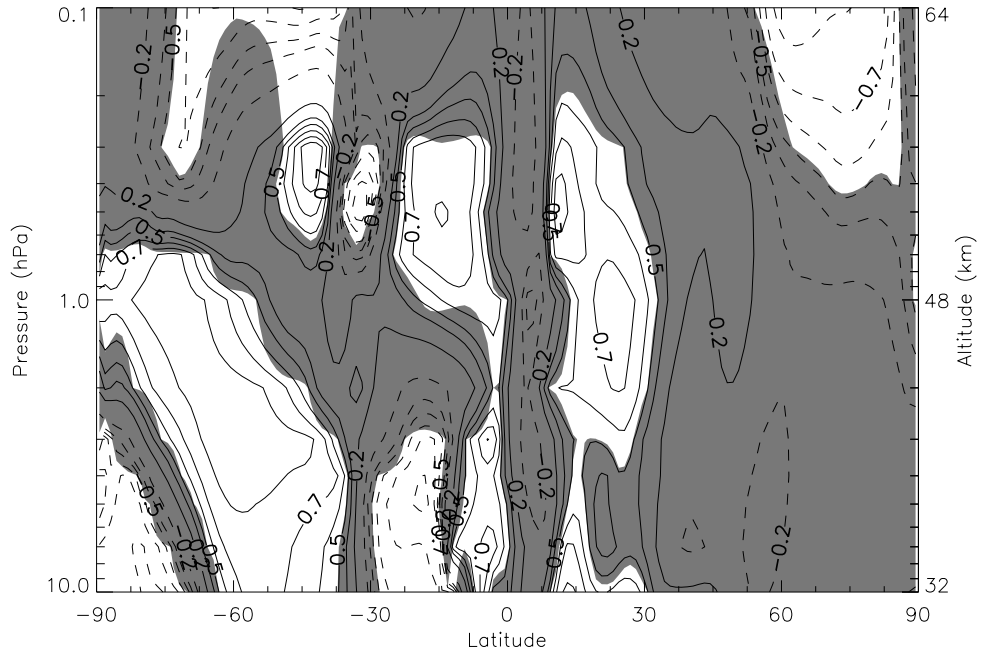

Figure 4.62: Correlation map of SPW2 V on 2005 - 277-291 with a lag of 0. Solid contour lines represent a positive correlation and dashed lines mean negative correlation. Shaded areas mean that the statistical significance of a correlation point is less than 95%.

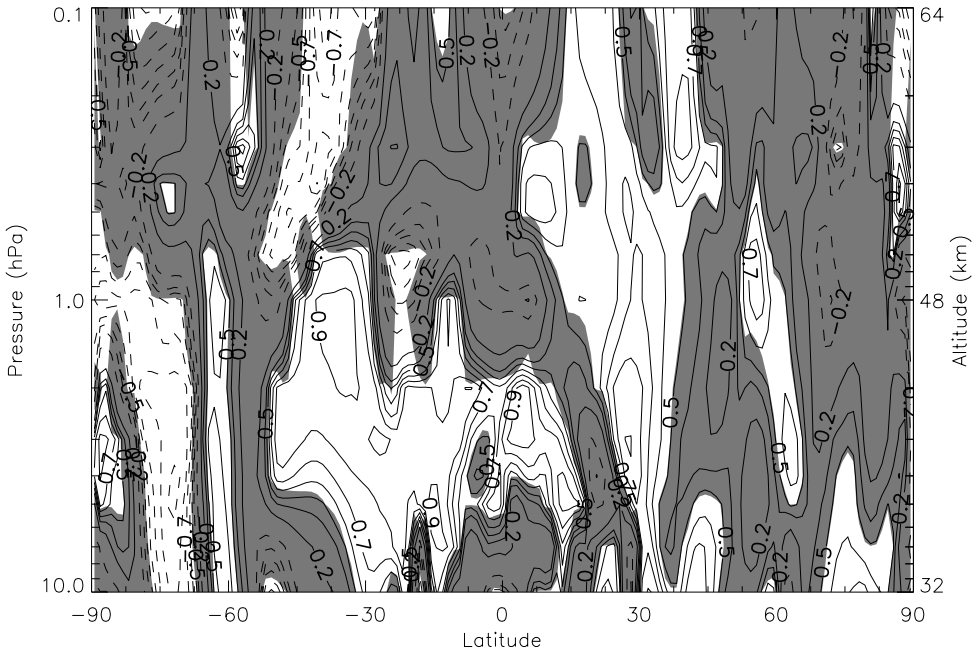

Figure 4.63: Correlation map of SPW3 U on 2005 - 277-291 for lag=0

Correlation map of SPW3 U on 2005 - 277-291 with a lag of 0. Solid contour lines represent a positive correlation and dashed lines mean negative correlation. Shaded areas mean that the statistical significance of a correlation point is less than 95%.

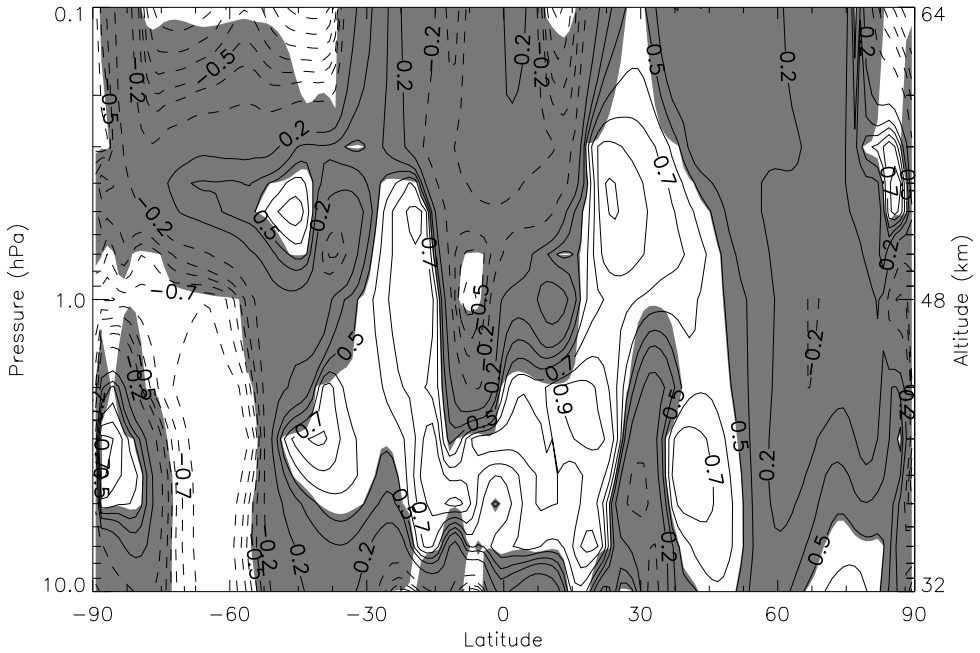

Figure 4.64: Correlation map of SPW3 V on 2005 - 277-291 with a lag of 0. Solid contour lines represent a positive correlation and dashed lines mean negative correlation. Shaded areas mean that the statistical significance of a correlation point is less than 95%.

4.2.4.3 2005 - 317-333

Another event of interest happened during the days 317-333 of 2005. During this period SPMR 12hW1 increases rapidly to what ends up being its highest amplitude of the whole season, as can be seen from Figure 4.58. Then Figure 4.65 shows very significant correlation results for SPW1, SPW2 and SPW3.

Figures 4.66 and 4.67 show the correlation of SPW1 U and V respectively. The figures clearly show a very strong correlation that dominates almost all of the winter hemisphere.

Around the region where SPW2 peaks, figures 4.68 and 4.69 show that there's a strong anti-correlation. Moving northward there's a smaller region of strong positive correlation.

Also in the latitudes where SPW3 peaks, figures 4.70 and 4.71 show a strong positive correlation dominating most of the mid to high latitudes of the winter hemisphere.

The analysis performed for SPW U negative lags, as shown by figures C.19, C.21 and C.23, show a very similar structure. SPW1 has a strong positive correlation dominating most of the winter hemisphere. SPW2 has a region of strong anti-correlation around its peak and then a region of strong positive correlation close to the North Pole. SPW3 has most a strong positive correlation covering the majority of the winter hemisphere. Figures C.20, C.22 and C.24 show the exact same behavior for the SPW V correlation for negative lags.

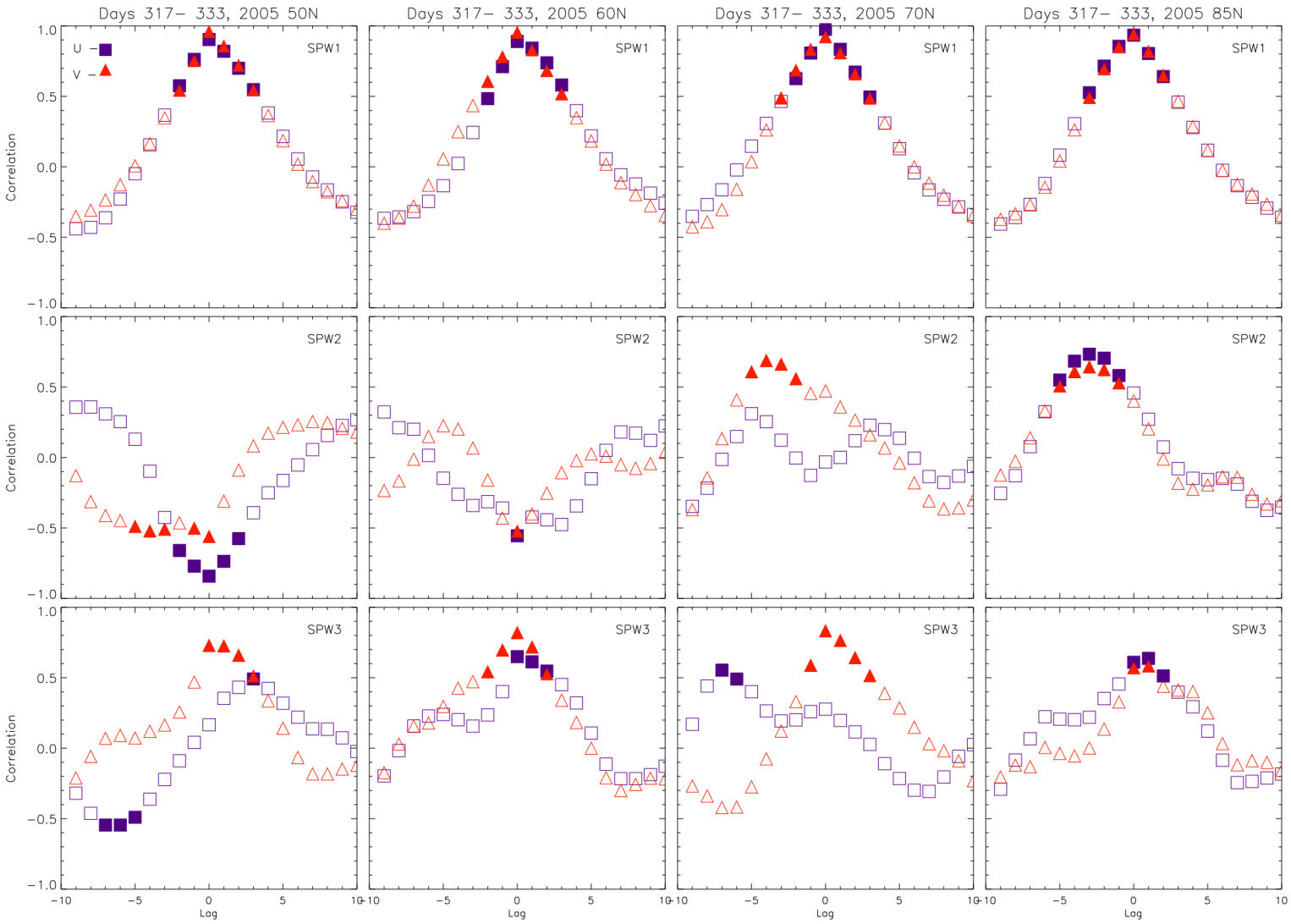

Figure 4.65: This figure shows the correlation between MERRA zonal and meridional winds and SPMR data in 2005, days 317-333 as a function of lag. Left column shows correlations using data from MERRA at 50°N, second column at 60°N, third column at 70°N and last column at 85°N. First row correlates the MERRA SPW1 components with 12hW1 from SPMR, middle row correlates MERRA SPW2 and bottom row correlates MERRA SPW3. Correlation of zonal winds is shown by blue squares and meridional winds by red triangles. Filled symbols mean that the statistical significance of a correlation point is equal or greater than 95%.

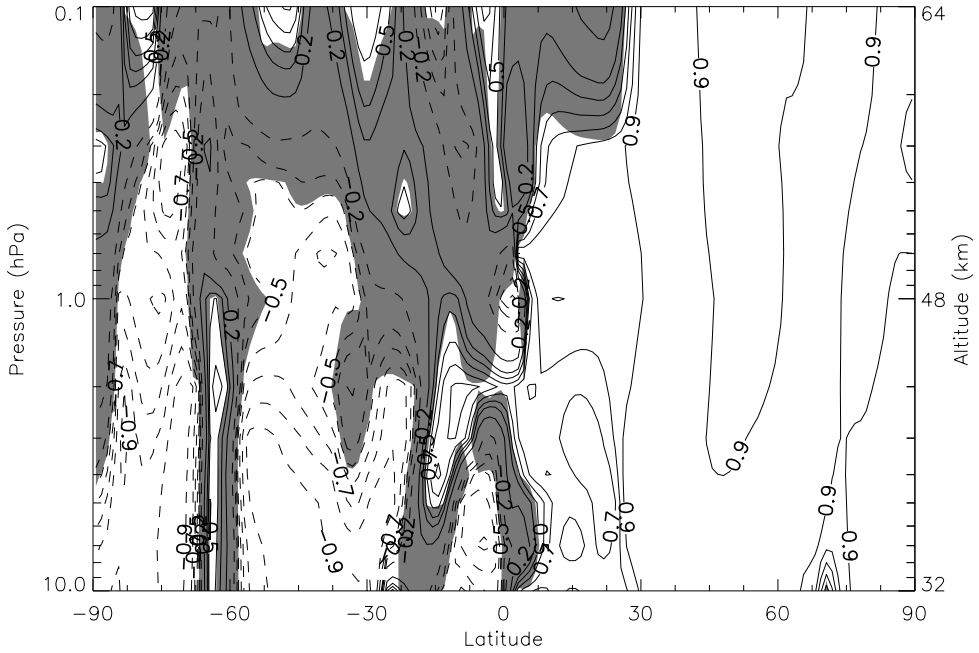

Figure 4.66: Correlation map of SPW1 U on 2005 - 317-333 with a lag of 0. Solid contour lines represent a positive correlation and dashed lines mean negative correlation. Shaded areas mean that the statistical significance of a correlation point is less than 95%.

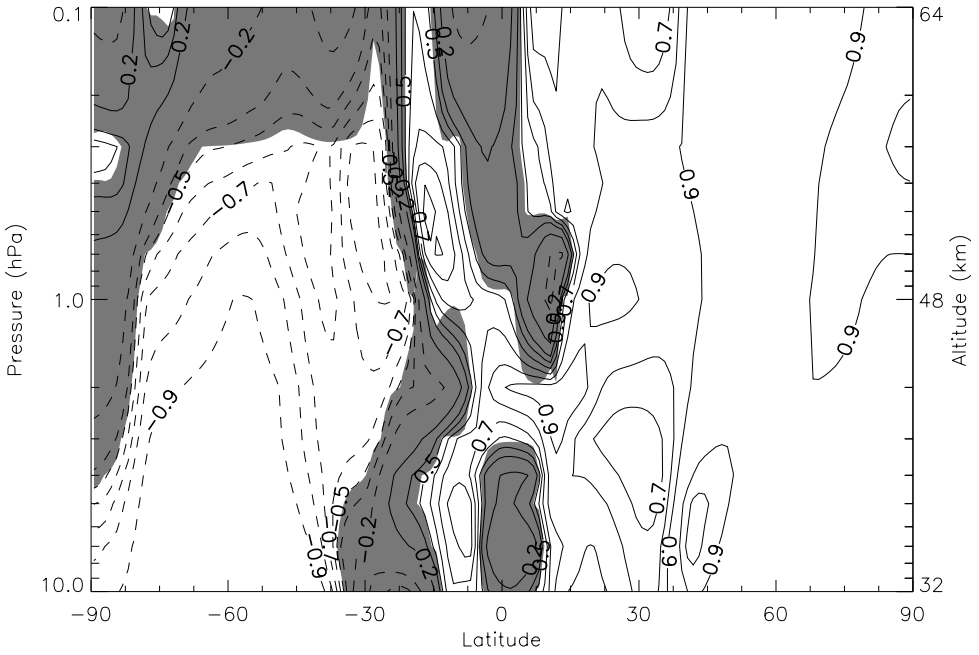

Figure 4.67: Correlation map of SPW1 V on 2005 - 317-333 with a lag of 0. Solid contour lines represent a positive correlation and dashed lines mean negative correlation. Shaded areas mean that the statistical significance of a correlation point is less than 95%.

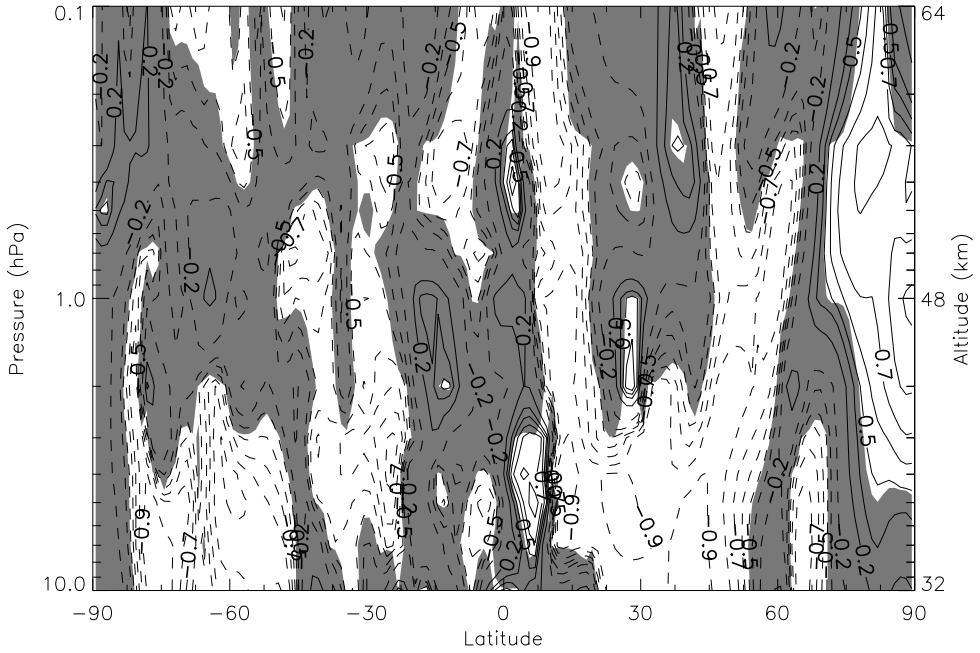

Figure 4.68: Correlation map of SPW2 U on 2005 - 317-333 with a lag of 0. Solid contour lines represent a positive correlation and dashed lines mean negative correlation. Shaded areas mean that the statistical significance of a correlation point is less than 95%.

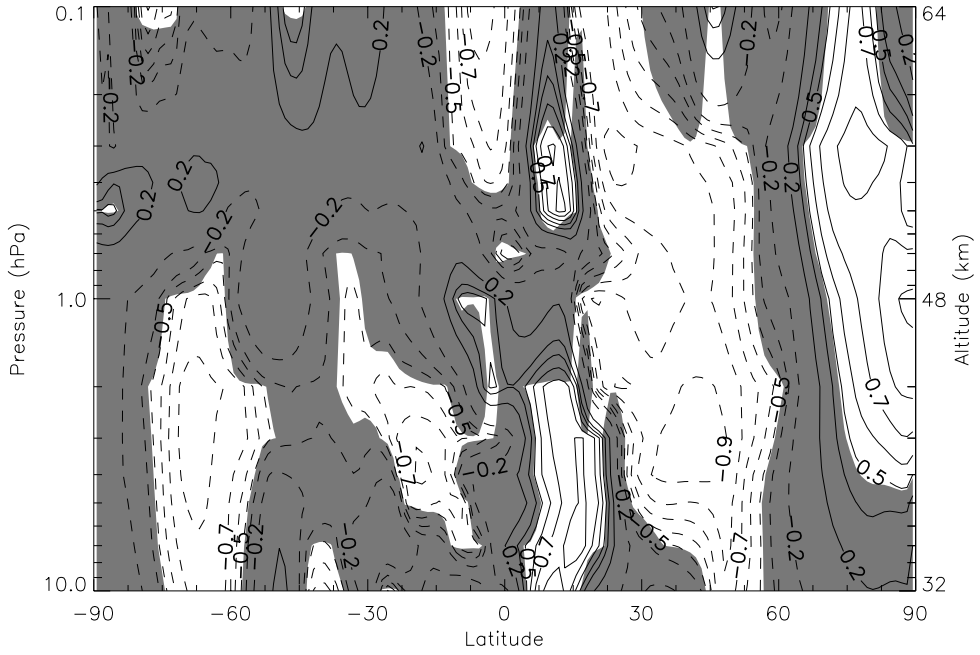

Figure 4.69: Correlation map of SPW2 V on 2005 - 317-333 with a lag of 0. Solid contour lines represent a positive correlation and dashed lines mean negative correlation. Shaded areas mean that the statistical significance of a correlation point is less than 95%.

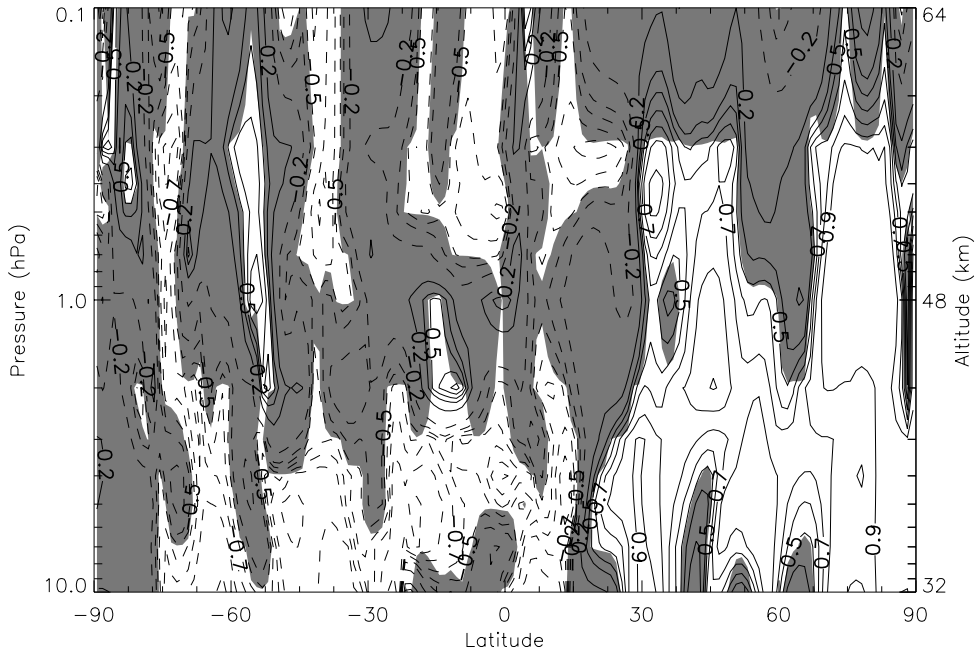

Figure 4.70: Correlation map of SPW3 U on 2005 - 317-333 for lag=0

Correlation map of SPW3 U on 2005 - 317-333 with a lag of 0. Solid contour lines represent a positive correlation and dashed lines mean negative correlation. Shaded areas mean that the statistical significance of a correlation point is less than 95%.

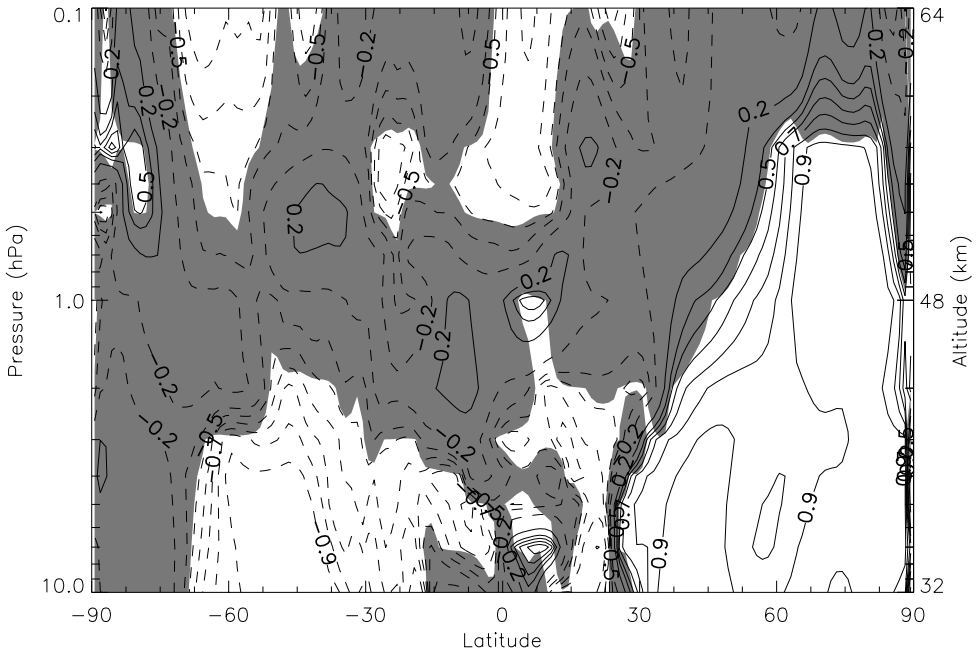

Figure 4.71: Correlation map of SPW3 V on 2005 - 317-333 with a lag of 0. Solid contour lines represent a positive correlation and dashed lines mean negative correlation. Shaded areas mean that the statistical significance of a correlation point is less than 95%.

4.2.5 2006 events

4.2.5.1 2006 - 45-62

Figures 4.72 and 4.73 show the correlation between 12hW1 and SPW1 U and V for this event. Both figures show a very strong and positive correlation in the region where SPW1 has its peak.

Figures 4.74 and 4.75 show that during this event the correlations with SPW2 U and V are negative but very limited spatially, therefore not making SPW2 so relevant during this event.

During this event, SPW3 had its peak at lower altitudes than usual. Figures 4.76 and 4.77 show that the correlation with SPW3 U and V are strong, negative and cover a large region from mid-to-high latitudes and lower altitudes.

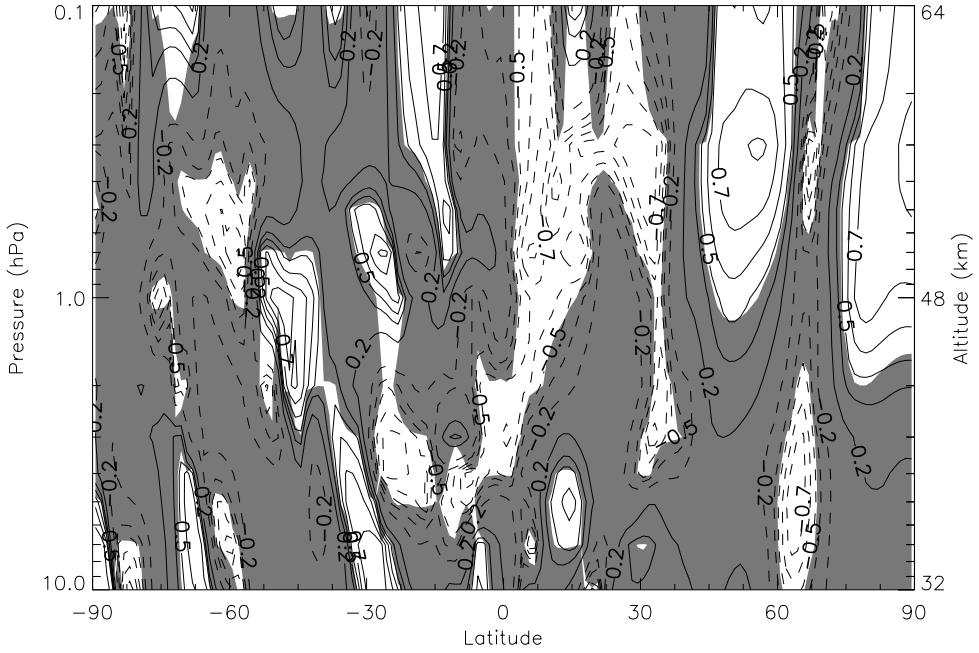

Figure 4.72: Correlation map of SPW1 U on 2006 - 45-62 with a lag of 0. Solid contour lines represent a positive correlation and dashed lines mean negative correlation. Shaded areas mean that the statistical significance of a correlation point is less than 95%.

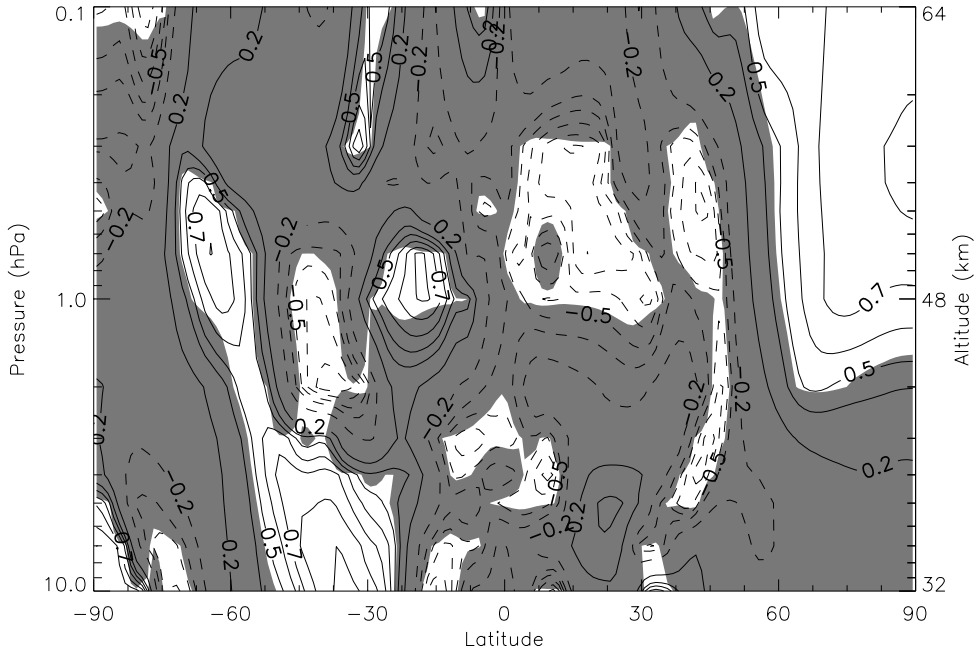

Figure 4.73: Correlation map of SPW1 V on 2006 - 45-62 with a lag of 0. Solid contour lines represent a positive correlation and dashed lines mean negative correlation. Shaded areas mean that the statistical significance of a correlation point is less than 95%.

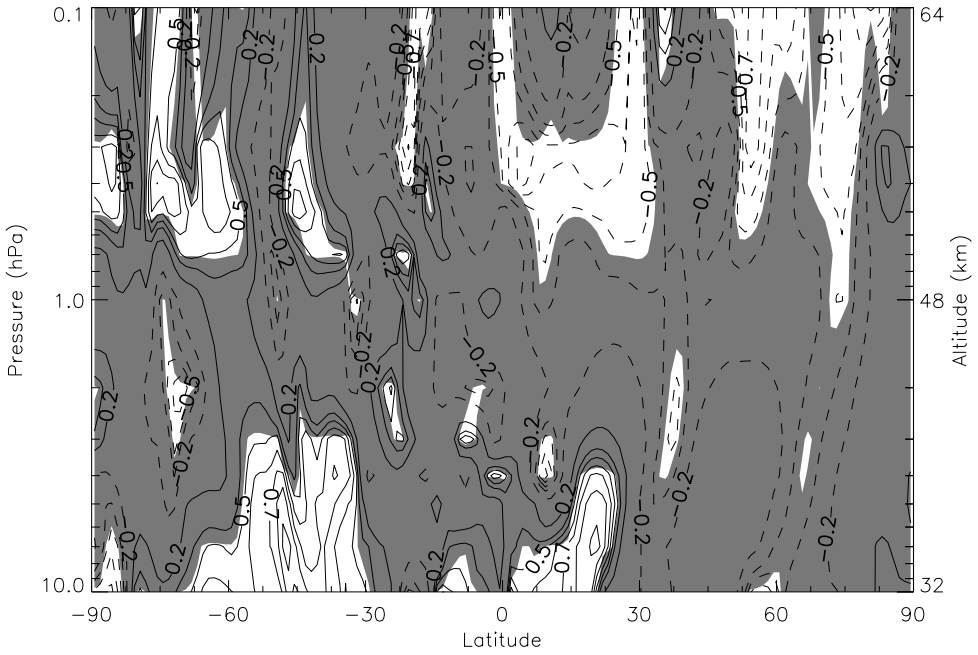

Figure 4.74: Correlation map of SPW2 U on 2006 - 45-62 with a lag of 0. Solid contour lines represent a positive correlation and dashed lines mean negative correlation. Shaded areas mean that the statistical significance of a correlation point is less than 95%.

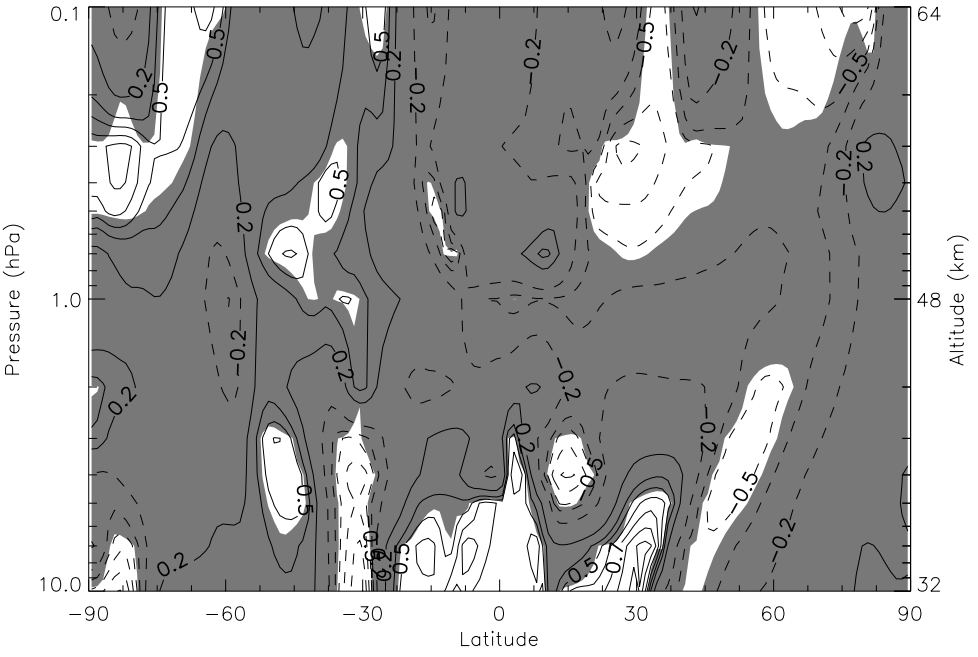

Figure 4.75: Correlation map of SPW2 V on 2006 - 45-62 with a lag of 0. Solid contour lines represent a positive correlation and dashed lines mean negative correlation. Shaded areas mean that the statistical significance of a correlation point is less than 95%.

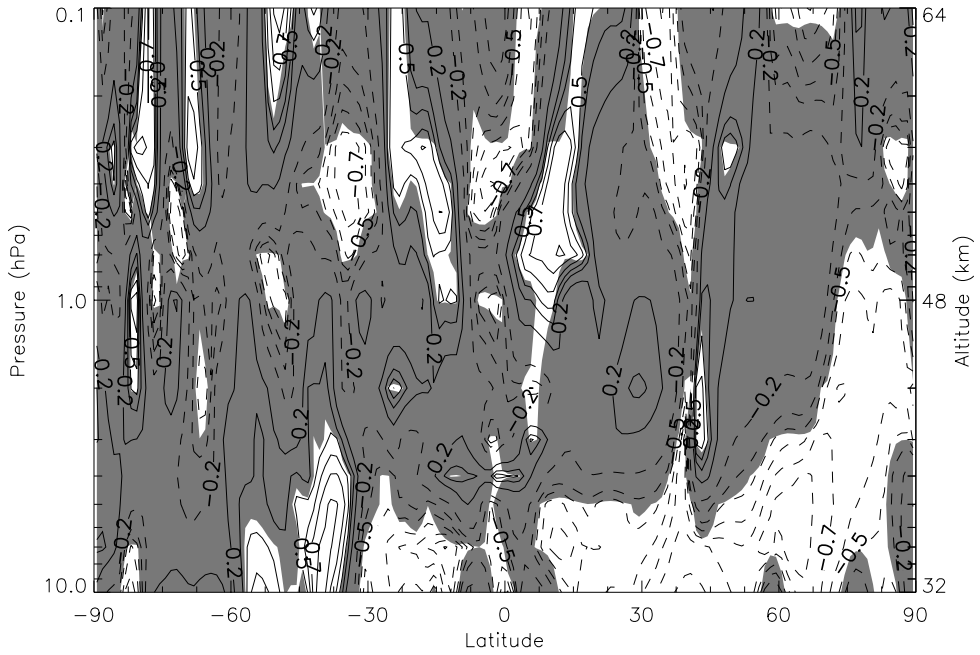

Figure 4.76: Correlation map of SPW3 U on 2006 - 45-62 for lag=0

Correlation map of SPW3 U on 2006 - 45-62 with a lag of 0. Solid contour lines represent a positive correlation and dashed lines mean negative correlation. Shaded areas mean that the statistical significance of a correlation point is less than 95%.

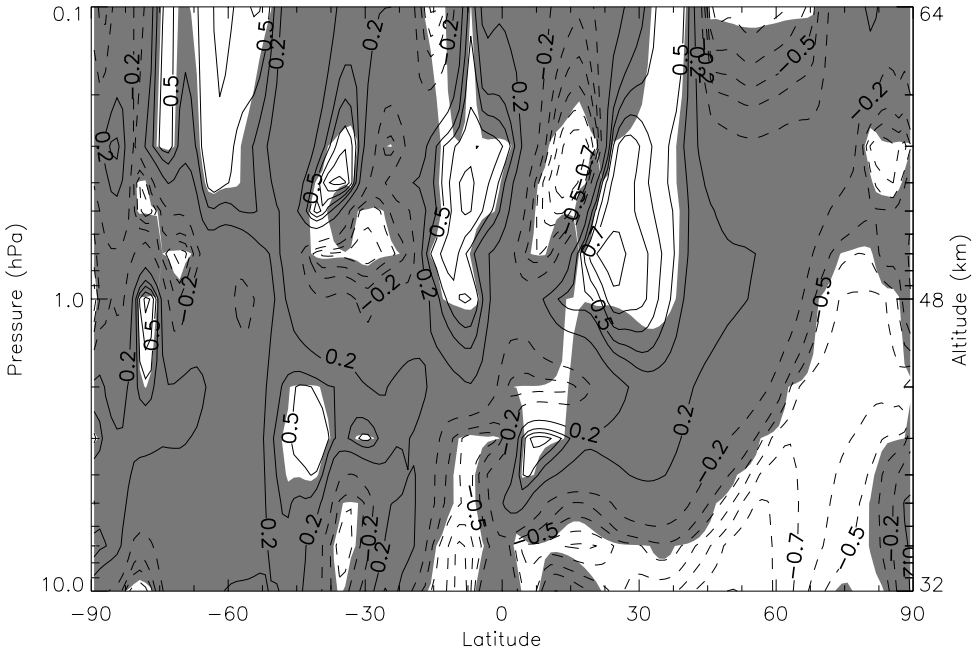

Figure 4.77: Correlation map of SPW3 V on 2006 - 45-62 with a lag of 0. Solid contour lines represent a positive correlation and dashed lines mean negative correlation. Shaded areas mean that the statistical significance of a correlation point is less than 95%.

4.2.5.2 2006 - 60-90

This event covers the last 30 days of the austral summer season, during days 60 through 90 of 2006. This is an interesting event because it follows the decreasing activity of the SPW components as they start to reduce its amplitude and move to the southern hemisphere (as the winter starts in that hemisphere).

Figures 4.78 and 4.79 show a strong positive correlation with SPW1 U and V components at lower latitudes than usual because the SPW1 activity is starting to move south and switch hemispheres.

Figures 4.80 and 4.81 show an anti-correlation with SPW2 U and V, but with very limited spatial coverage.

Figures 4.82 and 4.83 show a positive correlation with SPW3 U and V but also on a very small region.

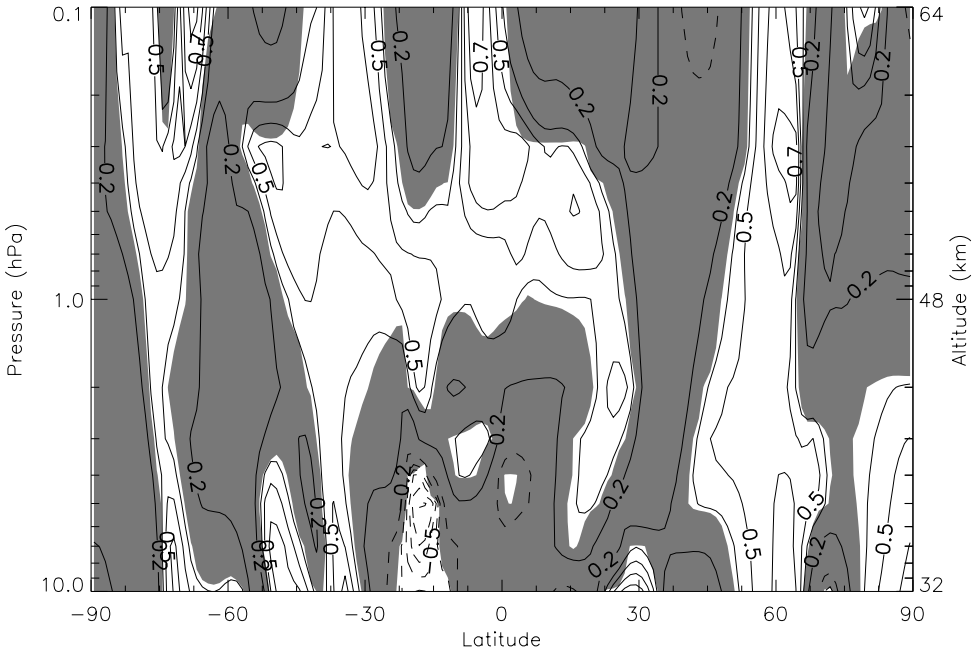

Figure 4.78: Correlation map of SPW1 U on 2006 - 60-90 with a lag of 0. Solid contour lines represent a positive correlation and dashed lines mean negative correlation. Shaded areas mean that the statistical significance of a correlation point is less than 95%.

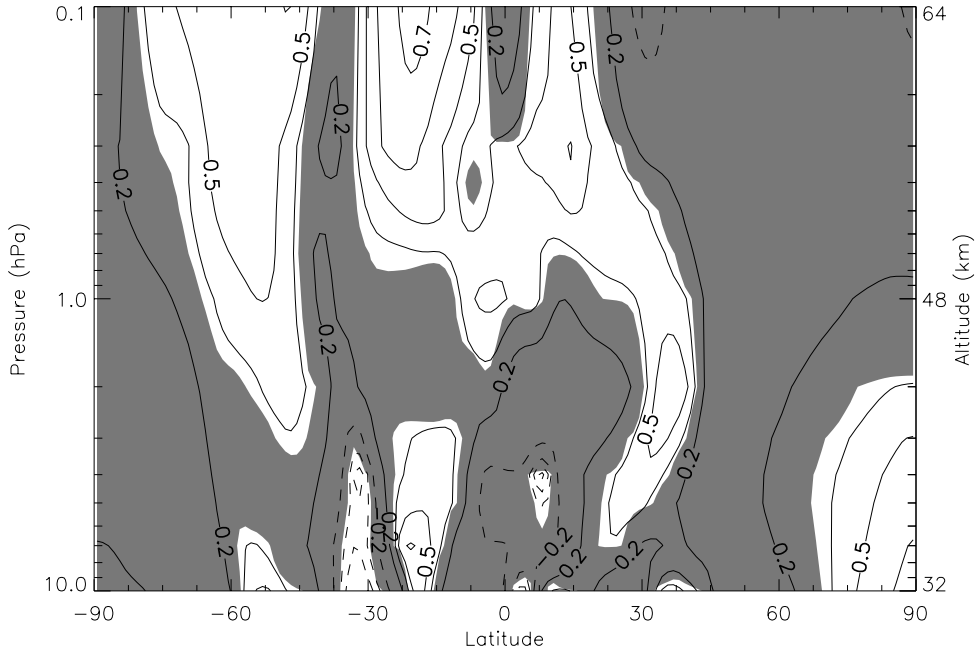

Figure 4.79: Correlation map of SPW1 V on 2006 - 60-90 with a lag of 0. Solid contour lines represent a positive correlation and dashed lines mean negative correlation. Shaded areas mean that the statistical significance of a correlation point is less than 95%.

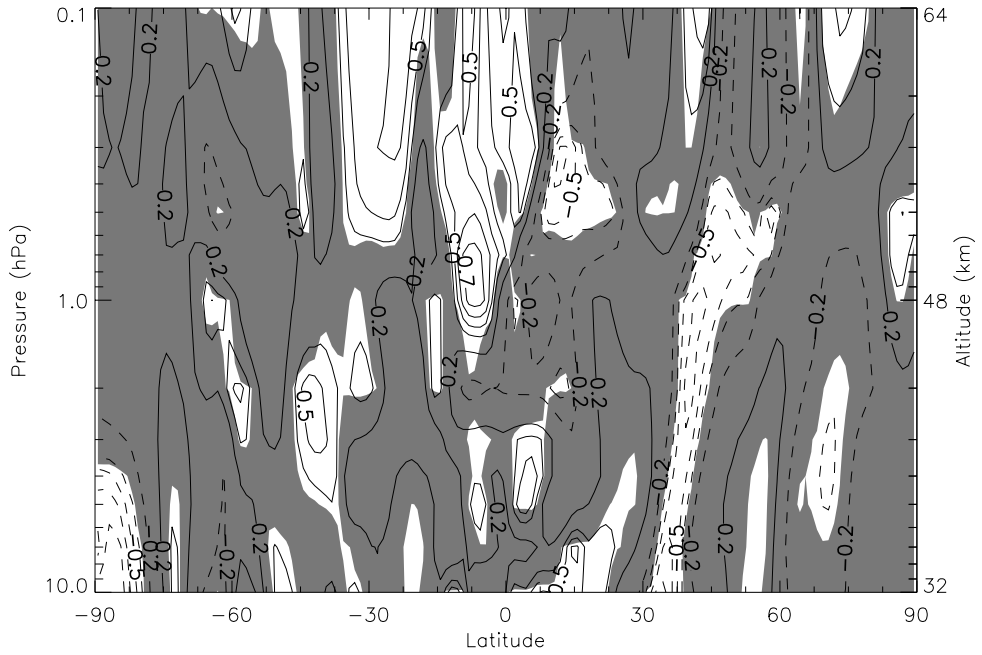

Figure 4.80: Correlation map of SPW2 U on 2006 - 60-90 with a lag of 0. Solid contour lines represent a positive correlation and dashed lines mean negative correlation. Shaded areas mean that the statistical significance of a correlation point is less than 95%.

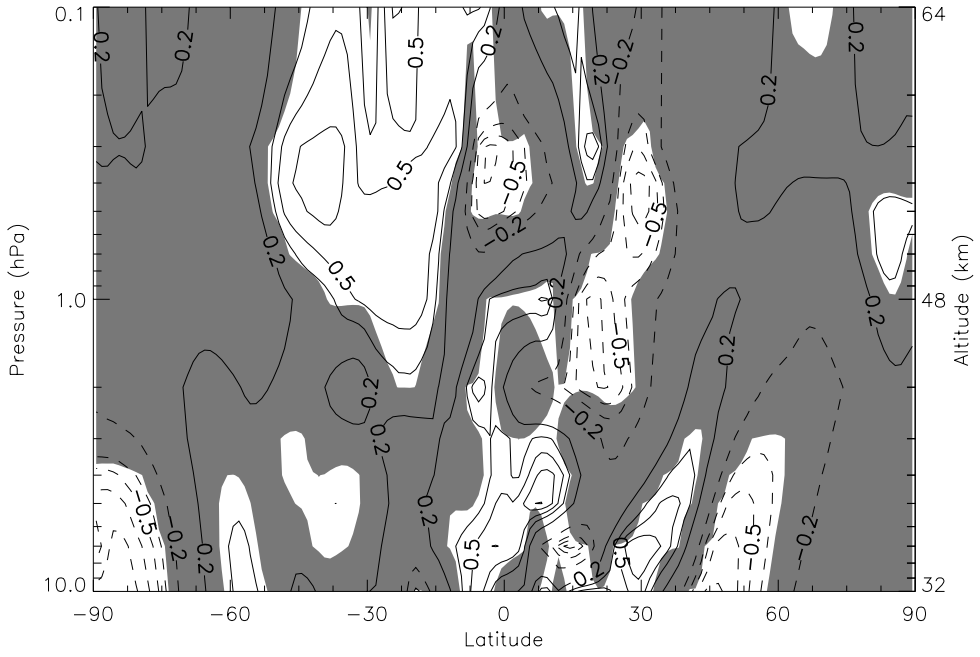

Figure 4.81: Correlation map of SPW2 V on 2006 - 60-90 with a lag of 0. Solid contour lines represent a positive correlation and dashed lines mean negative correlation. Shaded areas mean that the statistical significance of a correlation point is less than 95%.

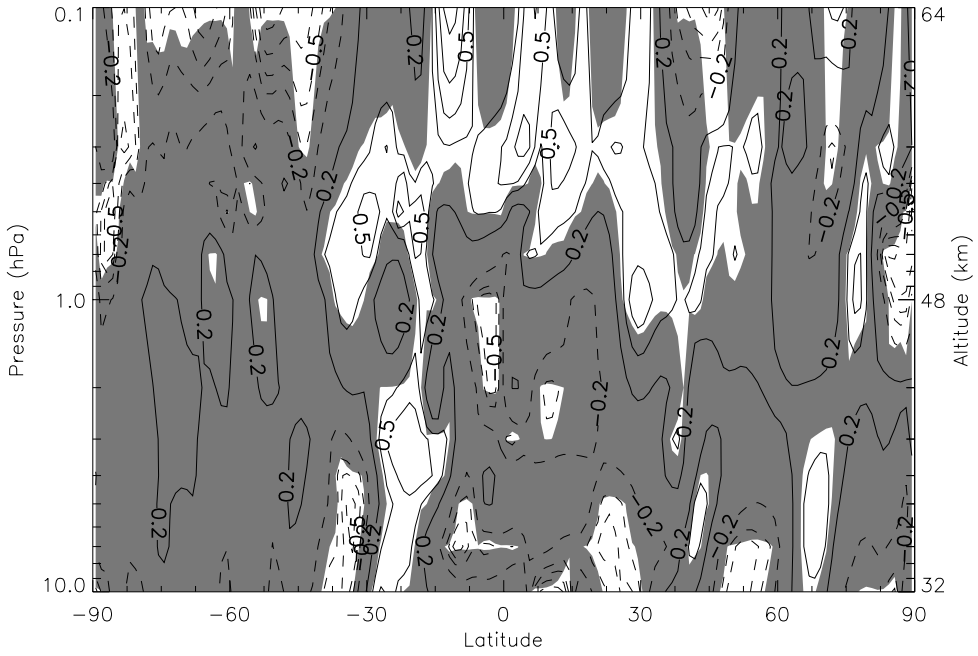

Figure 4.82: Correlation map of SPW3 U on 2006 - 60-90 for lag=0

Correlation map of SPW3 U on 2006 - 60-90 with a lag of 0. Solid contour lines represent a positive correlation and dashed lines mean negative correlation. Shaded areas mean that the statistical significance of a correlation point is less than 95%.

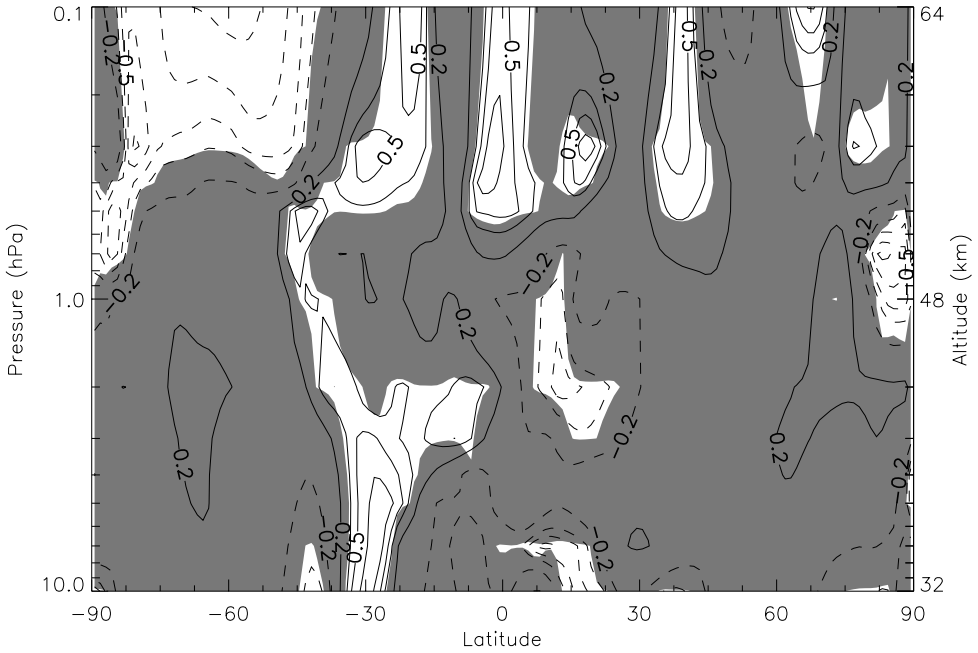

Figure 4.83: Correlation map of SPW3 V on 2006 - 60-90 with a lag of 0. Solid contour lines represent a positive correlation and dashed lines mean negative correlation. Shaded areas mean that the statistical significance of a correlation point is less than 95%.

4.2.6 2007 events

4.2.6.1 2007 - 1-9

The next event to be studied is relatively short, covering days 1 through 9 in 2007. Figure 4.84 shows the normalized 12hW1 and SPW activity during the 2006-2007 season.

Figure 4.85 shows that the correlation with SPW1 U is very strong and negative, covering most of the winter hemisphere. Similarly, figure 4.86 shows an even broader structure for SPW1 V.

Figures 4.87 and 4.88 show a small region of strong positive correlation with SPW2 U and V at the location where SPW2 peaks during this event, and a region of negative correlation just below it, which corresponds to the vertical propagation of SPW2 during this event.

Figures 4.89 and 4.90 show that SPW3 has a strong negative correlation for both U and V in regions towards higher and lower latitudes than where it peaks.

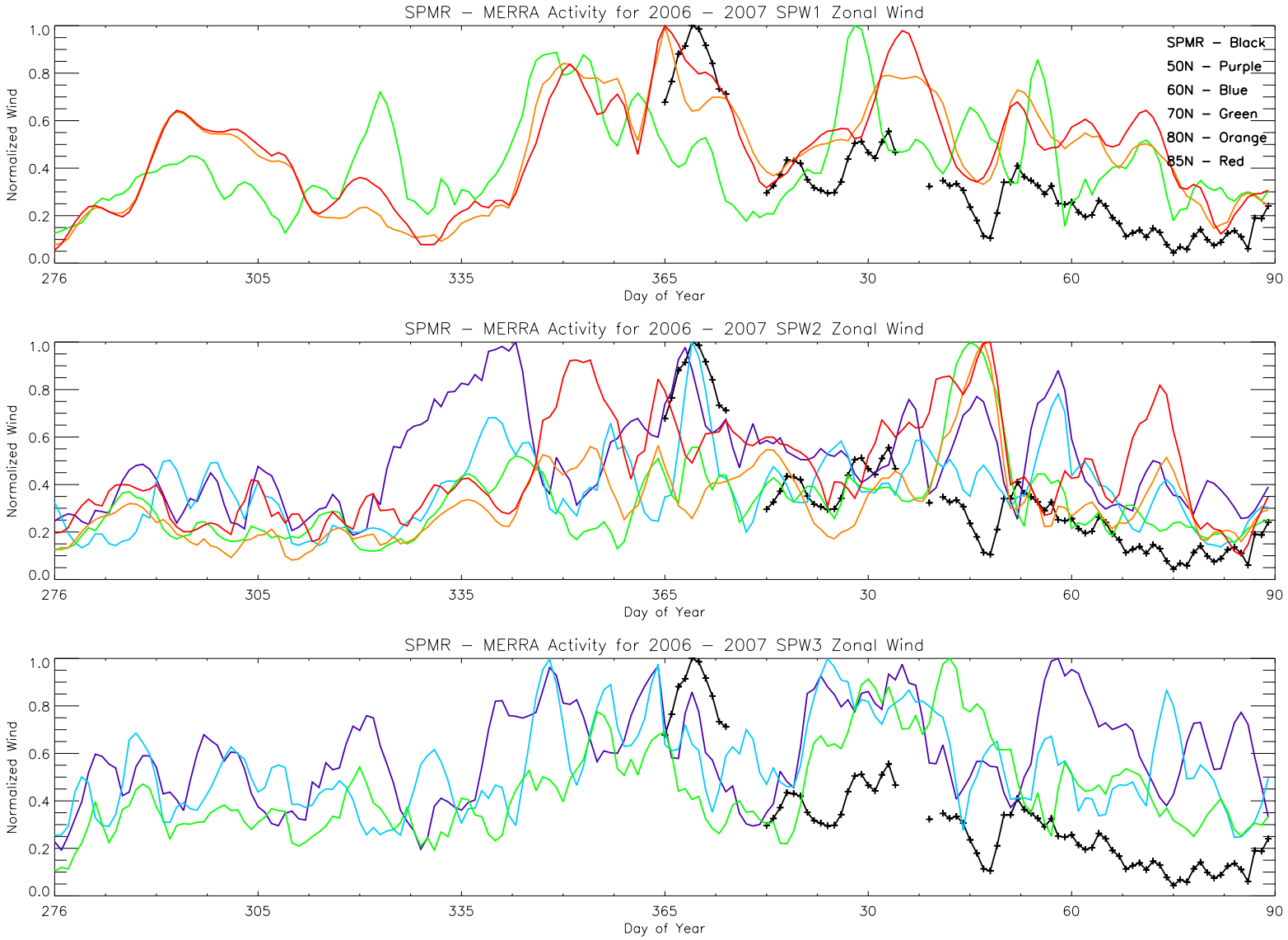

Figure 4.84: Top panel shows normalized SPW1 zonal wind and SPMR data. Middle panel shows SPW2 and SPMR, and bottom panel shows SPW3 and SPMR data. SPMR data shown by the black line, MERRA at 50°N is purple, 60°N is blue, 70°N is green, 80°N is orange and 85°N is red. Data is from 2003-2004.

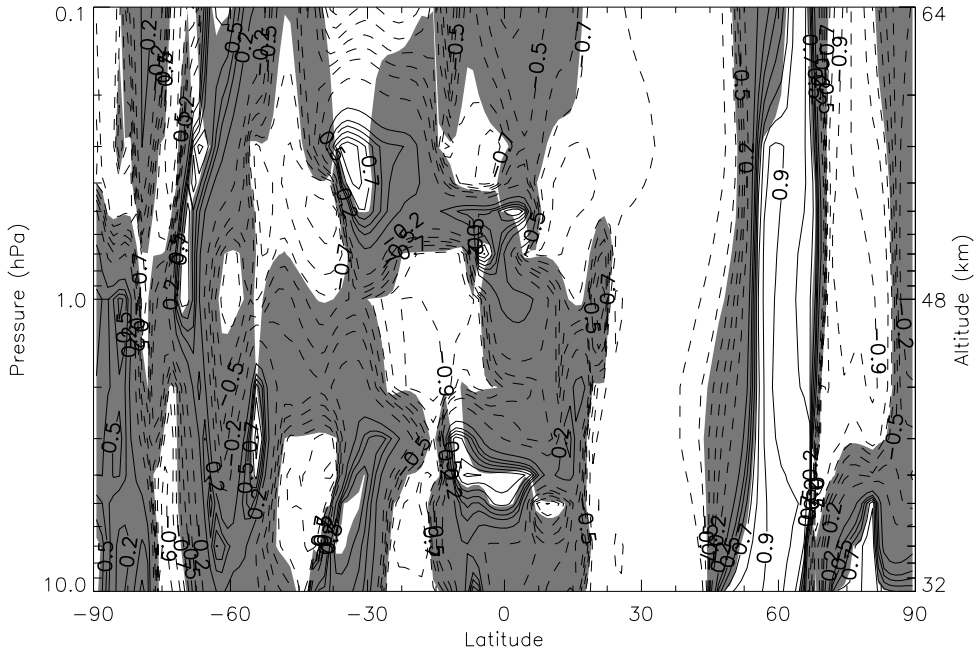

Figure 4.85: Correlation map of SPW1 U on 2007 - 1-9 with a lag of 0. Solid contour lines represent a positive correlation and dashed lines mean negative correlation. Shaded areas mean that the statistical significance of a correlation point is less than 95%.

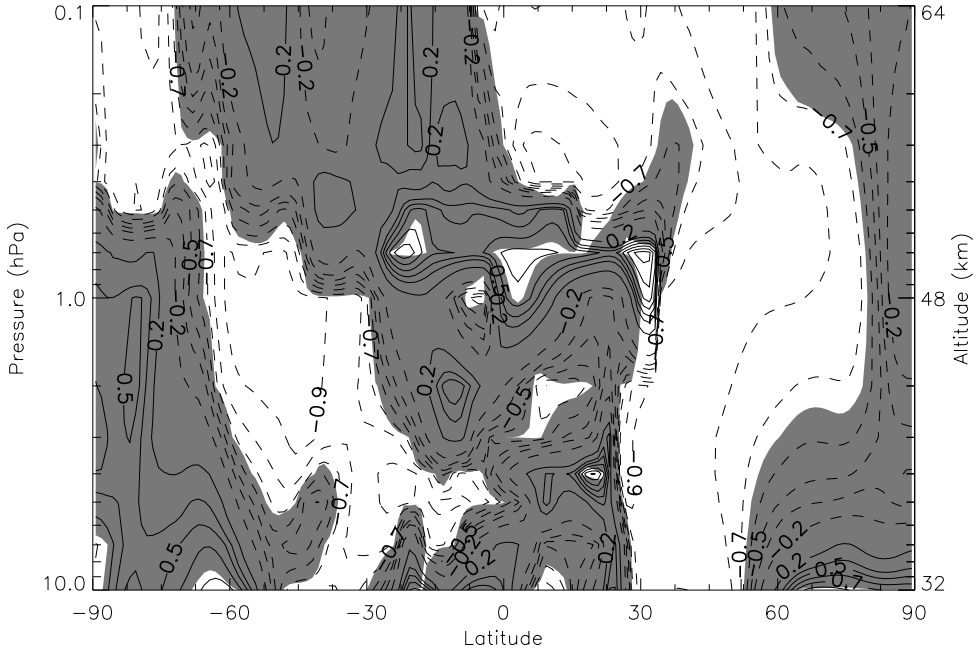

Figure 4.86: Correlation map of SPW1 V on 2007 - 1-9 with a lag of 0. Solid contour lines represent a positive correlation and dashed lines mean negative correlation. Shaded areas mean that the statistical significance of a correlation point is less than 95%.

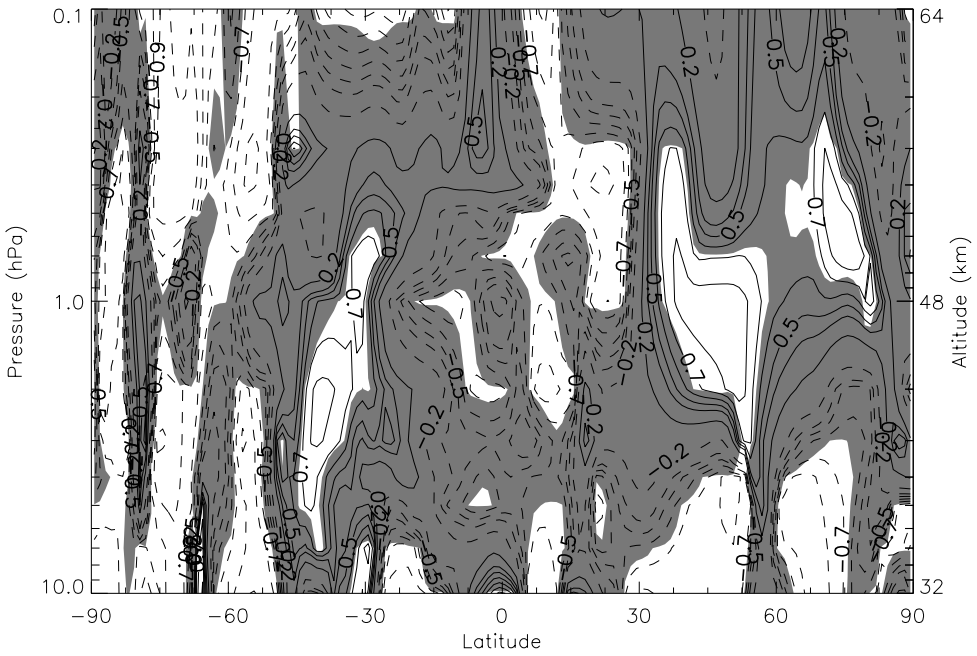

Figure 4.87: Correlation map of SPW2 U on 2007 - 1-9 with a lag of 0. Solid contour lines represent a positive correlation and dashed lines mean negative correlation. Shaded areas mean that the statistical significance of a correlation point is less than 95%.

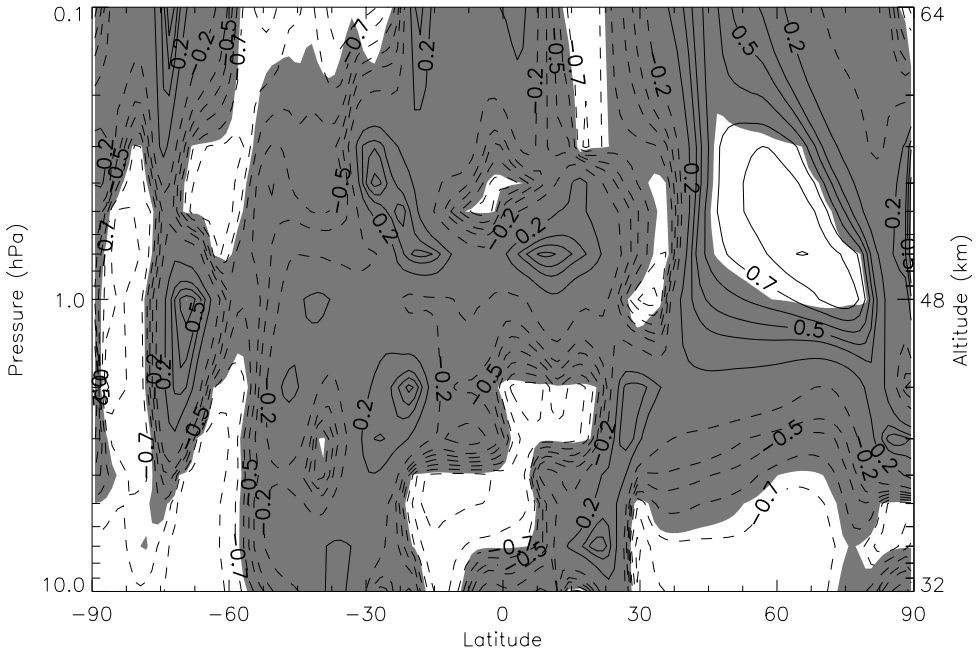

Figure 4.88: Correlation map of SPW2 V on 2007 - 1-9 with a lag of 0. Solid contour lines represent a positive correlation and dashed lines mean negative correlation. Shaded areas mean that the statistical significance of a correlation point is less than 95%.

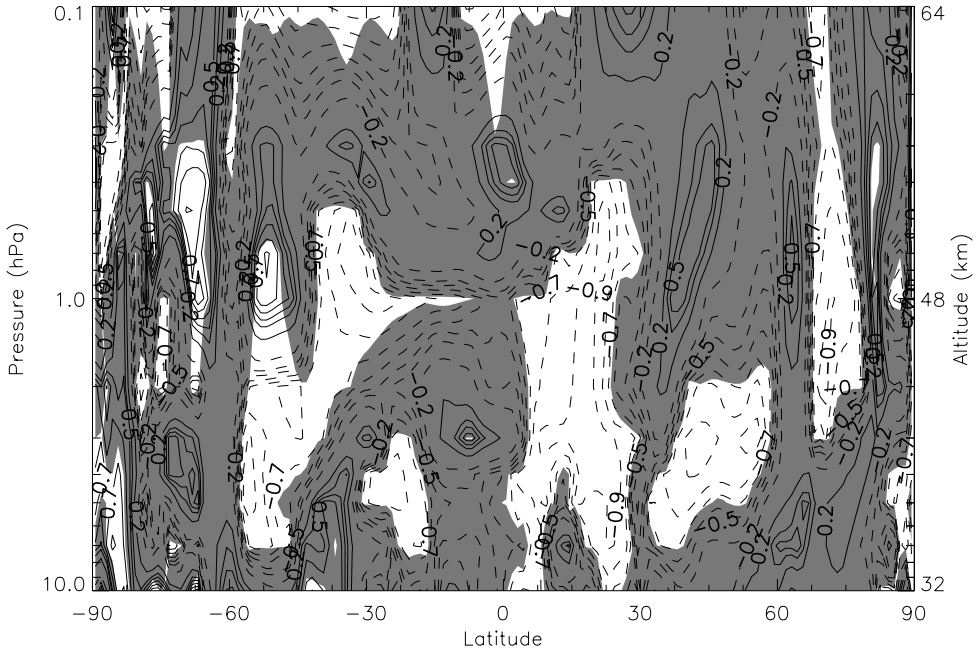

Figure 4.89: Correlation map of SPW3 U on 2007 - 1-9 for lag=0

Correlation map of SPW3 U on 2007 - 1-9 with a lag of 0. Solid contour lines represent a positive correlation and dashed lines mean negative correlation. Shaded areas mean that the statistical significance of a correlation point is less than 95%.

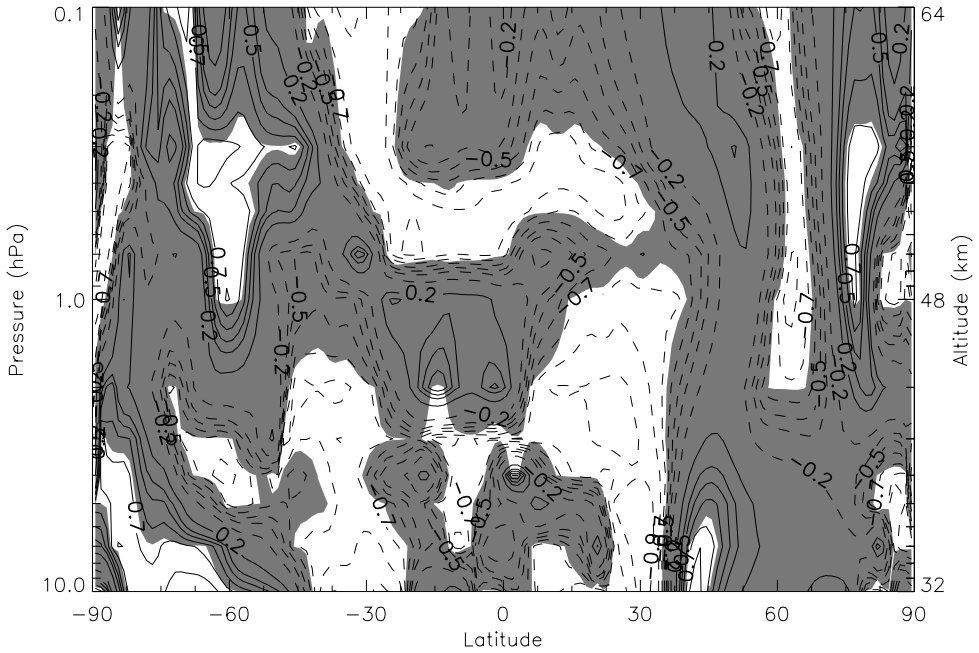

Figure 4.90: Correlation map of SPW3 V on 2007 - 1-9 with a lag of 0. Solid contour lines represent a positive correlation and dashed lines mean negative correlation. Shaded areas mean that the statistical significance of a correlation point is less than 95%.

4.2.6.2 2007 - 15-32

The next event to be analyzed happened during days 15 and 32 on 2007.

Figure 4.91 shows that the correlation with SPW1 U is very strong and positive, covering most of the region where SPW1 peaks. Figure 4.92 also shows a strong positive correlation with SPW1 V, but with an even larger correlation region.

Figure 4.93 correlates SPW2 U and shows almost no significant correlation during this period. Figure 4.94 shows a positive correlation region with SPW2 V.

Figures 4.95 and 4.96 correlate 12hW1 with SPW3 U and V, respectively. Both components of SPW3 show a strong, positive correlation around the region where SPW3 has its peak during this event.

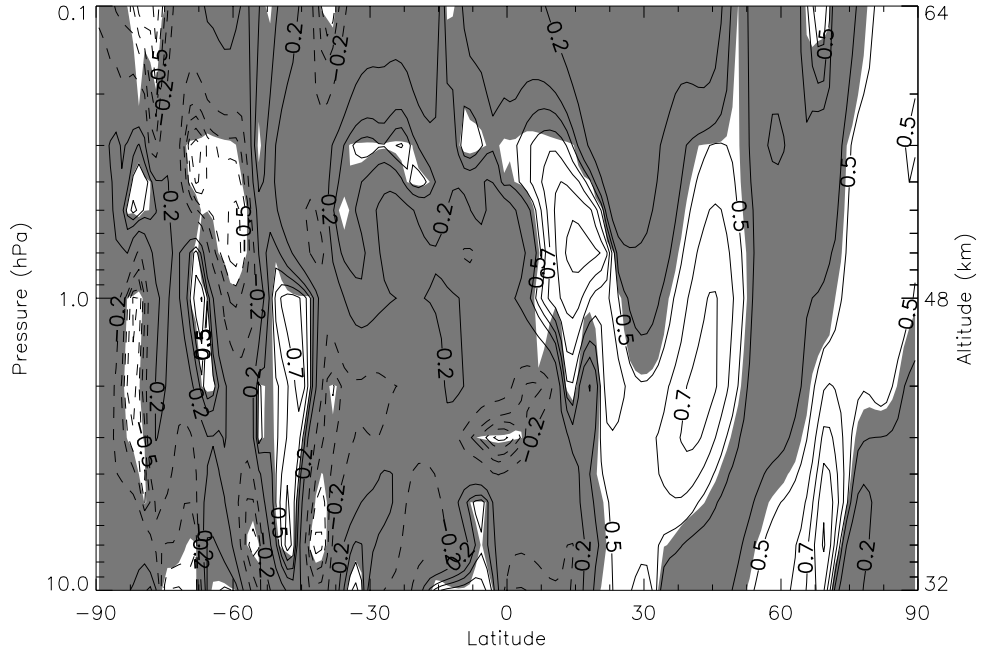

Figure 4.91: Correlation map of SPW1 U on 2007 - 15-32 with a lag of 0. Solid contour lines represent a positive correlation and dashed lines mean negative correlation. Shaded areas mean that the statistical significance of a correlation point is less than 95%.

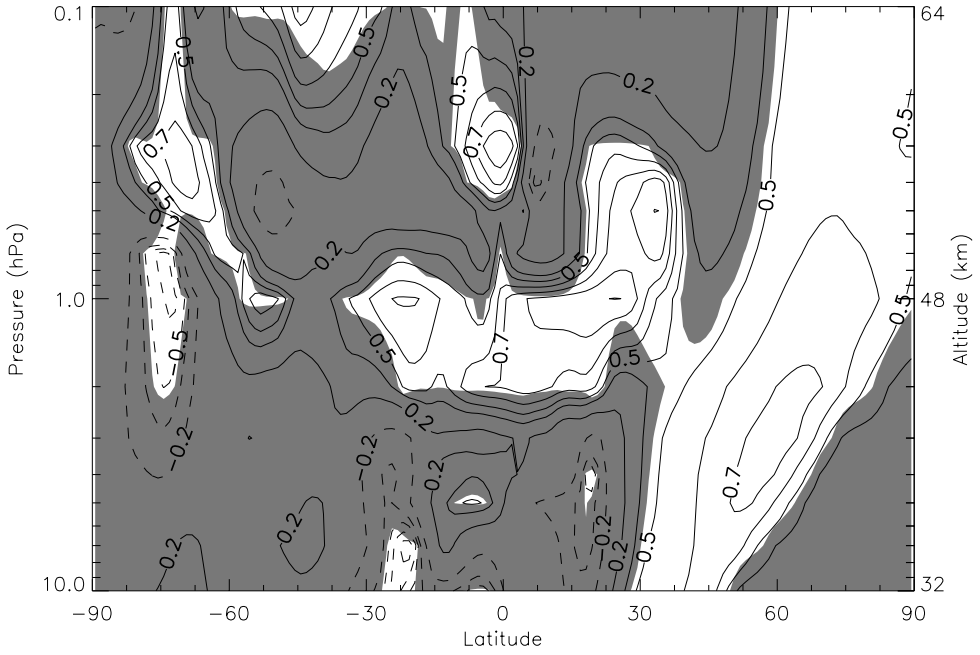

Figure 4.92: Correlation map of SPW1 V on 2007 - 15-32 with a lag of 0. Solid contour lines represent a positive correlation and dashed lines mean negative correlation. Shaded areas mean that the statistical significance of a correlation point is less than 95%.

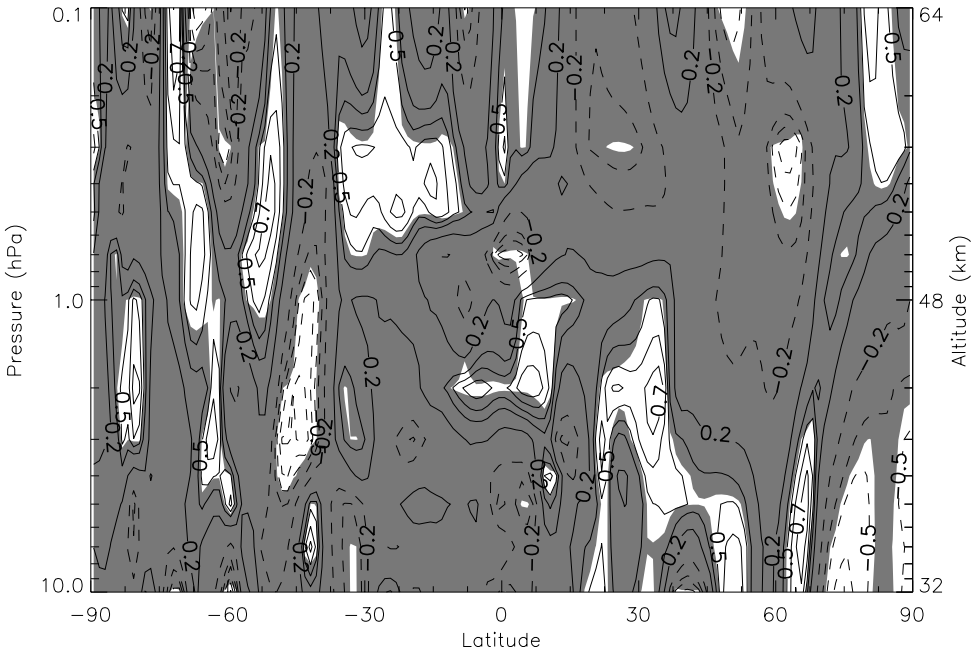

Figure 4.93: Correlation map of SPW2 U on 2007 - 15-32 with a lag of 0. Solid contour lines represent a positive correlation and dashed lines mean negative correlation. Shaded areas mean that the statistical significance of a correlation point is less than 95%.

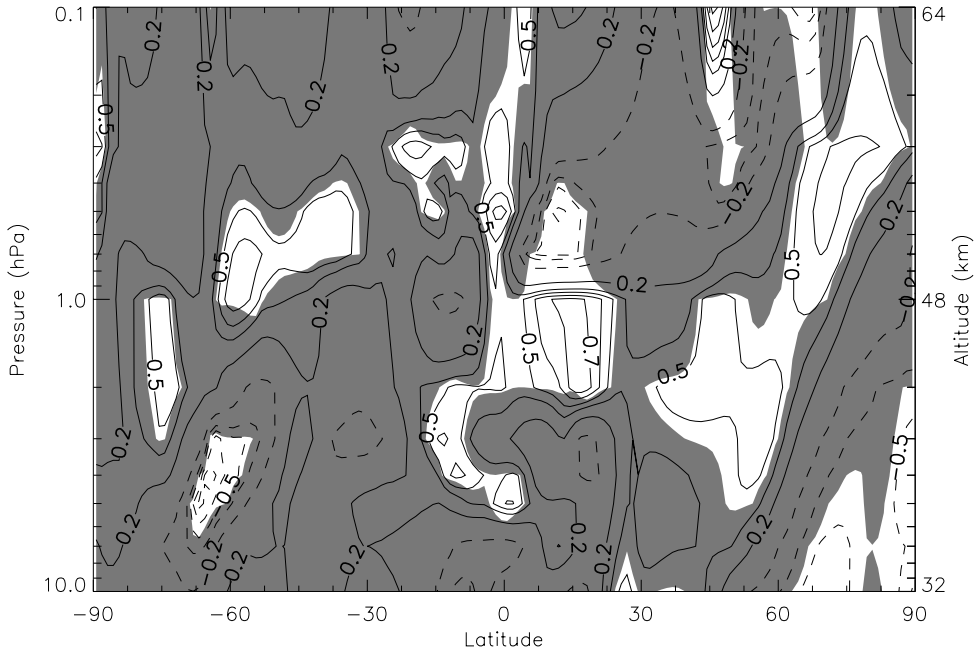

Figure 4.94: Correlation map of SPW2 V on 2007 - 15-32 with a lag of 0. Solid contour lines represent a positive correlation and dashed lines mean negative correlation. Shaded areas mean that the statistical significance of a correlation point is less than 95%.

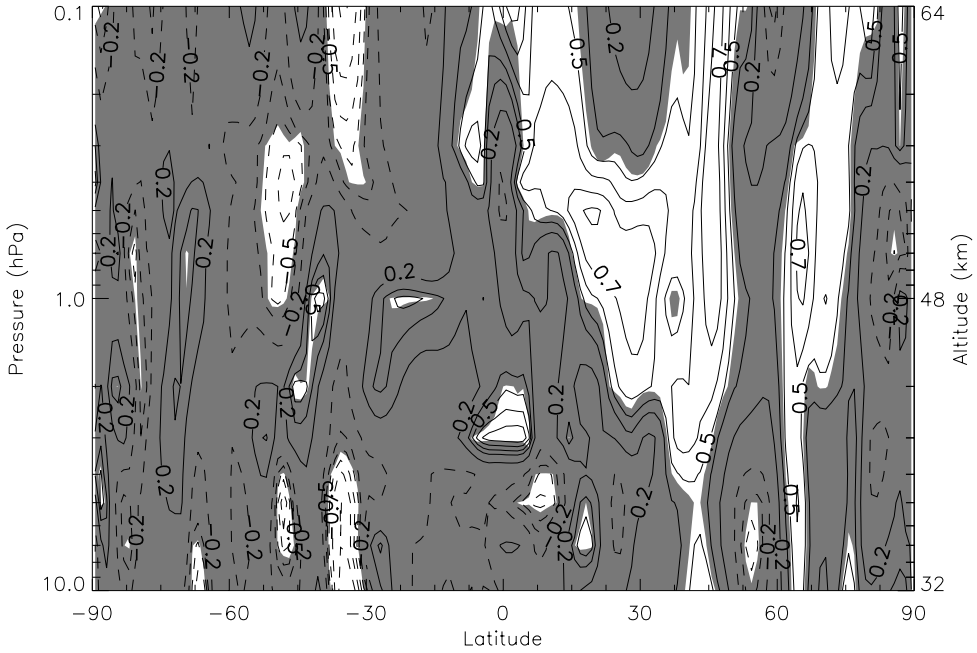

Figure 4.95: Correlation map of SPW3 U on 2007 - 15-32 for lag=0

Correlation map of SPW3 U on 2007 - 15-32 with a lag of 0. Solid contour lines represent a positive correlation and dashed lines mean negative correlation. Shaded areas mean that the statistical significance of a correlation point is less than 95%.

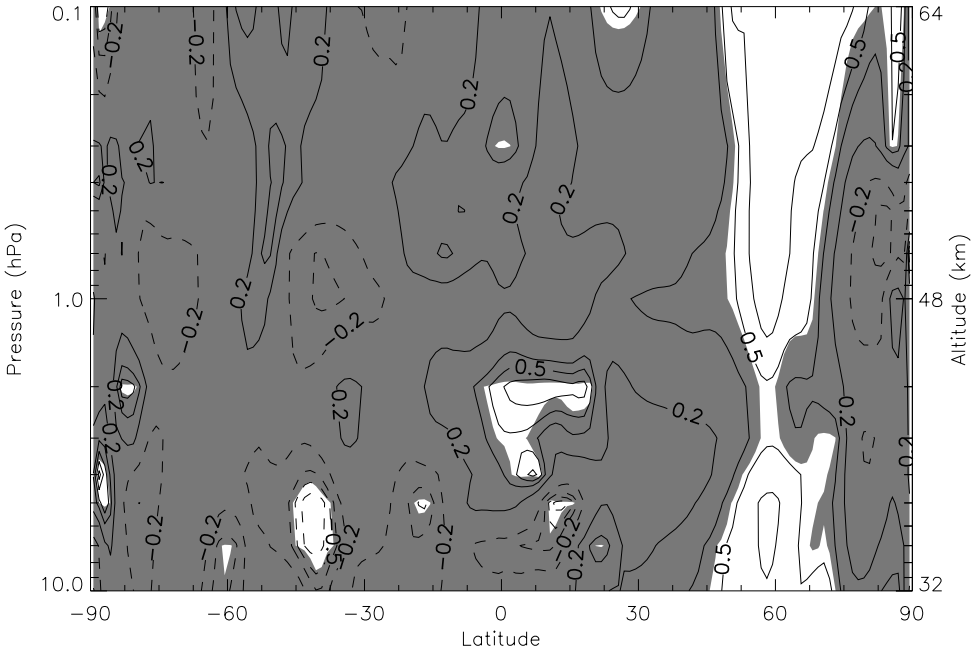

Figure 4.96: Correlation map of SPW3 V on 2007 - 15-32 with a lag of 0. Solid contour lines represent a positive correlation and dashed lines mean negative correlation. Shaded areas mean that the statistical significance of a correlation point is less than 95%.

4.2.6.3 2007 - 45-75

This event covers days 45 through 75 in 2007, towards the end of the 2006-2007 austral summer season.

Figure 4.97 shows the correlation between 12hW1 and SPW1 U. This correlation has a narrow region of strong positive correlation at high latitudes and low altitudes, and then a region of strong anti-correlation on the higher altitudes, which is related to the motion of SPW1. Figure 4.98 has a small region of negative correlation around 60°N and lower altitudes.

Figure 4.99 shows the correlation with SPW2 U. It has a region of very strong positive correlation at mid-latitudes. Figure 4.100 shows a similar structure, with a positive correlation region happening at lower latitudes and higher altitudes.

Figures 4.101 and 4.102 show a region of strong positive correlation around mid-to-high latitudes, where SPW3 peaks during this event.

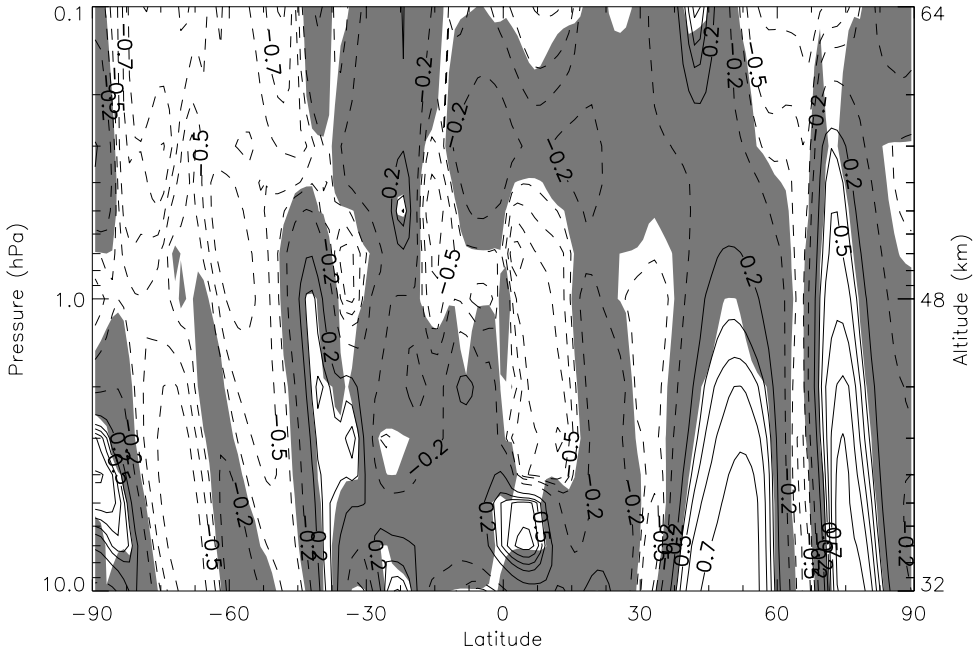

Figure 4.97: Correlation map of SPW1 U on 2007 - 45-75 with a lag of 0. Solid contour lines represent a positive correlation and dashed lines mean negative correlation. Shaded areas mean that the statistical significance of a correlation point is less than 95%.

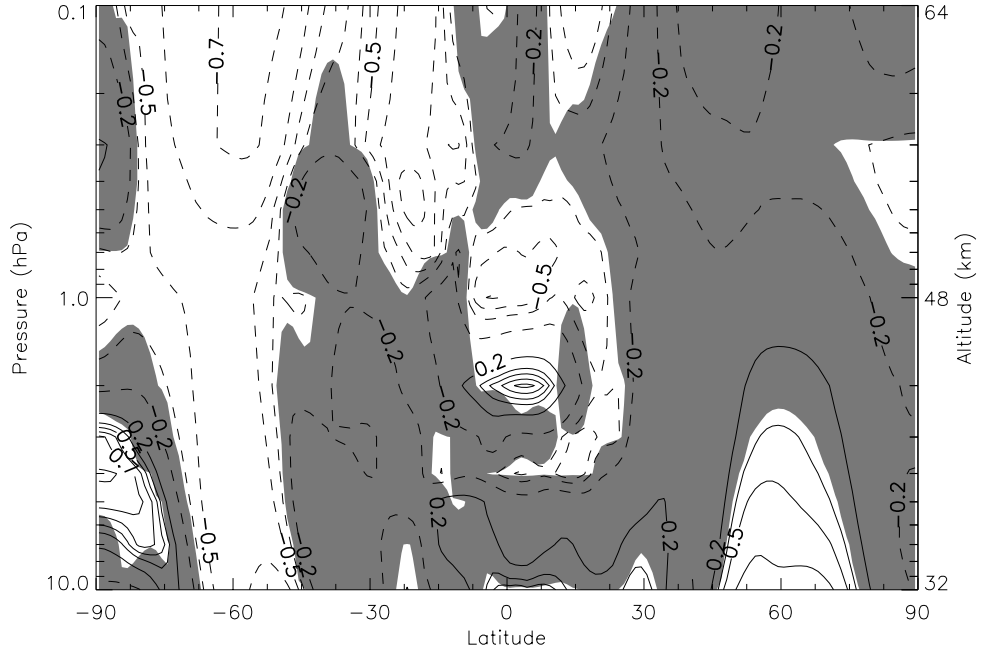

Figure 4.98: Correlation map of SPW1 V on 2007 - 45-75 with a lag of 0. Solid contour lines represent a positive correlation and dashed lines mean negative correlation. Shaded areas mean that the statistical significance of a correlation point is less than 95%.

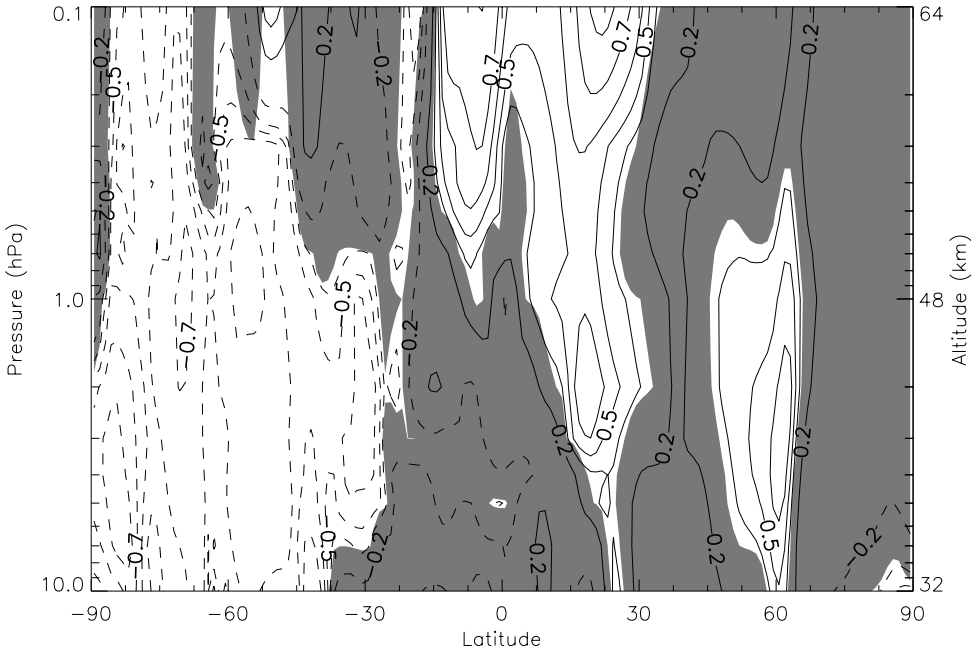

Figure 4.99: Correlation map of SPW2 U on 2007 - 45-75 with a lag of 0. Solid contour lines represent a positive correlation and dashed lines mean negative correlation. Shaded areas mean that the statistical significance of a correlation point is less than 95%.

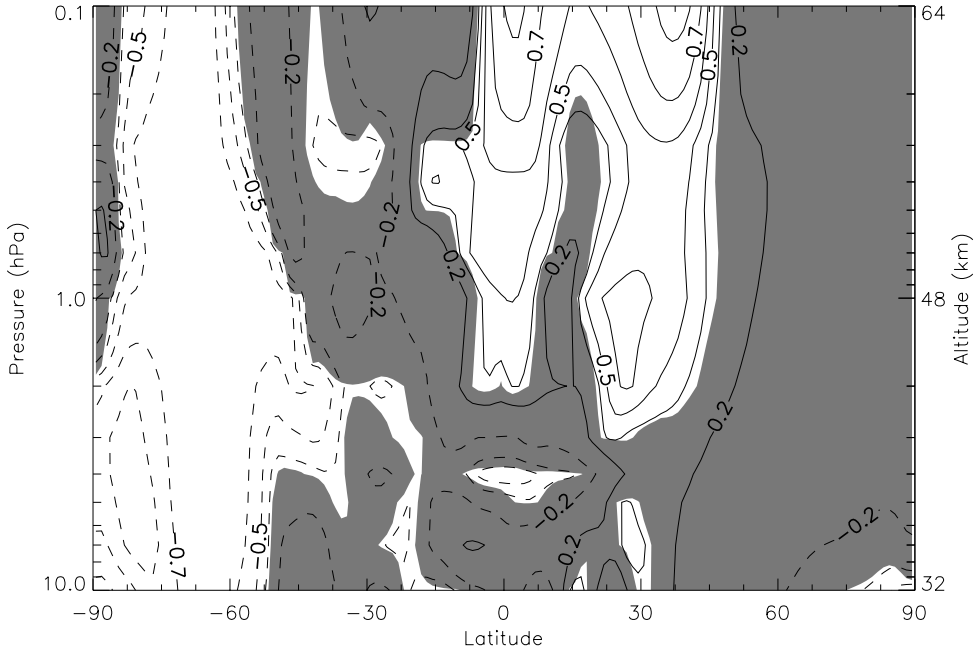

Figure 4.100: Correlation map of SPW2 V on 2007 - 45-75 with a lag of 0. Solid contour lines represent a positive correlation and dashed lines mean negative correlation. Shaded areas mean that the statistical significance of a correlation point is less than 95%.

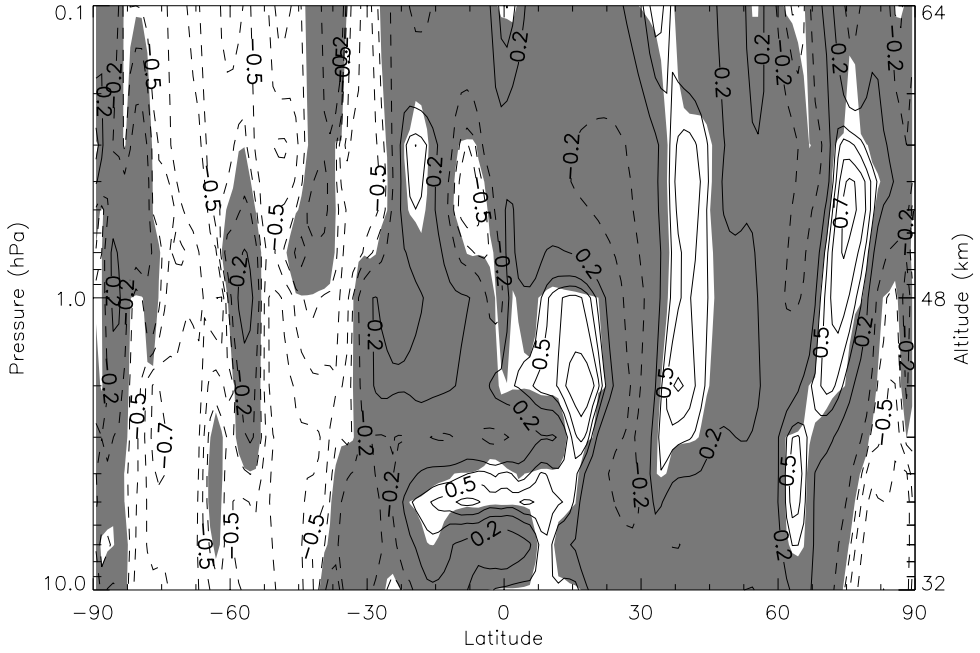

Figure 4.101: Correlation map of SPW3 U on 2007 - 45-75 for lag=0

Correlation map of SPW3 U on 2007 - 45-75 with a lag of 0. Solid contour lines represent a positive correlation and dashed lines mean negative correlation. Shaded areas mean that the statistical significance of a correlation point is less than 95%.

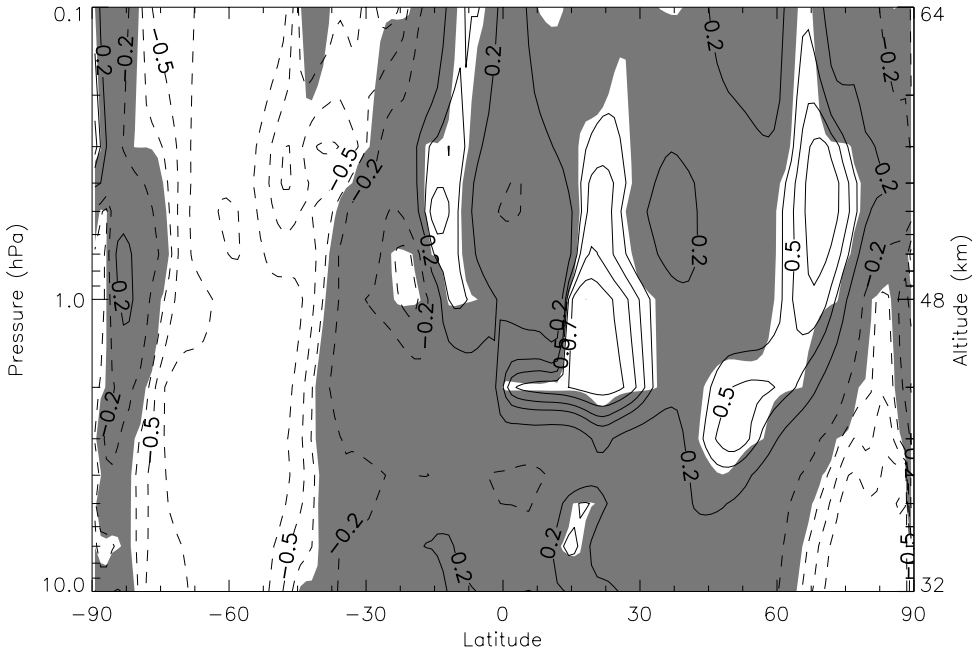

Figure 4.102: Correlation map of SPW3 V on 2007 - 45-75 with a lag of 0. Solid contour lines represent a positive correlation and dashed lines mean negative correlation. Shaded areas mean that the statistical significance of a correlation point is less than 95%.

4.2.6.4 2007 - 342-350

The next event to be considered happened during the days 342 and 350 of 2007. This is a relatively short event, but with interesting characteristics. Figure 4.103 shows the 12hW1 and SPW data for the 2007-2008 austral summer season.

Figures 4.104 and 4.105 show the correlation between 12hW1 and SPW1 U and V. Both components show a similar behavior, with a strong positive correlation in the mid-latitudes, south from the peak.

Figures 4.106 and 4.107 show the correlation of 12hW1 with SPW2 U and V. Both components show a strong anti-correlation in the mid-latitudes, where SPW2 peaks during this period.

Another important feature of this event is the correlation with SPW3. Figures 4.108 and 4.109 show a very strong positive correlation.

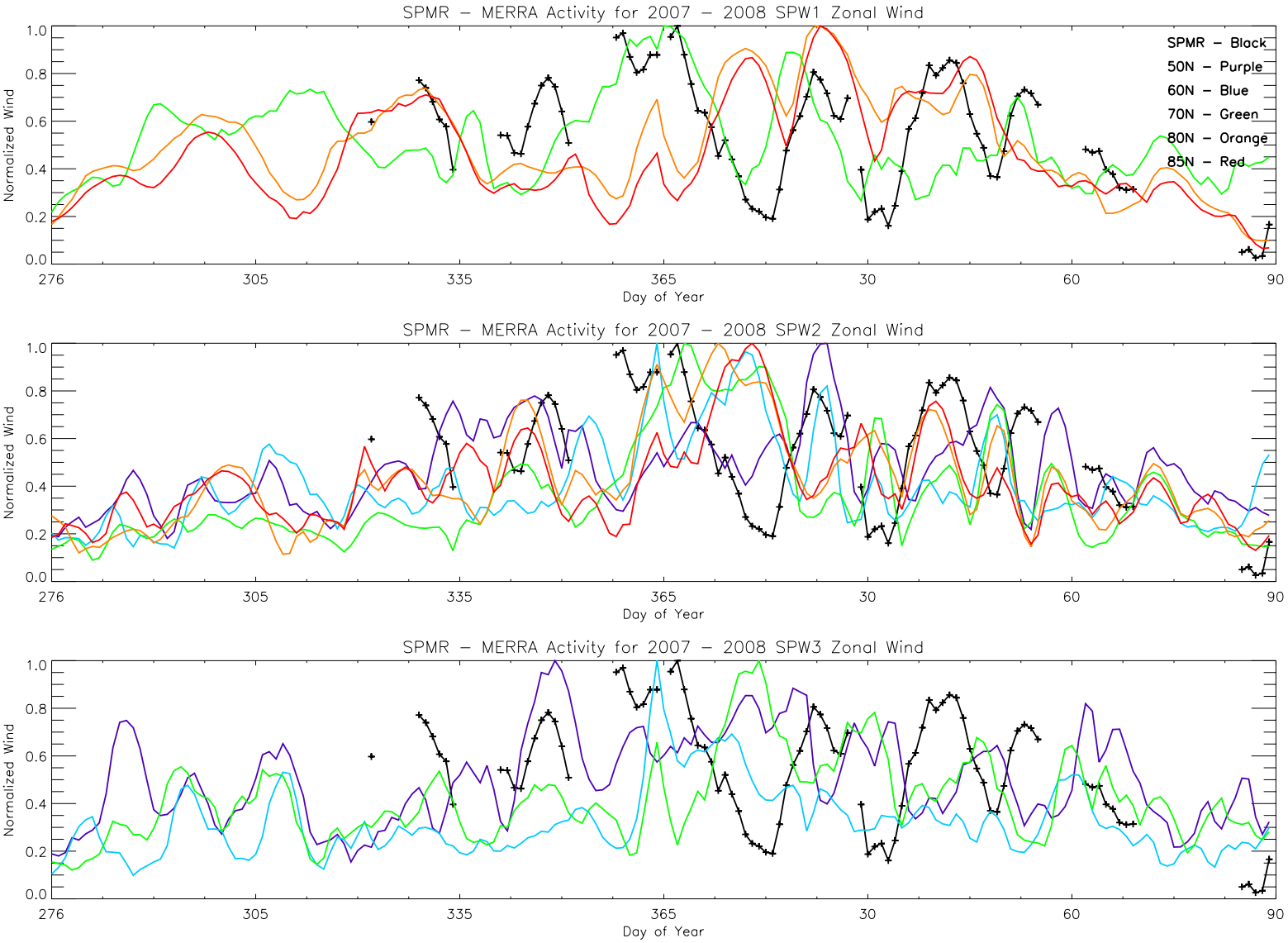

Figure 4.103: Top panel shows normalized SPW1 zonal wind and SPMR data. Middle panel shows SPW2 and SPMR, and bottom panel shows SPW3 and SPMR data. SPMR data shown by the black line, MERRA at 50°N is purple, 60°N is blue, 70°N is green, 80°N is orange and 85°N is red. Data is from 2003-2004.

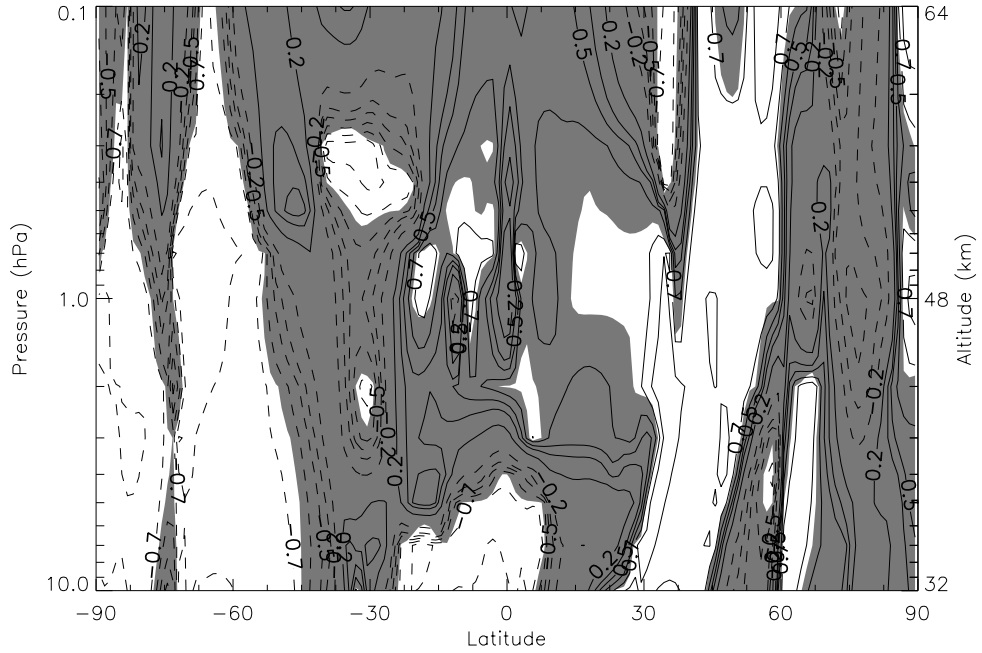

Figure 4.104: Correlation map of SPW1 U on 2007 - 342-350 with a lag of 0. Solid contour lines represent a positive correlation and dashed lines mean negative correlation. Shaded areas mean that the statistical significance of a correlation point is less than 95%.

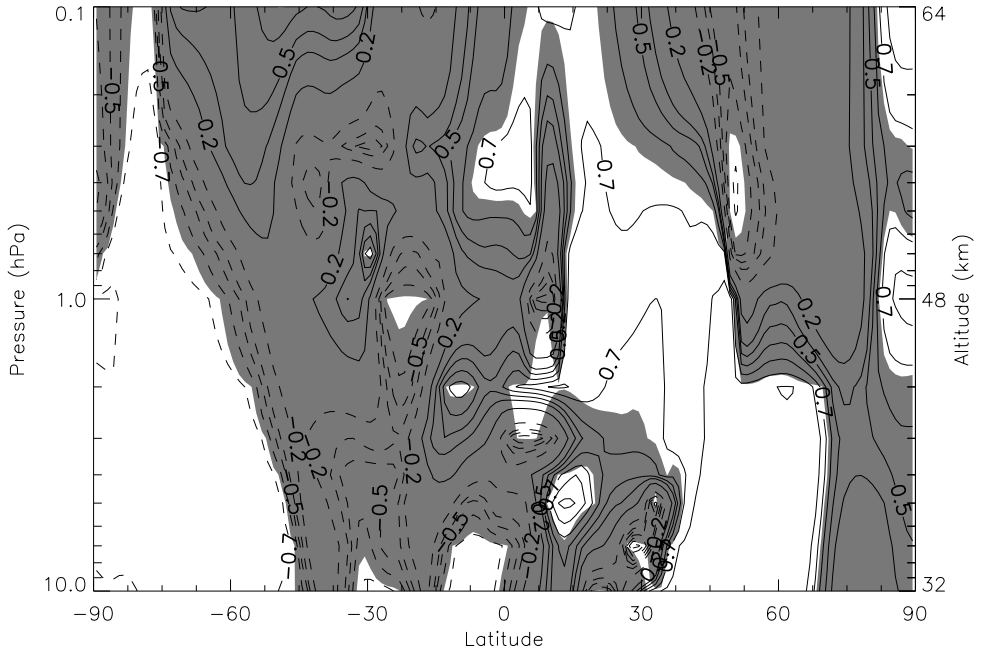

Figure 4.105: Correlation map of SPW1 V on 2007 - 342-350 with a lag of 0. Solid contour lines represent a positive correlation and dashed lines mean negative correlation. Shaded areas mean that the statistical significance of a correlation point is less than 95%.

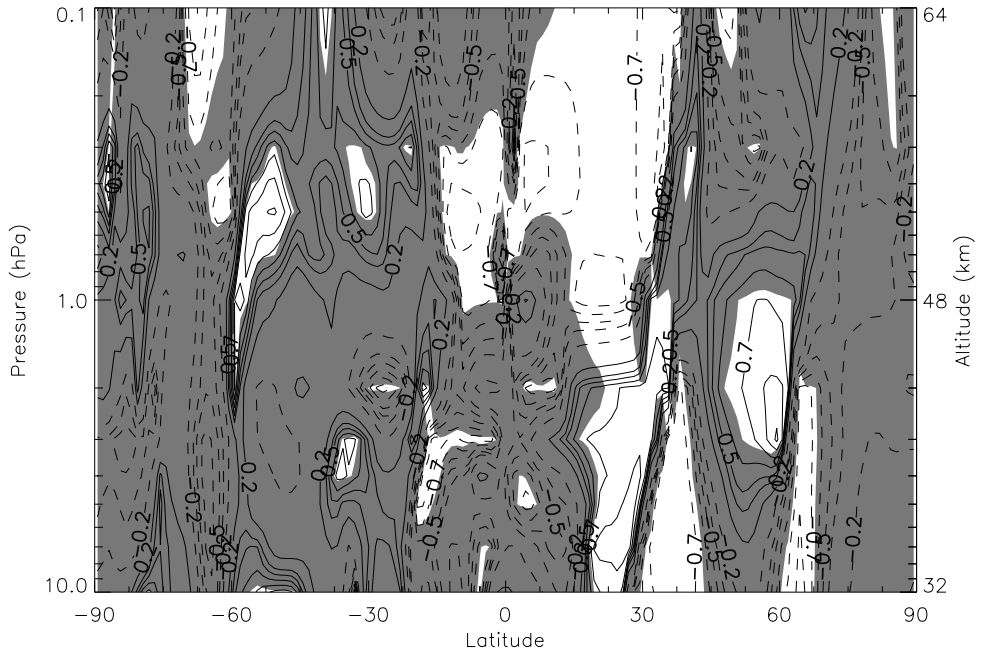

Figure 4.106: Correlation map of SPW2 U on 2007 - 342-350 with a lag of 0. Solid contour lines represent a positive correlation and dashed lines mean negative correlation. Shaded areas mean that the statistical significance of a correlation point is less than 95%.

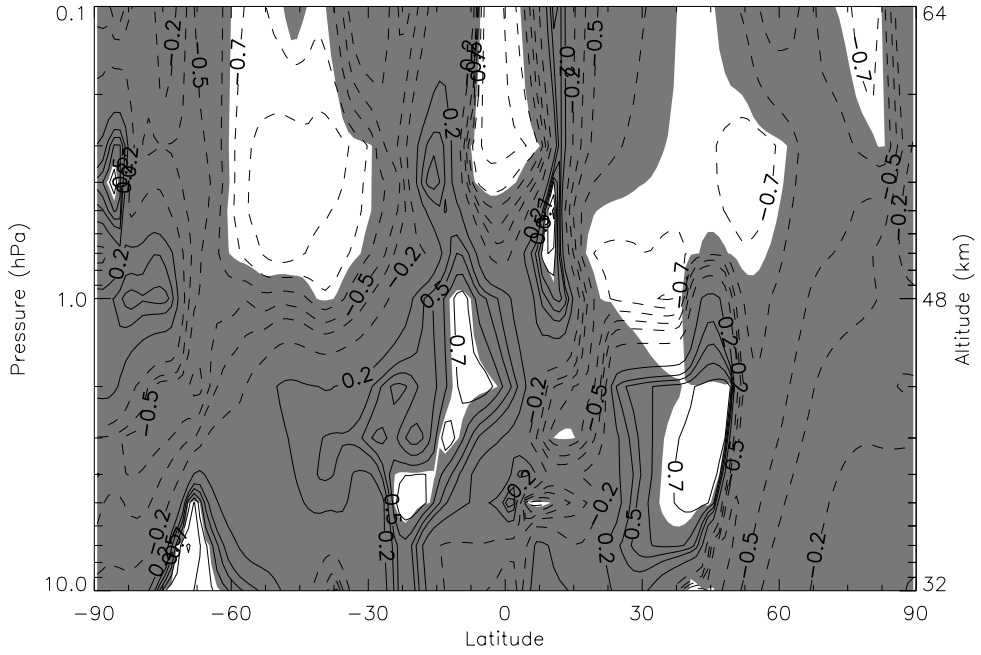

Figure 4.107: Correlation map of SPW2 V on 2007 - 342-350 with a lag of 0. Solid contour lines represent a positive correlation and dashed lines mean negative correlation. Shaded areas mean that the statistical significance of a correlation point is less than 95%.

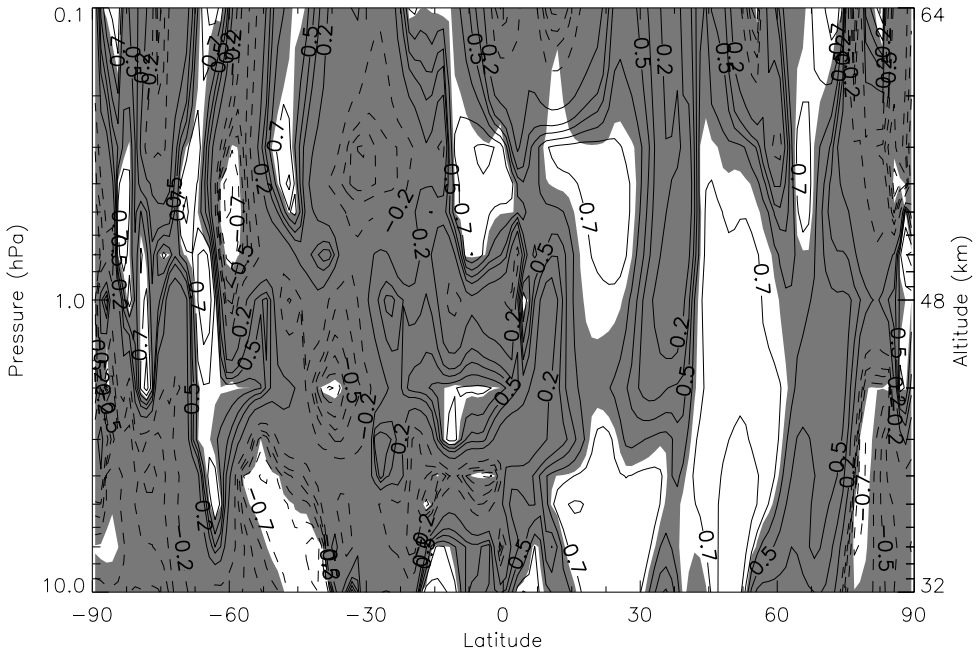

Figure 4.108: Correlation map of SPW3 U on 2007 - 342-350 for lag=0

Correlation map of SPW3 U on 2007 - 342-350 with a lag of 0. Solid contour lines represent a positive correlation and dashed lines mean negative correlation. Shaded areas mean that the statistical significance of a correlation point is less than 95%.

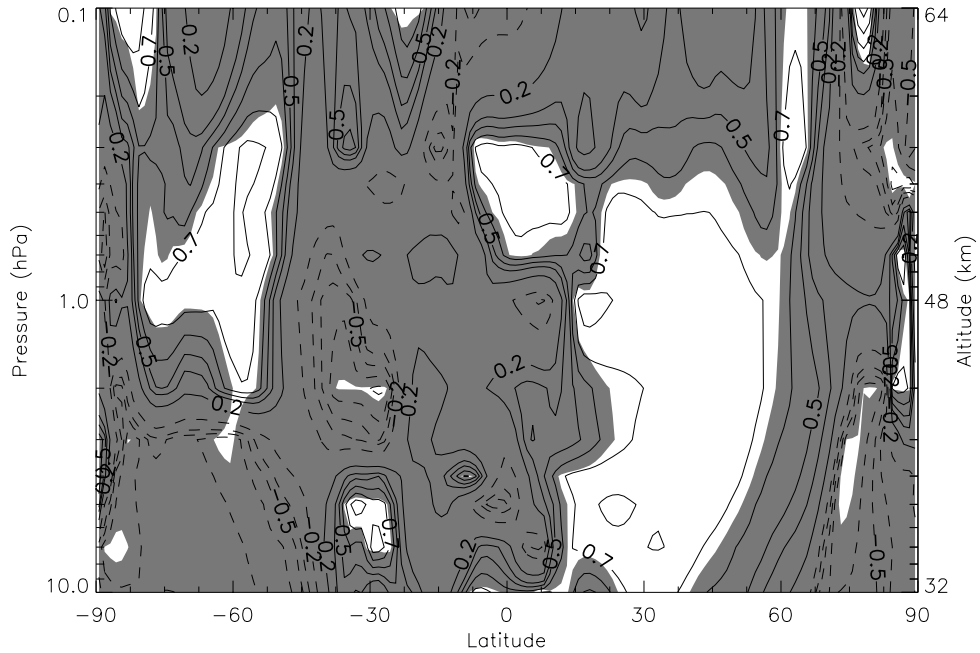

Figure 4.109: Correlation map of SPW3 V on 2007 - 342-350 with a lag of 0. Solid contour lines represent a positive correlation and dashed lines mean negative correlation. Shaded areas mean that the statistical significance of a correlation point is less than 95%.

4.2.7 2008 events

4.2.7.1 2008 - 2-16

This event happened early in 2008, during days 2 through 16. The first feature to stand out is a strong anti-correlation between 12hW1 and SPW1 U and V, as it can be seen on figures 4.110 and 4.111.

Figure 4.112 shows a region of positive correlation with SPW2 U in mid-latitudes and lower altitudes, and a smaller region of negative correlation at higher altitudes. Figure 4.113 shows the correlation with SPW2 V, which is mostly negative around the regions of interest.

Figures 4.114 and 4.115 show the correlation with SPW3 U and V, respectively. Both components show a strong anti-correlation covering a large part of the winter hemisphere.

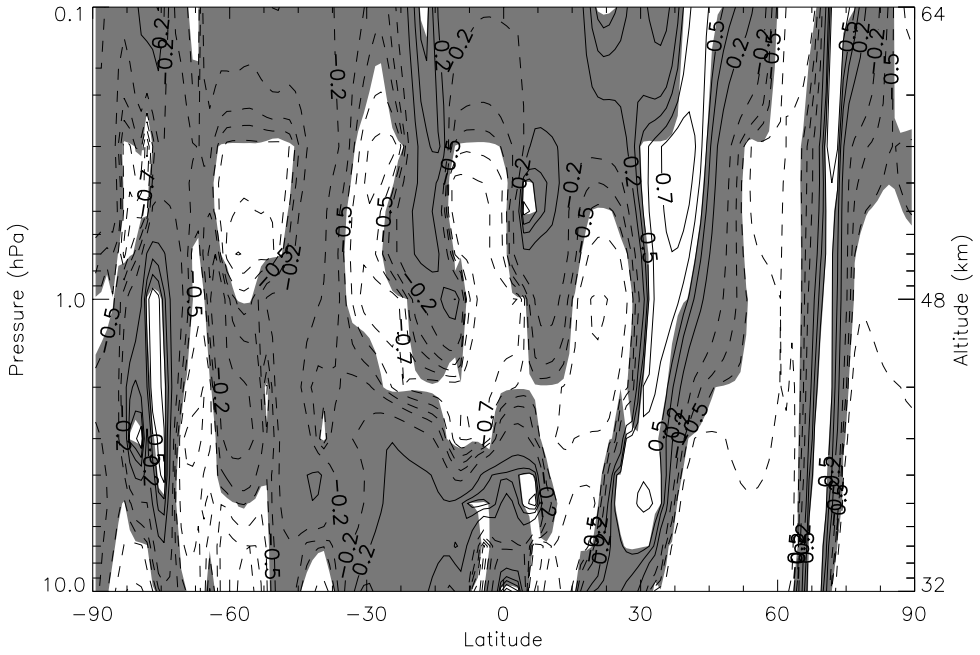

Figure 4.110: Correlation map of SPW1 U on 2008 - 2-16 with a lag of 0. Solid contour lines represent a positive correlation and dashed lines mean negative correlation. Shaded areas mean that the statistical significance of a correlation point is less than 95%.

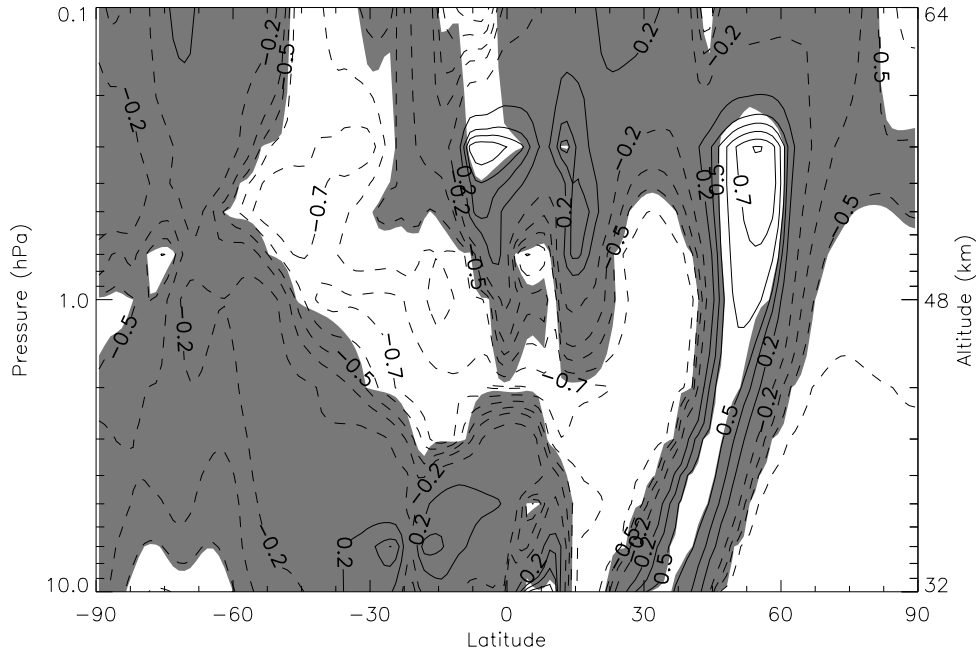

Figure 4.111: Correlation map of SPW1 V on 2008 - 2-16 with a lag of 0. Solid contour lines represent a positive correlation and dashed lines mean negative correlation. Shaded areas mean that the statistical significance of a correlation point is less than 95%.

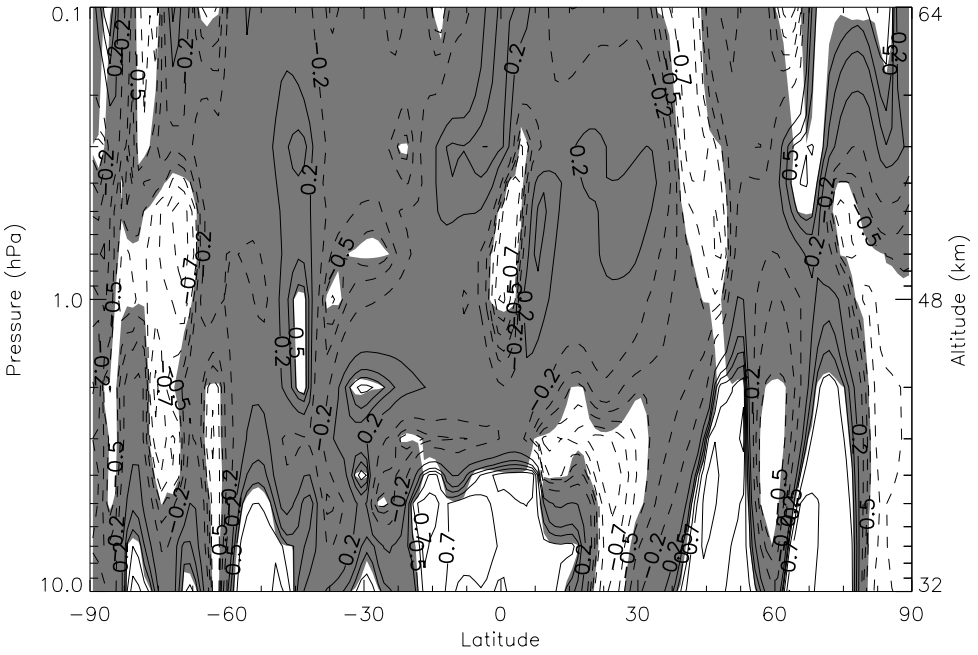

Figure 4.112: Correlation map of SPW2 U on 2008 - 2-16 with a lag of 0. Solid contour lines represent a positive correlation and dashed lines mean negative correlation. Shaded areas mean that the statistical significance of a correlation point is less than 95%.

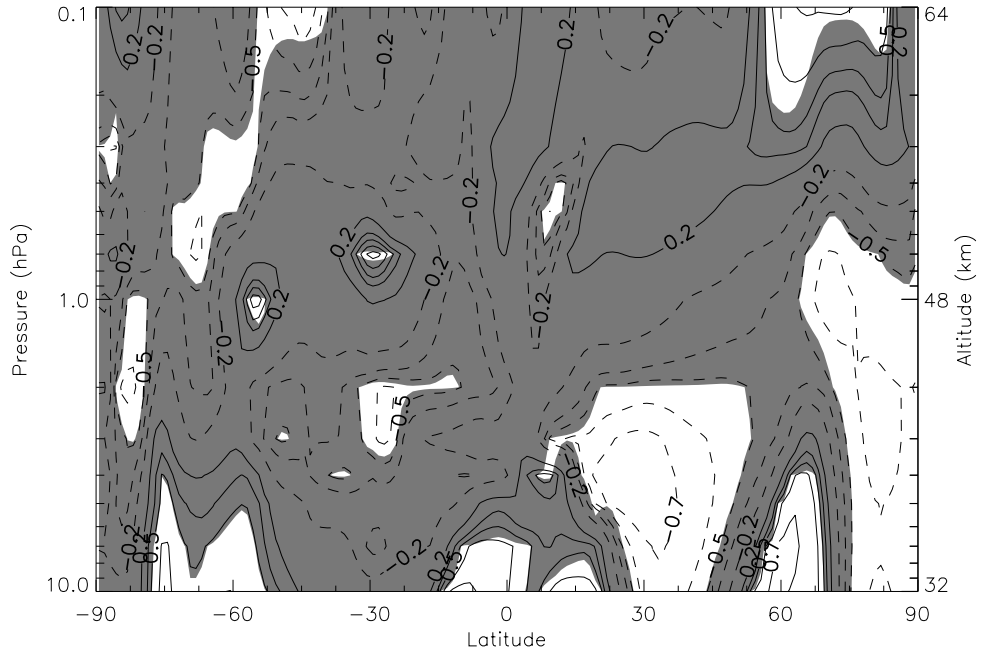

Figure 4.113: Correlation map of SPW2 V on 2008 - 2-16 with a lag of 0. Solid contour lines represent a positive correlation and dashed lines mean negative correlation. Shaded areas mean that the statistical significance of a correlation point is less than 95%.

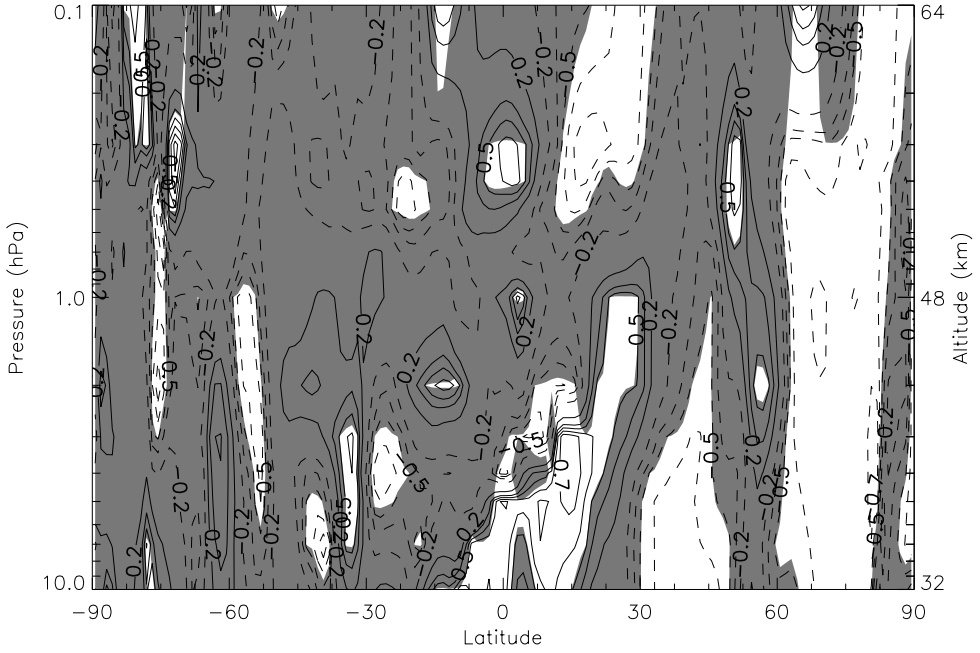

Figure 4.114: Correlation map of SPW3 U on 2008 - 2-16 for lag=0

Correlation map of SPW3 U on 2008 - 2-16 with a lag of 0. Solid contour lines represent a positive correlation and dashed lines mean negative correlation. Shaded areas mean that the statistical significance of a correlation point is less than 95%.

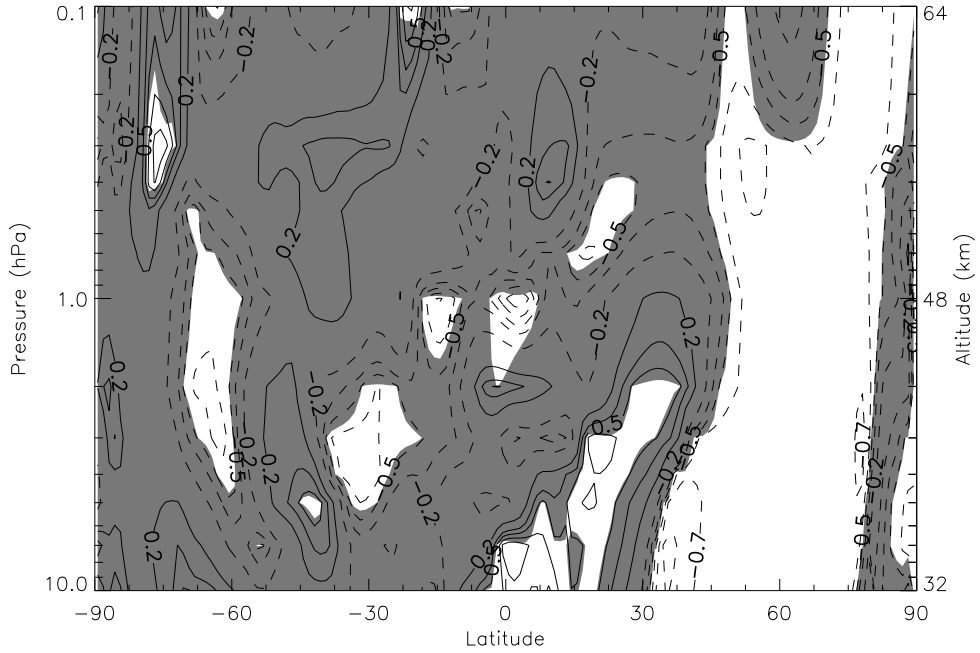

Figure 4.115: Correlation map of SPW3 V on 2008 - 2-16 with a lag of 0. Solid contour lines represent a positive correlation and dashed lines mean negative correlation. Shaded areas mean that the statistical significance of a correlation point is less than 95%.

4.2.7.2 2008 - 33-50

The last event being analyzed in this project happened during days 33 through 50 in 2008. During this event we see on figures 4.116 and 4.117 that there is a strong positive correlation at very high latitudes.

Figures 4.118 and 4.119 show the correlation with SPW2 U and V. Both components show a strong anti-correlation covering most of the low-to-mid latitudes, where SPW2 peaks.

Figures 4.120 and 4.121 show a region of positive correlation around mid latitudes and another region of negative correlation at slightly higher latitudes. These regions are around the peak, which indicates that during this period SPW3 was moving around.

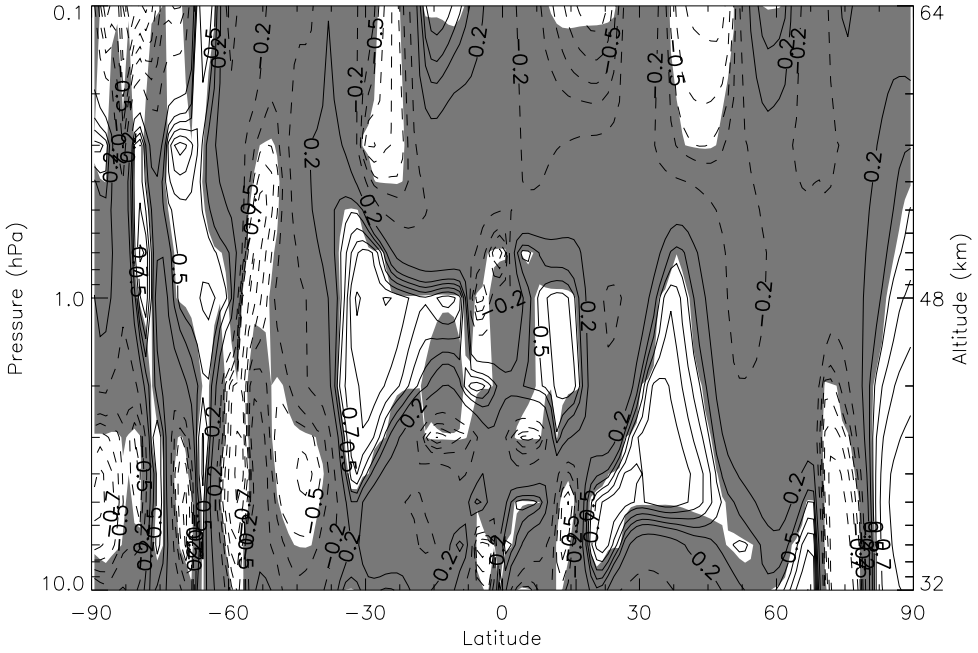

Figure 4.116: Correlation map of SPW1 U on 2008 - 33-50 with a lag of 0. Solid contour lines represent a positive correlation and dashed lines mean negative correlation. Shaded areas mean that the statistical significance of a correlation point is less than 95%.

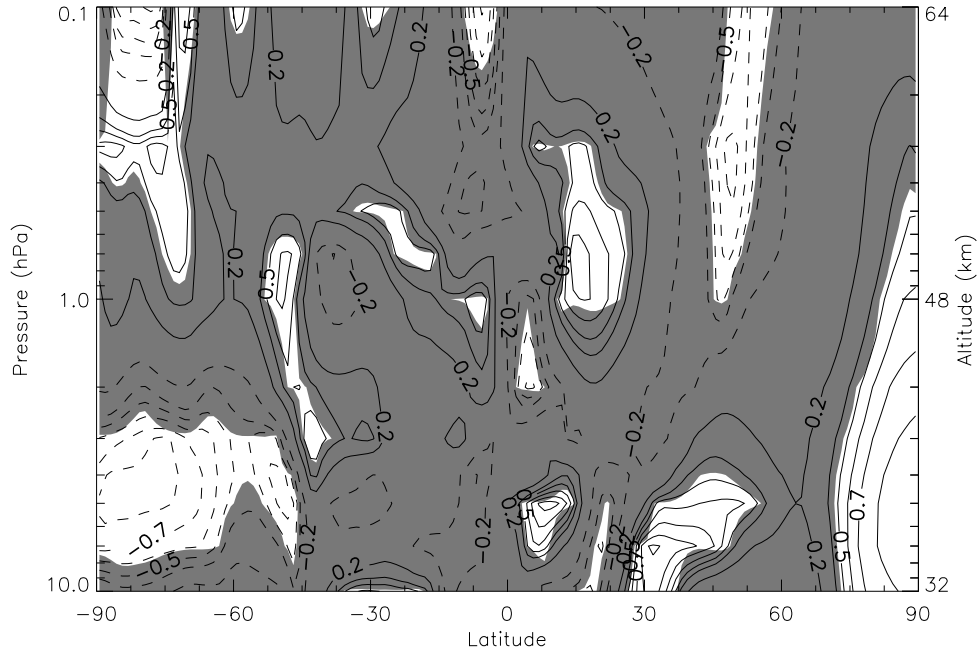

Figure 4.117: Correlation map of SPW1 V on 2008 - 33-50 with a lag of 0. Solid contour lines represent a positive correlation and dashed lines mean negative correlation. Shaded areas mean that the statistical significance of a correlation point is less than 95%.

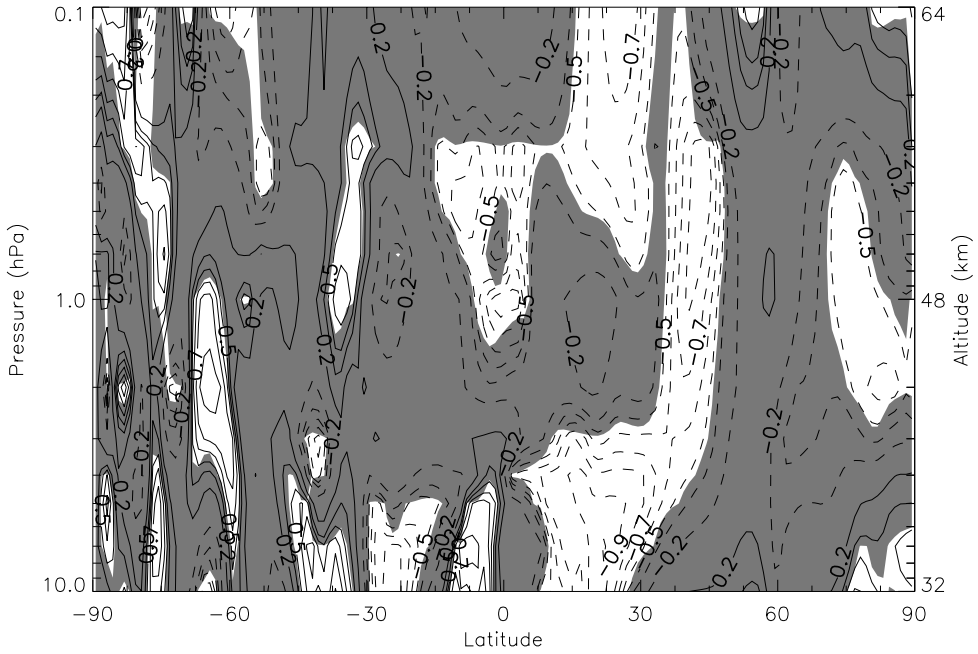

Figure 4.118: Correlation map of SPW2 U on 2008 - 33-50 with a lag of 0. Solid contour lines represent a positive correlation and dashed lines mean negative correlation. Shaded areas mean that the statistical significance of a correlation point is less than 95%.

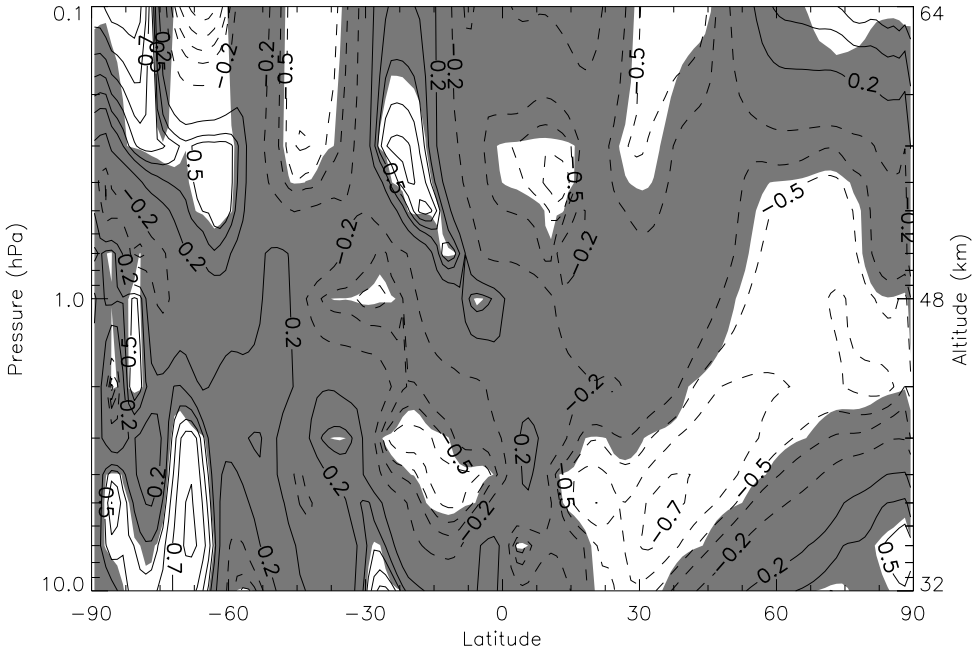

Figure 4.119: Correlation map of SPW2 V on 2008 - 33-50 with a lag of 0. Solid contour lines represent a positive correlation and dashed lines mean negative correlation. Shaded areas mean that the statistical significance of a correlation point is less than 95%.

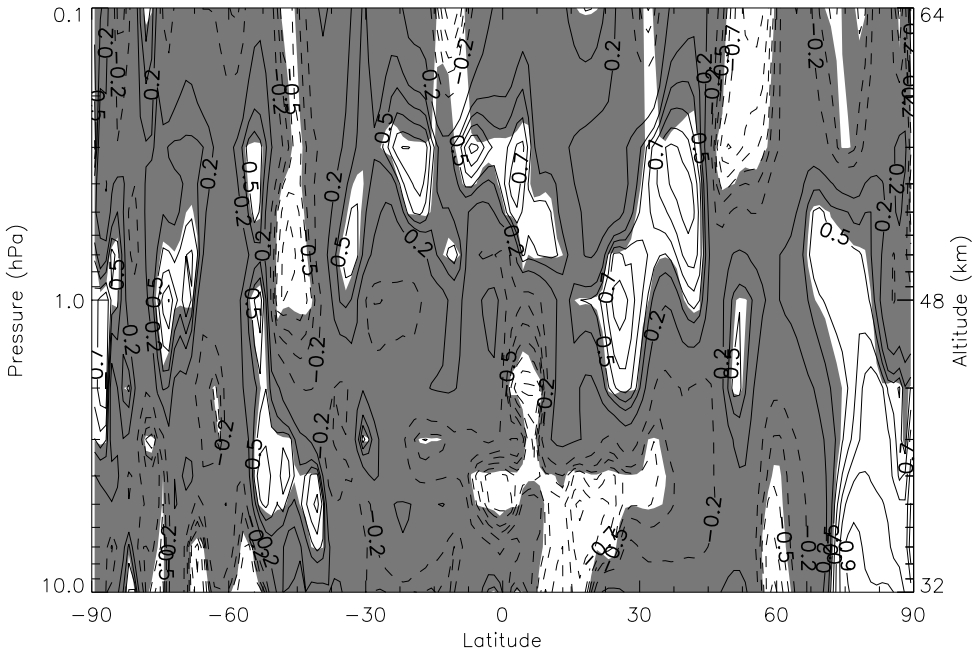

Figure 4.120: Correlation map of SPW3 U on 2008 - 33-50 for lag=0

Correlation map of SPW3 U on 2008 - 33-50 with a lag of 0. Solid contour lines represent a positive correlation and dashed lines mean negative correlation. Shaded areas mean that the statistical significance of a correlation point is less than 95%.

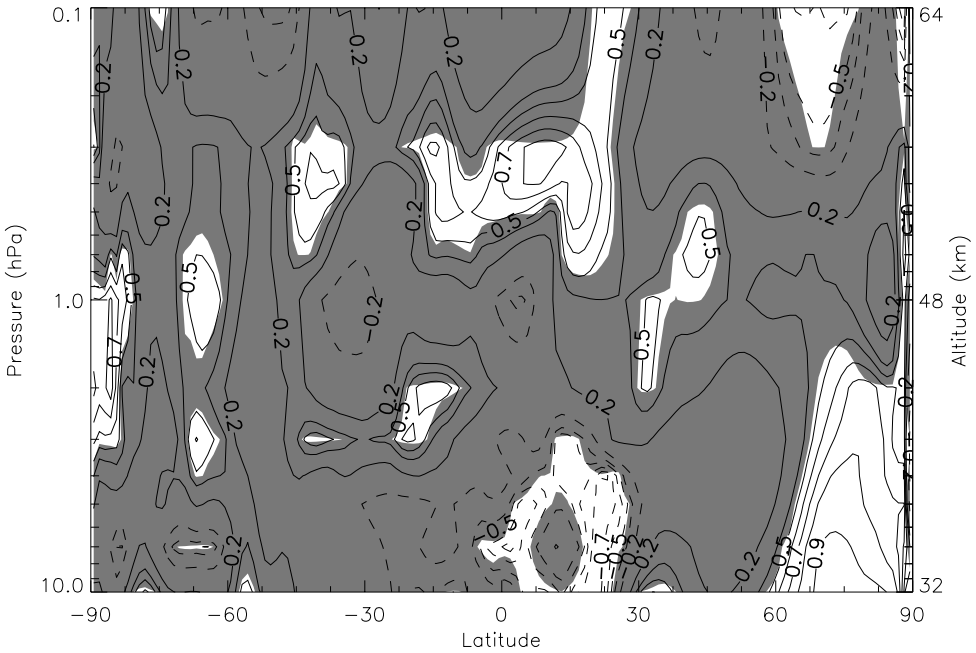

Figure 4.121: Correlation map of SPW3 V on 2008 - 33-50 with a lag of 0. Solid contour lines represent a positive correlation and dashed lines mean negative correlation. Shaded areas mean that the statistical significance of a correlation point is less than 95%.

Chapter 5

DISCUSSION

5.1 Summary of events

This section presents a summary of the correlations that dominate each of components of each of the events presented in Chapter 4. This was done by looking at each plot and deciding the most dominant sign of statistically significant correlation at lower altitudes (<48km) and higher altitudes (>48km), based on where each component usually peaks. Then from these two values from each plot the common result was obtained.

Table 5.1 brings these statistics for all the events between 2002 and 2005. Table 5.2 shows the events from 2006 to 2008. In both tables, next to the correlation analysis just described it also shown for each event analyzed, what the QBO phase was and also if there was a SSW event that happened relatively close. The SSW event is described as the center day of the event and in parenthesis is how many days it lasted (e.g. on event 2004 - 10-50, SSW was centered on day 2004-7 and was 9 days long).

Based on the overall data from tables 5.1 and 5.2, a histogram of the correlation signs of each SPW component on each event was computed, as it can be seen on figure 5.1. This histogram shows the histogram for each of the three SPW components. Each histogram has three vertical bars. The blue bars indicate the quantity of events (out of the 18 presented in Chapter 4) that had a significant positive correlation, the green bars indicate the events that had a significant negative correlation and the red bars indicate events that had both positive and negative correlations around the region of interest (due to significant SPW movement).

Table 5.1: Summary of the correlations of the 2002-2005 events

Year	Days	SPW U	Low Altitude <48km	High Altitude >48km	Overall	QBO Phase	SSW
2002	325-342	SPW1	n/a	+	+	W	–
		SPW2	+	-	+/-		
		SPW3	-	-	-		
	345-365	SPW1	+	+	+	W	–
		SPW2	+/-	+/-	+/-		
		SPW3	-	-	-		
2003	1-13	SPW1	+	-	+/-	W	18 (1)
		SPW2	-	-	-		
		SPW3	-	-	-		
	10-30	SPW1	n/a	n/a	n/a	W	18 (1)
		SPW2	+	+	+		
		SPW3	+	+	+		
	45-70	SPW1	-	+	+/-	W	18 (1)
		SPW2	+/-	+/-	+/-		
		SPW3	+	+	+		
2004	10-50	SPW1	+	+	+	E	7 (9)
		SPW2	+/-	+/-	+/-		
		SPW3	-	+	+/-		
	55-85	SPW1	+	+	+	E	7 (9)
		SPW2	+	+	+		
		SPW3	+	+	+		
2005	50-75	SPW1	+	+	+	E	–
		SPW2	-	+	+/-		
		SPW3	+	+	+/-		
	277-291	SPW1	+	+	+	E	–
		SPW2	+/-	n/a	+/-		
		SPW3	+	+	+		
	317-333	SPW1	+	+	+	E	–
		SPW2	+/-	+/-	+/-		
		SPW3	+	+	+		

Table 5.2: Summary of the correlations of the 2006-2008 events

Year	Days	SPW U	Low Altitude <48km	High Altitude >48km	Overall	QBO Phase	SSW
2006	45-62	SPW1	+	+	+	E	21 (26)
		SPW2	-	-	-		
		SPW3	-	+	+/-		
	60-90	SPW1	+	+	+	E	21 (26)
		SPW2	-	-	-		
		SPW3	+	+	+		
2007	1-9	SPW1	-	-	-	W	55 (4)
		SPW2	-	+	+/-		
		SPW3	-	-	-		
	15-32	SPW1	+	+	+	W	55 (4)
		SPW2	+	n/a	+		
		SPW3	+	+	+		
	45-75	SPW1	+	-	+/-	W	55 (4)
		SPW2	+	+	+		
		SPW3	+	+	+		
	342-350	SPW1	+	+	+	W	–
		SPW2	+	-	+/-		
		SPW3	+	+	+		
2008	2-16	SPW1	-	-	-	E	74 (7)
		SPW2	+	-	+/-		
		SPW3	-	+	+/-		
	33-50	SPW1	+	+	+	E	74 (7)
		SPW2	-	-	-		
		SPW3	-	+	+/-		

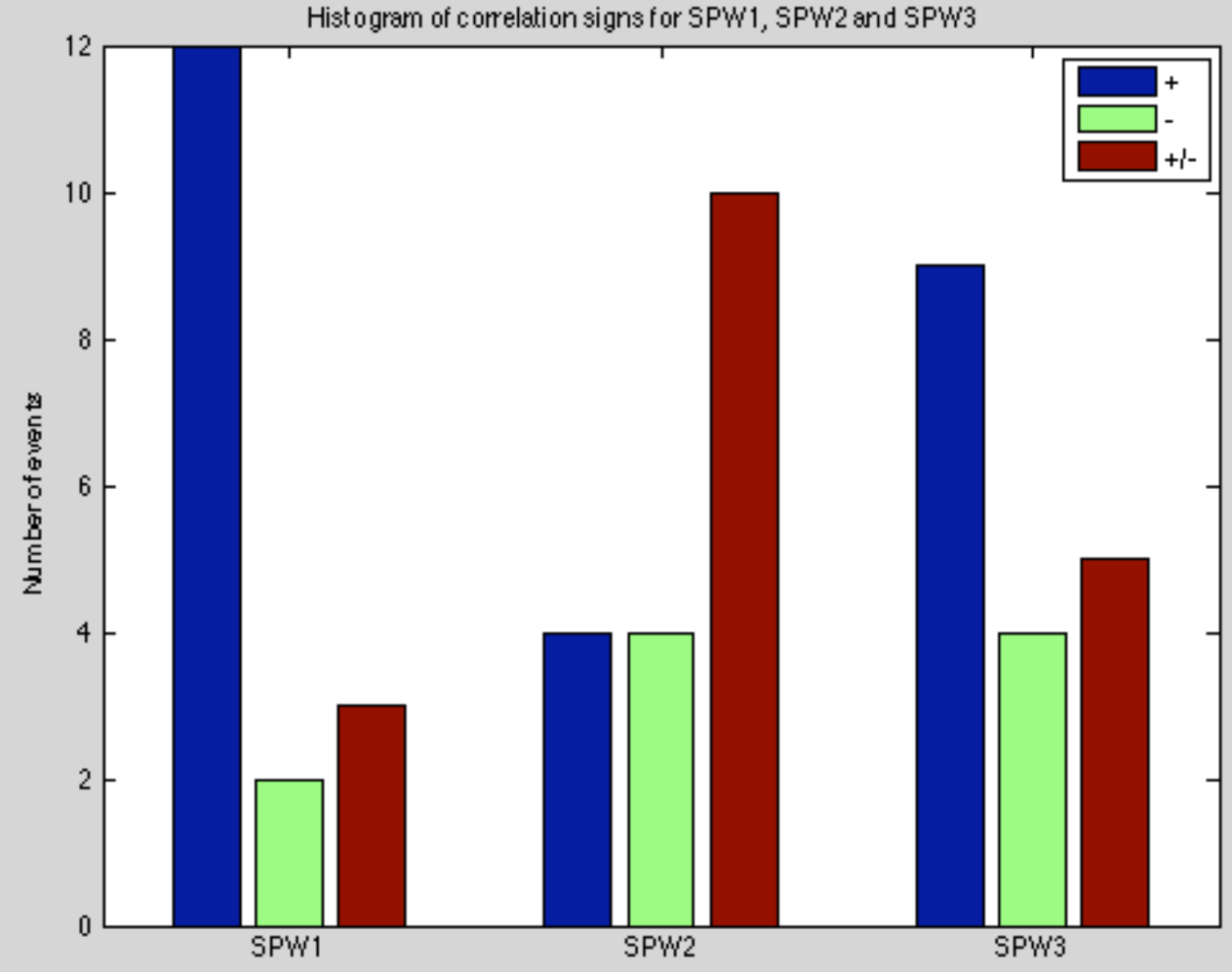

Figure 5.1: This is a histogram plot of the dominant correlation signs during the 18 events analyzed for SPW1, SPW2 and SPW3. Blue bars correspond the quantity of positive correlations, green bars correspond the quantity of negative correlations and red bars represent the quantity of events that had both positive and negative significant correlations

5.2 10-day Correlations Throughout the 2002-2008 Austral Summer Seasons

Figures 5.2 - 5.7 depict another way to look at structure of the correlation between SPW1, SPW2 and SPW3 with 12hW1. On these plots a correlation coefficient was calculated at each day of austral summer season (as long as there was available SPMR data) by using a 10-day window centered on this date. The SPW data obtained for the correlation was by collecting the maximum amplitude present in each, regardless of its geographical position (we basically followed the peak at each day). This process was repeated through the 2002-2008 seasons and plotted together (but separated by SPW components). All the plots follow a color scheme that is represented by: Red blocks correspond to a positive correlation of at least 0.6, green blocks correspond to a negative correlation of at least -0.6, purple blocks represent correlations between -0.6 and 0.6 and black blocks represent missing SPMR data.

Figure 5.2 shows this analysis for SPW1 U. The first feature that can be easily recognized that basically for every season in which SPMR data are present in the beginning and end of the season there seems to be a strong positive correlation on these ends of the season. Another feature is that for most of the cases, both positive and negative correlations tend to dominate for a reasonable amount of time (at least 30 days) before switching to the other kind of correlation. Figure 5.3 shows the analysis for SPW1 V. Its structure is extremely similar to SPW1 U, with regards to the fact that there seems to exist more periods with a positive correlation.

The analysis for SPW2 U can be seen on figure 5.4. SPW2 U also seems to have a positive correlation in the beginning and end of most of the seasons. From the available data it also seems that during the middle of the season SPW2 U tends to have mostly a positive correlation. It also presents long periods for a correlation, before switching to the other correlation. Figure 5.5 shows that the correlation for SPW2 V is almost identical to SPW2 U.

SPW3 U and V correlations can be seen on figures 5.6 and 5.7, respectively. Both

components of SPW3 show a very similar structure, which has as its most interesting feature the fact that in the most recent years (since 2004) a strong negative correlation seems to dominate almost all of the second half of the austral summer season.

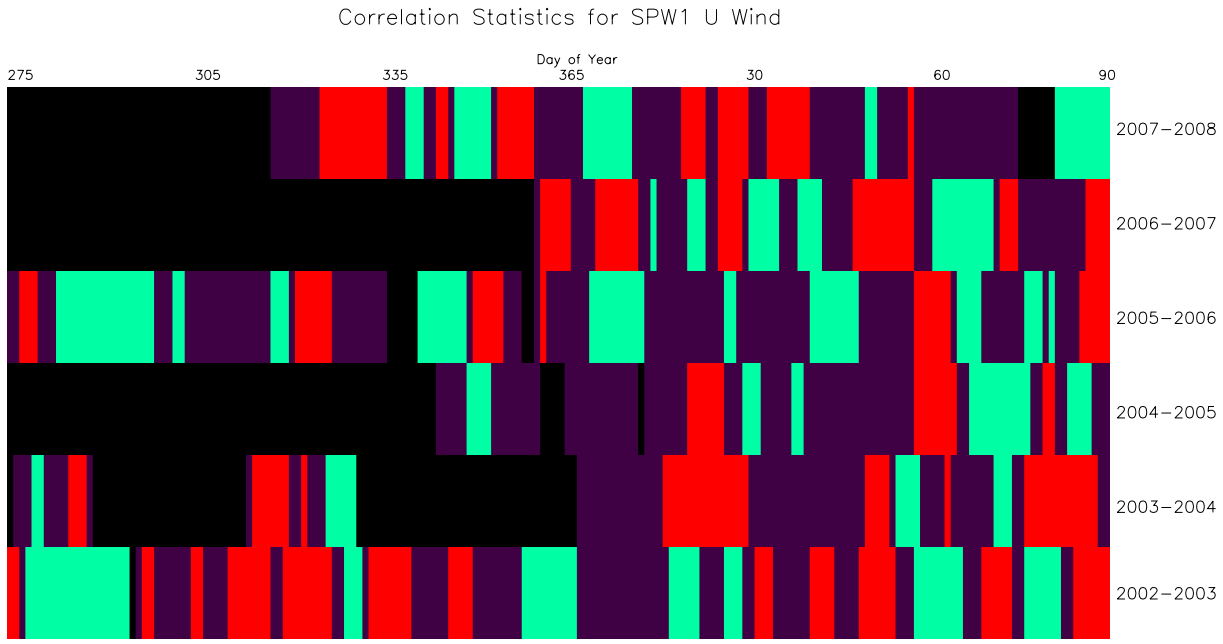

Figure 5.2: This plot represents 10-day SPW1 U correlations centered on each day of the austral summer season from 2002-2008. Red blocks mean a positive correlation of at least 0.6, green means a negative correlation of at least -0.6, purple means a correlation between -0.6 and 0.6 and black represents missing data (due to SPMR being offline)

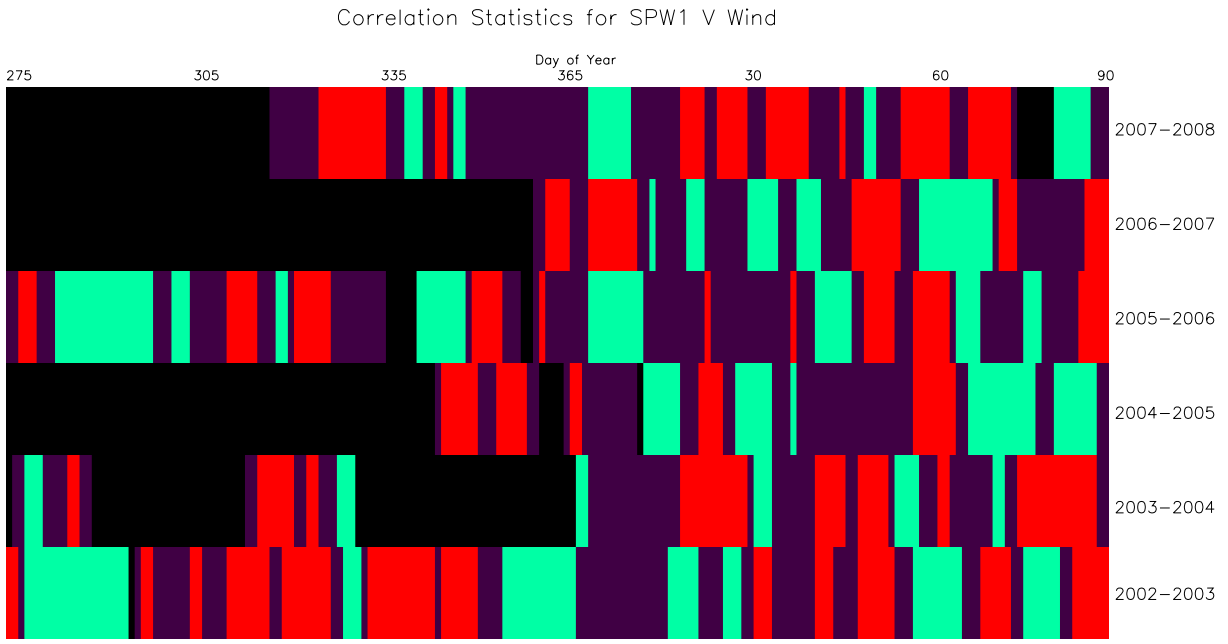

Figure 5.3: This plot represents 10-day SPW1 V correlations centered on each day of the austral summer season from 2002-2008. Red blocks mean a positive correlation of at least 0.6, green means a negative correlation of at least -0.6, purple means a correlation between -0.6 and 0.6 and black represents missing data (due to SPMR being offline).

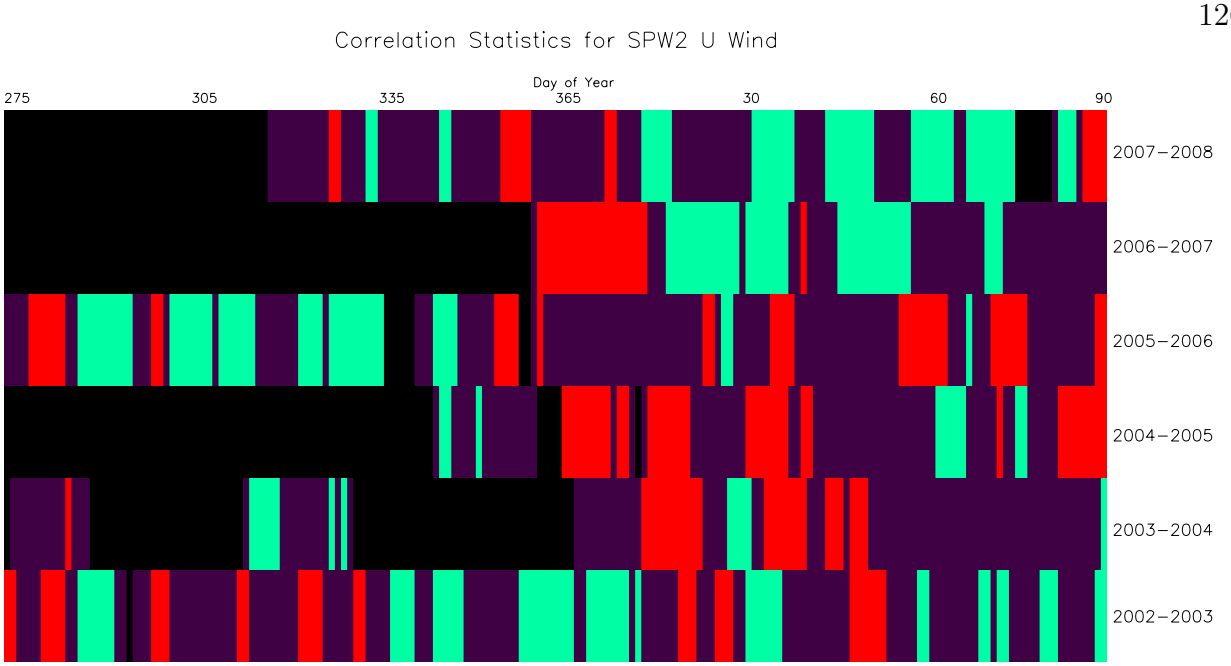

Figure 5.4: This plot represents 10-day SPW2 U correlations centered on each day of the austral summer season from 2002-2008. Red blocks mean a positive correlation of at least 0.6, green means a negative correlation of at least -0.6, purple means a correlation between -0.6 and 0.6 and black represents missing data (due to SPMR being offline)

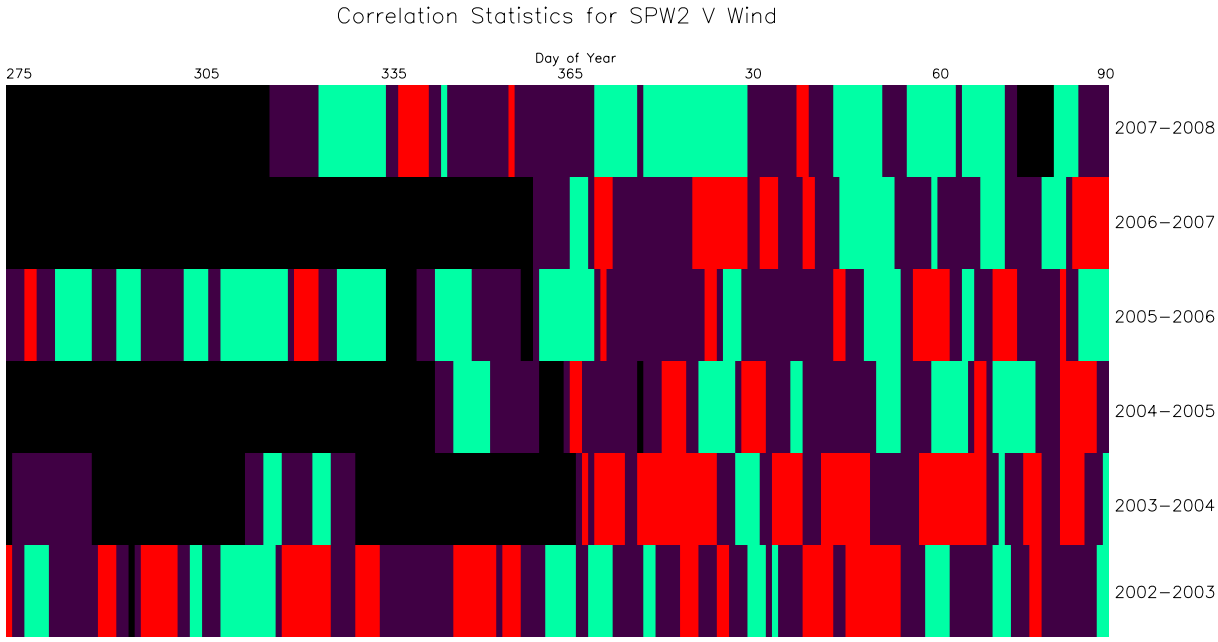

Figure 5.5: This plot represents 10-day SPW2 V correlations centered on each day of the austral summer season from 2002-2008. Red blocks mean a positive correlation of at least 0.6, green means a negative correlation of at least -0.6, purple means a correlation between -0.6 and 0.6 and black represents missing data (due to SPMR being offline).

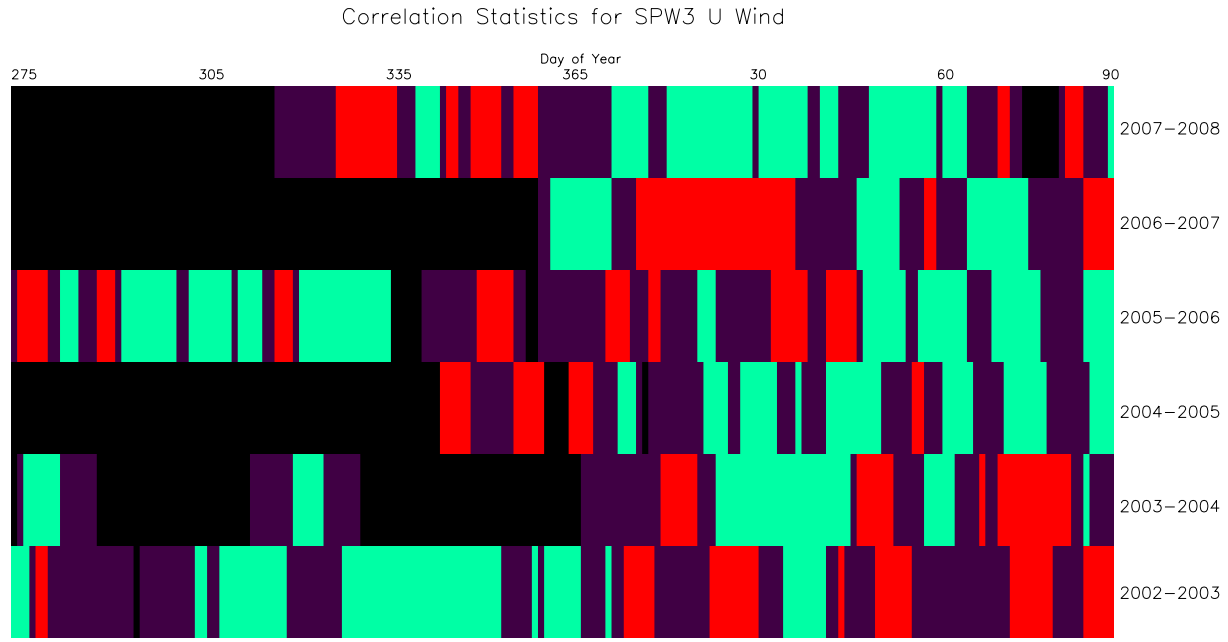

Figure 5.6: This plot represents 10-day SPW3 U correlations centered on each day of the austral summer season from 2002-2008. Red blocks mean a positive correlation of at least 0.6, green means a negative correlation of at least -0.6, purple means a correlation between -0.6 and 0.6 and black represents missing data (due to SPMR being offline)

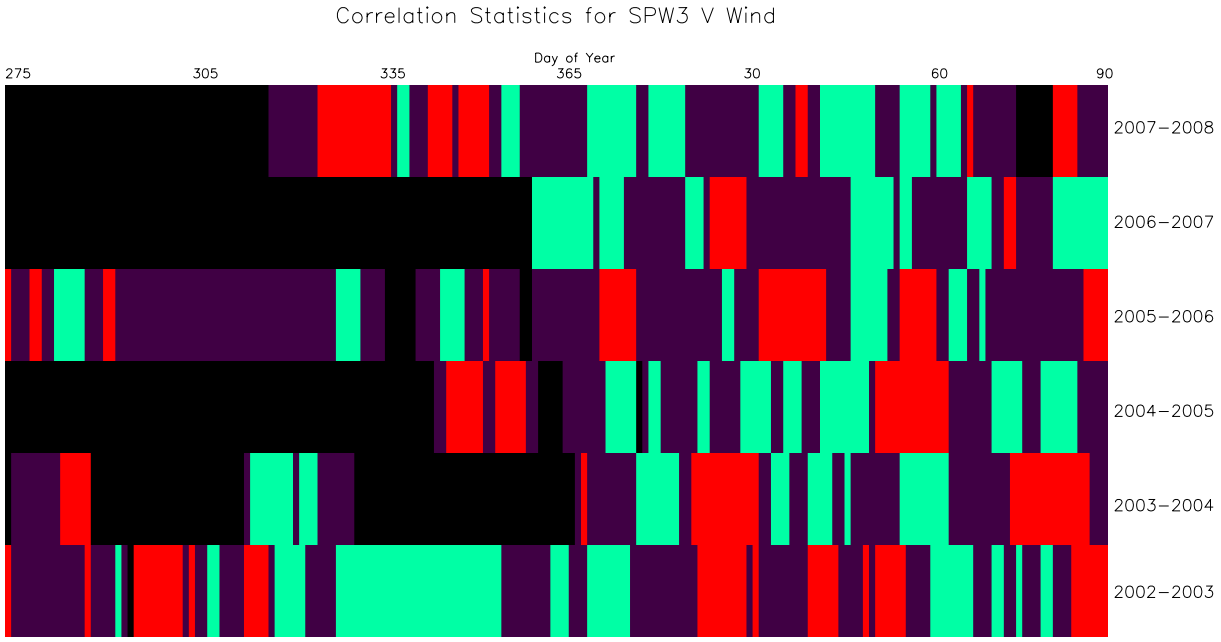

Figure 5.7: This plot represents 10-day SPW3 V correlations centered on each day of the austral summer season from 2002-2008. Red blocks mean a positive correlation of at least 0.6, green means a negative correlation of at least -0.6, purple means a correlation between -0.6 and 0.6 and black represents missing data (due to SPMR being offline).

5.3 Recurring Mechanisms from the Statistical Analysis

Based on the information provided by tables 5.1 and 5.1 and by figure 5.1, some more statistics were obtained. All the following analysis were obtained by taking into account the behavior of the correlation close to the region where the specific SPW component is usually more excited.

Regarding SPW1, 17 out of the 18 events analyzed provided significant correlation. Out of these, 12 had a positive correlation, 2 had a negative correlation and 3 had a +/− correlation, which happens due to significant movement of the SPW during the event.

During events that there was a SSW event inside or near the period of each event all SPW1 correlations had a +/− sign and were on the West phase of the QBO. When QBO was on East phase, 8 out of 9 events had a positive correlation. When QBO was on West phase, 4 events had a positive correlation, 1 had negative and 3 had +/− correlations.

SPW2 had 4 events with positive correlation, 4 with negative and 10 with +/−. Due to high variability of SPW2 geographically and also of its amplitude, it is not straight forward to define a metric to analyze each case. It can be seen that SPW2 definitely has a correlation with the behavior of 12hW1, but it might be just a minor player (if at all) in the dynamics of the 12hW1 in the south pole.

Regarding SPW3, 9 events had a strong positive correlation, 4 had a negative correlation and 5 had +/− correlation signs around the region of interest (which means significant movement of SPW3 in the northern hemisphere). During the events that there was a SSW event inside or near the period of each event analyzed, SPW3 had 5 positive correlations, 1 negative and 3 events with a +/− correlation.

When QBO had an East phase, SPW3 had 4 positive events and 5 with a +/− sign. When QBO has a West phase, 4 events were negative and 5 were positive.

Chapter 6

CONCLUSION

6.1 Conclusion

In this investigation a diagnostic study was carried out in order to characterize the features that might be important in the evolution and variability of the non-migrating semidiurnal tide at the South Pole. The conclusions of the study are summarized below:

(1) It has been proposed in literature that the SPW1 is a driving mechanism for the 12hW1, which can be observed at the South Pole. It has been found in this study that SPW1 is not clearly correlated with the 12hW1 in a SSW or pre-SSW configuration. It was also shown that there exists a significant correlation with the variability of the 12hW1 and SPW1 when QBO is in its East phase.

(2) SPW2 is extremely variable both in its amplitude and location of maximum. Even though the analysis presented here shows strong positive and negative correlations in most of the events, SPW2 is not believed to be a major driving mechanism because through a non-linear interaction it gives the wrong wavenumber.

(3) SPW3 is relatively dynamical in the northern hemisphere, like SPW2, but it seems to be more consistent with the analysis of the variability of 12hW1. During SSW or pre-SSW atmospheric conditioning SPW3 is not a clear metric (or at least is not well understood), however there seems to be a pattern on the behavior of SPW1 and

SPW3 as a system. However, through a non-linear interaction with SPW3 we still get a wrong sign for the wavenumber.

It has been shown in this work that there is a statistically significant relationship between stationary planetary wave activity in the northern hemisphere affecting the structure and variability of the non-migrating semidiurnal tide over the south pole. The stationary planetary wave wavenumber 1 (SPW1) appears to be the most important feature in almost all of the events analyzed. SPW2 has a minor role in this interaction, since there is a correlation but it does not follow a specific pattern. SPW3 seems to be well correlated with 12hW1, although its amplitudes are not nearly as strong as SPW1 and also its non-linear interaction does not yield the right tidal component.

A specific metric is difficult to obtain at this point in time since it is complicated to find recurring mechanisms due to different non-linear interactions that exist, and also due to the occurrence of Sudden Stratospheric Warming events. Furthermore, constant interaction with the QBO presents different dynamics depending on its current phase.

There is still not a definite answer to this problem, however this study will further help characterize this non-linear relationship and future works can focus on the interactions with different waves and tides in order to achieve a concise understanding of this process.

6.2 Future work

This work characterized through a series of events that there is a strong connection between the non-migrating semidiurnal tide and stationary planetary wave s=1,2 and 3. However, the non-linear dynamics that drives this variability is still not very well understood. In order to try to understand this interaction better, the correlation of 12hW1 and SPW1 also needs to be analyzed close to the region where SPW1 maximizes in the northern winter hemisphere. As previously discussed, one must pay attention to SSW events and also the QBO phase, since there might be a deeper connection which is still not understood.

Another way to tackle this problem would be to use TIME-GCM to try to reproduce the variability of the 12hW1 seen in these events by forcing the model with the waves used in the analysis obtained from MERRA.

Bibliography

[1] Goddard earth sciences data and information services center. http://disc.sci.gsfc.nasa.gov/daac-bin/FTPSubset.pl, October 2010.

[2] National center for atmospheric research. http://www.ncl.ucar.edu/Applications/heighttime.shtml, March 2012.

[3] The ozone hole. http://www.theozonehole.com/atmosphere.htm, March 2012.

[4] S. M. I. Azeem, E. R. Talaat, G. G. Sivjee, and J.-H. Yee. Mesosphere and lower thermosphere temperature anomalies during the 2002 antarctic stratospheric warming event. Annales Geophysicae, 2010.

[5] M. P. Baldwin, L. J. Gray, T. J. Dunkerton, K. Hamilton, P. H. Haynes, W. J. Randel, J. R. Holton, M. J. Alexander, I. Hirota, T. Horinouchi, D. B. A. Jones, J. S. Kinnersley, C. Marquardt, K. Sato, and M. Takahashi. The quasi-biennial oscillation. Reviews of Geophysics, 2001.

[6] A. G. Beard, N. J. Mitchell, P. J. S. Williams, and M. Kunitake. Non-linear interaction between tides and planetary waves resulting in period tidal variability. Journal of Atmospheric and Solar-Terrestrial Physics, 1999.

[7] P. O. Canziani. On tidal variability and the existence of planetary wave-like oscillations in the upper thermosphere - ii. non-linear interactions and global scale oscillations. Journal of Atmospheric and Terrestrial Physics, 1994.

[8] L. C. Chang. Analysis of the migrating diurnal tide in the whole atmosphere community climate model. Master's thesis, University of Colorado at Boulder, 2006.

[9] L. C. Chang. Migrating Diurnal Tide Variability Induced by Propagating Planetary Waves. PhD thesis, University of Colorado at Boulder, 2010.

[10] L. C. Chang, S. E. Palo, and H.-L. Liu. Short-term variation of the s=1 nonmigrating semidiurnal tide during the 2002 stratospheric sudden warming. Journal of Geophysical Research, 2009.

[11] S. Chapman and R. S. Lindzen. Atmospheric Tides: Thermal and Gravitation. Gordon and Breach Science Publishers, 1970.

[12] A. J. Charlton and L. M. Polvani. A new look at stratospheric sudden warmings. part i: Climatology and modeling benchmarks. American Meteorological Society, 2007.

[13] W. Chen, M. Takahashi, and H-F. Graf. Interannual variations of stationary planetary wave activity in the northern winter troposphere and stratosphere and their relations to nam and sst. Journal of Geophysical Research, 2003.

[14] A. Ebel. Contributions of gravity waves to the momentum, heat and turbulent energy budget of the upper mesosphere and lower thermosphere. Journal of Atmospheric and Terrestrial Physics, 1984.

[15] J. M. Forbes. Atmospheric tides 1. model description and results for the solar diurnal component. Journal of Geophysical Research, 1982.

[16] J. M. Forbes. Modelling the propagation of atmospheric tides from the lower to the middle and upper atmosphere. Physica Scripta, 1987.

[17] J. M. Forbes. Tidal and planetary waves. Geophysical Monograph, American Geophysical Union, 1995.

[18] J. M. Forbes, N. A. Makarov, and Y. I Portnyagin. First results form the meteor radar at south pole: A large 12-hour oscillation with zonal wavenumber one. Geophysical Research Letters, 1995.

[19] J. M. Forbes, Y. I Portnyagin, N. A. Makarov, S. E. Palo, E. G. Merzlyakov, and X. Zhang. Dynamics of the lower thermosphere over south pole from meteor radar wind measurements. Earth Planets Space, 1999.

[20] J. M. Forbes, X. Zhang, M. E. Hagan, J. M. Russell III, S. E. Palo, C. J. Mertens, and M. G. Mlynczak. Monthly tidal temperatures 20-120km from timed/saber.

[21] R. R. Garcia, R. Lieberman, J. M. Russell III, and M. G. Mlynczak. Large-scale waves in the mesosphere and lower thermosphere observed by saber. Journal of the Atmospheric Sciences, 2005.

[22] M. E. Hagan, C. McLandress, and J. M. Forbes. Diurnal tidal variability in the upper mesosphere and lower thermosphere. Annales Geophysicae, 1997.

[23] M. E. Hagan, R. G. Roble, and J. Hackney. Migrating thermospheric tides. Journal of Geophysical Research, 2001.

[24] G. Hernandez, G. J. Fraser, and R. W. Smith. Mesospheric 12-hour oscillation near south pole, antarctica. Geophysical Research Letters, 1993.

[25] J. R. Holton. An Introduction to Dynamic Meteorology. Elsevier Academic Press, fourth edition edition, 2004.

[26] S. S. Hough. On the application of harmonic analysis to the dynamical theory of tides, part i., on laplace's 'oscillation of the first species', and on the dynamics of ocean current. Phil. Trans. Royal Society of London, 1897.

[27] S. S. Hough. On the application of harmonic analysis to the dynamical theory of tides, part ii., on the general integration of laplace's dynamical equations. Phil. Trans. Royal Society of London, 1898.

[28] M. Angelats i Coll and J. M. Forbes. Nonlinear interactions in the upper atmosphere: The s=1 and s=3 nonmigrating semidiurnal tides. Journal of Geophysical Research, 2002.

[29] J. M. Russell III, M. G. Mlynczak, L. L. Gordley, J. Tansock, and R. Esplin. An overview of the saber experiment and preliminary calibration results. In SPIE Conference on Optical Spectroscopic Techniques and Instrumentation for Atmospheric and Space Research, 1999.

[30] H. Iimura, S. E. Palo, Q. Wu, T. L. Killeen, S. C. Solomon, and W. R. Skinner. Structure of the nonmigrating semidiurnal tide above antarctica observed from the timed doppler interferometer. Journal of Geophysical Research, 114, 2009.

[31] T. J. Immel, E. Sagawa, S. L. England, S. B. Henderson, M. E. Hagan, S. B. Mende, H. U. Frey, C. M. Swenson, and L. J. Paxton. Control of equatorial ionospheric morphology by atmospheric tides. Journal of Atmospheric and Solar-Terrestrial Physics, 2006.

[32] D. Janches, S. E. Palo, E. M. Lau, S. K. Avery, J. P. Avery, S. de la Peña, and N. A. Makarov. Diurnal and seasonal variability of the meteoric flux at the south pole measured with radars. Geophysical Research Letters, 2004.

[33] K. Kruger, B. Naujokat, and K. Labitzke. The unusual midwinter warming in the southern hemisphere stratosphere 2002: A comparison to northen hemisphere phenomena. American Meteorological Society, 2004.

[34] E. M. Lau, S. K. Avery, J. P. Avery, D. Janches, S. E. Palo, R. Schafer, and N. A. Makarov. Statistical characterization of the meteor trail distribution at the south pole as seen by a vhf interferometric meteor radar. Radio Science, 2006.

[35] T. Matsuno. Vertical propagation of stationary planetary waves in the winter northern hemisphere. Journal of the Atmospheric Sciences, 1970.

[36] S. E. Palo. Analysis of the Equatorial Semiannual Oscillation and Quasi Two-Day Wave in the Mesosphere and Lower Thermopshere Using a Spectral Model and Data Collected with the Christmas Island Radar Systems. PhD thesis, University of Colorado at Boulder, 1994.

[37] S. E. Palo, J. M. Forbes, X. Zhang, J. M. Russell III, C. J. Mertens, M. G. Mlynczak, G. B. Burns, P. J. Espy, and T. D. Kawahara. Planetary wave coupling from the stratosphere to the thermosphere during the 2002 southern hermisphere pre-stratwarm period. Geophysical Research Letters, 2005.

[38] S. E. Palo, Y. I Portnyagin, J. M. Forbes, N. A. Makarov, and E. G. Merzlyakov. Transient eastward-propagating long-period waves observed over the south pole. Annales Geophysicae, 1998.

[39] M. De La Place. Celestial mechanics. 1825.

[40] Y. I Portnyagin, J. M. Forbes, N. A. Makarov, E. G. Merzlyakov, and S. E. Palo. The summertime 12-h wind oscillation with zonal wavenumber s=1 in the lower thermosphere over the south pole. Annales Geophysicae, 1998.

[41] Y. I Portnyagin, J. M. Forbes, E. G. Merzlyakov, N. A. Makarov, and S. E. Palo. Intradiurnal wind variations observed in the lower thermosphere over the south pole. Annales Geophysicae, 2000.

[42] Y. I Portnyagin, T. V. Solovjova, N. A. Makarov, E. G. Merzlyakov, A. H. Manson, C. E. Meek, W. Hocking, N. Mitchell, D. Pancheva, P. Hoffmann, W. Singer, Y. Murayama, K. Igarashi, J. M. Forbes, S. E. Palo, C. Hall, and S. Nozawa. Monthly mean climatology of the prevailing winds and tides in the arctic mesosphere/lower thermosphere. Annales Geophysicae, 2004.

[43] W. H. Press, B. P. Flannery, S. A. Teukolsky, and W. T. Vetterling. Numerical Recipes in C: The Art of Scientific Computing. Cambridge University Press, 1988.

[44] G. W. Prölss. Physics of the Earth's Space Environment. Springer, 2004.

[45] L. Qian, S. C. Solomon, and T. J. Kane. Seasonal variation of thermospheric density and composition. Journal of Geophysical Research, 2009.

[46] E. G. Remsberg, E. R. Lingenfelser, V. L. Harvey, W. Grose, J. M. Russell III, M. Mlynczak, and L. L. Gordley. On the verification of the quality of saber temperature, geopotential height, and wind fields by comparison with met office assimilated analyses. Journal of Geophysical Research, 2003.

[47] M. M. Rienecker, M. J. Suarez, R. Gelaro, R. Todling, J. Bacmeister, E. Liu, M. G. Bosilovich, S. D. Schubert, L. Takacs, G. Kim, S. bloom, J. Chen, D. Collins, A. Conaty, A. Silva, W. Gu, J. Joiner, R. D. Koster, R. Lucchesi, A. Molod, T. Owens, S. Pawson, P. Pegion, C. R. Redder, R. Reichle, F. R. Robertson, A. G. Ruddick, M. Sienkiewicz, and J. Woolen. Merra: Nasa's modern-era retrospective analysis for research and applications. Journal of Climate, 24, 2011.

[48] M. M. Rienecker, M. J. Suarez, R. Todling, J. Bacmeister, L. Takacs, H.-C. Liu, W. Gu, M. Sienkiewicz, R. D. Koster, R. Gelaro, I. Stajner, and J. E. Nielsen. The geos-5 data assimilation system. Technical report, NASA, 2008.

[49] R. G. Roble and I. Tzur. The global atmospheric-electrical circuit. Studies in Geophysics, 1986.

[50] M. R. Schoeberl. Stratospheric warmings: Observations and theory. Reviews of Geophysics and Space Physics, 1978.

[51] A. K. Smith, N. J. Mitchell D. V. Pancheva, D. R. Marsh, J. M. Russell III, and M. G. Mlynczak. A link between variability of the semidiurnal tide and planetary waves in the opposite hemisphere. Geophysical Research Letters, 2007.

[52] H. Teitelbaum and F. Vial. On tidal variability induced by nonlinear interaction with planetary waves. Journal of Geophysical Research, 96, 1991.

[53] H. Teitelbaum, F. Vial, A. H Manson, R. Giraldez, and M. Massebeuf. Non-linear interaction between the diurnal and semidiurnal tides: terdiurnal and diurnal secondary waves. Journal of Atmospheric and Terrestrial Physics, 1989.

Appendix A

Nomenclature

Throughout this thesis, all quantities that appear primed $\{u', v', \Phi'\}$ denote perturbations of the atmospheric fields. Complex quantities are denoted by a hat over the variable, such as $\{\hat{u}, \hat{v}, \hat{\Phi}\}$. Quantities that have bars $\{\bar{u}, \bar{v}, \bar{\Phi}\}$ denote a zonal mean of the atmospheric field.

T	Temperature
Φ	Geopotential
ϕ	Latitude
λ	Longitude
H	Scale Height
ψ	Phase
u	Zonal Wind Velocity
v	Meridional Wind Velocity
w	Vertical Wind Velocity
ρ_0	Density
a	Radius of the Earth
f	Coriolis Parameter
ω	Angular Frequency
Ω	Rotation Rate of the Earth
s	Zonal Wavenumber

r	Correlation
s(r)	Statistical Significance
J	Adiabatic Heating
N	Buoyancy Frequency
g	Gravity
R	Gas Constant
κ	$\frac{R}{c_p} \approx \frac{2}{7}$

Appendix B

Acronyms

12hW1	Non-migrating semidiurnal tide s=1
3DVAR	Three Dimension Variational Data Assimilation
AGCM	Atmospheric General Circulation Model
GEOS-5	Goddard Earth Observing System Data Assimilation System Version 5
GPS	Global Positioning System
LEO	Low Earth Orbit
MERRA	Modern Era Retrospective Analysis for Research and Applications
MLT	Mesosphere and Lower Thermosphere
NASA	National Aeronautics and Space Administration
QBO	Quasi-Biennial Oscillation
SABER	Sounding the Atmosphere by Broadband Emission Radiometry
SPMR	South Pole Meteor Radar
SPW	Stationary Planetary Wave
SSW	Sudden Stratospheric Warming
TIMED	Thermosphere Ionosphere Mesosphere Energetics and Dynamics

Appendix C

Additional Correlation Analysis

C.1 2002 event

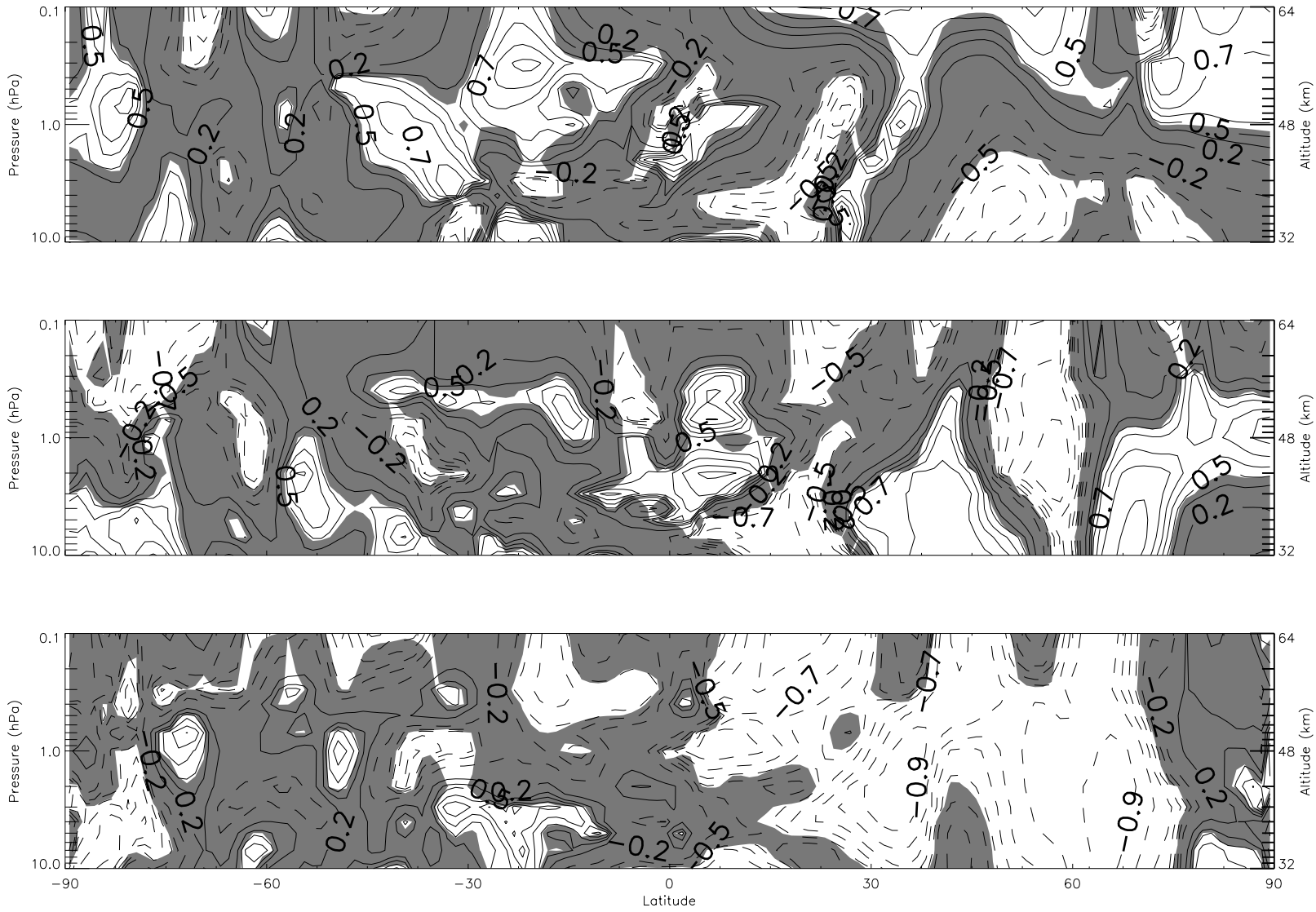

Figure C.1: Correlation map of SPW U s=1,2,3 on 2002 - 325-342 for lag=0

Correlation map of SPW U s=1,2 and 3 on 2002 - 325-342 for lag=0. Top graph shows correlation with SPW1, middle graph with SPW2 and bottom with SPW3. Solid contour lines represent a positive correlation and dashed lines mean negative correlation. Shaded areas mean that the statistical significance of a correlation point is less than 95%.

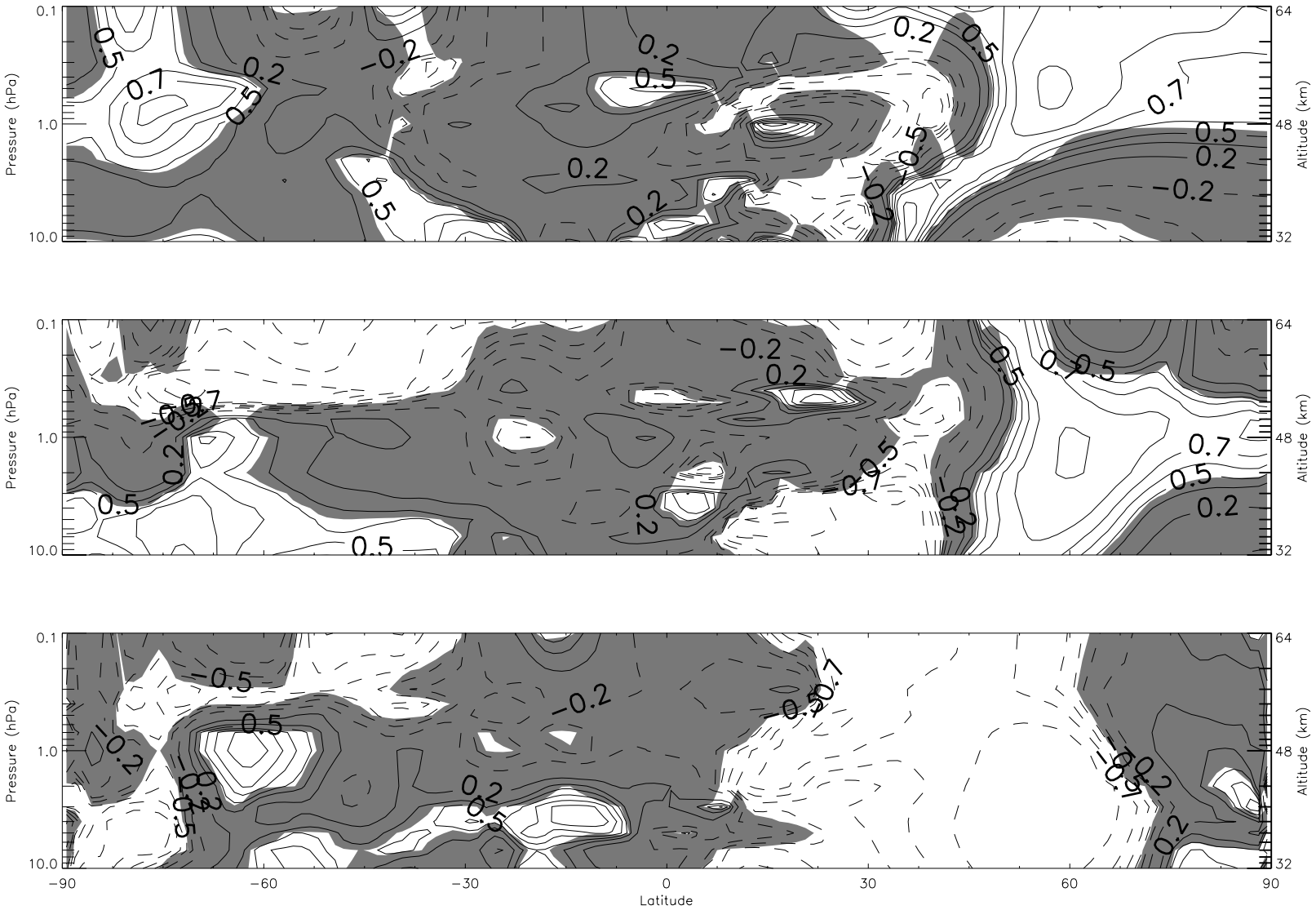

Figure C.2: Correlation map of SPW V s=1,2,3 on 2002 - 325-342 for lag=0

Correlation map of SPW V s=1,2 and 3 on 2002 - 325-342 for lag=0. Top graph shows correlation with SPW1, middle graph with SPW2 and bottom with SPW3. Solid contour lines represent a positive correlation and dashed lines mean negative correlation. Shaded areas mean that the statistical significance of a correlation point is less than 95%.

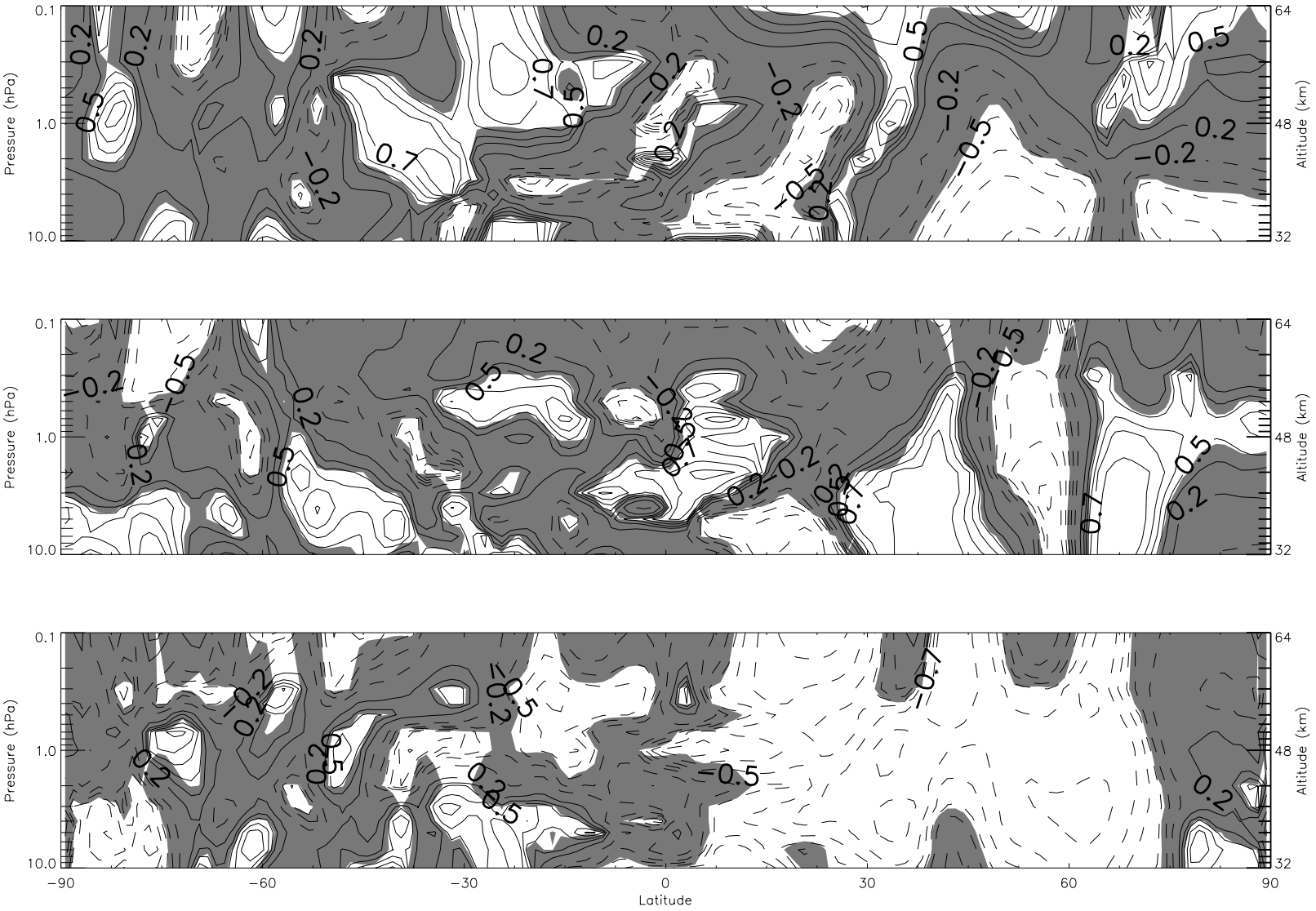

Figure C.3: Correlation map of SPW U s=1,2,3 on 2002 - 325-342 for lag=-1

Correlation map of SPW U s=1,2 and 3 on 2002 - 325-342 for lag=-1. Top graph shows correlation with SPW1, middle graph with SPW2 and bottom with SPW3. Solid contour lines represent a positive correlation and dashed lines mean negative correlation. Shaded areas mean that the statistical significance of a correlation point is less than 95%.

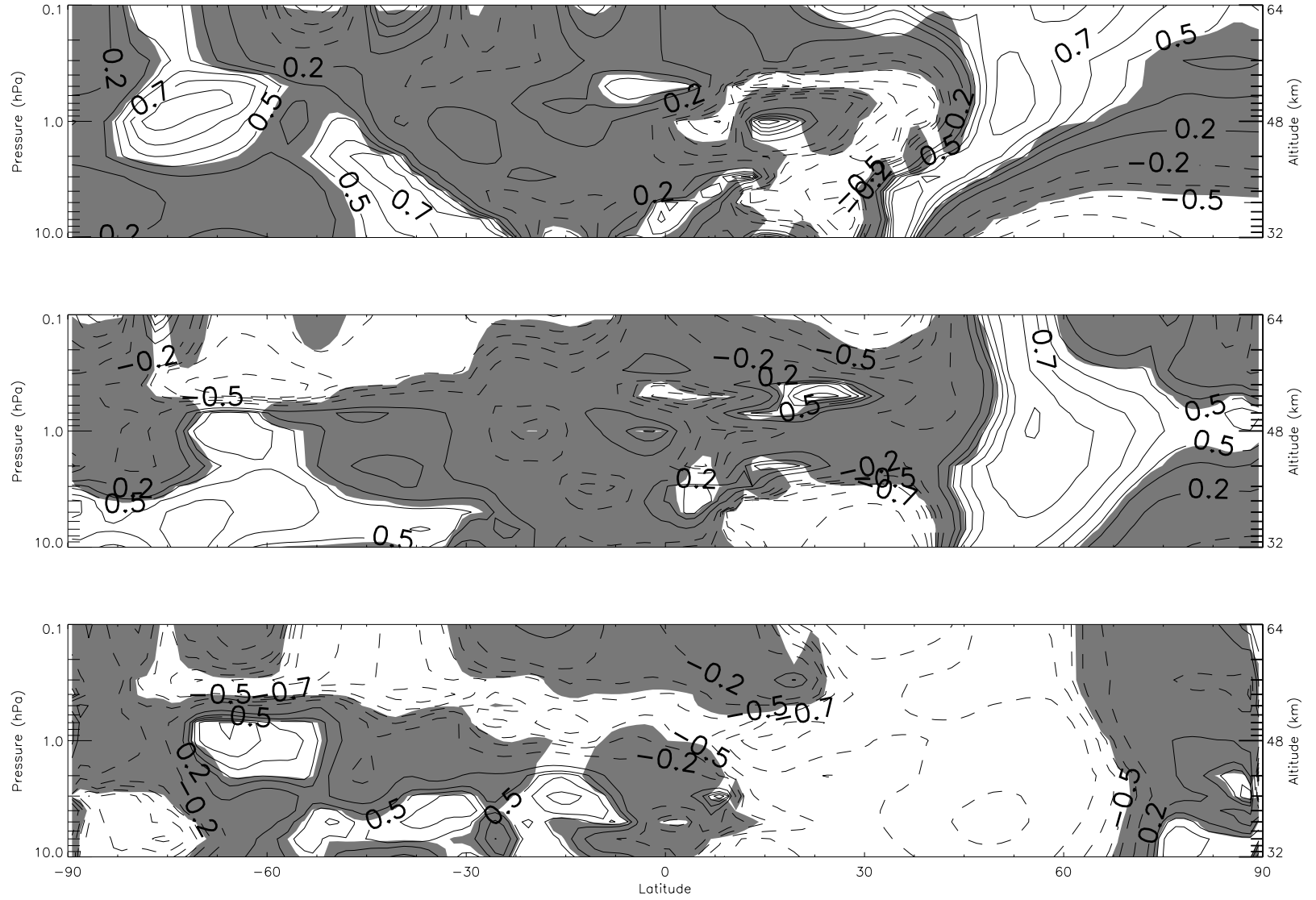

Figure C.4: Correlation map of SPW V s=1,2,3 on 2002 - 325-342 for lag=-1

Correlation map of SPW V s=1,2 and 3 on 2002 - 325-342 for lag=-1. Top graph shows correlation with SPW1, middle graph with SPW2 and bottom with SPW3. Solid contour lines represent a positive correlation and dashed lines mean negative correlation. Shaded areas mean that the statistical significance of a correlation point is less than 95%.

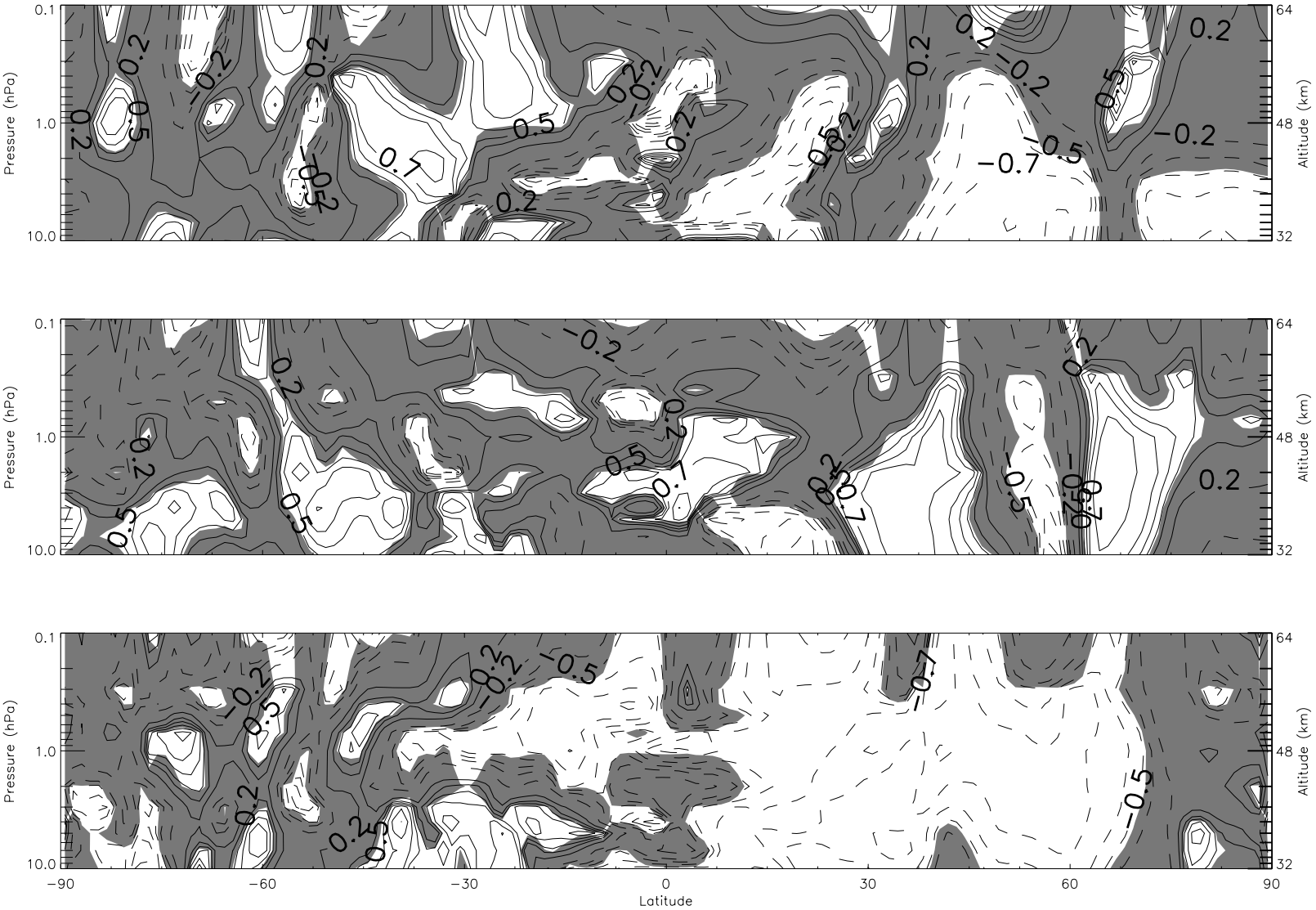

Figure C.5: Correlation map of SPW U s=1,2,3 on 2002 - 325-342 for lag=-2

Correlation map of SPW U s=1,2 and 3 on 2002 - 325-342 for lag=-2. Top graph shows correlation with SPW1, middle graph with SPW2 and bottom with SPW3. Solid contour lines represent a positive correlation and dashed lines mean negative correlation. Shaded areas mean that the statistical significance of a correlation point is less than 95%.

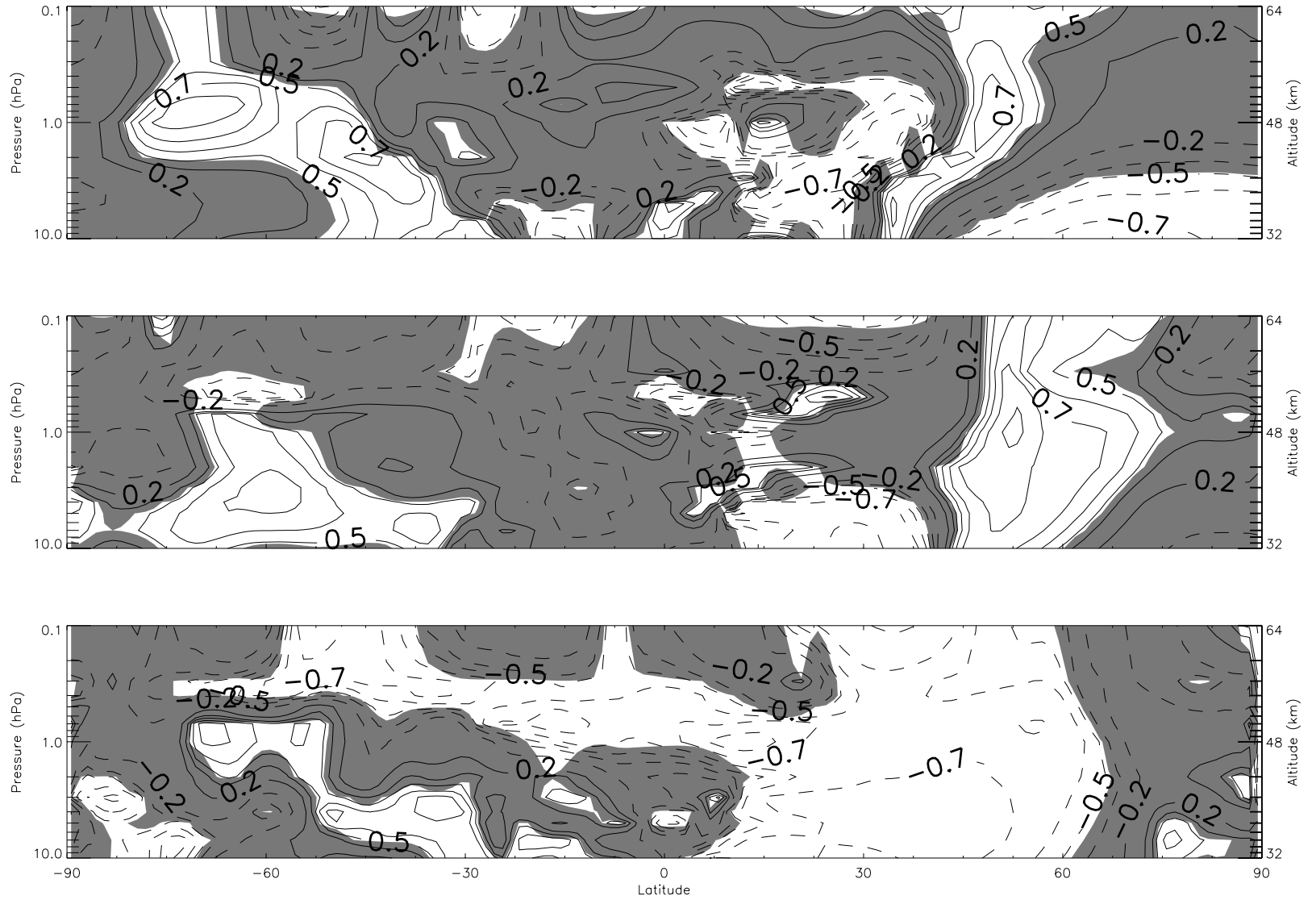

Figure C.6: Correlation map of SPW V s=1,2,3 on 2002 - 325-342 for lag=-2

Correlation map of SPW V s=1,2 and 3 on 2002 - 325-342 for lag=-2. Top graph shows correlation with SPW1, middle graph with SPW2 and bottom with SPW3. Solid contour lines represent a positive correlation and dashed lines mean negative correlation. Shaded areas mean that the statistical significance of a correlation point is less than 95%.

C.2 2003 event

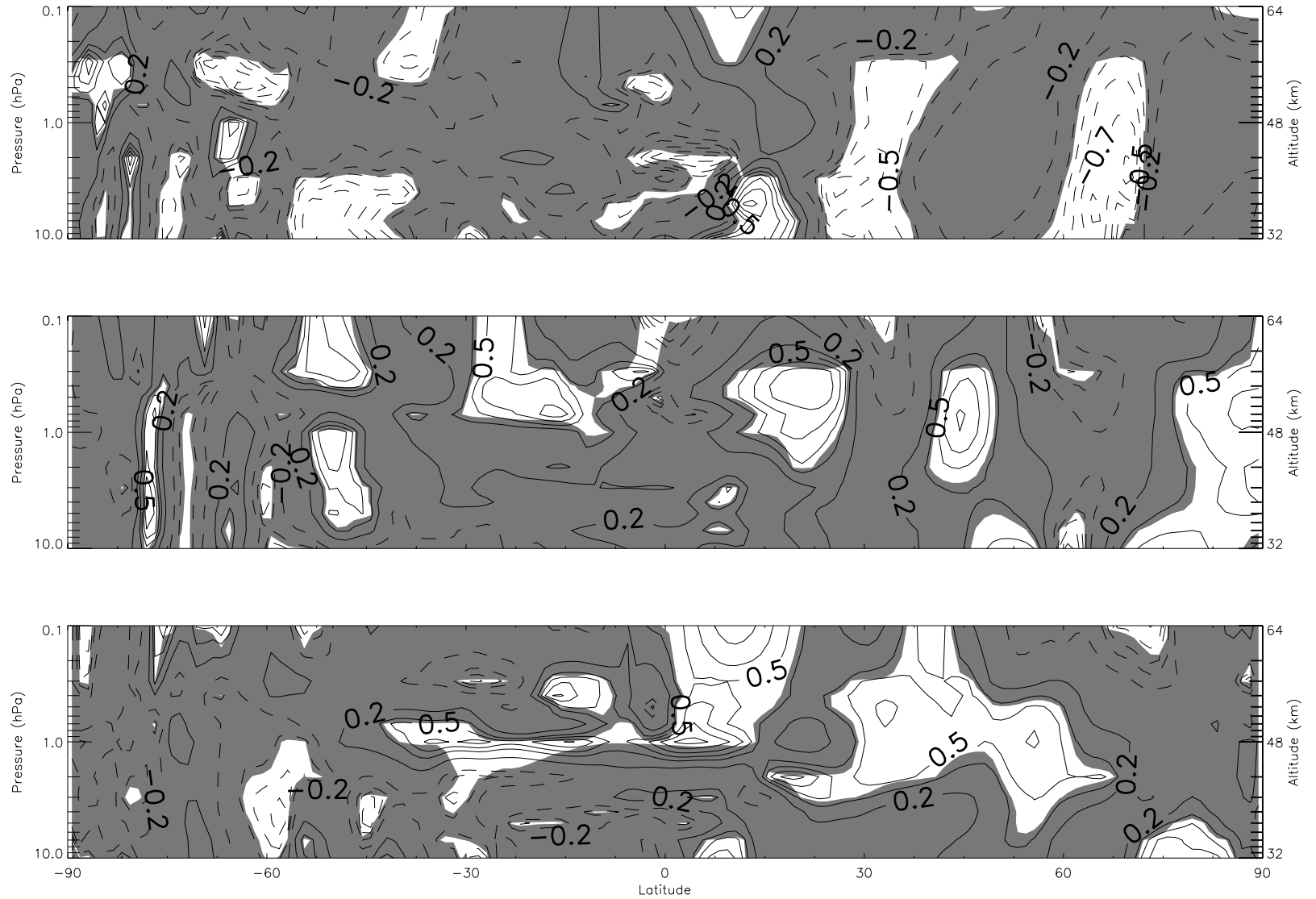

Figure C.7: Correlation map of SPW U s=1,2,3 on 2003 - 10-30 for lag=0

Correlation map of SPW U s=1,2 and 3 on 2003 - 10-30 for lag=0. Top graph shows correlation with SPW1, middle graph with SPW2 and bottom with SPW3. Solid contour lines represent a positive correlation and dashed lines mean negative correlation. Shaded areas mean that the statistical significance of a correlation point is less than 95%.

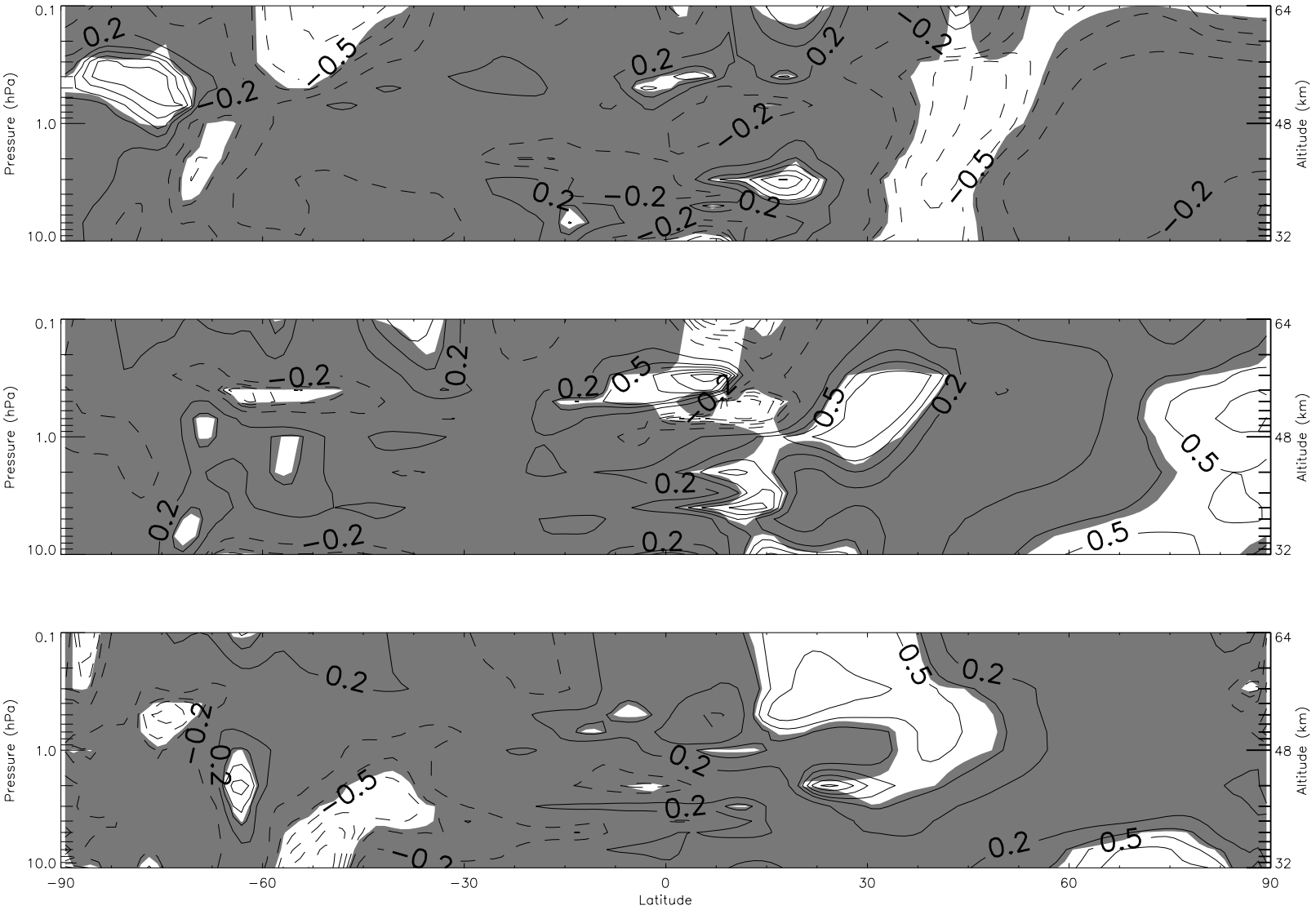

Figure C.8: Correlation map of SPW V s=1,2,3 on 2003 - 10-30 for lag=0

Correlation map of SPW V s=1,2 and 3 on 2003 - 10-30 for lag=0. Top graph shows correlation with SPW1, middle graph with SPW2 and bottom with SPW3. Solid contour lines represent a positive correlation and dashed lines mean negative correlation. Shaded areas mean that the statistical significance of a correlation point is less than 95%.

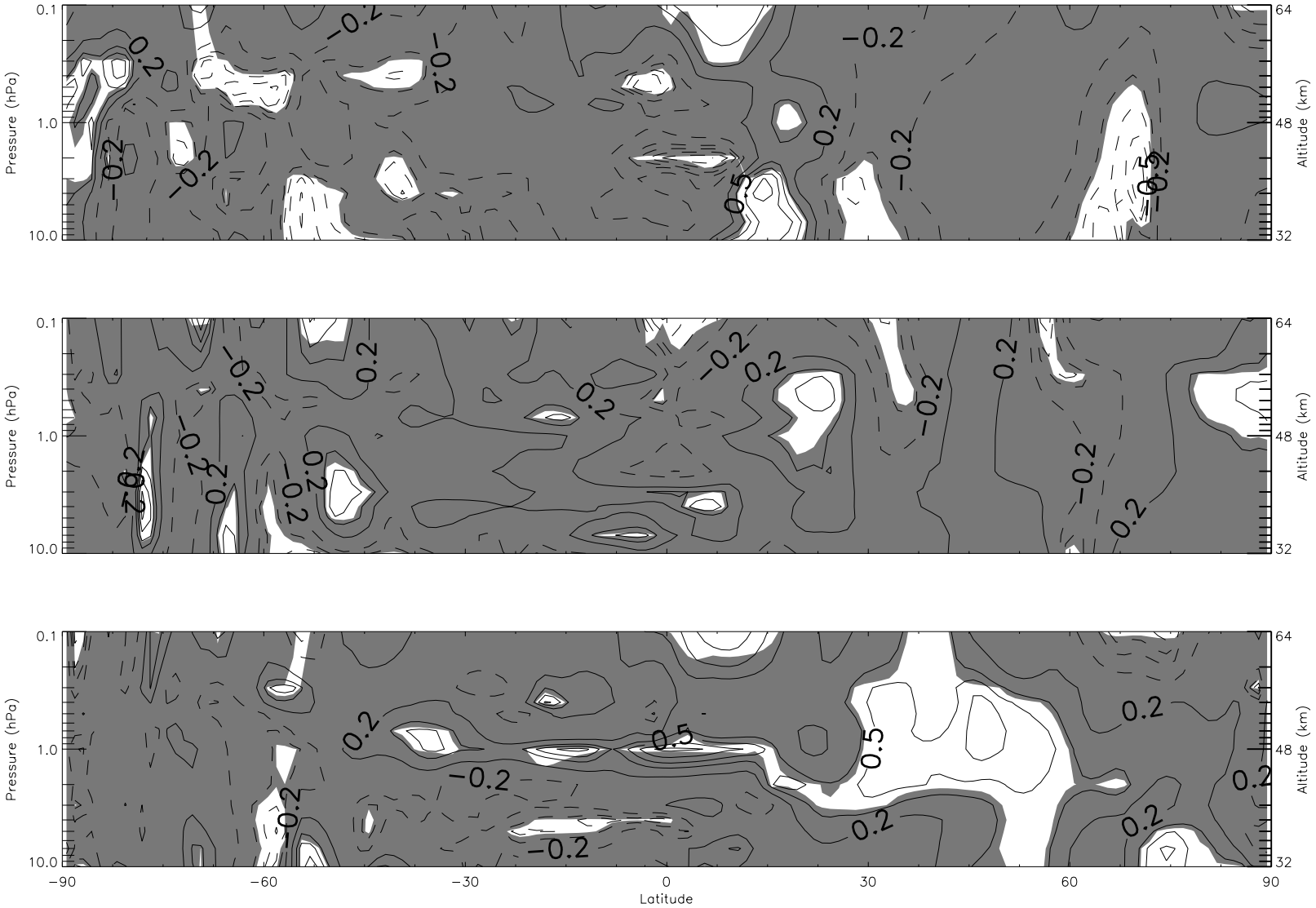

Figure C.9: Correlation map of SPW U s=1,2,3 on 2003 - 10-30 for lag=-1

Correlation map of SPW U s=1,2 and 3 on 2003 - 10-30 for lag=-1. Top graph shows correlation with SPW1, middle graph with SPW2 and bottom with SPW3. Solid contour lines represent a positive correlation and dashed lines mean negative correlation. Shaded areas mean that the statistical significance of a correlation point is less than 95%.

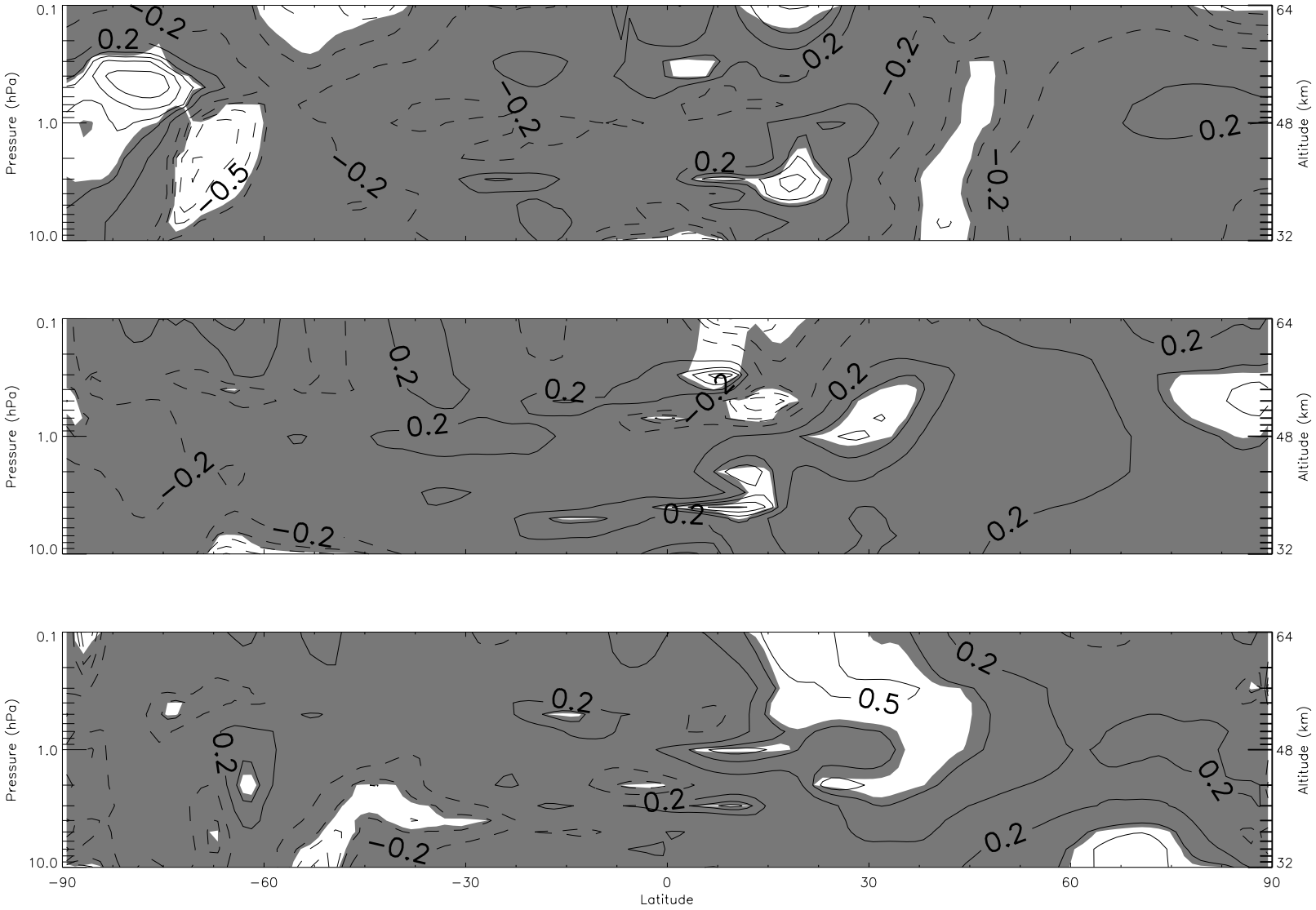

Figure C.10: Correlation map of SPW V s=1,2,3 on 2003 - 10-30 for lag=-1

Correlation map of SPW V s=1,2 and 3 on 2003 - 10-30 for lag=-1. Top graph shows correlation with SPW1, middle graph with SPW2 and bottom with SPW3. Solid contour lines represent a positive correlation and dashed lines mean negative correlation. Shaded areas mean that the statistical significance of a correlation point is less than 95%.

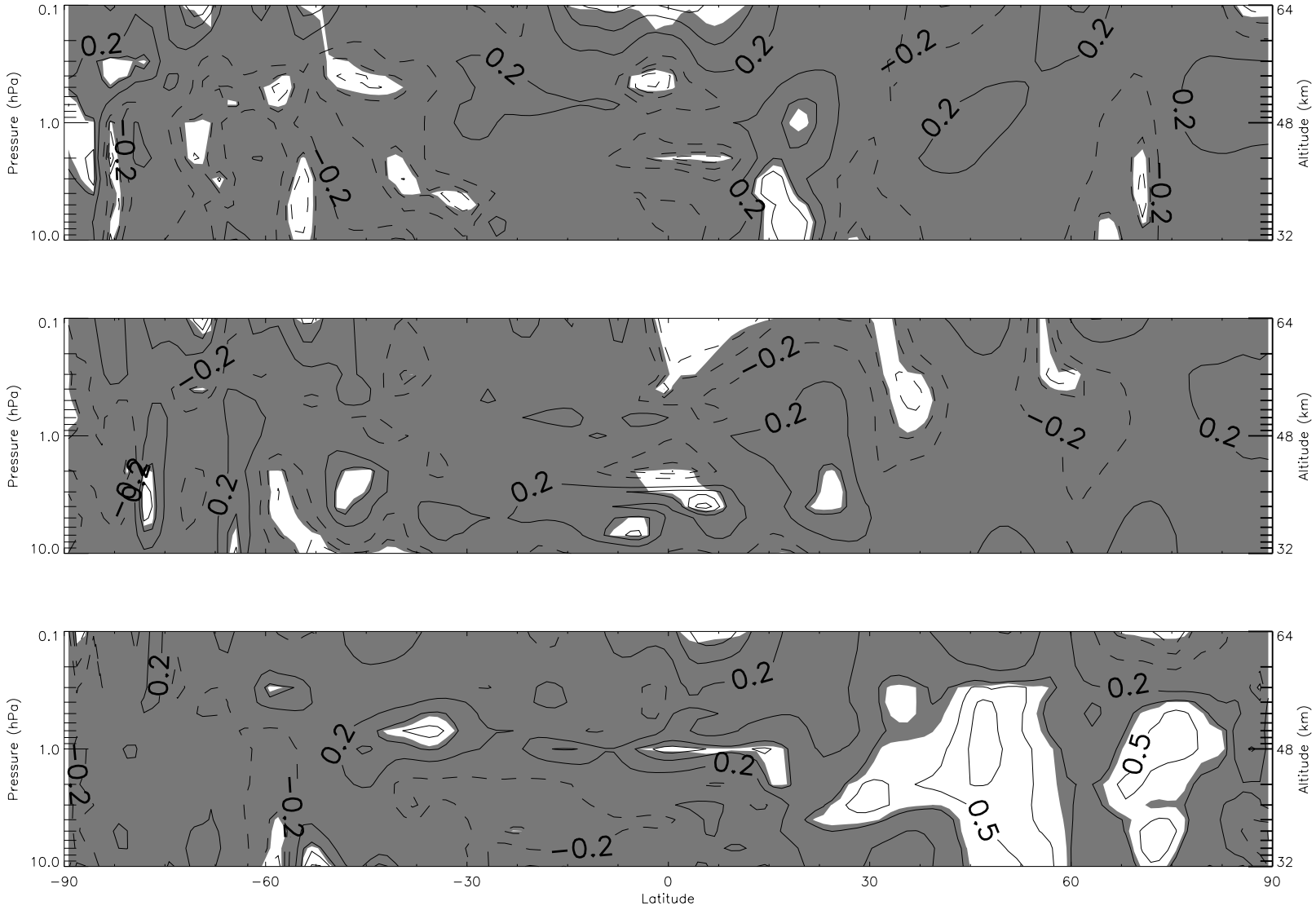

Figure C.11: Correlation map of SPW U s=1,2,3 on 2003 - 10-30 for lag=-2

Correlation map of SPW U s=1,2 and 3 on 2003 - 10-30 for lag=-2. Top graph shows correlation with SPW1, middle graph with SPW2 and bottom with SPW3. Solid contour lines represent a positive correlation and dashed lines mean negative correlation. Shaded areas mean that the statistical significance of a correlation point is less than 95%.

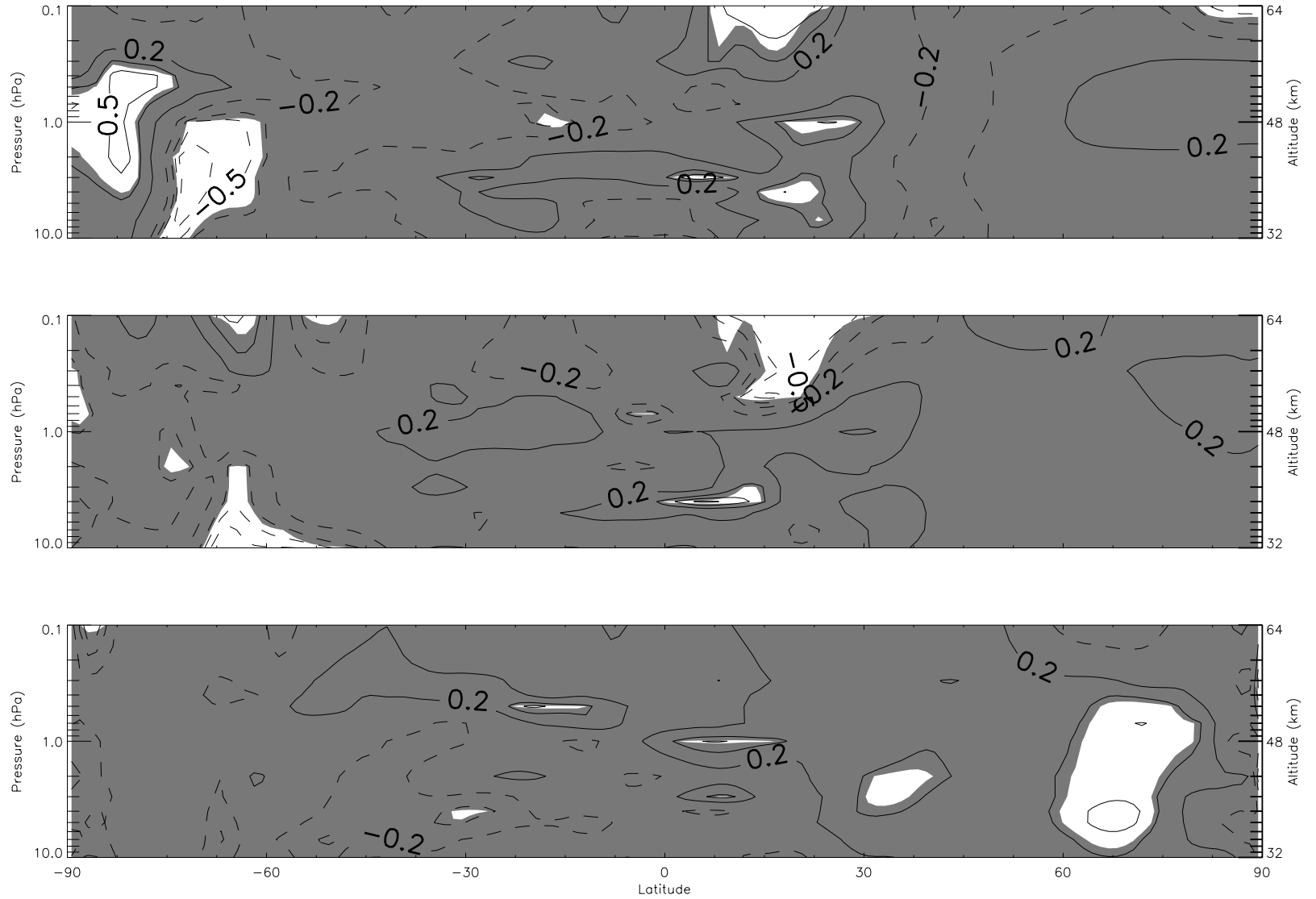

Figure C.12: Correlation map of SPW V s=1,2,3 on 2003 - 10-30 for lag=-2

Correlation map of SPW V s=1,2 and 3 on 2003 - 10-30 for lag=-2. Top graph shows correlation with SPW1, middle graph with SPW2 and bottom with SPW3. Solid contour lines represent a positive correlation and dashed lines mean negative correlation. Shaded areas mean that the statistical significance of a correlation point is less than 95%.

C.3 2004 event

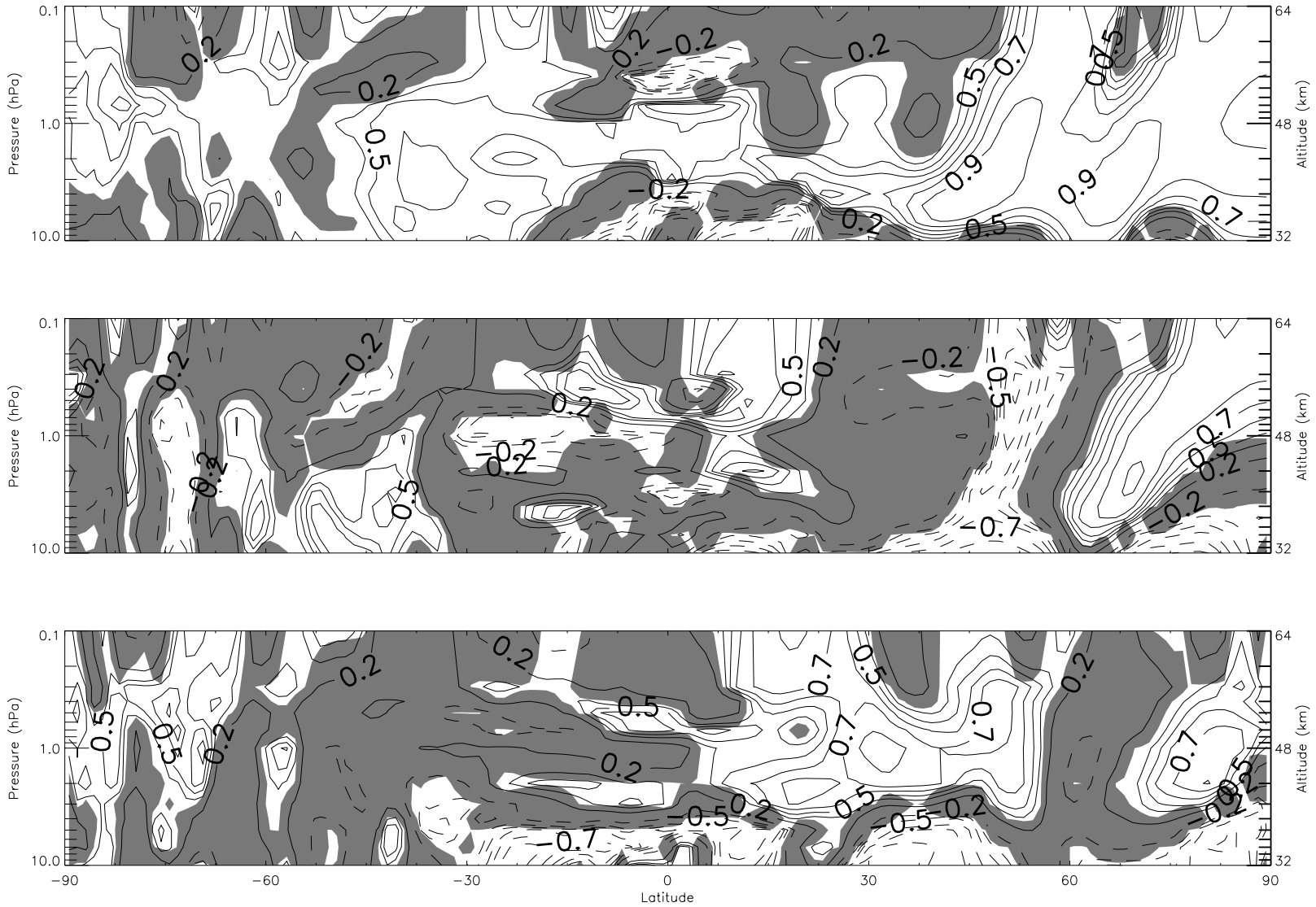

Figure C.13: Correlation map of SPW U s=1,2,3 on 2004 - 10-50 for lag=0

Correlation map of SPW U s=1,2 and 3 on 2004 - 10-50 for lag=0. Top graph shows correlation with SPW1, middle graph with SPW2 and bottom with SPW3. Solid contour lines represent a positive correlation and dashed lines mean negative correlation. Shaded areas mean that the statistical significance of a correlation point is less than 95%.

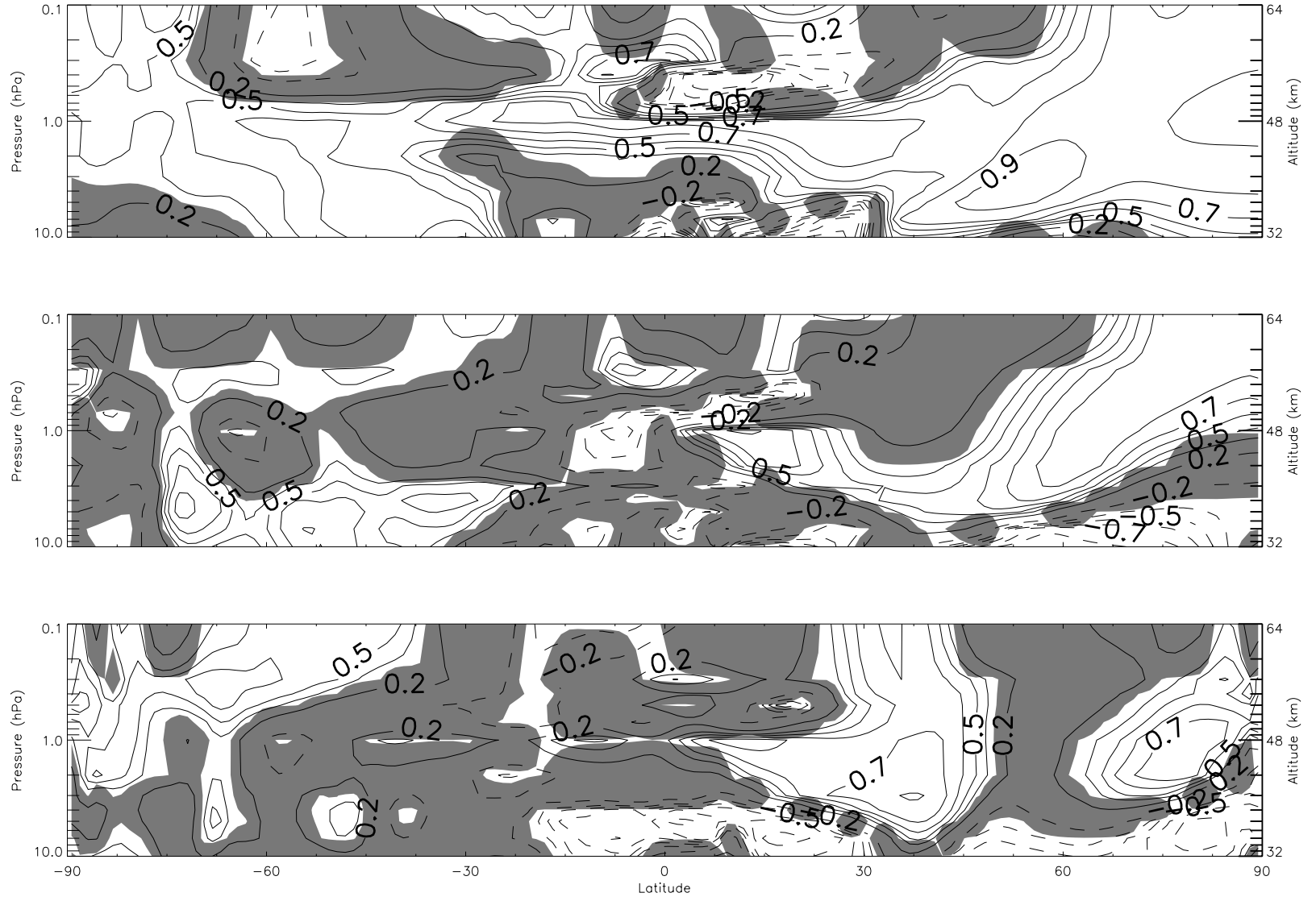

Figure C.14: Correlation map of SPW V s=1,2,3 on 2004 - 10-50 for lag=0

Correlation map of SPW V s=1,2 and 3 on 2004 - 10-50 for lag=0. Top graph shows correlation with SPW1, middle graph with SPW2 and bottom with SPW3. Solid contour lines represent a positive correlation and dashed lines mean negative correlation. Shaded areas mean that the statistical significance of a correlation point is less than 95%.

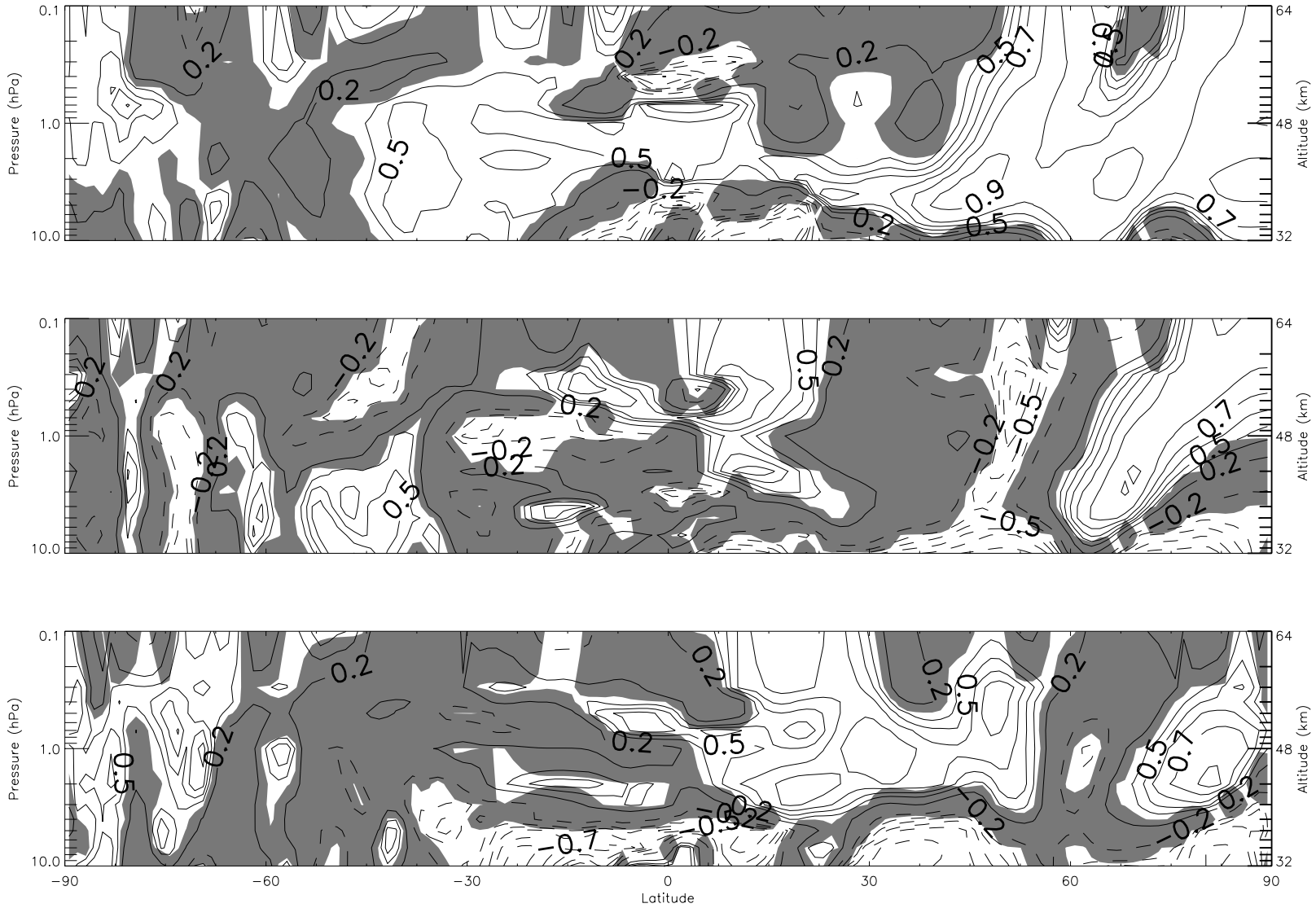

Figure C.15: Correlation map of SPW U s=1,2,3 on 2004 - 10-50 for lag=-1

Correlation map of SPW U s=1,2 and 3 on 2004 - 10-50 for lag=-1. Top graph shows correlation with SPW1, middle graph with SPW2 and bottom with SPW3. Solid contour lines represent a positive correlation and dashed lines mean negative correlation. Shaded areas mean that the statistical significance of a correlation point is less than 95%.

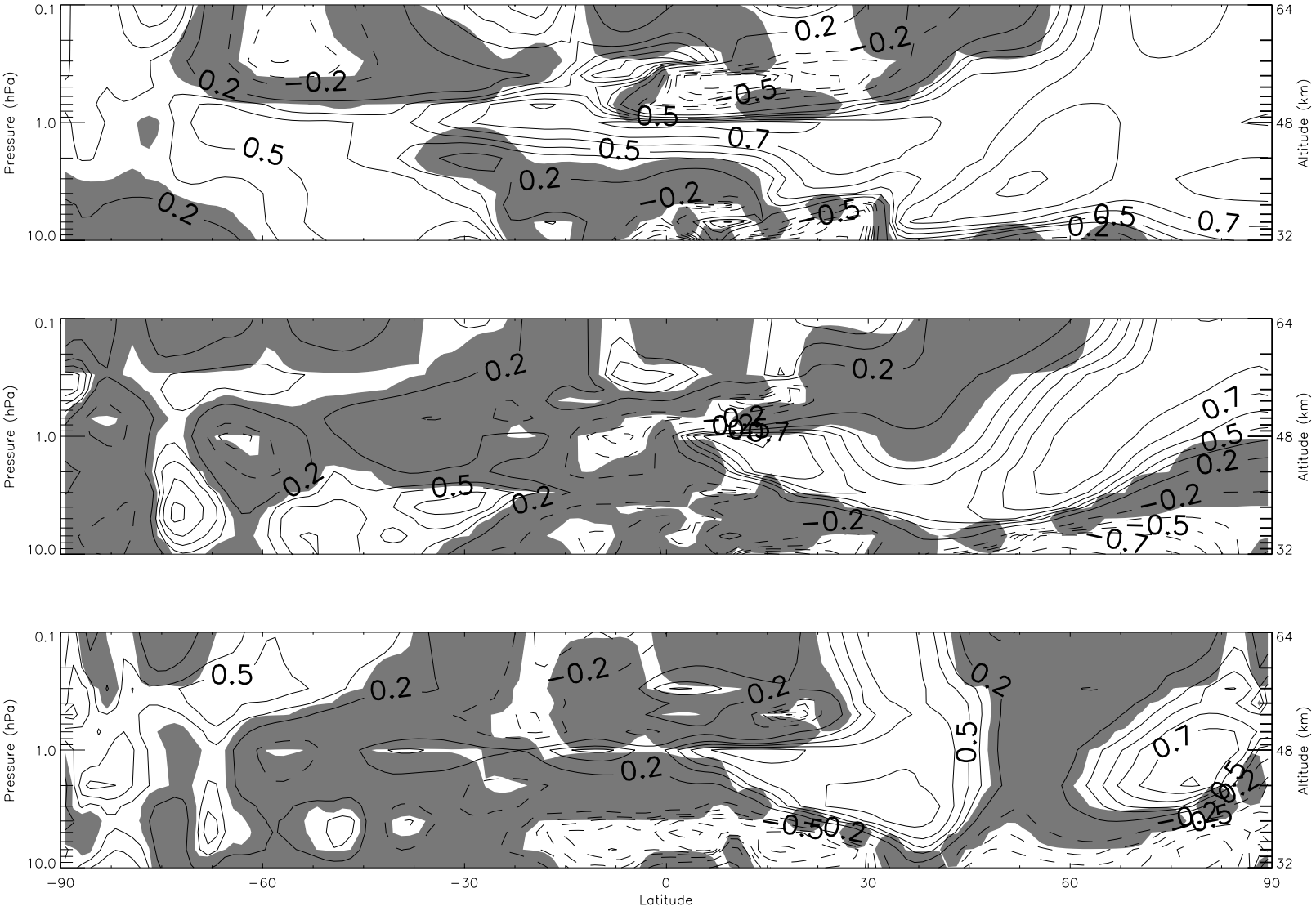

Figure C.16: Correlation map of SPW V s=1,2,3 on 2004 - 10-50 for lag=-1

Correlation map of SPW V s=1,2 and 3 on 2004 - 10-50 for lag=-1. Top graph shows correlation with SPW1, middle graph with SPW2 and bottom with SPW3. Solid contour lines represent a positive correlation and dashed lines mean negative correlation. Shaded areas mean that the statistical significance of a correlation point is less than 95%.

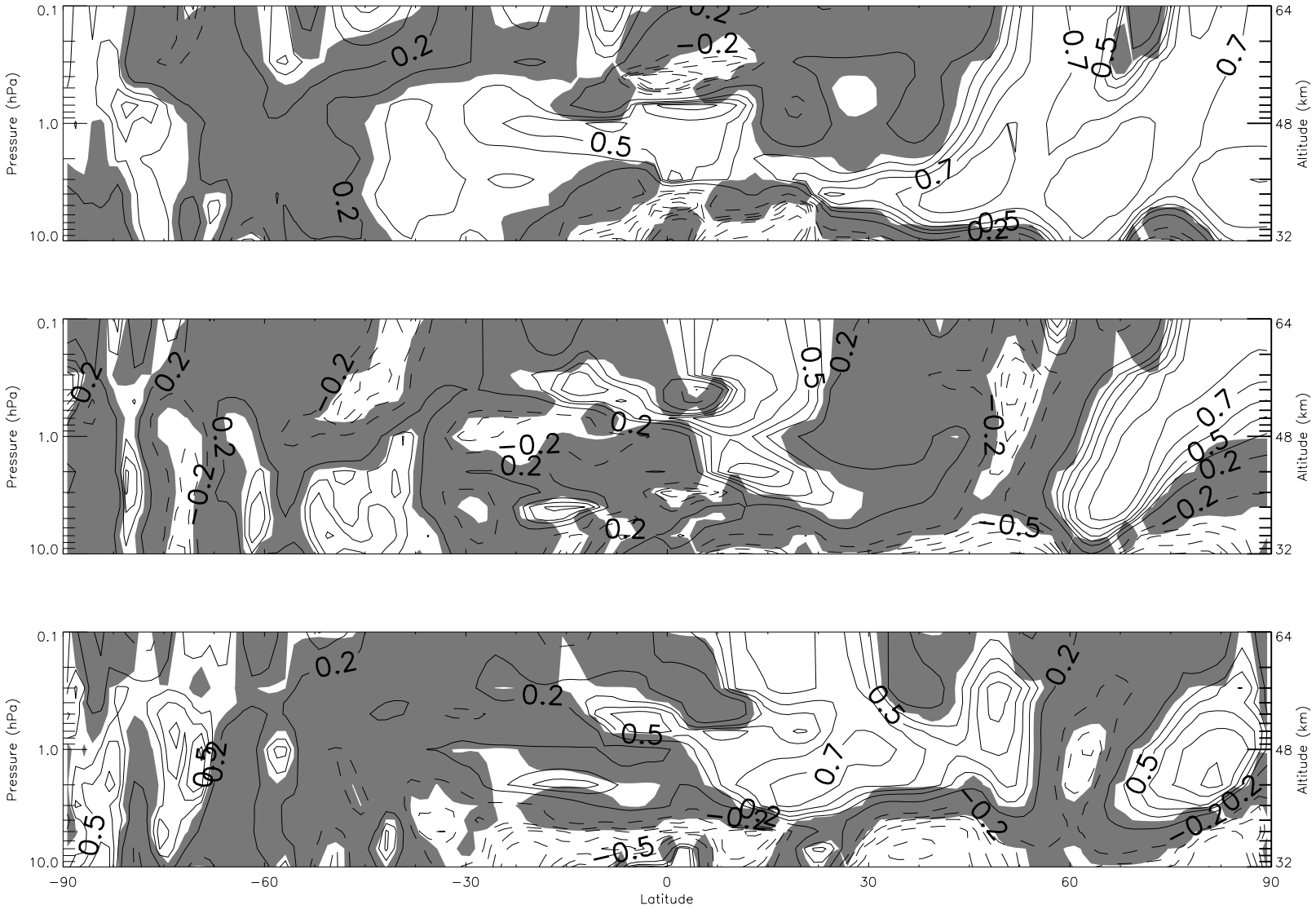

Figure C.17: Correlation map of SPW U s=1,2,3 on 2004 - 10-50 for lag=-2

Correlation map of SPW U s=1,2 and 3 on 2004 - 10-50 for lag=-2. Top graph shows correlation with SPW1, middle graph with SPW2 and bottom with SPW3. Solid contour lines represent a positive correlation and dashed lines mean negative correlation. Shaded areas mean that the statistical significance of a correlation point is less than 95%.

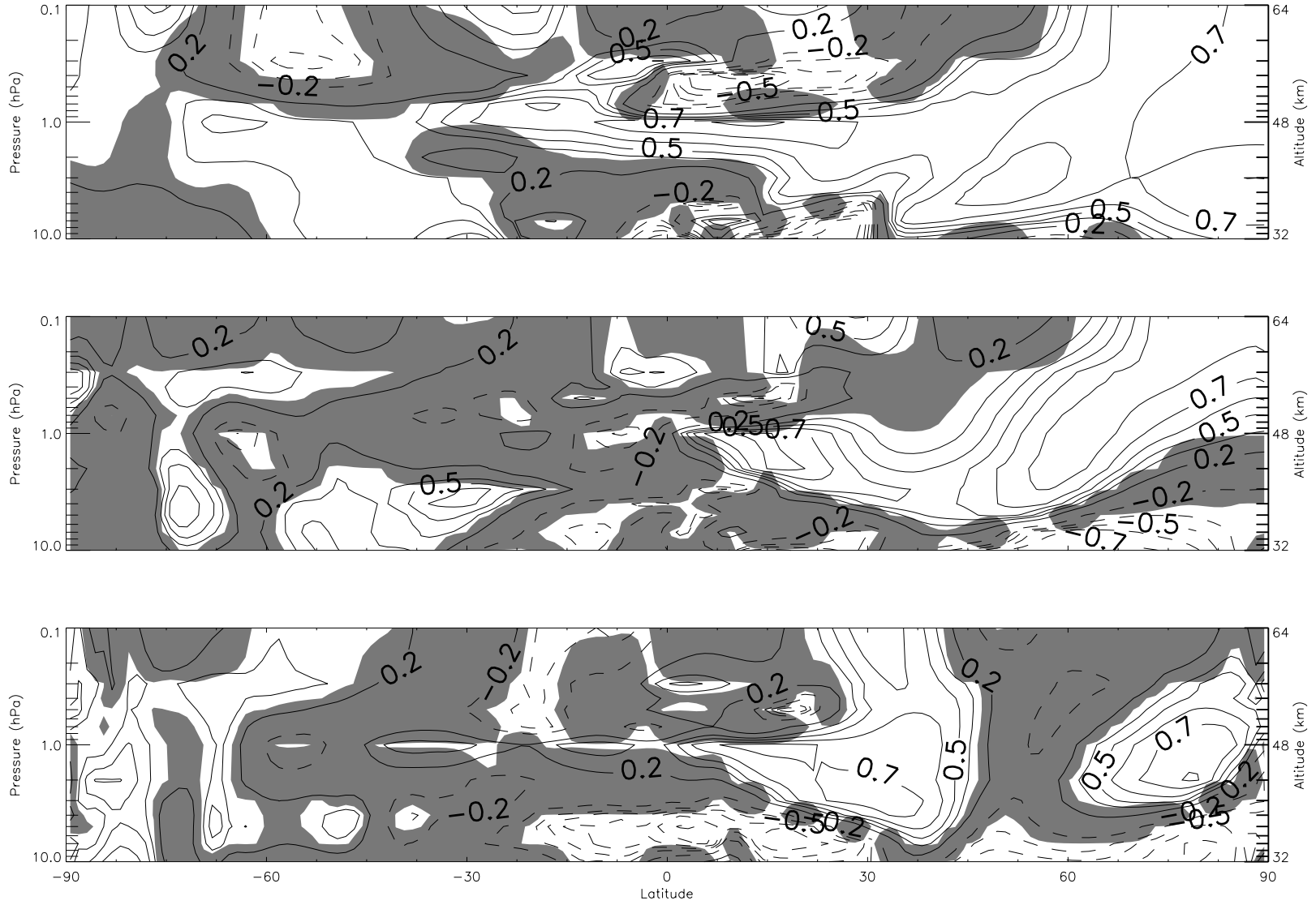

Figure C.18: Correlation map of SPW V s=1,2,3 on 2004 - 10-50 for lag=-2

Correlation map of SPW V s=1,2 and 3 on 2004 - 10-50 for lag=-2. Top graph shows correlation with SPW1, middle graph with SPW2 and bottom with SPW3. Solid contour lines represent a positive correlation and dashed lines mean negative correlation. Shaded areas mean that the statistical significance of a correlation point is less than 95%.

C.4 2005 event

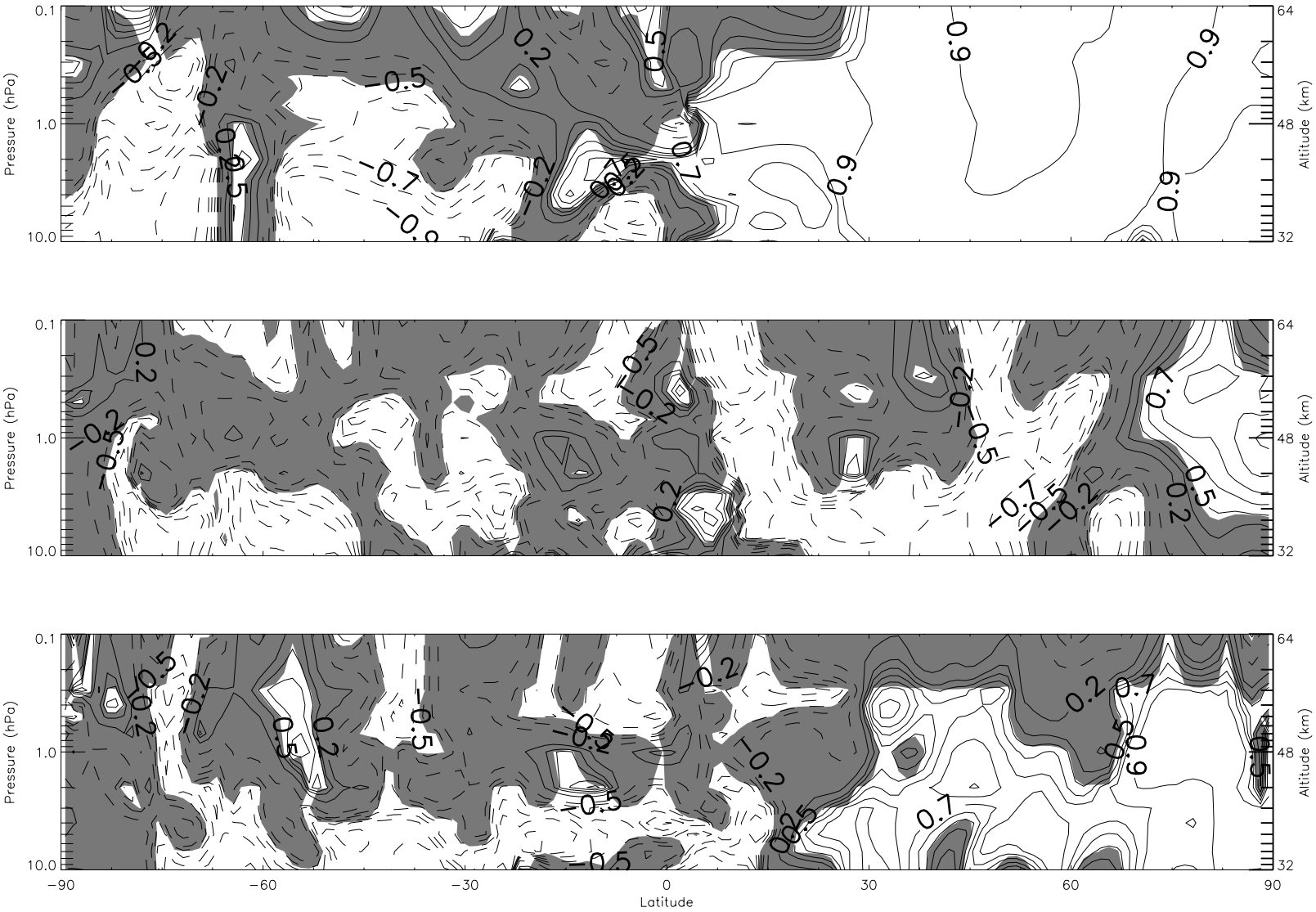

Figure C.19: Correlation map of SPW U s=1,2,3 on 2005 - 317-333 for lag=0

Correlation map of SPW U s=1,2 and 3 on 2005 - 317-333 for lag=0. Top graph shows correlation with SPW1, middle graph with SPW2 and bottom with SPW3. Solid contour lines represent a positive correlation and dashed lines mean negative correlation. Shaded areas mean that the statistical significance of a correlation point is less than 95%.

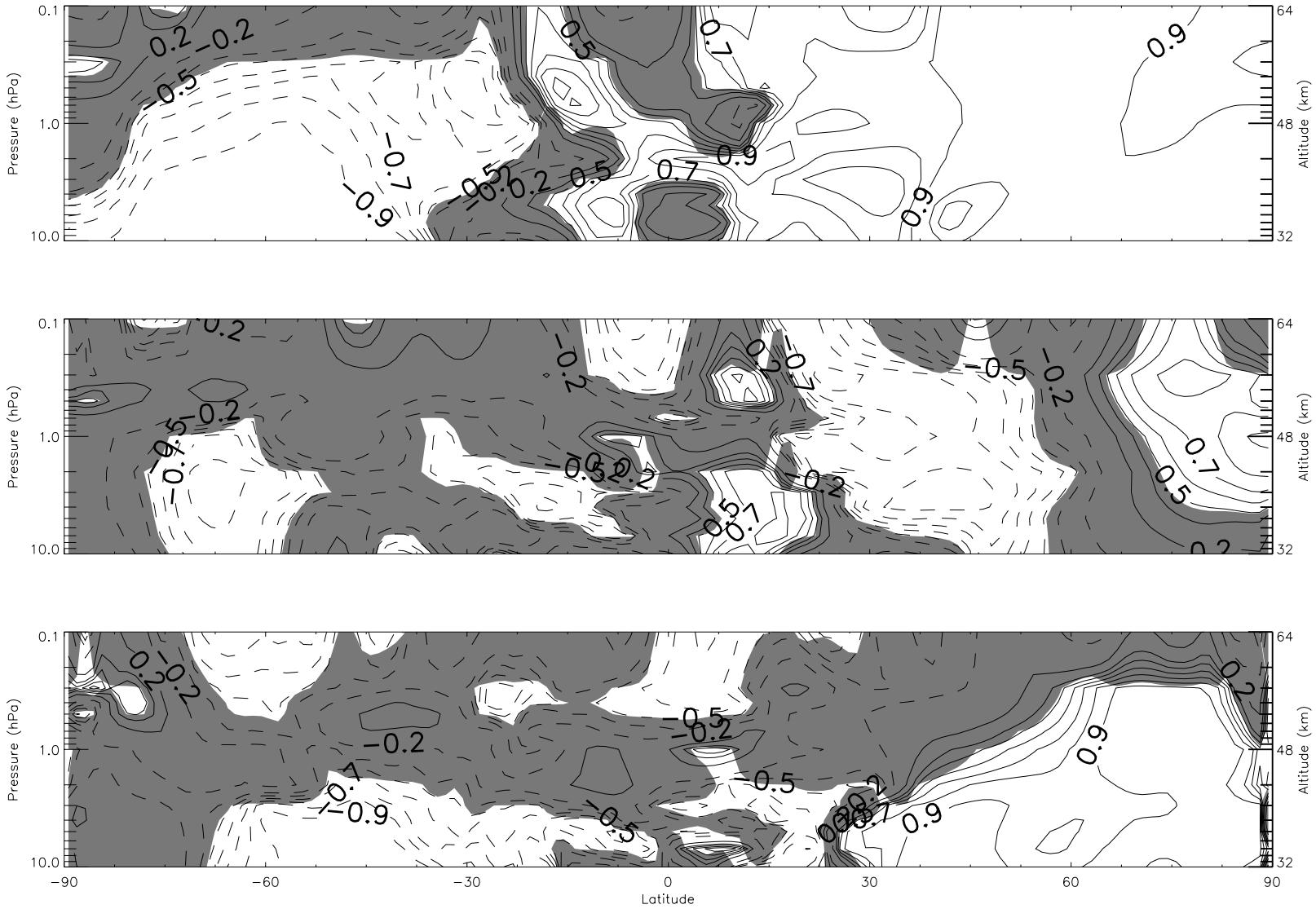

Figure C.20: Correlation map of SPW V s=1,2,3 on 2005 - 317-333 for lag=0

Correlation map of SPW V s=1,2 and 3 on 2005 - 317-333 for lag=0. Top graph shows correlation with SPW1, middle graph with SPW2 and bottom with SPW3. Solid contour lines represent a positive correlation and dashed lines mean negative correlation. Shaded areas mean that the statistical significance of a correlation point is less than 95%.

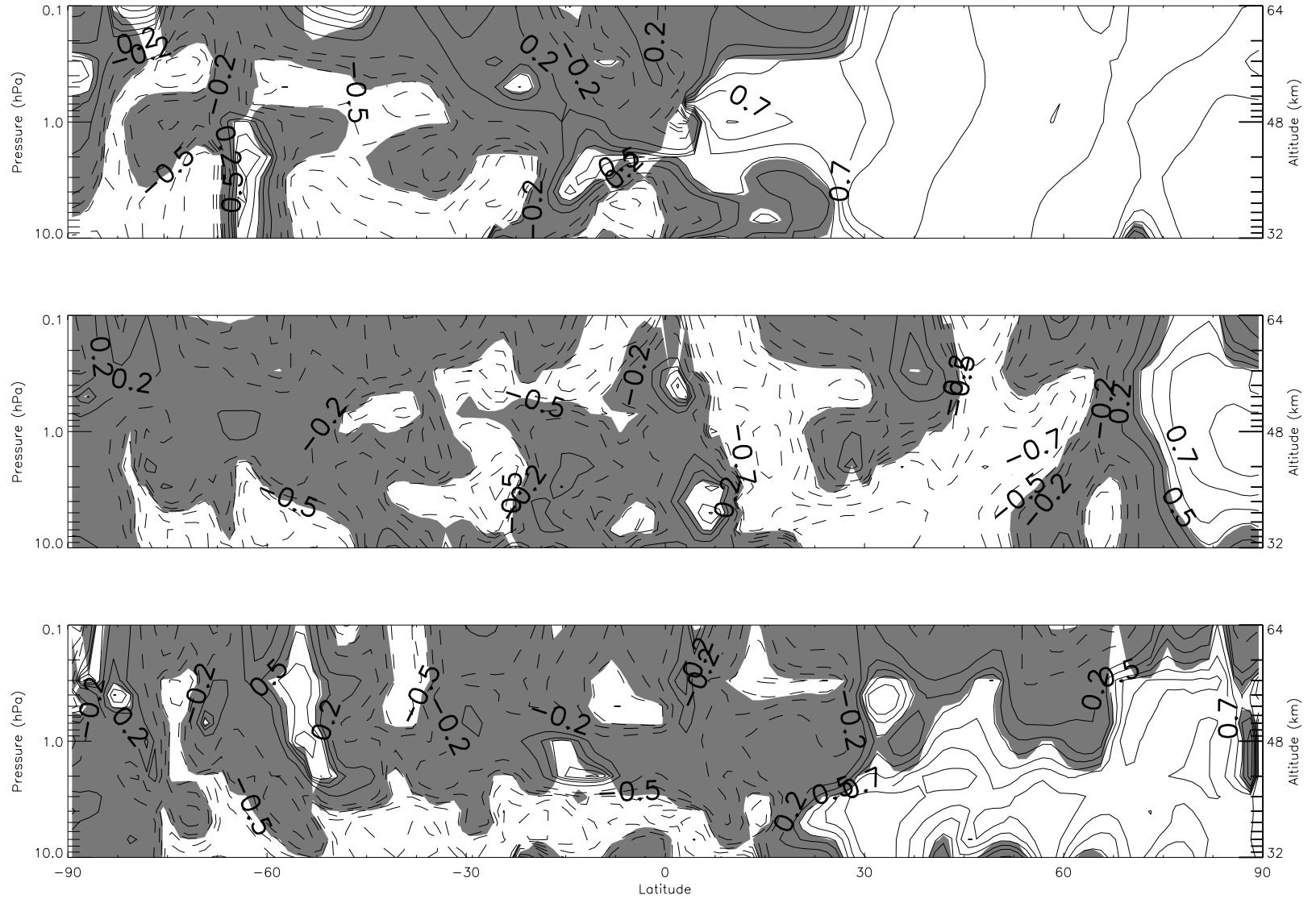

Figure C.21: Correlation map of SPW U s=1,2,3 on 2005 - 317-333 for lag=-1

Correlation map of SPW U s=1,2 and 3 on 2005 - 317-333 for lag=-1. Top graph shows correlation with SPW1, middle graph with SPW2 and bottom with SPW3. Solid contour lines represent a positive correlation and dashed lines mean negative correlation. Shaded areas mean that the statistical significance of a correlation point is less than 95%.

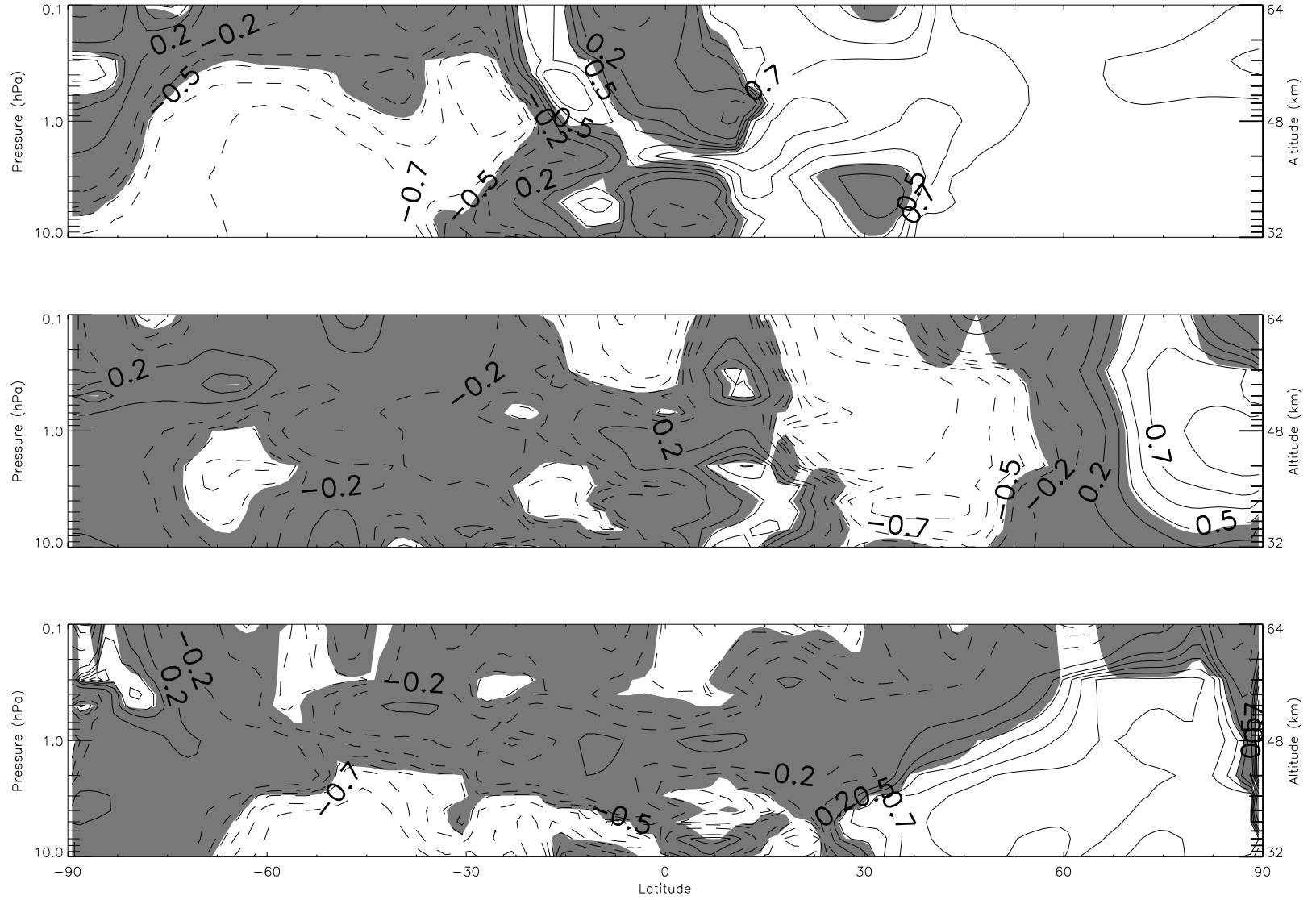

Figure C.22: Correlation map of SPW V s=1,2,3 on 2005 - 317-333 for lag=-1

Correlation map of SPW V s=1,2 and 3 on 2005 - 317-333 for lag=-1. Top graph shows correlation with SPW1, middle graph with SPW2 and bottom with SPW3. Solid contour lines represent a positive correlation and dashed lines mean negative correlation. Shaded areas mean that the statistical significance of a correlation point is less than 95%.

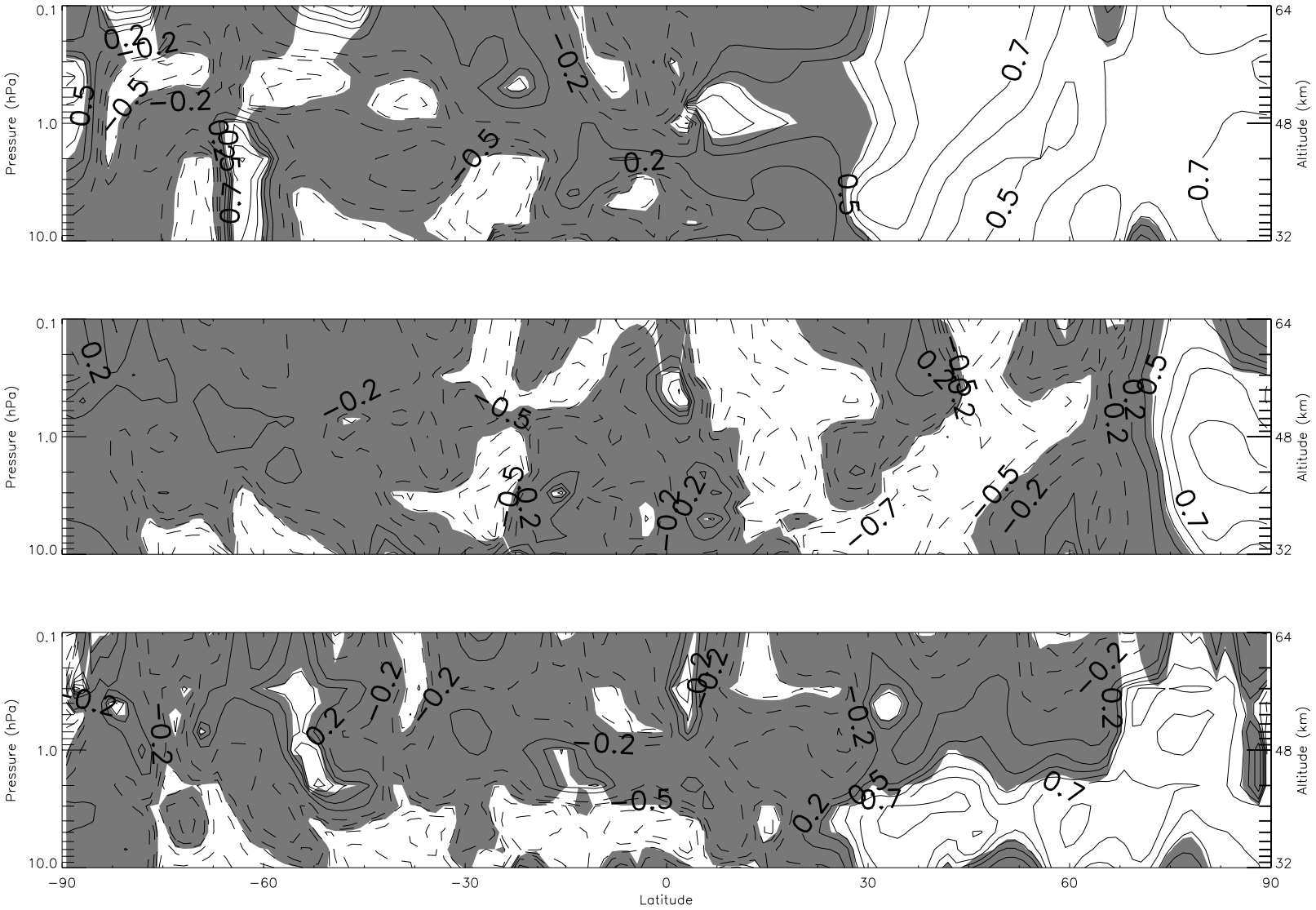

Figure C.23: Correlation map of SPW U s=1,2,3 on 2005 - 317-333 for lag=-2

Correlation map of SPW U s=1,2 and 3 on 2005 - 317-333 for lag=-2. Top graph shows correlation with SPW1, middle graph with SPW2 and bottom with SPW3. Solid contour lines represent a positive correlation and dashed lines mean negative correlation. Shaded areas mean that the statistical significance of a correlation point is less than 95%.

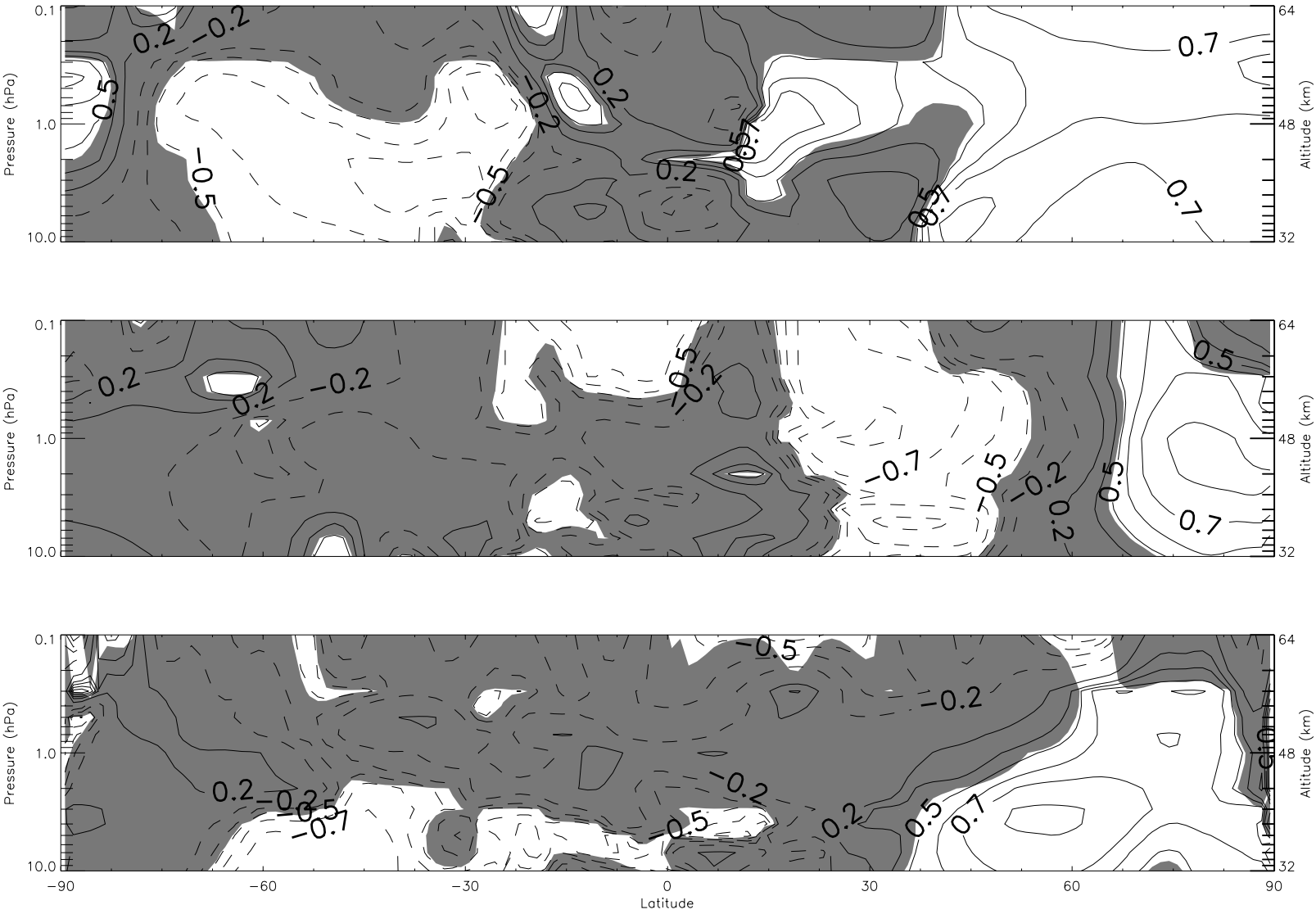

Figure C.24: Correlation map of SPW V s=1,2,3 on 2005 - 317-333 for lag=-2

Correlation map of SPW V s=1,2 and 3 on 2005 - 317-333 for lag=-2. Top graph shows correlation with SPW1, middle graph with SPW2 and bottom with SPW3. Solid contour lines represent a positive correlation and dashed lines mean negative correlation. Shaded areas mean that the statistical significance of a correlation point is less than 95%.